FE(II) OXIDATION BY ANAEROBIC PHOTOTROPHIC BACTERIA: MOLECULAR MECHANISMS AND GEOLOGICAL IMPLICATIONS

Thesis by

Laura Rosemary Croal

In Partial Fulfillment of the Requirements

for the Degree of

Doctor of Philosophy

California Institute of Technology

Pasadena, California

2005

(Defended May 31, 2005)

Acknowledgements

When I came to graduate school, I didn't know how to use Excel or Powerpoint. I didn't know how to efficiently find scientific references. I didn't know the difference between rocks and minerals. I didn't really understand how electron transfer in photosynthesis worked, nor did I care; and while I had a bit of an idea that theoretically, if one was so inclined, one could calculate the free energy yield of a metabolism, I certainly had no idea why one would ever want to do such a thing. Thus, there are many, many people to thank here, as I now know and understand the significance of all these things (and more!) because people here helped and challenged me to learn them.

I must start by thanking and telling the story of how I came to be the graduate student of the person who has had, by far, the most influence on my ability to do the research that I have written about in this thesis – Dianne Newman. I had the outstanding luck to meet Dianne at a key time in my life - the summer before my last year as an undergraduate. It was during this time that I was deciding what graduate schools I would apply to in the fall. I knew two things: that I wanted to go west and that I wanted to do molecular genetics in environmentally relevant microorganisms. I spent that summer doing research in the lab of Roberto Kolter - not so incidentally Dianne's post-doctoral advisor. Dianne was at Wood's Hole that summer TA'ing the Microbial Diversity class - I almost missed her as she didn't come back to the lab until almost the end of summer and my time there! Fortunately she did return and one day over tea we started talking about our future plans, I and my graduate school choices and she and her new position at Caltech, in Pasadena, CALIFORNIA. During my conversation with her I learned a new word - molecular geomicrobiology. I was hooked, and it seemed Dianne would soon need graduate students, but who was this woman? I had only known her a few days, what was she really like? And how the hell was she already a professor at Caltech when she was just 5 years older than me?! A thorough background check and a "rigorous" interrogation over the phone gave me the answers I needed to justify applying to Caltech. And justification I needed, as all my trusted advisors told me: 1) don't go to a school where there is only one person you want to work for, it's too risky and 2) don't work for a new faculty member, it's even more risky! I was made so leery that before I came to visit Caltech for a recruiting weekend, I thought I knew for sure that I wouldn't end up there. How could it possibly compete with my other microbiology powerhouse choices? Once I did visit, however, the beautiful campus setting, the smell of the gardenias, the brilliance of the people and the rocking recruiting weekend all made me to realize that this was no risk I was taking, Caltech and Dianne were a sure thing. As it turns out it, I was right: five and a half years later I have an amazingly, unbelievably, accomplished advisor who has given me countless opportunities and un-ending support and this thesis to prove it. Thank you so much Dianne.

And so, here comes the rest of the list…

Thanks to the NSF, for funding the first three years of my graduate work and providing me with an opportunity to do research in Germany. Thanks also to the Packard Foundation, whose generous support made my project possible.

Thanks to Liz Arredondo, Chi Ma, Jared Leadbetter, Kosuke Ishii, Randy Mielke, Sue Welch and Rebecca Poulson for technical assistance.

Thanks to Tina Salmassi, who also provided technical assistance and who, as my TA for Janet Hering's aquatic chemistry class, helped me endlessly and patiently, taking me from being unable to input log numbers in my calculator to being able to construct Eh/pH diagrams at the drop of a hat (it is because of you that I know how to use Excel!)

Thanks to Clark Johnson and Brian Bead, for patiently helping me learn all the Fe isotopic geochemistry I could handle!

Great thanks to Professors Friedrich Widdel and Bernard Schink, who allowed me the amazing opportunity to work in their labs in Germany for a summer. I couldn't have asked for a more worthwhile and fulfilling graduate experience.

Thanks to Arash Komeili, Jeff Gralnick, and Andreas Kappler for being a constant source of reference and aid and to all the Newman Lab members past and present, for continual helpful scientific discussion as well as entertainment! In particular, thanks to Yongqin Jiao for being a BIF team member extraordinaire! Without your help and support over the past five months, those cell suspension assays would NEVER have gotten done!

Thanks to all my friends at Caltech who have made my time here more enjoyable, my girl's lunch crew in particular!

Thanks to my previous mentors and teachers: Diana Downs, Julie Zilles, Jorge Escalante, Roberto Kolter, Paula Watnick, Enrique Massa, and Fred Kittel for preparing me well for the challenge of graduate school.

Thanks to my committee members, Mel Simon, George Rossman, Elliot Meyerowitz, and Joe Kirschvink for their time and support.

And finally, special and profound thanks to: 1) my brother and sister who offered invaluable support and humor over the years, 2) my mother who constantly reminded me and demonstrated that all I had to do was say the word and she would be here, if for nothing else than to just make me dinner, 3) my father, who through a two hour phone conversation at a crucial time, helped me find the strength to continue my work here and helped me come to the decision, once and for all, that obtaining this degree would not be the first challenge in my life that I would not rise to meet and 4) Chris, who was there to make me that dinner when my mother wasn't and who offered unconditional and complete support through out it all. Words can't express how much I love you all and how grateful I am for your support. With out you five, I most certainly would not be where I am today.

Abstract

In this thesis, the hypothesis that photoautotrophic Fe(II)-oxidizing bacteria catalyzed the deposition of Banded Iron Formations (BIFs), an enigmatic class of ancient sedimentary rocks is explored. Ecophysiological, geochemical, genetic and biochemical approaches are taken to elucidate the molecular mechanism of photoautotrophic Fe(II) oxidation in an effort to identify molecular biosignatures that are unique to this metabolism and capable of being preserved BIFs. In an ecophysiological approach, we show that Fe(II) oxidation by these phototrophs proceeds at appreciable rates in the presence of high concentrations of H_2 when CO_2 is abundant. These findings substantiate a role for the involvement of these phototrophs in BIF deposition under the presumed geochemical conditions of the Archean. In a geochemical approach, we find that although phylogenetically distinct phototrophs fractionate Fe isotopes in a way that is consistent with Fe isotopic values found in Precambrian BIFs, it is unlikely that this fractionation can be used as a biosignature for this metabolism given its similarity to fractionations produced by abiotic Fe(II) oxidation reactions. In two distinct genetic approaches, we identify genes involved in Fe(II) oxidation in *Rhodopseudomonas palustris* TIE-1 and *Rhodobacter* SW2. Genes identified in TIE-1 encode a predicted integral membrane protein that appears to be part of an ABC transport system and a putative CobS, an enzyme involved in cobalamin (vitamin B_{12}) biosynthesis. Candidate genes on a cloned fragment of the *Rhodobacter* SW2 genome that confer Fe(II) oxidation activity to a non-oxidizing strain include those predicted to encode permeases and a protein with potential redox capability. Finally, in a preliminary biochemical approach, *c*-type cytochromes and other proteins that are exclusive or more highly expressed under Fe(II) growth conditions in TIE-1 and SW2 are identified in SDS-PAGE gels. The work described here furthers our search for a biosignature unique to photoautotrophic Fe(II) oxidation by providing mechanistic information on this metabolism.

TABLE OF CONTENTS

LIST OF FIGURES

LIST OF TABLES

1. Introduction

WERE FE(II) OXIDIZING PHOTOAUTOTROPHS INVOLVED IN THE DEPOSITION OF PRECAMBRIAN BANDED IRON FORMATIONS?

Banded Iron Formations (BIFs) are ancient sedimentary rocks characterized by laminations consisting of the siliceous mineral chert (SiO_2) and various Fe minerals [96]. The Fe minerals in these rocks, which by definition contain >15 wt.% Fe [80], are generally oxidized minerals, such as magnetite (Fe_3O_4) and hematite (Fe_2O_3); however formations containing reduced Fe minerals including Fe-carbonates, -sulfides or -silicates also exist [94]. Given the massive volume of these depositions, which can extend laterally hundreds to thousands of kilometers with thicknesses of hundreds of meters, BIFs are important from an economic perspective, as they provide the source for approximately 90% of the Fe ore mined globally [172].

BIFs were deposited during a period of Earth history known as the Precambrian, with the majority of these rocks having an age that ranges from ~3.8 to 1 billion years (Ga) [96]. Models to explain the formation of BIFs are both numerous and controversial and hinge on knowing when free oxygen (O_2) appeared on the Earth. Traditionally, the origin of these rocks are explained by the precipitation of iron oxide minerals that occurred when episodic upwellings

brought deep, anoxic ocean waters high in ferrous Fe [Fe(II)] concentration in contact with more oxygenated surface waters [95]. The source of this O_2 is presumed to be oxygenic photosynthetic bacteria (cyanobacteria), however, whether cyanobacteria capable of producing O_2 had evolved at the time when the most ancient of these BIFs were deposited (*e.g.,* 3.8 Ga) remains questionable [23, 148, 166]. In addition, several lines of geological evidence suggest that before approximately 2.3 Ga, the Earth's atmosphere was essentially devoid of O_2 and that reducing conditions prevailed [58, 74, 91, 145]. Thus, an open question is whether O_2 would have been present in sufficient quantities to form these ancient BIFs. Hypotheses invoking the direct oxidation of Fe(II) by UV light under anaerobic conditions have been proposed [24, 32, 62]; however, under the presumed chemical conditions of the Precambrian ocean [73], it is unlikely that this process accounts for the amount of Fe(III) required to explain these depositions [101].

A alternate hypothesis for the deposition of these formations under anoxic conditions is that they were formed as a metabolic by-product of anoxygenic phototrophic bacteria able to use Fe(II) as an electron donor for photosynthesis [67, 101, 182]. This metabolism proceeds by the reaction:

$$HCO^{3-} + 4\ Fe^{2+} + 10\ H_2O \rightarrow <CH_2O> + 4\ Fe(OH)_3 + 7\ H^+$$

and is likely to represent one of the most ancient forms of metabolism (see background and [20, 185]). While the majority of isolated Fe(II) photoautotrophs

are freshwater strains [52, 69, 70, 182], marine strains have been isolated as well [163]. Thus, ancient relatives of these bacteria likely inhabited the oceanic environments in which BIFs were deposited.

RESEARCH OBJECTIVES AND SUMMARY

The goal of this thesis has been to investigate the possibility that Fe(II) oxidizing phototrophs were involved in the deposition of BIFs. My approaches have ranged from the ecophysiological, to the geochemical, to the genetic and biochemical, with the objective being to characterize Fe(II) photoautotrophy at the molecular level in an effort to identify chemical signatures unique to this metabolism that are preserved in BIFs. The results of these investigations are described and discussed in detail in the subsequent chapters of this thesis.

In chapter two, further details concerning the search for biosignatures and their limitations, why we have chosen to focus on Fe(II)-oxidizing phototrophs and what is known about the molecular mechanism Fe(II) oxidation by *Acidithiobacillus ferrooxidans* are discussed. Portions of this chapter have been published in an article entitled “The Genetics of Geochemistry” in *Annual Review of Genetics*.

To investigate if the presence of H_2, which is reported to have been present in the Archean at concentrations of up to 300,000 ppm [170], would have inhibited Fe(II) oxidation by these phototrophs in an ancient ocean (potentially precluding a role for these organisms in BIF deposition), we investigated the effects of H_2 on the Fe(II) oxidation activity of *Rhodopseudomonas palustris* TIE-

1 (TIE-1) and *Rhodobacter* sp. SW2 (SW2). The findings of this work, described in chapter three, show that Fe(II) oxidation still proceeds under an atmosphere containing ~3 times the maximum predicted concentration of H_2 in the Archean when CO_2 is abundant. Additionally, the amount of H_2 dissolved in a 100 m photic zone of Archean ocean over an area equivalent to the Hamersley basin may have been less than 0.24 ppm. We thus conclude that H_2 would pose no barrier to Fe(II) oxidation by ancient anoxygenic phototrophs at depth in the photic zone and would not have prevented these organisms from catalyzing BIF deposition. Portions of this work will be submitted to *Geobiology*.

After demonstrating that Fe(II) photoautotrophy would have been an active metabolism in the environments where BIFs were deposited, we undertook a geochemical investigation to determine if a biologically unique Fe isotope fractionation was produced during photoautotrophic growth on Fe(II) of a pure strain, *Thiodictyon* strain F4, and two enrichment cultures. This work is the topic of chapter four and was published in an article entitled “Fe Isotope Fractionation by Fe(II)-oxidizing Photoautotrophic Bacteria” in *Geochimica et Cosmochimica Acta*. We found that these bacteria produce Fe isotope fractionations of +1.5 ± 0.2‰ where the $^{56}Fe/^{54}Fe$ ratios of the ferric precipitate metabolic products are enriched in the heavier isotope relative to aqueous ferrous iron [$Fe(II)_{(aq)}$]. This fractionation was relatively constant at early stages of the reaction and apparently independent of the Fe(II)-oxidation rates investigated. Given that our measured fractionation is similar to that measured for dissimilatory Fe(III)-reducing bacteria and abiotic oxidation of $Fe(II)_{aq}$ to ferrihydrite by molecular

oxygen, yet significantly smaller than the abiotic equilibrium fractionation between aqueous $Fe(II)_{(aq)}$and Fe(III) [$Fe(III)_{(aq)}$], we proposed two mechanistic interpretations that are consistent with our data: (1) there is an equilibrium isotope fractionation effect mediated by free, biologically produced Fe ligands common to Fe(II)-oxidizing and Fe(III)-reducing biological systems, or (2) the measured fractionation results from a kinetic isotope fractionation effect, produced during the precipitation of Fe(III) to iron oxyhydroxide, overlain by equilibrium isotope exchange between $Fe(II)_{(aq)}$ and $Fe(III)_{(aq)}$ species. Investigations performed by Andreas Kappler concurrent with this work, however, provided no evidence for the involvement of free biological ligands [89]. Thus, although these bacteria do fractionate Fe isotopes in a way that is consistent with Fe isotopic values found in Precambrian BIFs [84], we currently favor an abiotic mechanism for our measured Fe isotope fractionation. In addition, recent work with *Acidithiobacillus ferrooxidans* provides conclusive evidence that the Fe isotope fractionation associated with Fe(II)-oxidizing metabolisms is reflective of abiotic processes [8].

Upon our discovery that Fe isotopes would not be useful in identifying the activity of Fe(II)-oxidizing phototrophs in the rock record, we endeavored to define the molecular mechanism of photoautotrophic Fe(II) oxidation so that novel biosignatures for this metabolism might be identified. The results of our genetic investigations are presented in chapter five where two approaches to identify genes involved in Fe(II) photoautotrophy in TIE-1 and SW2 are described. In the portion of this chapter related to *Rhodopseudomonas palustris*

TIE-1, we describe the results of a transposon mutagenesis screen to identify mutants of TIE-1 specifically defective in Fe(II)-oxidation. The isolation of this strain and this screen are the primary work of Yongqin Jiao, a graduate student in the lab, and this work will be published as an article entitled “Isolation and Characterization of a Genetically Tractable Photoautotrophic Fe(II)-oxidizing Bacterium, *Rhodopseudomonas palustris* strain TIE-1” in *Applied and Environmental Microbiology*. I, however, was a co-author on this paper, as I developed the assay used to screen for mutants defective in Fe(II) oxidation and contributed to the interpretation of the isolated mutants. From this work, we identified two types of mutants defective in Fe(II)-oxidation and the disrupted genes of these stains are predicted to encode an integral membrane protein that appears to be part of an ABC transport system and CobS, an enzyme involved in cobalamin (vitamin B_{12}) biosynthesis. This suggests that components of the Fe(II) oxidation system of this bacterium may reside at least momentarily in the periplasm and that a protein involved in Fe(II) oxidation may require cobalamin as cofactor. In the work done on SW2, a genomic cosmid library of this genetically intractable strain was heterologously expressed in *Rhodobacter capsulatus* SB1003 (1003), a strain unable to grow photoautotrophically on Fe(II) and four cosmids that conferred Fe(II)-oxidation activity to 1003 were identified. The insert of one of these cosmids was sequenced to ~78% completion and likely gene candidates inferred from the sequence include two genes encoding predicted permeases and a gene that encodes a protein that may have redox capability. Sequence data obtained for the portion of this work related to SW2 is

presented in Appendix 1 and follow up work that I will complete subsequent to my graduation is described.

In chapter six, we present our biochemical work initiated to identify proteins upregulated or expressed uniquely under Fe(II) phototrophic growth conditions in SW2 and TIE-1. Preliminary results suggest that *c*-type cytochromes and other proteins that are exclusive or more highly expressed under Fe(II) growth conditions are present in these two strains. Whether these proteins are involved in phototrophic Fe(II)-oxidation remains to be investigated, however, precedent exists for the involvement of *c*-type cytochromes in Fe(II) oxidizing respiratory processes [6, 38, 174, 177, 189].

Conclusions, the implications of this work and perspectives for future research are the subject of Chapter 7.

Ultimately, the work done here provides a basis for understanding the molecular mechanism of photoautotrophic Fe(II)-oxidation and it is my hope that further investigations of this metabolism will lead us to new targets for biosignature development.

2. Background

FINDING TRACES OF MICROBIAL METABOLISMS IN THE ROCK RECORD

Microbial metabolisms contribute to the maintenance of the hydro-, atmo-, and lithospheres on the Earth and have done so since they first evolved on this planet billions of years ago [98, 114, 126]. While determining the impact of microbes in modern environments is a tractable problem, given that the activities of these organisms can be monitored directly *in situ* or in pure culture [21, 115, 129, 135], investigating the impact microbes had on the chemistry of the environment billions of years ago presents a formidable challenge.

When the organisms are macroscopic, relationships between biology and the geochemical evolution of the Earth can be inferred from morphological fossils [100]. While this approach can also be applied to microorganisms, when considering the impact microbes have had during remote periods of Earth history (*e.g.,* the Archean, >2.5 Ga), the fossil record of these organisms becomes increasingly poor as the rocks we look at increase in age and even when microfossils are found, they can be highly controversial [23, 148]. Moreover, these fossils provide little evidence regarding the physiology of the organisms they represent.

An alternate, accepted approach to recognizing biological activity in the ancient rock record is to identify organic or inorganic signatures unique to extant

microbial metabolisms that are preserved in rocks through time (*i.e.,* biosignatures). When biosignatures indicative of a particular metabolism are identified, inferences regarding the impact the metabolism may have had on the environment can be made [31, 143, 153, 166, 171]. And while we can never know the extent to which modern metabolisms are good proxies for ancient ones, because we cannot study extinct organisms, the assumption that they are is accepted as a necessary one in this field [3].

It is important to note that, just like morphological fossils, biosignatures are subject to controversy and misinterpretation [121, 147, 175]. Thus, identifying robust biosignatures unique to a particular metabolism that cannot be confused with abiotic processes represents a true challenge. Nonetheless, the identification of such signatures is a necessary first step towards understanding how microbial metabolisms have influenced the chemistry of the Earth over time.

To make inferences about the cycling of elements on the ancient Earth, it is important to identify biosignatures of organisms that carry out an ancient form of metabolism. A particular metabolism that has had a profound impact on the chemical evolution of the Earth and that is believed be among the first metabolisms to have evolved is photosynthesis. The antiquity of the oxygenic form of this metabolism is supported by the finding of 2-methylhopane hydrocarbon derivatives of cyanobacterial membrane lipids in rocks as old as 2.7 Ga [25, 166].

Further, phylogenetic relationships between genes that are involved in bacteriochlorophyll and chlorophyll biosynthesis show that the anoxygenic form

of photosynthesis evolved before the oxygenic form [185]. If true, the evolution of anoxygenic photosynthesis would logically predate the evolution of respiratory metabolisms that are based on oxygen or other highly oxidized species (*i.e.,* nitrate) as well. Therefore, the metabolism of anoxygenic photoautotrophic bacteria is of primary interest in our considerations of the geochemical evolution of the Earth.

FE(II) OXIDATION BY PHOTOAUTOTROPHIC BACTERIA

Microbial Fe(II) oxidation is an important component of the Fe geochemical cycle [125, 158, 160]. In modern environments, microorganisms that are able to oxidize Fe(II) are ubiquitous, inhabiting and affecting a wide variety of environments where Fe(II) is present. These environments include: marine coastal sediments and brackish water lagoons [161, 163], sediments from freshwater creeks, ponds, lakes and ditches [68-70, 182], low pH environments associated with acid mine waters [39, 50], groundwater springs [54], sediments and the rhizosphere of plants from freshwater wetlands [56, 157], the seafloor near active hydrothermal fields [51, 55], and swine waste lagoons [34].

Microorganisms that are able to oxidize Fe(II) are diverse in their phylogeny and overall physiology (Table 2-1). Representative examples of bacteria and archaea capable of coupling Fe(II) oxidation to growth include psychro-, hyperthermo- and mesophiles that couple Fe(II) oxidation to the reduction of nitrate at neutral pH [14, 162], or to the reduction of oxygen at either

low [50, 169], or neutral pH [54], and the anaerobic Fe(II)-oxidizing phototrophs [52, 70, 182].

Table 2-1: Metabolisms where Fe(II) is the electron donor and the genes that have been implicated in these processes.

Metabolism	Reaction	Genes
Acidophilic iron oxidation	$4Fe^{2+} + 4H^{+} + O_2 \rightarrow 4Fe^{3+} + 2H_2O$	*iro, cyc1, cyc2, coxA,B,C,D, rus*
Phototrophic iron oxidation	$4\ Fe^{2+} + HCO_3^{-} + 10H_2O \rightarrow 4\ Fe(OH)_3 + (CH_2O) + 7H^{+}$	None known
Neutrophilic iron oxidation	$4Fe^{2+} + 10H_2O + O_2 \rightarrow 4Fe(OH)_3 + 8H^{+}$	None known
Nitrate-dependent iron oxidation	$10\ Fe^{2+} + 2\ NO_3^{-} + 24\ H_2O \rightarrow 10\ Fe(OH)_3 + N_2 + 18H^{+}$	None known

The use of Fe(II) as an electron donor likely arose early in Earth history given the abundant availability of Fe(II) in the ancient oceans, relative to today [57, 72, 184] and of the organisms able to grow on Fe(II), it is thought that the anoxygenic phototrophs are the most ancient [20, 41, 185]. Thus, in addition to contributing to Fe cycling in modern environments, Fe(II)-oxidizing bacteria have likely affected the Fe cycle over geological time. Indeed, both direct photoautotrophic Fe(II) oxidation and indirect Fe(II) oxidation mediated by cyanobacteria [37] have been proposed as being responsible for the deposition of Banded Iron Formations as discussed in the introduction [67, 101, 182]. To distinguish these two biological processes from each other, as well as from other

proposed abiotic mechanisms of Fe(II) oxidation, biosignatures that uniquely represent the activity of Fe(II)-oxidizing organisms must be identified. An informed search for such biosignatures and their rigorous interpretation requires a detailed understanding of the mechanism and products of Fe(II) photoautotrophy. To date, very little is known about the mechanism of this metabolism. Therefore, our studies have been focused on elucidating the molecular basis of Fe(II) oxidation by these bacteria.

MECHANISMS OF FE(II) OXIDATION BY ACIDITHIOBACILLUS FERROOXIDANS

Although little is known about Fe(II) oxidation in phototrophic bacteria at the mechanistic level, a substantial body of knowledge concerning the mechanism of this metabolism exists for the acidophilic, Fe(II)-oxidizing organism, *Acidithiobacillus ferrooxidans*. Members of this species are gram-negative, mesophilic, obligately autotrophic and acidophilic bacteria capable of aerobic respiration on Fe(II) and reduced forms of sulfur (H_2S, S^o, $S_2O_3^{2-}$) [53, 139]. Because they can grow chemolithoautotrophically on sulfide ores, these bacteria are able to solubilize a variety of valuable metals such as copper, uranium, cobalt, and gold that are embedded within the ores [138]. Given this property, understanding the metabolism of these bacteria is particularly interesting to industries wishing to use this strain (or genetically modified derivatives) for leaching purposes [7, 137, 183].

Most of what is known about Fe(II) oxidation by *A. ferrooxidans* stems from biochemical studies, yet how the different components of the electron transport pathway (Figure 2-1) work together is uncertain and controversial [7, 19, 77, 186]. Comparatively little is known about the genetics of Fe(II) oxidation in *A. ferrooxidans* as genetic analysis has been constrained by the culturing requirements for this organism. For example, a number of antibiotics are inhibited by low pH and high Fe(II) concentrations [183], resulting in a dearth of suitable selective markers. To circumvent this problem, toxic metal resistance genes have been used as selective markers, but only with limited success [103]. Additionally, while some of the standard tools required for genetic studies (*e.g.,* appropriate shuttle vectors and transformation methods) have been developed and/or optimized for various strains of *A. ferrooxidans* [103, 130, 138], until recently [109], these methods have not been used for the construction of mutants. Consequently, no defined mutants defective in Fe(II) oxidation exist, although spontaneous mutants that have lost the ability to oxidize Fe(II) have been identified [149]. The recent report of the construction of a *recA* mutant of *A. ferrooxidans* strain ATCC 33020 via marker exchange mutagenesis represents a step towards improved genetic analysis of this strain [109].

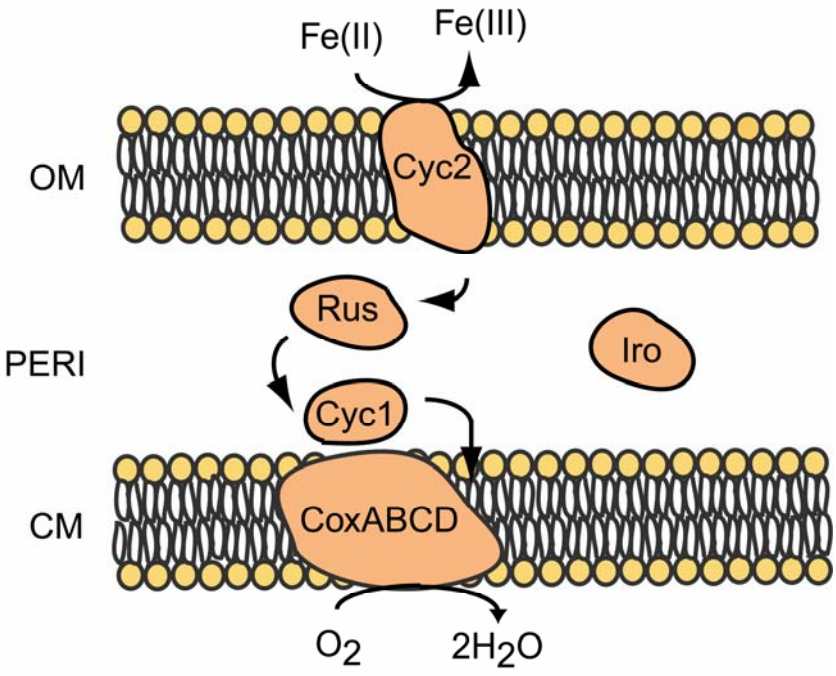

Figure 2-1: Cartoon representation of the components implicated in electron transfer for Fe(II) oxidation by *Acidithiobacillus ferrooxidans* strain ATCC 33020. The product of the *iro* gene is not thought to play a role in this strain, but may in others.

Despite these limitations, several genes thought to be involved in Fe(II) oxidation are known. The majority have been identified using degenerate primers derived from N-terminal sequences of purified proteins. The first of these genes to be identified using reverse genetics was the *iro* gene of *A. ferrooxidans* strain Fe1. This gene encodes a high potential Fe-S protein that is homologous to the soluble ferredoxins commonly found in purple photosynthetic bacteria. Additionally, Northern blot and RNA primer extension analyses suggest that this gene is transcribed on its own, but expression studies under different growth conditions have not yet been conducted [104]. Because of its high redox

potential, Fe(II)-cytochrome *c*-552 oxidoreductase activity and acid stability *in vitro,* it has been proposed that the product of this gene catalyzes the first step in the transfer of electrons from Fe(II) to O_2 [63, 104, 187]. However, this does not appear to be the case for all strains of *A. ferrooxidans* [7] and genetic evidence to support this function in *A. ferrooxidans* Fe1 does not exist.

A second gene thought to encode a protein involved in Fe(II)-oxidation by *A. ferrooxidans* is the *rus* gene. Again, using reverse genetics, the *rus* gene was cloned from *A. ferrooxidans* ATCC 33020 [13, 66]. This gene encodes the small type 1 blue copper protein, rusticyanin; a protein that has received much attention in biochemical studies given that it represents up to 5% of the total soluble protein of *A. ferrooxidans* cells when grown on Fe(II), displays a high degree of acid tolerance and has a high redox potential [40, 76]. In the region upstream of the *rus* gene, a sequence similar to a rho-independent terminator and two potential *Escherichia coli*-like, σ^{70}-specific promoter sequences are present. Downstream of the gene are two putative stem loop structures, one of which is followed by a T rich region. This suggests that the *rus* gene can be transcribed from its own promoter [13]. Further investigations of *rus* gene transcription by Northern, RT-PCR and primer extension analyses have shown that this gene is part of an operon comprising eight genes, of which *rus* is the last [7, 13]. Putative promoters in this operon have been identified both by sequence and primer extension analyses. Primer analysis with RNA extracted from cells grown on sulfur or Fe(II) indicates that two promoters upstream of *cyc2* and one promoter upstream of *rus* are active in cells grown on sulfur whereas only one of

the promoters upstream of *cyc2* is active in Fe(II)-grown cells [7]. Additionally, while it has been observed that the *rus* transcript is present in both Fe(II) and sulfur grown cells, it is more abundant in Fe(II)-grown cells and present throughout all growth phases (in contrast to sulfur-grown cells, where it appears only in exponential phase) [188, 191].

Since the discovery that *rus* is co-transcribed with several other genes in an operon (Figure 2-2), the genes in this operon have been analyzed [6, 7, 190]. Strikingly, seven of the eight genes in this operon appear to encode redox proteins. The *cyc2* gene encodes a high molecular weight, outer membrane, *c*-type cytochrome [6, 190] while *cyc1* encodes a c_4-type cytochrome with a signal peptide sequence indicative of translocation to the periplasm [6]. *coxB*, *coxA,* and *coxC* encode proteins with homology to subunits II, I, and III, respectively, of an aa_3-type cytochrome *c* oxidase. The protein encoded by *coxD* shares similarity with nothing in the database, however, given the position of this gene relative to the other *cox* gene homologs and what is known about the organization of these genes in other organisms, it was assumed that *coxD* represents subunit IV of an aa_3-type cytochrome *c* oxidase [7]. Lastly, ORF1 encodes a putative protein of unknown function with a terminal signal sequence suggesting that it is translocated to the periplasm. Given that biochemical studies have implicated proteins of these types in Fe(II) oxidation [17, 38, 40, 63, 76, 174, 177], it is assumed that the products of this operon are involved in the Fe(II) respiratory pathway of this organism (Figure 2-1) [7].

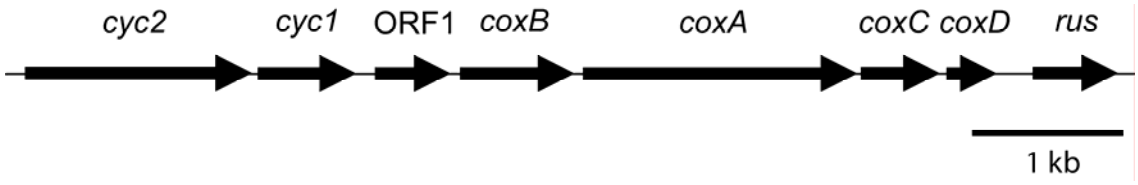

Figure 2-2: Genes proposed to encode the components of Fe(II) oxidation in *Acidithiobacillus ferrooxidans* strain ATCC 33020.

3. Fe(II) photoautotrophy under a H_2 atmosphere: implications for Banded Iron Formations

ABSTRACT

Both H_2 and Fe(II) can serve as electron donors for anoxygenic photosynthesis and are predicted to have been present in the atmosphere and ocean of the Archean in quantities sufficient for energy metabolism. If H_2, given its more favorable redox potential, is the preferred substrate for anoxygenic phototrophs, this may preclude the involvement of phototrophs capable of Fe(II) photoautotrophy in Banded Iron Formation (BIF) deposition. Here we investigate the effect of H_2 on Fe(II) oxidation by cell suspensions of two strains of Fe(II)-oxidizing purple non-sulfur bacteria. We find that Fe(II) oxidation still proceeds under an atmosphere containing ~3 times the maximum predicted concentration of H_2 in the Archean when CO_2 is abundant. Additionally, the amount of H_2 dissolved in a 100 m photic zone of Archean ocean over an area equivalent to the Hamersley basin may have been less than 0.24 ppm. Therefore, H_2 would pose no barrier to Fe(II) oxidation by ancient anoxygenic phototrophs at depth in the photic zone and would not have precluded the involvement of these bacteria in BIF deposition.

INTRODUCTION

Recent debates in the literature have called into question the idea that evidence for the earliest life in the rock record can be inferred from morphology [23, 148] or chemical composition alone [59, 107, 121]. The value of a search strategy that considers not only morphology and chemical analyses (*e.g.,* isotopic compositions or REE (rare earth element) analyses), but also the ecophysiological context of the fossils in question is becoming increasingly appreciated. An illustration of the power of such a search strategy comes from a recent analysis of the carbonaceous laminations preserved in the shallow water facies of the 3.4 billion year old (Ga) Buck Reef Chert in South Africa [171]. In this work, a synthesis of data from the morphology of the mats as well as sedimentological, petrographic and geochemical investigations allowed for a reconstruction of the environmental setting in which these mat structures were found. This ecological reconstruction enabled the authors to convincingly argue that the mats found in this chert were formed in a euphotic zone that was anoxic, and conclude that the organisms that formed the mats were likely anoxygenic phototrophs, rather than oxygenic.

Further, the authors found a lack of ferric oxide or ferrous sulfide minerals present in the depositional environment of these mats. H_2, however, is thought to have been present in the Archean atmosphere at concentrations between 1000 and 300,000 ppm as a result of volcanic emissions and atmospheric photochemistry [33, 90, 170]. Given the paucity of possible electron donors for photosynthesis in the depositional environment of this ancient mat, Tice and

Lowe deduced that these anoxygenic phototrophs likely used H_2 as their electron donor for carbon fixation, rather than Fe(II) or S^{2-} and thus, H_2-based photoautotrophy was the active metabolism in this environment [111].

In ancient environments where the chemistry is more complex, however, can the dominant active physiologies still be inferred? To address such questions, knowledge concerning the molecular mechanisms of how a particular physiology of interest is regulated must be taken into account. For example, it has been suggested that anoxygenic photoautotrophs able to use ferrous iron [Fe(II)] as an electron donor for photosynthesis were involved in the deposition of the Banded Iron Formations (BIFs) that appear in the rock record prior to the advent of atmospheric O_2 [67, 101, 182]. This model assumes that these bacteria used Fe(II) as an electron donor for photosynthesis; however, if the atmosphere of the early Earth contained quantities of H_2 sufficient to support H_2-based photoautotrophy, would H_2, given its more favorable redox potential [113], be preferred over Fe(II)? If so, would this diminish the likelihood that these bacteria were involved in BIF deposition in certain environments? Coupling an understanding how Fe(II) based photoautotrophy is regulated with biogeochemical/ecological reconstructions of environmental setting can help refine models that consider whether these phototrophs could have catalyzed BIF deposition.

A key assumption that we must make to integrate such physiological and geological information, however, is that the activities of modern organisms are representative and comparable to those of ancient organisms and this

assumption is accepted as a necessary one in this field [3]. Recent studies of the isotopic record of sedimentary sulfides where such assumptions were made have given new insights into when microbial sulfate reduction evolved and the concentrations of sulfate and O_2 in the early Archean ocean and atmosphere [31, 153]. In addition, carbon isotopic studies have revealed traces of autotrophy in the rock record [99, 142, 143]

Here, making the assumption that Fe(II) phototrophy is an ancient metabolism [41] and that extant organisms capable of this metabolism are representative of their ancient relatives, we investigate the effects of H_2 on the Fe(II) oxidation activity of two strains of Fe(II)-oxidizing purple non-sulfur anoxygenic phototrophs and show that Fe(II) oxidation can occur in the presence of H_2 under conditions broadly similar to an Archean ocean.

EXPERIMENTAL PROCEDURES

Organisms and Cultivation

Rhodobacter sp. strain SW2 (SW2) was a gift from F. Widdel (MPI, Bremen, Germany) and *Rhodopseudomonas palustris* strain TIE-1 (TIE-1) was isolated in our lab [83]. Cultures were maintained in a previously described anoxic minimal salts medium for freshwater cultures [52] and were incubated 20 to 30 cm from a 34 W tungsten, incandescent light source at 30°C for TIE-1 and 16°C for SW2. Electron donors for photosynthetic growth were added to the basal medium as follows: thiosulfate was added from an anoxic filter sterilized stock to a final concentration of 10 mM and H_2 was provided as a headspace of

80% H_2: 20% CO_2. For growth on Fe(II), 4 mls of a filter sterilized, anoxic 1 M Fe(II)$Cl_2 \cdot H_2O$ stock solution was added per 1 liter (L) of anaerobic, basal medium (final concentration ~4 mM). To avoid the precipitation of ferrous Fe minerals that results upon addition of Fe(II)$Cl_2 \cdot H_2O$ to the bicarbonate buffered basal medium and the precipitation of ferric Fe minerals that form during the growth of these bacteria on Fe, the metal chelator, nitrilotriacetic acid (NTA, disodium salt from Sigma), was supplied from a 1 M filter sterilized stock solution to a final concentration of 10 mM. This NTA addition greatly facilitated the harvesting of cells, free of Fe minerals, from Fe(II) grown cultures.

Cell suspension assays

All cell suspension assays were prepared under anoxic conditions in an anaerobic chamber (Coy Laboratory Products, Grasslake, MI) to minimize exposure of the cells to oxygen. Cells of SW2 or TIE1 grown on H_2, thiosulfate, or Fe(II)-NTA were harvested in exponential phase (OD_{600} ~0.15 to 0.18) by centrifugation (10,000 rpm on a Beckman JLA 10.5 rotor for 20 min). Pellets were washed once with an equal volume of 50 mM Hepes buffer containing 20 mM NaCl at pH 7 (assay buffer) to remove residual medium components and resuspended in assay buffer containing the appropriate amount of $NaHCO_3$ and Fe(II)$Cl_2 \cdot H_2O$ to a final OD_{600} of 0.1. Resuspending the cells to the same final OD_{600} ensured that the assays were normalized to cell number, as verified by cell counts using a Petroff-Hauser counting chamber. Concentrations of $NaHCO_3$ were 1 or 20 mM and concentrations of Fe(II) were 0.5, 1 or 2 mM. When

appropriate, the protein synthesis inhibiting antibiotic, gentamicin, was added to a final concentration of 0.1, 0.2, 0.5, 1, 2, 4 mg/ml. Unless otherwise stated, assay volumes were 3 mls and cell suspensions of TIE1 and SW2 were incubated at 30°C and 16°C, respectively, in 12 ml stoppered serum bottles at 30 cm from a 34 W tungsten incandescent light bulb. The headspace of the assay bottles contained either 80% N_2:20% CO_2 or 80% H_2:20% CO_2 depending on the particular experiment (see results and figure legends for specific details).

Analytical methods

Fe(II) and Fe(III) concentrations were measured in triplicate by the *Ferrozine* assay [159]. 10 µl of cell suspension was added to 90 µl of 1 N HCL to which 100 µl of *Ferrozine* solution (1 g of *Ferrozine* plus 500 g of ammonia acetate in 1 L of ddH_2O) was added. After 10 minutes, the absorbance at 570 nm was read and the concentration of Fe(II) was determined by comparison to Fe(I) standards. To measure hydrogenase activity, benzyl viologen (Sigma) was added to the assay to a final concentration of 5 mM and the reduction of benzyl viologen was measured at 570 nm in duplicate samples. The program MINEQL$^+$ (Environmental Research Software; http://www.mineql.com/homepage.html) was used to calculate the concentrations of the various Fe(II) and NTA species in the phototrophic minimal salts medium (pH 6.8) when 4 mM Fe(II)$Cl_2 \cdot H_2O$ and 20 mM NTA were added. A closed system was assumed, the ionic strength of the solution was not considered, the temperature was set at 25°C and component concentrations were: H_2O, $1*10^0$; H^+, $1.58*10^{-7}$; Ca^{2+}, $3.69*10^{-6}$; Cl^-, $6.97*10^{-3}$;

CO_3^{2-}, 4.79*10^{-6}; Fe^{2+}, 5.73*10^{-8}; K^+, 3.55*10^{-3}; Mg^{2+}, 1.27*10^{-4}; NH_4^+, 5.47*10^{-3}; SO_4^{2-}, 1.81*10^{-3}; $EDTA^{-4}$, 1.36*10^{-14}; NTA^{-3}, 4.5*10^{-6}.

RESULTS AND DISCUSSION

Effects of NTA

The products of Fe(II) oxidation by TIE-1 and SW2 are poorly crystalline ferric (hydr)oxide precipitates [41, 89]. These precipitates greatly hinder our ability to harvest cells for physiological studies. To prevent the precipitation of ferric phases in our cultures, we added varying concentrations of the chelator NTA to our growth medium containing Fe(II) and found that a concentration of at least 10 mM NTA was necessary to keep Fe(III) in solution for both cultures. As has been observed before for the Fe(II)-oxidizing phototrophic strain, *Rhodomicrobium vannielli* [70], the addition of NTA accelerated the rate of Fe(II) oxidation. For TIE-1, the addition of 7.5, 15, and 20 mM NTA increased the Fe(II) oxidation rate approximately 44, 52 and 55%, respectively, and for SW2, the rate increased approximately 22% upon addition of 7.5 or 10 mM of NTA (Figure 3-1A and 1B). The acceleration of Fe(II) oxidation does not result from stimulation of growth by the addition of this organic compound, as control experiments showed that neither TIE-1 nor SW2 could grow on NTA alone (data not shown). In some Fe(II)-oxidizing phototrophs, the ferric precipitate products of this form of metabolism completely encrust the cells and impede further oxidation [70]. While such severe consequences of ferric precipitation are not evident with TIE-1 or SW2, it is possible that the deposition of these precipitates

at the surface of the cell does have inhibitory effects of the rate of Fe(II) oxidation. Given this, an alternative explanation for the increased rate of Fe(II) oxidation upon addition of NTA may be that solubilization of the ferric precipitates alleviates product inhibition of this metabolism by these precipitates.

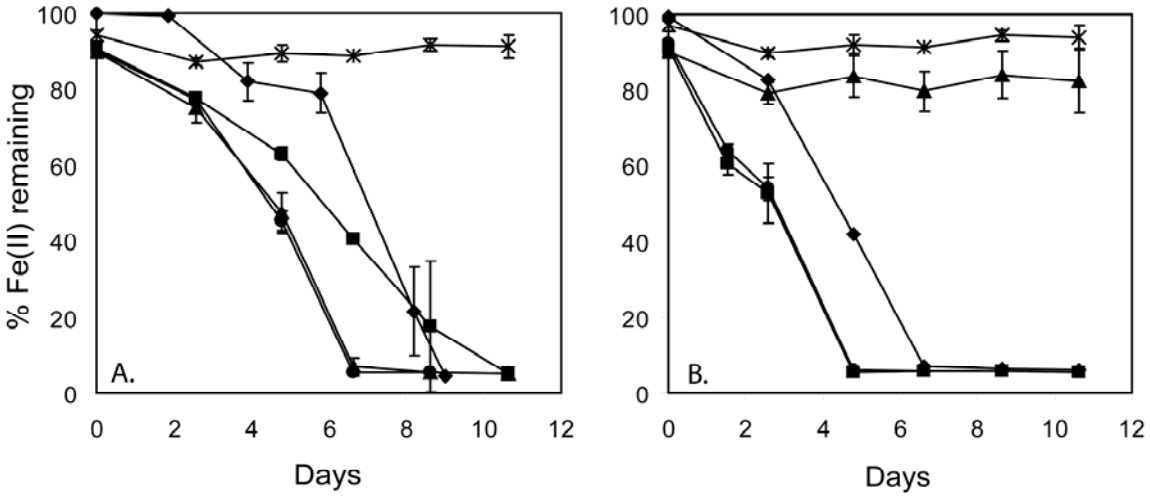

Figure 3-1: Growth of TIE-1 and SW2 on 4 mM Fe(II)$Cl_2 \cdot H_2O$ + varying concentrations of NTA. A. Data for TIE-1: ♦ - 0 mM NTA, ■ - 7.5 mM NTA, ▲ - 15 mM NTA, ● - 20 mM NTA, ✳ - Abiotic + 20 mM NTA. B. Data for SW2: ♦ - 0 mM NTA, ■ - 7.5 mM NTA, ● - 10 mM NTA, ▲ - 15 mM NTA, ✳ - Abiotic + 20 mM NTA. No growth was observed in cultures of TIE-1 or SW2 where only NTA and no Fe(II) was added, indicating that these strains cannot use NTA as a substrate for growth. The lower concentration of Fe(II) at time 0 in the cultures where NTA has been added as compared to the cultures with no NTA addition indicates there is a pool of Fe(II) we cannot measure with the *Ferrozine* assay. Error bars represent the error on duplicate cultures.

The concentration of NTA tolerated by the two strains differed. TIE-1 could tolerate up to 20 mM NTA (higher concentrations were not tested) (Figure 3-1A) whereas concentrations higher the 10 mM were inhibitory for SW2 (Figure 3-1B). MINEQL^{+} modeling of the chemical speciation of the medium shows that upon initial addition of 4 mM Fe(II)$Cl_2 \cdot H_2O$ to medium containing 5-20 mM NTA, 99.8% of the total Fe(II) is present as the Fe[NTA] species (Figure 3-2A and 2B and Table 3-1 and 2 for 20 mM NTA). It is, therefore, unlikely that the increased resistance of TIE-1 to NTA, relative to SW2, results from the production of Fe(II) chelators by this strain, because the Fe-NTA speciation remains the same within our tested NTA concentration span. Rather, it may result from a more general mechanism, related perhaps to differences in cell wall permeability or the efficiency/number of generalized solute efflux pumps. This later hypothesis would be consistent with the observation that TIE-1 is resistant to a greater concentration of the antibiotics kanamycin, gentamicin, tetracycline and chloramphenicol (the mechanisms of resistance of the latter two being via efflux) than most purple non-sulfur bacteria on solid and liquid media [83].

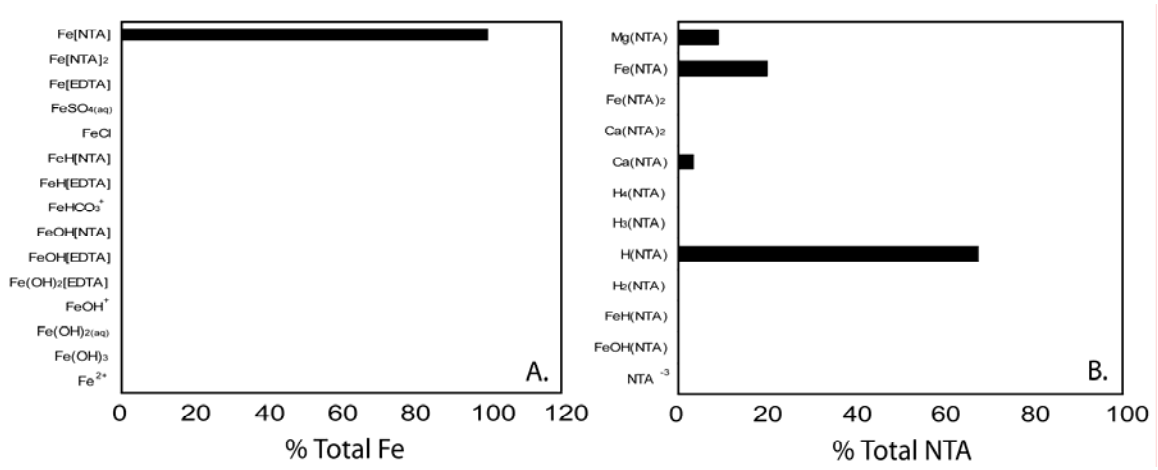

Figure 3-2: Concentrations of A. Fe(II) and B. NTA species in the phototrophic basal medium (pH 6.8). Concentrations are represented as % of total Fe(II) (4 mM $Fe(II)Cl_2 \cdot H_2O$) and NTA (20 mM Na_2NTA) as calculated with MINEQL$^+$. See text for model parameters.

Table 3-1: Molar concentrations the NTA species in the phototrophic basal medium with 4 mM $Fe(II)Cl_2 \cdot H_2O$ and 20 mM NTA at pH 6.8, as calculated with MINEQL$^+$.

NTA species	Molar concentration
FeOH(NTA)	4.50E-06
FeH(NTA)	1.41E-07
H_2(NTA)	7.96E-08
H(NTA)	1.87E-06
H_3(NTA)	1.35E-02
H_4(NTA)	2.97E-11
Ca(NTA)	4.70E-17
$Ca(NTA)_2$	6.73E-04
$Fe(NTA)_2$	4.82E-08
Fe(NTA)	4.82E-06
Mg(NTA)	3.99E-03
Total NTA	2.00E-02

Table 3-2: Molar concentrations of the Fe(II) species in the phototrophic basal medium with 4 mM Fe(II)$Cl_2 \cdot H_2O$ and 20 mM NTA at pH 6.8, as calculated with MINEQL$^+$.

Fe(II) species	Molar concentration
Fe^{2+}	5.73E-08
$Fe(OH)_3$	1.47E-16
$Fe(OH)_{2(aq)}$	7.31E-15
$FeOH^+$	1.45E-10
$Fe(OH)_2$ [EDTA]	3.10E-12
FeOH[EDTA]	1.55E-08
FeOH[NTA]	1.41E-07
$FeHCO_3^+$	1.17E-08
FeH[EDTA]	1.42E-09
FeH[NTA]	7.96E-08
FeCl	2.52E-10
$FeSO_{4(aq)}$	2.54E-08
Fe[EDTA]	7.79E-06
$Fe[NTA]_2$	4.82E-06
Fe[NTA]	3.99E-03
Total Fe(II)	4.00E-03

Fe(II) oxidation under a H_2 atmosphere

A general assumption in bacterial physiology is that electron donors that yield the most energy for growth will be preferred over those that yield less. Thus, in a bicarbonate containing system where the relevant Fe couple, $Fe(OH)_3$ + $HCO_3^-/FeCO_3$, has a redox potential of +0.2 V [52], H_2, with the redox potential of the relevant couple, $2H^+/H_2$, being -0.41 V [113], is expected to be preferred as a source of electrons for growth over Fe(II). This implies that in an environment where H_2 and Fe(II) co-exist, photoautotrophic Fe(II) oxidation may not be a relevant physiology to consider.

Interested in whether the availability of H_2 as an electron donor might inhibit Fe(II) oxidation by ancient relatives of TIE-1 and SW2, we investigated the effects of H_2 on the Fe(II) oxidation activity of these two strains in cell suspension assays where the concentrations of Fe(II), $NaHCO_3$ and H_2 were comparable to those predicted for an ancient Archean ocean. Namely, our initial Fe(II) concentration of ~0.4 to 0.45 mM is within the range of 0.054 to 0.54 mM predicted by Holland and Ewers [57, 72], our $NaHCO_3$ concentration of 20 mM is on the same order as the 70 mM predicted for an Archean ocean and an order of magnitude higher than the present day concentration of 2 mM [65], and our H_2 concentration of 800,000 ppm is also on the same order as the recently proposed concentration in the early atmosphere of 300,000 ppm [170].

In our experiments containing 1 mM $NaHCO_3$, in the absence of H_2, we observed initial rates of Fe(II) oxidation for TIE-1 and SW2 of 0.07 mM/hr and 0.15 mM/hr, respectively (Figure 3-3A and 3B, Table 3-3). Under the same low $NaHCO_3$ conditions, in the presence of H_2, the rate of Fe(II) oxidation by TIE-1 decreased by 44% as compared to the absence of H_2 (Figure 3-3A, Table 3-3). SW2, however, showed a much more dramatic inhibition by H_2 under low $NaHCO_3$ conditions. Here, the rate of Fe(II) oxidation decreased to 0.03 mM/hr during the first 5 hours (78% of the rate in the absence of H_2) and further decreased to 0.01 (on average) thereafter, resulting in only 22% of the total Fe(II) being oxidized within the 10 hour course of the experiment (Figure 3-3B, Table 3-3).

Under 20 mM $NaHCO_3$, however, while the rates of Fe(II) oxidation in the presence of H_2 decreased for the two strains, we did not observe such dramatic decreases, as compared to the 1 mM $NaHCO_3$ conditions. For TIE-1, in the presence of H_2 the initial rate of Fe(II) oxidation decreased 26% as compared to the rate of oxidation in absence of H_2 (Figure 3-3A, Table 3-3). For SW2 the initial rate of Fe(II) oxidation decreased 39% when H_2 is present (Figure 3-3B, Table 3-3). Regardless of the slight decreases in Fe(II) oxidation rate in the presence of H_2, however, for SW2, all of the Fe(II) is oxidized to completion within 2 hours and for TIE-1, after 8 hours, the same amount of Fe(II) is oxidized as in the absence of H_2 (Figure 3-3A and 3B).

These results indicate that Fe(II) oxidation by some anoxygenic phototrophs may be severely inhibited by the presence of H_2 in modern environments where the concentration of $NaHCO_3$ is low (2 mM). However, if the concentration of $NaHCO_3$ is high (*i.e.*, at least 20 mM), as is assumed to be the case in an Archean ocean, even in the presence of H_2, Fe(II) oxidation by these phototrophs could still have proceeded at appreciable, although slightly reduced, rates. Further, these results demonstrate that the utilization of substrates may change under different conditions and the co-utilization of substrates during anoxygenic photosynthesis is possible. Substrate preference must, therefore, be experimentally demonstrated under the particular conditions of interest.

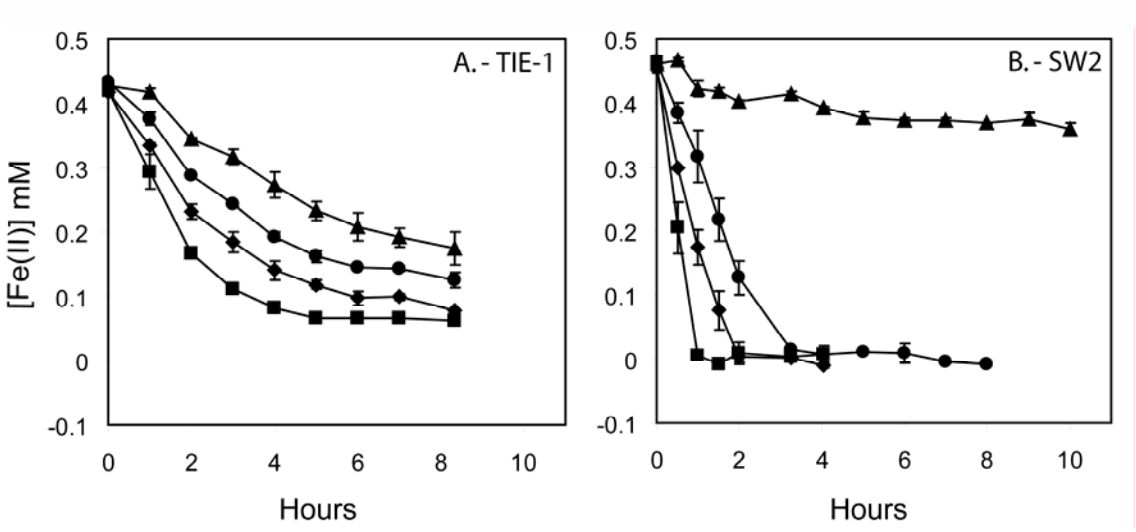

Figure 3-3: H_2 inhibits the Fe(II) oxidation activity of both TIE-1 and SW2 to varying degrees depending on the concentration of $NaHCO_3$. A. Data for TIE-1: ▲ - H_2 + 1 mM $NaHCO_3$ + 0.5 mM $FeCl_2 \cdot H_2O$; ● - N_2 + 1 mM $NaHCO_3$ + 0.5 mM $FeCl_2 \cdot H_2O$; ♦ - H_2 + 20 mM $NaHCO_3$ + 0.5 mM $FeCl_2 \cdot H_2O$; ■ - N_2 + 20 mM $NaHCO_3$ + 0.5 mM $FeCl_2 \cdot H_2O$. B. Data for SW2: ▲ - H_2 + 1 mM $NaHCO_3$ + 0.5 mM $FeCl_2 \cdot H_2O$; ● - N_2 + 1 mM $NaHCO_3$ + 0.5 mM $FeCl_2 \cdot H_2O$; ♦ - H_2 + 20 mM $NaHCO_3$ + 0.5 mM $FeCl_2 \cdot H_2O$; ■ - N_2 + 20 mM $NaHCO_3$ + 0.5 mM $FeCl_2 \cdot H_2O$. Data are representative of at least two independent experiments. The volume of the assay was 1 ml and the assay bottles were shook vigorously to ensure maximal H_2 saturation of the cell suspension solution. Error bars represent the error on duplicate cell suspension assays for TIE-1 and triplicate assays for SW2.

Table 3-3: Rates of Fe(II) oxidation by cell suspensions of TIE-1 and SW2. The rate of Fe(II) oxidation for the TIE-1 + H_2/CO_2 + 1 mM $NaHCO_3$ + 0.5 mM Fe(II)$Cl_2 \cdot H_2O$ assay was calculated using the first four time points, all others were calculated using the first three time points. The rate of Fe(II) oxidation for the SW2 + H_2/CO_2 + 1 mM $NaHCO_3$ + 0.5 mM $FeCl_2 \cdot H_2O$ assay was calculated using the first five time points, all others were calculated using the first three time points.

Assay Condition	mM Fe(II) oxidized/hour	R^2	% decrease in rate relative to no H_2 conditions
TIE-1 + H_2/CO_2 + 1 mM $NaHCO_3$ + 0.5 mM $FeCl_2 \cdot H_2O$	0.04	0.93	44
TIE-1 - N_2/CO_2 + 1 mM $NaHCO_3$ + 0.5 mM $FeCl_2 \cdot H_2O$	0.07	0.99	
TIE-1 + H_2/CO_2 + 20 mM $NaHCO_3$ + 0.5 mM $FeCl_2 \cdot H_2O$	0.09	1	26
TIE-1 - N_2/CO_2 + 20 mM $NaHCO_3$ + 0.5 mM $FeCl_2 \cdot H_2O$	0.13	1	
SW2 - H_2/CO_2 + 1 mM $NaHCO_3$ + 0.5 mM $FeCl_2 \cdot H_2O$	0.03 – first 2 hours 0.01 – 2 to 10 hours	0.86 0.71	78
SW2 - N_2/CO_2 + 1 mM $NaHCO_3$ + 0.5 mM $FeCl_2 \cdot H_2O$	0.15	1	
SW2 + H_2/CO_2 + 20 mM $NaHCO_3$ + 0.5 mM $FeCl_2 \cdot H_2O$	0.28	1	39
SW2 - N_2/CO_2 + 20 mM $NaHCO_3$ + 0.5 mM $FeCl_2 \cdot H_2O$	0.45	1	

Inferences on the mechanism of Fe(II) oxidation inhibition by H_2

The molecular mechanism by which H_2 inhibits Fe(II) oxidation is not understood. Cell suspensions of TIE-1 and SW2 cells incubated in the dark show that all the Fe(II) oxidation activity observed in H_2 pre-grown cells is light dependent (Figure 3-4).

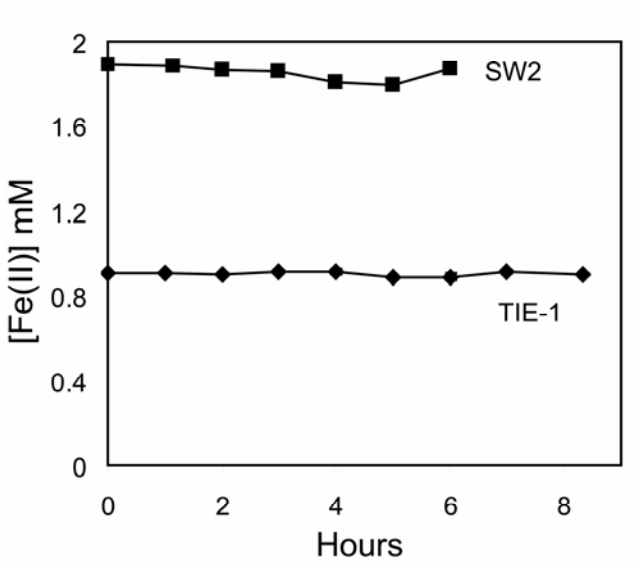

Figure 3-4: The Fe(II) oxidation activity of cell suspensions of TIE-1 and SW2 is completely light dependent. ♦ - H_2 pre-grown TIE-1 cells + N_2 + 20 mM $NaHCO_3$ + 1 mM $FeCl_2 \cdot H_2O$, incubated in the dark. ■ - H_2 pre-grown SW2 cells + N_2 + 20 mM $NaHCO_3$ + 2 mM $FeCl_2 \cdot H_2O$, incubated in the dark.

This implies that electron flow from Fe(II) is specific to the photosynthetic electron transport system. If the same is true for electrons derived from H_2, there exist a number of possibilities by which H_2 might inhibit Fe(II) oxidation. These possibilities include: 1) Hydrogenase, the enzyme that oxidizes H_2, delivering the

electrons to the photosynthetic electron transport chain at the level of the quinone pool [178], is the same enzyme that oxidizes Fe(II) and this enzyme has a higher affinity or faster rate of reaction with H_2 than Fe(II). If the enzyme that oxidizes Fe(II) (Fe oxidase) is not the hydrogenase enzyme, 2) H_2 may inhibit the expression of the Fe(II) oxidase, 3) H_2 may directly inhibit the Fe(II) oxidase itself, or 4) hydrogenase is active in these cells and is effectively out-competing the Fe(II) oxidase to donate electrons to the photosynthetic electron transport chain.

Although the formal possibility exists that the Fe(II) oxidase and the hydrogenase are the same enzyme, this seems highly unlikely given the very different redox potentials and molecular structures of these substrates. Moreover, there is no precedent in the literature for a hydrogenase with Fe(II) oxidation activity. In addition, if the hydrogenase enzyme catalyzes Fe(II) oxidation, cells pre-grown on H_2 would be expected to have greater Fe(II) oxidation activity than cells pre-grown on thiosulfate, as less hydrogenase would be expressed when H_2 is not present to induce its expression [178]. Cells pre-grown on thiosulfate, however, show a rate of Fe(II) oxidation equivalent to cells pre-grown on H_2 (Figure 3-5).

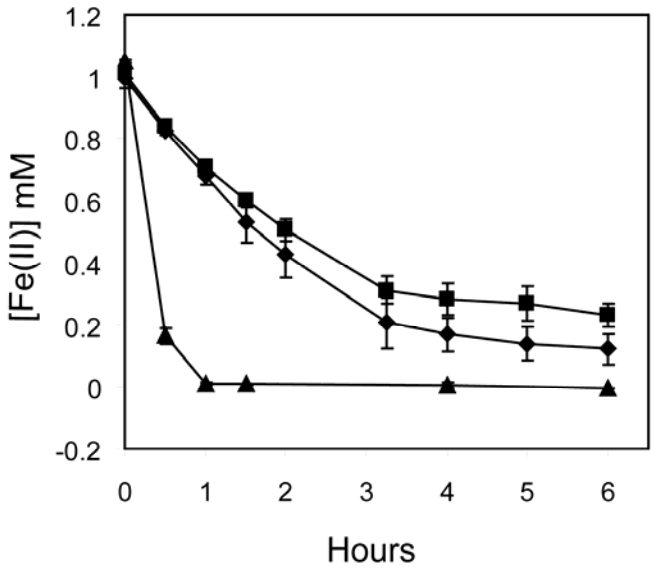

Figure 3-5: Fe(II) oxidation activity of cell suspensions of TIE-1 pre-grown photoautotrophically on different inorganic electron donors. ■ - TIE-1 pre-grown on 10 mM thiosulfate, ♦ - TIE-1 pre-grown on H_2, ▲ - TIE-1 pre-grown on 4 mM $FeCl_2 \cdot H_2O$ + 10 mM NTA. Cells used in this assay were normalized for cell number and the error bars represent the error on triplicate cell suspension assays.

Interestingly, cells pre-grown on Fe(II)-NTA show a greater rate of Fe(II) oxidation than those pre-grown on thiosulfate or H_2 (Figure 3-5). This shows that components necessary for Fe(II) oxidation are expressed to varying degrees under different conditions and implies that their expression is inducible. Further, evidence for the inducible nature of this activity comes from cell suspension assays conducted on H_2 pre-grown cells where the protein synthesis gentamicin was added at increasing concentrations. Here, the Fe(II) oxidation activity decreased with increasing concentration of gentamicin (Figure 3-6).

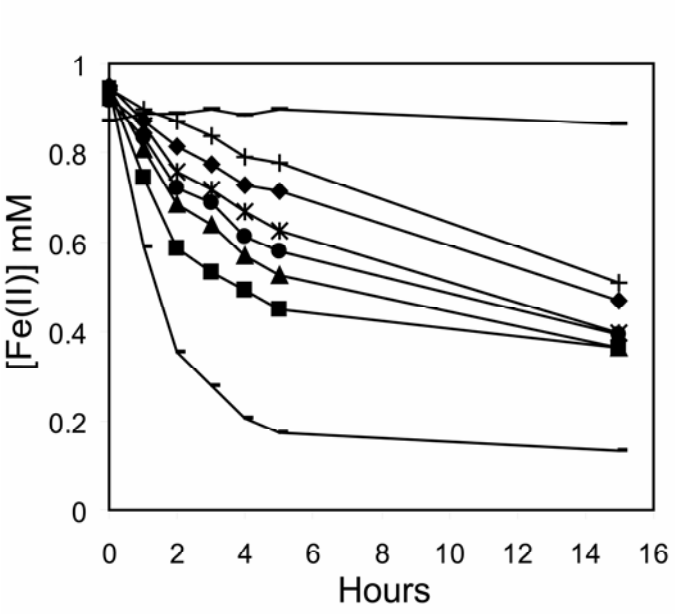

Figure 3-6: The Fe(II) oxidation activity of H_2 pre-grown cells of TIE-1 decreases with increasing concentration of gentamicin. All assays here contain 1 mM $FeCl_2 \cdot H_2O$ and 20 mM $NaHCO_3$. – (short dash) - no gentamicin added; ■ - 0.1 mg/ml gentamicin; ♦ - 0.2 mg/ml gentamicin; ▲ - 0.5 mg/ml gentamicin; ● - 1 mg/ml gentamicin; + - 2 mg/ml gentamicin; ✳ - 4 mg/ml gentamicin; — (long dash) abiotic control + 4 mg/ml gentamicin.

If gentamicin is acting to inhibit novel protein synthesis as expected, these results show that new protein synthesis must be induced and is required for maximal Fe(II) oxidation activity under our assay conditions. The factors that induce this activity are currently unknown, however, based on analogy to the hydrogenase and the sulfide quinone reductase enzymes (the enzyme responsible for the oxidation of S^{2-} during photoautotrophic growth on S^{2-} in many purple non-sulfur phototrophs) [64, 178], it is likely that the Fe(II) oxidase is induced to some level by its substrate, Fe(II).

Assuming that Fe(II) and H_2 oxidation are catalyzed by different enzymes, if H_2 inhibits expression of the Fe(II) oxidase or the Fe(II) oxidase enzyme itself, cells pre-grown on H_2 and transferred to assay conditions containing both Fe(II) and H_2 would be expected to have no Fe(II) oxidation activity (during H_2 pre-growth the Fe(II) oxidase would be repressed and upon transfer to the assay containing H_2, the repression of the Fe(II) oxidase would continue due to the presence of H_2). On the contrary, in our experiments where we add H_2 to the assay to investigate its effects on Fe(II) oxidation, we see that the cells do have Fe(II) oxidation activity (albeit, less than the activity observed for H_2 pre-grown cells transferred to an assay with only Fe(II) (Figure 3-3A and 3B). This observation implies that the Fe(II) oxidase can be expressed in the presence of H_2 and thus, is not repressed transcriptionally, or post-translationally by H_2, itself.

This leaves us to consider the possibility that the observed inhibition of Fe(II) oxidation by H_2 results from the fact that both the hydrogenase and Fe(II) oxidase enzymes are present and active under our assay conditions and compete to donate electrons to the photosynthetic electron transport chain and ultimately CO_2; the implication of this being that the electrons from H_2 out-compete those from Fe(II).

The flow of electrons from Fe(II) and H_2 to the photosynthetic electron transport chain and CO_2 is shown in Figure 3-7.

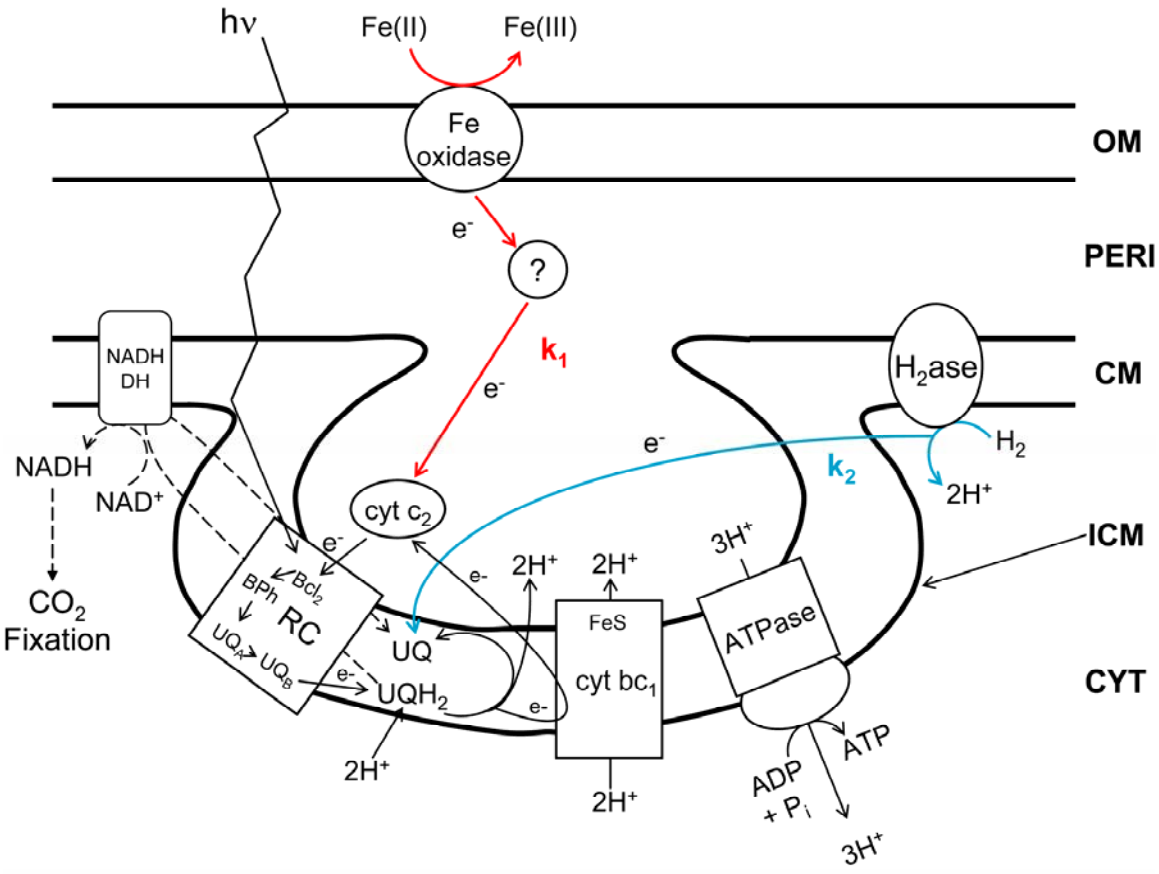

Figure 3-7: A cartoon representation of the flow of electrons from Fe(II) and H_2 to the photosynthetic electron transport chain and CO_2. For simplicity, Fe(II) oxidation is represented as occurring outside the cell. The red lines, associated with k_1, represent the pathway and the overall rate of electron flow from Fe(II) to the photosynthetic electron transport chain. The blue lines, associated with k_2, represent the pathway and the overall rate of electron flow from H_2 to the photosynthetic electron transport chain. OM: outer membrane; PERI: periplasm; CM: cytoplasmic membrane; ICM: intracytoplasmic membrane; CYT: cytoplasm.

The hydrogenase enzyme, presumably located in the cytoplasmic membrane (CM) of TIE-1 and SW2 by comparison to *Rhodobacter capsulatus*

[178], donates electrons from H_2 to the quinone pool. These electrons can then flow through the photosynthetic electron transport chain in a cyclic fashion to produce ATP or feed into NAD^+ reduction (catalyzed by the NADH dehydrogenase also located in the CM). NADH can then be used to fix CO_2.

The location of the Fe(II) oxidase is not yet known. Because Fe(III) formed in the periplasm or cytoplasm would precipitate given the neutral pH at which these organisms grow, it has been proposed that oxidation of Fe(II) occurs at the cell surface and that the electrons are shuttled to the phototrophic reaction center within the intracytoplasmic membrane via a periplasmic transport system involving Cyt c_2 [52]. Alternatively, it is possible that Fe(II) is oxidized internal to the outer membrane (OM). If this is the case, we expect that Fe-chelators (be they organic or inorganic) keep the Fe(III) from precipitating until it can be exported from cell or that subtle changes in local pH control Fe(III) precipitation [41, 89]. In Figure 3-7, the Fe oxidase is depicted as residing in the OM for simplicity. Here, the electrons from Fe(II) flow into the photosynthetic electron transport chain via Cyt c_2 and, as is the case for electrons from H_2, continue to flow through the chain in a cyclic fashion to produce ATP or feed into NAD^+ reduction. Whether intermediate carries between the Fe(II) oxidase and Cyt c_2 also play a role is unknown.

Under conditions where the physiological electron acceptor, CO_2, is abundant (*i.e.*, 20 mM $NaHCO_3$), H_2 inhibition of Fe(II) oxidation is observed as a slight decrease in the rate of Fe(II) oxidation for both TIE-1 and SW2 (Figure 3-3A and 3B, Table 3-3). If these enzymes are competing to donate electrons to

the photosynthetic electron transport chain and ultimately CO_2, when the concentration of the electron acceptor is low (*i.e.*, 1 mM $NaHCO_3$), we might expect the competition between the two enzymes to become more intense and be manifested as a greater inhibition of Fe(II) oxidation by H_2. In support of this hypothesis, we observe that the rate of Fe(II) oxidation for both strains under low $NaHCO_3$ concentrations decreased more so in the presence of H_2 as compared to higher $NaHCO_3$ concentrations, particularly for SW2 (Figure 3-3A and 3B, Table 3-3).

To further test this competition hypothesis, we measured the hydrogenase activity of cell suspensions of TIE-1 pre-grown on H_2 in the presence and absence of Fe(II) to determine if the hydrogenase enzyme is in fact present and active in our assay conditions. The H_2-dependent reduction of benzyl viologen observed indicates that the cells used for our assay do have an active hydrogenase, the activity of which does not seem to be affected by the presence or absence of Fe(II) (Figure 2A & B). These findings are as expected given that the cell are pre-grown on H_2, a condition where the hydrogenase is expected to be highly expressed [178].

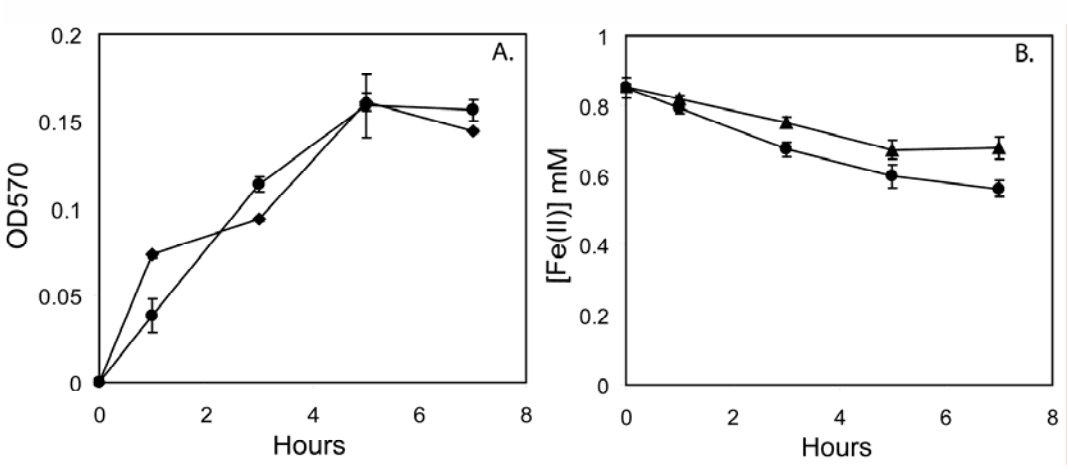

Figure 3-8: Hydrogenase and Fe(II) oxidation activity for TIE-1 as measured by benzyl viologen (BV) reduction and *Ferrozine*, respectively. A. Hydrogenase activity for TIE-1: ♦ - H_2 + 20 mM $NaHCO_3$ + 1 mM $FeCl_2 \cdot H_2O$ + 5 mM BV; ● - H_2 + 20 mM $NaHCO_3$ + 5 mM BV. B. Fe(II) oxidation activity for TIE-1: ▲ H_2 + 20 mM $NaHCO_3$ + 1 mM $FeCl_2 \cdot H_2O$; ● - N_2 + 20 mM $NaHCO_3$ + 1 mM $FeCl_2 \cdot H_2O$. The volume of the assay was 1 ml and the assay bottles were shook vigorously to ensure maximal H_2 saturation of the cell suspension solution. Error bars represent the error on triplicate cell suspension assays.

That the extent of Fe(II) oxidation in the presence of H_2 is limited by the concentration of $NaHCO_3$ in both TIE-1 and SW2 implies that in both strains, the overall rate at which electrons are delivered to the photosynthetic electron transport chain from Fe(II) (k_1, Figure 3-7) is slower than the overall rate at which electrons are delivered to the photosynthetic electron transport chain from H_2 (k_2, Figure 3-7). Reasons why k_2 may be greater than k_1 cannot be determined from our current data, but there are a number of possibilities. First, it is possible that the rate(s) of reaction of the enzymes in the H_2 pathway are faster relative to the

rates of reaction of the enzymes in the Fe(II) pathway. Second, there may be a greater abundance of hydrogenase in these cells relative to the Fe(II) oxidase, which is likely given that these cells are pre-grown on H_2. A final possibility hinges on the fact that that electrons from H_2 are delivered to the photosynthetic electron transport chain via the quinone pool, whereas electrons from Fe(II) are presumably delivered at the level of Cyt c_2. Given that the quinone pool is larger than the Cyt c_2 pool with reported ratios of 20-25 molecules of quinone to each reaction center versus 2 molecules of Cyt c_2 per reaction center [49, 167, 176], the quinone pool represents a larger sink for electrons than the Cyt c_2 pool, and is thus likely to be less limiting in terms of the amount of electrons that can be accepted from the substrate. Further, because the pathway to the NADH dehydrogenase of electrons donated directly to the quinone pool is shorter than that of electrons fed in though the Cyt c_2 pool (which must first go through the reaction center), electrons from H_2 get fed into NAD+ reduction and subsequent CO_2 fixation faster than those from Fe(II). These factors together may serve to accelerate the overall rate of H_2 oxidation relative to Fe(II) oxidation.

The physiological basis for the difference in sensitivity to H_2 under low $NaHCO_3$ concentrations that is observed for the two strains remains to be determined. The greater degree of inhibition by H_2 observed for SW2 relative to TIE-1, however, may imply that k_1 for SW2 is effectively less than k_1 for TIE-1 (Figure 3-7). Such a scenario may result if k_1 is less than k_2 in SW2, whereas k_1 and k_2 are more equivalent in TIE-1, or if there is a greater concentration of hydrogenase relative to Fe(II) oxidase in SW2 versus TIE-1. Such questions

concerning the rates of individual reactions within a physiological pathway cannot be resolved with cell suspension experiments and require further investigations with purified enzymes. Thus, purification of the Fe(II) oxidase is a priority for future work.

Implications for Banded Iron Formations

Inferences on mechanism aside, the implication of our results for Banded Iron Formations are that when the physiological electron acceptor for photosynthesis (CO_2), is abundant (as would be the case in an ancient Achaean ocean) some Fe(II) oxidizing phototrophs have the capacity to oxidize Fe(II) even in the presence of the alternative electron donor, H_2. Thus, the presence of H_2 in an ancient atmosphere up to concentrations of even 800,000 ppm would not necessarily preclude Fe(II) oxidation by these bacteria. That our $NaHCO_3$ concentrations (20 mM) are lower than the predicted concentrations in an Archean ocean by ~3.5 fold implies that the slight inhibitory effects of H_2 observed under our conditions might be negligible at concentrations of 70 mM.

If we assume that photochemical reactions and volcanic emissions were the major source of H_2 and calculate the concentration of H_2 in a photic zone of 100 m over an area of 10^{11} m^2 (equivalent to the depositional basin of the Hamersley Group, which contains among the largest BIFs [101]), using a hydrogen mixing ratio of 30% (which is at the upper limit of what has been predicted [170]), and a Henry's constant for H_2 of $10^{-3.1}$ [122], we find the concentration of H_2 expected in this volume of ocean water to be 0.24 ppm (0.24

mM). Given that diffusion and H_2 consumption rates by other bacteria are not considered in this calculation, we expect the concentration of H_2 to further decrease with depth. Additionally, the solubility of H_2 in water decreases with increasing temperature [60]. If estimations of Archean ocean temperatures at 70±15°C are correct [97], our calculated value represents a maximum for the amount of H_2 dissolved in the photic zone of this basin and is several orders of magnitude less than those used for our experiments. Therefore, it is likely that at depths approaching 100 m in the ancient open ocean, H_2 would pose no barrier to Fe(II) oxidation by these anoxygenic phototrophs. Further, in sulfide depleted environments, which are thought to prevail in the ancient oceans prior to 1.8 Ga [134], Fe(II) may be the predominant inorganic electron donor for anoxygenic photosynthesis in an Archean ocean.

CONCLUSIONS

We find that even in the presence of 800,000 ppm H_2, Fe(II) is still oxidized at appreciable rates by two species of Fe(II)-oxidizing purple non-sulfur phototrophs when the concentration of $NaHCO_3$ is 20 mM. This implies that the presence of H_2 in an ancient atmosphere at the currently predicted values would not preclude the involvement of these organisms in BIF deposition. Additionally, our calculations predict that the concentration of dissolved H_2 in the photic zone of an Archean ocean would be less than 0.24 ppm; a concentration that is expected to have no effect on Fe(II) oxidation by anoxygenic phototrophs at depth in the photic zone. Further, in sulfide depleted environments, which are

thought to prevail in the ancient oceans prior to 1.8 Ga [134], Fe(II) may be the predominant inorganic electron donor for anoxygenic photosynthesis in an Archean ocean.

The molecular mechanism by which H_2 inhibits Fe(II) oxidation by these phototrophs when $NaHCO_3$ concentrations are low remains to be determined, but the most likely explanation appears to be that it results from a competition between hydrogenase and the Fe(II) oxidase to donate electrons to the photosynthetic electron transport chain and ultimately CO_2. The physiological differences between TIE-1 and SW2 that result in differential sensitivity to H_2 are also not known, but the difference may result from different rates of reaction for enzymes in the Fe(II) and/or H_2 oxidation pathways of the two strains.

A consideration that remains to be investigated is the effect that organic compounds may have on phototrophic Fe(II) oxidation. Further studies that combine microbial physiology and the geological approaches that allow biogeochemical reconstructions of ancient environments will help shed light on this and other questions related to BIF deposition and the ecology of the Archean.

4. Iron Isotope Fractionation by Fe(II)-oxidizing Photoautotrophic Bacteria

ABSTRACT

Photoautotrophic bacteria that oxidize ferrous iron [Fe(II)] under anaerobic conditions are thought to be ancient in origin, and the ferric (hydr)oxide mineral products of their metabolism are likely to be preserved in ancient rocks. Here, two enrichment cultures of Fe(II)-oxidizing photoautotrophs and a culture of the genus *Thiodictyon* were studied with respect to their ability to fractionate Fe isotopes. Fe isotope fractionations produced by both the enrichment cultures and the *Thiodictyon* culture were relatively constant at early stages of the reaction progress, where the ^{56}Fe /^{54}Fe ratios of poorly crystalline hydrous ferric oxide (HFO) metabolic products were enriched in the heavier isotope relative to aqueous ferrous iron ($Fe(II)_{aq}$) by ~1.5±0.2 per mil (‰). This fractionation appears to be independent of the rate of photoautotrophic Fe(II)-oxidation, and is comparable to that observed for Fe isotope fractionation by dissimilatory Fe(III)-reducing bacteria. Although there remain a number of uncertainties regarding how the overall measured isotopic fractionation is produced, the most likely mechanisms include 1) an equilibrium effect produced by biological ligands, or 2) a kinetic effect produced by precipitation of HFO overlaid upon equilibrium exchange between Fe(II) and Fe(III) species. The fractionation we observe is similar in direction to that measured for abiotic oxidation of $Fe(II)_{aq}$ by molecular

oxygen. This suggests that the use of Fe isotopes to identify phototrophic Fe(II)-oxidation in the rock record may only be possible during time periods in Earth's history when independent evidence exists for low ambient oxygen contents.

INTRODUCTION

Geochemical cycling of iron (Fe) is primarily controlled by redox conditions, which vary markedly in different environments on the modern Earth, and have likely changed over geologic time. It is widely (though not universally) accepted that the terrestrial atmosphere has been oxidizing for at least the last two billion years [58, 74, 91, 106, 128, 145]. As a result, chemical oxidation of ferrous iron [Fe(II)] under "modern" atmospheric conditions often occurs through the interaction of reduced fluids with oxygenated waters. An important exception to this, however, is Fe(II)-oxidation that occurs in microaerobic or anoxic environments as a result of the activity of microorganisms that oxidize Fe(II) to generate energy for growth. Microorganisms of this type include those that couple Fe(II)-oxidation to the reduction of nitrate at neutral pH [14, 162], or to the reduction of oxygen at either low [18, 50], or neutral pH [54], and the anaerobic Fe(II)-oxidizing phototrophs [52, 70, 182]. Under oxygen-deplete conditions, microbially mediated Fe(II)-oxidation is an important component of the Fe redox cycle.

In most cases, the products of biologically oxidized Fe are highly insoluble ferric [Fe(III)] (hydr)oxide minerals that are likely to be preserved in rocks. Indeed, direct photoautotrophic Fe(II)-oxidation under anaerobic conditions (as

opposed to indirect photoautotrophic Fe(II)-oxidation mediated by oxygen produced by cyanobacteria [37]), has been proposed as a mechanism for producing the extensive ferric oxide deposits found in ancient Banded Iron Formations (BIFs) [67, 101, 182]. Therefore, studies of the mechanisms of direct biological Fe(II)-oxidation and the structure and composition of the resulting Fe(III) mineral products may be useful in furthering our understanding of the geochemical cycling of Fe that occurred on the ancient Earth. To evaluate the role of microbes in Fe cycling today and over geological time, however, we are faced with the challenge of distinguishing between Fe(III) minerals that formed via biological or abiotic pathways.

It has been suggested that Fe isotope geochemistry may be useful in such a context [10], and a number of measurements of Fe isotope fractionation have been made in biological [10, 11, 22, 85, 116], and abiotic [4, 10-12, 27, 86, 117, 141, 155, 181] experimental systems. Although most igneous rocks and many clastic sedimentary materials are isotopically homogeneous within ±0.05‰ [11], significant variations (~ 4‰) in Fe isotope compositions are found in late Archean BIFs [84].

If Fe isotopes are to be used to broaden our understanding of the Fe cycle, and the isotopic variations observed in BIFs, a better understanding of the Fe isotope fractionations that are produced by abiotic and biological transformations of Fe is needed. In particular, biological redox processes that alter the oxidation state of Fe are of interest because Fe isotopic fractionations in low temperature natural systems are predicted to be greatest between Fe(II) and

Fe(III) phases [146]. Although Fe isotope fractionations produced during dissimilatory Fe(III)-reduction by *Shewanella alga* have been measured [10, 11], no data currently exist to constrain Fe isotope fractionations that may occur during microbial Fe(II)-oxidation.

To make inferences about Fe cycling on the ancient Earth using Fe isotopes, it is important to study Fe(II)-oxidizing organisms that carry out an ancient form of metabolism. The use of Fe(II) as an electron donor in anoxygenic photosynthesis likely arose early in Earth history. This assumption rests on the fact that phylogenetic relationships between genes that are involved in bacteriochlorophyll and chlorophyll biosynthesis show that the anoxygenic form of photosynthesis evolved before the oxygenic form [185], as well as the logic that the evolution of oxygenic photosynthesis predates the evolution of respiratory metabolisms that are based on oxygen or other highly oxidized species (*i.e.*, nitrate). In addition, the high estimated concentrations of reduced Fe that appear to have existed in the early Earth's oceans relative to today [57, 72, 184], suggest that Fe(II) was available to fuel microbial metabolism early in Earth history. Therefore, this study focuses on Fe isotope fractionation produced by anoxygenic Fe(II)-oxidizing photoautotrophic bacteria, as opposed to other Fe(II)-oxidizing bacteria.

EXPERIMENTAL PROCEDURES

Organisms and cultivation

Two enrichment cultures of Fe(II)-oxidizing anoxygenic phototrophs were obtained from an Fe-rich ditch in Bremen, Germany. The Fe(II)-oxidizing phototroph, strain F4, was isolated from a marsh in Woods Hole, MA

For routine cultivation, all cultures were maintained in an anoxic minimal salts medium for freshwater cultures [52]. One liter (L) of medium contained: 0.3 grams (g) NH_4Cl, 0.5 g KH_2PO_4, 0.4 g $MgCl_2 \cdot 6H_2O$, 0.1 g $CaCl_2 \cdot 2H_2O$. After sterilization by autoclaving, the basal salts solution was equilibrated with a 20% CO_2:80% N_2 gas mix. Additions to the cooled medium included: 22 milliliters (ml) 1 Molar (M) $NaHCO_3$, 1 ml of a trace elements solution (3 g Na_2-EDTA, 1.1 g $FeSO_4 \cdot 7H_2O$, 190 mg $CoCl_2 \cdot 6H_2O$, 42 mg $ZnCl_2$, 24 mg $NiCl_2 \cdot 6\ H_2O$, 18 mg $Na_2MoO_4 \cdot 2H_2O$, 300 mg H_3BO_3, 2 mg $CuCl_2 \cdot 2H_2O$ and 50 mg $MnCl_2 \cdot 4H_2O$ in 1 L ultra-pure H2O), 1 ml of a vitamin solution (4 mg 4-aminobenzoic acid, 1 mg D(+)-biotin, 10 mg nicotinic acid, 5 mg Ca D(+)-pantothenate, 15 mg pyridoxine dihydrochloride, and 10 mg thiamine chloride dihydrochloride in 1 L ultra-pure H_2O), and 1 ml of a vitamin B_{12} solution (5 mg in 50 ml ultra-pure H_2O). The medium was adjusted to pH 7 with 1 M HCl.

Fe(II) additions to the basal medium were made in an anaerobic chamber (Coy Laboratory Products, Grasslake, MI). 10 ml of an anoxic, 1 M $FeCl_2 \cdot H_2O$ stock solution was added to the medium batch used to grow the enrichments, whereas 15 ml was added to the batch used to grow strain F4. Upon addition of Fe(II) to the medium, a fluffy white precipitate, most likely vivianite ($Fe_3(PO_4)$

$_2$·8H_2O) or a vivianite and siderite ($FeCO_3$) mixture, formed. To eliminate this precipitate from Fe(III) precipitates that would later be produced during biological Fe(II)-oxidation, precipitation was allowed to proceed for approximately 14-18 hours, after which all precipitates were filtered out (0.2 µm, cellulose nitrate, Millipore), leaving a clear medium with ~6-10 mM $Fe(II)_{aq}$. Filtration was performed in the anaerobic chamber. Twenty-five ml aliquots of the Fe(II)-containing medium were dispensed anaerobically into 58 ml serum bottles, stoppered and maintained under a 20% CO_2:80% N_2 gas atmosphere. Most cultures were incubated at a distance of 40 cm from a 40 Watt (W) standard incandescent light source at 22°C, except for those incubated at 80 and 120 cm distances; all were gently inverted daily to mix the cultures.

The ferrous precipitates were ~0.3‰ heavier in ^{56}Fe /^{54}Fe ratios than the starting 1 M $FeCl_2$·H_2O stock solutions, producing a medium supernatant that was lower in $\delta^{56}Fe$ values than the starting $FeCl_2$·H_2O reagent (Table 4-1). The fact that the $\delta^{56}Fe$ values in the aqueous fractions of the uninoculated controls for the microbial experiments were different from the controls listed in the Table 4-1 is surprising, but may be explained by differences in timing of medium sampling (*i.e.*, we sampled our reagent controls after only 2-3 hours, and it is probable that not all of the ferrous solids had precipitated by this point, whereas ferrous solid precipitation appears to have been complete in the medium used for the microbial experiments). Note that the solid $FeCl_2$·H_2O reagent is isotopically heterogeneous on the ~100 µg scale (Table 4-1), although this scale of isotopic

heterogeneity is homogenized by the large amounts of solid used in the $FeCl_2 \cdot H_2O$ regent preparation.

Table 4-1: Fe isotope compositions of the experimental reagents and enrichment culture inoculums. In the analyses column, up to triplicate mass spectrometry runs of a sample conducted on different days are reported; the errors are 2-SE from in-run statistics and reflect machine uncertainties and/or processing errors. The Mass Spec Average is the average of up to three analyses of a single sample, 1-SD is one standard deviation external; note that if there is only one mass spectrometry analysis, the error is 2-SE. The Average of Replicate is the average of processing replicates of a sample throughout the entire analytical procedure; the best estimate of external reproducibility. [1]Inoculum refers to the cells and small amount of Fe(III) precipitates (~1.2 millimoles) transferred from a grown culture of the enrichments to the fresh filtered Fe(II) medium used for these experiments. Inoculum cultures where the Fe(II) substrate initially provided was oxidized to completion were used to minimize Fe carryover. [2]Yellow crystals among the bulk of the green crystals of the solid $FeCl_2 \cdot H_2O$ used for the isotopic experiments indicate slight oxidation of the reagent. The isotopic composition of the solid $FeCl_2 \cdot H_2O$ reagent is heterogeneous on the 100 mg scale. [3]1M $FeCl_2 \cdot H_2O$ stock solution used for enrichment medium preparation. [4]10 mM $FeCl_2 \cdot H_2O$ was added to 25 mls of medium. The resulting ferrous minerals were allowed to precipitate to completion. Under an aerobic atmosphere, the medium was mixed well and 1 ml

was extracted with a syringe and transferred to a microcentrifuge tube. The precipitate and soluble phases were separated by centrifugation. The soluble phase was removed with a pipette and filtered through a 0.22 μm filter into a clean microcentrifuge tube. The precipitate fraction was washed three times with ultra pure water equilibrated with an anoxic atmosphere. Supernatant 1, 2 and 3 are triplicate samples of the soluble phase and precipitate 1 and 2 are duplicate samples of the precipitate phase.

Table 4-1:

Sample	Analyses				Mass Spec Average				Average of Replicates			
	δ^{56}Fe	2-SE	δ^{56}Fe	2-SE	δ^{56}Fe	1-SD	δ^{56}Fe	1-SD	δ^{56}Fe	1-SD	δ^{56}Fe	1-SD
Inoculum for enrichment culture 1[1]	-0.31	0.06	-0.48	0.03	-0.31	0.01	-0.46	0.02	---	---	---	---
	-0.31	0.08	-0.45	0.04								
Inoculum for enrichment culture 2[1]	-0.35	0.06	-0.55	0.04	---	---	---	---	---	---	---	---
0.36 mg of $FeCl_2 \cdot H_2O$ salt crystals	-0.04	0.06	0.08	0.04	-0.06	0.03	-0.03	0.15	---	---	---	---
	-0.08	0.13	-0.13	0.06								
0.38 mg of green $FeCl_2 \cdot H_2O$ salt crystals[2]	-0.41	0.14	-0.68	0.06	-0.48	0.09	-0.68	0.06	---	---	---	---
	-0.45	0.06	-0.62	0.03								
	-0.57	0.08	-0.75	0.04								
0.44 mg of green $FeCl_2 \cdot H_2O$ salt crystals[2]	-0.13	0.06	-0.17	0.03	-0.14	0.02	-0.21	0.06	---	---	---	---
	-0.16	0.09	-0.25	0.04								
0.35 mg of yellow $FeCl_2 \cdot H_2O$ salt crystals[2]	-0.22	0.12	-0.33	0.07	-0.25	0.09	-0.42	0.15	---	---	---	---
	-0.36	0.06	-0.59	0.03								
	-0.19	0.07	-0.34	0.04								
0.47 mg of yellow $FeCl_2 \cdot H_2O$ salt crystals[2]	-0.11	0.13	-0.09	0.06	-0.07	0.12	-0.08	0.22	---	---	---	---
	0.07	0.05	0.14	0.05								
	-0.16	0.07	-0.30	0.03								
~200mg of $FeCl_2 \cdot H_2O$ salt crystals dissolved into a 400 ppm Fe solution	-0.41	0.11	-0.48	0.06	-0.37	0.04	-0.46	0.09	---	---	---	---
	-0.33	0.07	-0.36	0.04								
	-0.36	0.07	-0.53	0.03								

1 M $FeCl_2 \cdot H_2O$ stock solutions – 1^3	-0.42	0.07	-0.53	0.04	---	---	---	---	-0.36	0.03	-0.51	0.01
1 M $FeCl_2 \cdot H_2O$ stock solutions – 2^3	-0.36	0.08	-0.55	0.04	-0.32	0.05	-0.50	0.08	---	---	---	---
	-0.29	0.12	-0.45	0.06								
Supernatant 1^4	-0.63	0.09	-1.03	0.04	-0.72	0.10	-1.14	0.11	-0.70	0.09	-1.09	0.12
	-0.84	0.09	-1.25	0.05								
	-0.71	0.09	-1.15	0.04								
Supernatant 2^4	-0.69	0.08	-1.02	0.10	-0.68	0.10	-1.04	0.11	---	---	---	---
	-0.78	0.05	-1.15	0.04								
	-0.59	0.08	-0.94	0.04								
Supernatant 3^4	-0.69	0.10	-0.94	0.05	-0.77	0.11	-1.08	0.19	---	---	---	---
	-0.85	0.07	-1.21	0.04								
Precipitate 1^4	-0.07	0.13	-0.12	0.06	-0.11	0.05	-0.18	0.06	-0.08	0.05	-0.12	0.11
	-0.16	0.08	-0.22	0.06								
	-0.09	0.12	-0.22	0.05								
Precipitate 2^4	-0.04	0.09	-0.08	0.06	-0.05	0.02	-0.06	0.12	---	---	---	---
	-0.04	0.10	0.06	0.06								
	-0.07	0.12	-0.17	0.06								

After filtration, no further precipitation of Fe(II) minerals was observed in uninoculated controls or in inoculated dark controls throughout the course of the experiments. This can be seen in Tables 4-2 and 3, which show invariant Fe(II) concentrations and Fe isotope compositions of the uninoculated controls, as well as the inoculated control that was incubated in the dark. Therefore, the current study avoids ambiguities in interpreting isotopic data that have been encountered by other researchers due to the simultaneous precipitation of Fe(II) and Fe(III) mineral phases during Fe(II)-oxidation [108].

Table 4-2: Fe isotope compositions of enrichments 1 and 2 and the uninoculated control. All cultures started at 25 ml total volume. Sampling volumes were always 1 ml, and were split into two 0.5 ml sub-volumes to obtain duplicate soluble and precipitate (ppt) fractions for that time point. Start volume is the volume of the culture on the day the sample was taken. Mmol Fe(III) is calculated by mass balance using the *Ferrozine* measurements for Fe(II). "*F*" represents the fraction of the total $Fe(II)_{aq}$ that has been oxidized. In the analyses column, up to triplicate mass spectrometry runs of a sample conducted on different days are reported; the errors are 2-SE from in-run statistics and reflect machine uncertainties and/or processing errors. The Mass Spec Average is the average of up to three analyses of a single sample, 1-SD is one standard deviation external; note that if there is only one mass spectrometry analysis, the error is 2-SE. The Average of Replicate is the average of processing replicates

of a sample throughout the entire analytical procedure; the best estimate of external reproducibility. [1]per 0.5 ml split

Table 4-2:

Sample/ Day/ Start Volume (ml)	Fe(II) mmol[1]	Fe(III) mmol[1]	*F*	Analyses				Mass Spec Average				Average of Replicates			
				δ^{56}Fe	2-SE	δ^{57}Fe	2-SE	δ^{56}Fe	1-SD	δ^{57}Fe	1-SD	δ^{56}Fe	1-SD	δ^{57}Fe	1-SD
Enrichment 1															
Soluble fraction 1/0/25	2.75	---	0.000	-0.40	0.07	-0.53	0.03	---	---	---	---	-0.40	0.07	-0.53	0.03
Soluble fraction 2/0/25	2.75	---	0.000	-0.41	0.07	-0.57	0.03	-0.46	0.07	-0.64	0.10				
				-0.51	0.08	-0.71	0.05								
Soluble fraction 1/3/24	2.94	---	0.000	-0.42	0.07	-0.65	0.04	-0.42	0.01	-0.66	0.02	-0.42	0.01	-0.62	0.05
				-0.42	0.06	-0.67	0.03								
Soluble fraction 2/3/24	2.94	---	0.000	-0.43	0.06	-0.56	0.03	-0.42	0.01	-0.58	0.02				
				-0.42	0.06	-0.59	0.03								
Soluble fraction 1/9/23	2.56	---	0.068	-0.71	0.07	-1.03	0.03	-0.69	0.03	-1.02	0.01	-0.77	0.14	-1.11	0.16
				-0.67	0.06	-1.02	0.03								
Soluble fraction 2/9/23	2.56	---	0.068	-0.93	0.05	-1.30	0.03	---	---	---	---				
Soluble fraction 1/11/22	0.55	---	0.801	-2.21	0.06	-3.17	0.03	-2.22	0.01	-3.17	0.00	-2.23	0.02	-3.22	0.06
				-2.22	0.11	-3.17	0.05								
Soluble fraction 2/11/22	0.55	---	0.801	-2.27	0.07	-3.28	0.04	-2.25	0.02	-3.27	0.01				
				-2.24	0.09	-3.27	0.04								
Soluble fraction 1/13/21	0.25	---	0.909	---	---	---	---	---	---	---	---	---	---	---	---
Soluble	0.25	---	0.909	---	---	---	---	---	---	---	---				

fraction 2/13/21															
Ppt. fraction 1/0/25	---	0.00	0.000	---	---	---	---	---	---	---	---	---	---	---	---
Ppt. fraction 2/0/25	---	0.00	0.000	---	---	---	---	---	---	---	---				
Ppt. fraction 1/3/24	---	0.00	0.000	---	---	---	---	---	---	---	---	---	---	---	---
Ppt. fraction 2/3/24	---	0.00	0.000	---	---	---	---	---	---	---	---				
Ppt. fraction 1/9/23	---	0.19	0.068	0.85	0.07	1.22	0.04	0.82	0.04	1.20	0.03	---	---	---	---
				0.80	0.06	1.18	0.04								
Ppt. fraction 2/9/23	---	0.19	0.068	---	---	---	---	---	---	---	---				
Ppt. fraction 1/11/22	---	2.20	0.801	0.01	0.07	-0.01	0.03	-0.01	0.02	0.01	0.02	-0.03	0.05	-0.02	0.04
				-0.03	0.06	0.02	0.04								
Ppt. fraction 2/11/22	---	2.20	0.801	-0.08	0.07	-0.07	0.03	---	---	---	---				
Ppt. fraction 1/13/21	---	2.50	0.909	-0.28	0.08	-0.40	0.04	---	---	---	---	-0.20	0.07	-0.29	0.07
Ppt. fraction 2/13/21	---	2.50	0.909	-0.10	0.07	-0.26	0.05	-0.17	0.06	-0.26	0.02				
				-0.19	0.06	-0.23	0.03								
				-0.22	0.07	-0.28	0.04								
Enrichment 2															
Soluble fraction 1/0/25	2.98	---	0.000	-0.41	0.08	-0.56	0.05	-0.43	0.03	-0.60	0.06	-0.43	0.03	-0.61	0.06
				-0.45	0.05	-0.65	0.03								

Soluble fraction 2/0/25	2.98	---	0.000	-0.40	0.13	-0.57	0.06	-0.42	0.03	-0.62	0.08				
				-0.45	0.06	-0.68	0.03								
Soluble fraction 1/3/24	2.59	---	0.131	-0.35	0.08	-0.62	0.04	-0.38	0.04	-0.60	0.02	-0.43	0.06	-0.64	0.06
				-0.41	0.06	-0.59	0.03								
Soluble fraction 2/3/24	2.59	---	0.131	-0.47	0.08	-0.65	0.18	-0.48	0.02	-0.68	0.05				
				-0.49	0.08	-0.72	0.04								
Soluble fraction 1/9/23	2.20	---	0.264	-0.87	0.08	-1.26	0.05	-0.88	0.01	-1.24	0.04	-0.86	0.04	-1.21	0.04
				-0.89	0.07	-1.21	0.04								
Soluble fraction 2/9/23	2.20	---	0.264	-0.80	0.09	-1.17	0.04	-0.84	0.05	-1.19	0.03				
				-0.88	0.09	-1.21	0.05								
Soluble fraction 1/11/22	1.95	---	0.345	-1.41	0.06	-2.00	0.04	---	---	---	---	-1.40	0.01	-2.00	0.00
Soluble fraction 2/11/22	1.95	---	0.345	-1.39	0.09	-2.01	0.04	---	---	---	---				
Soluble fraction 1/13/21	0.25	---	0.916	---	---	---	---	---	---	---	---	---	---	---	---
Soluble fraction 2/13/21	0.25	---	0.916	---	---	---	---	---	---	---	---				
Ppt. fraction 1/ 0/25	---	0.00	0.000	---	---	---	---	---	---	---	---	---	---	---	---
Ppt. fraction 2/0/25	---	0.00	0.000	---	---	---	---	---	---	---	---				
Ppt. fraction 1/3/24	---	0.39	0.131	---	---	---	---	---	---	---	---	---	---	---	---

Ppt. fraction 2/3/24	---	0.39	0.131	---	---	---	---	---	---	---	---				
Ppt. fraction 1/9/23	---	0.79	0.264	0.89	0.07	1.29	0.03	0.87	0.03	1.27	0.03	0.83	0.07	1.23	0.07
				0.84	0.07	1.24	0.03								
Ppt. fraction 2/9/23	---	0.79	0.264	0.74	0.08	1.15	0.04	---	---	---	---				
Ppt. fraction 1/11/22	---	1.03	0.345	0.71	0.09	1.07	0.05	0.69	0.04	1.05	0.03	0.68	0.03	1.05	0.02
				0.66	0.05	1.03	0.03								
Ppt. fraction 2/11/22	---	1.03	0.345	0.66	0.09	1.04	0.04	---	---	---	---				
Ppt. fraction 1/13/21	---	2.73	0.916	-0.12	0.09	-0.14	0.04	-0.12	0.01	-0.14	0.00	-0.07	0.08	-0.10	0.10
				-0.13	0.07	-0.14	0.04								
Ppt. fraction 2/13/21	---	2.73	0.916	0.04	0.17	0.06	0.06	-0.01	0.07	-0.06	0.16				
Uninoculated Control															
Soluble fraction 1/0/25	2.89	0.00	---	-0.30	0.05	-0.53	0.03	-0.33	0.05	-0.52	0.00	-0.38	0.06	-0.55	0.03
				-0.37	0.11	-0.52	0.04								
Soluble fraction 2/0/25	2.89	0.00	---	-0.41	0.08	-0.57	0.04	-0.42	0.01	-0.58	0.02				
				-0.43	0.05	-0.59	0.03								
Soluble fraction 1/3/24	3.00	0.00	---	-0.32	0.11	-0.55	0.05	---	---	---	---	-0.41	0.11	-0.62	0.08
Soluble fraction 2/3/24	3.00	0.00	---	-0.53	0.05	-0.71	0.02	-0.45	0.12	-0.65	0.08				
				-0.36	0.09	-0.60	0.04								
Soluble fraction	3.13	0.00	---	-0.54	0.06	-0.68	0.03	-0.58	0.05	-0.81	0.19	-0.50	0.09	-0.73	0.15
				-0.61	0.05	-0.94	0.04								

1/9/23															
Soluble fraction 2/9/23	3.13	0.00	---	-0.40	0.05	-0.65	0.02	-0.43	0.04	-0.64	0.02				
				-0.46	0.07	-0.63	0.04								
Soluble fraction 1/11/22	3.54	0.00	---	-0.29	0.07	-0.46	0.04	-0.25	0.05	-0.45	0.03	-0.31	0.08	-0.48	0.05
				-0.22	0.07	-0.43	0.04								
Soluble fraction 2/11/22	3.54	0.00	---	-0.36	0.06	-0.51	0.03	-0.38	0.02	-0.52	0.01				
				-0.39	0.09	-0.53	0.04								
Soluble fraction 1/13/21	3.83	0.00	---	-0.24	0.08	-0.44	0.03	---	---	---	---	-0.29	0.05	-0.44	0.02
Soluble fraction 2/13/21	3.83	0.00	---	-0.30	0.07	-0.47	0.03	-0.32	0.03	-0.45	0.03				
				-0.34	0.07	-0.43	0.03								

Table 4-3: Fe isotope compositions of the pure culture, F4, incubated at 40, 80 and 120 cm from the light and the uninoculated and dark controls. All cultures started at 25 ml total volume. Sampling volumes were always 1 ml, and were split into two 0.5 ml sub-volumes to obtain duplicate soluble and precipitate (ppt) fractions for that time point. Start volume is the volume of the culture on the day the sample was taken. Mmol Fe(III) is calculated by mass balance using the *Ferrozine* measurements for Fe(II). "*F*" represents the fraction of the total $Fe(II)_{aq}$ that has been oxidized. In the analyses column, up to triplicate mass spectrometry runs of a sample conducted on different days are reported; the errors are 2-SE from in-run statistics and reflect machine uncertainties and/or processing errors. The Mass Spec Average is the average of up to three analyses of a single sample, 1-SD is one standard deviation external; note that if there is only one mass spectrometry analysis, the error is 2-SE. The Average of Replicate is the average of processing replicates of a sample throughout the entire analytical procedure; the best estimate of external reproducibility. [1]per 0.5 ml split.

Table 4-3:

Sample/ Day/ Start Volume (ml)	Fe(II) mmol[1]	Fe(III) mmol[1]	*F*	Analyses				Mass Spec Average				Average of Replicates			
				δ^{56}Fe	2-SE	δ^{57}Fe	2-SE	δ^{56}Fe	1-SD	δ^{57}Fe	1-SD	δ^{56}Fe	1-SD	δ^{57}Fe	1-SD
F4 Culture - 40 cm															
Soluble fraction 1/0/25	4.66	---	0.000	-0.18	0.06	-0.28	0.03	---	---	---	---	-0.18	0.00	-0.22	0.08
Soluble fraction 2/0/25	4.66	---	0.000	-0.19	0.07	-0.17	0.04	---	---	---	---				
Soluble fraction 1/2/23	5.24	---	0.000	-0.13	0.07	-0.13	0.04	---	---	---	---	-0.13	0.01	-0.11	0.02
Soluble fraction 2/2/23	5.24	---	0.000	-0.14	0.06	-0.10	0.03	---	---	---	---				
Soluble fraction 1/4/21	4.58	---	0.017	-0.28	0.06	-0.48	0.03	-0.29	0.02	-0.41	0.11	-0.30	0.03	-0.39	0.08
				-0.30	0.05	-0.33	0.02								
Soluble fraction 2/4/21	4.58	---	0.017	-0.33	0.05	-0.35	0.03	---	---	---	---				
Soluble fraction 1/6/20	3.78	---	0.190	-0.77	0.06	-1.13	0.03	---	---	---	---	-0.78	0.03	-1.13	0.00
Soluble fraction 2/6/20	3.78	---	0.190	-0.80	0.05	-1.12	0.03	---	---	---	---				
Soluble fraction 1/8/19	2.01	---	0.570	-1.19	0.10	-1.76	0.05	-1.24	0.05	-1.85	0.08	-1.28	0.06	-1.85	0.06
				-1.28	0.05	-1.91	0.04								
				-1.26	0.04	-1.89	0.03								
Soluble	2.01	---	0.570	-1.34	0.05	-1.85	0.03	-1.34	0.01	-1.86	0.01				

fraction 2/8/19				-1.33	0.07	-1.87	0.03								
Soluble fraction 1/10/18	0.06	---	0.986	-2.44	0.10	-3.47	0.05	---	---	---	---	-2.39	0.06	-3.46	0.02
Soluble fraction 2/10/18	0.06	---	0.986	-2.35	0.07	-3.45	0.04	---	---	---	---				
Soluble fraction 1/12/17	0.00	---	1.00	---	---	---	---	---	---	---	---	---	---	---	---
Soluble fraction 2/12/17	0.00	---	1.00	---	---	---	---	---	---	---	---				
Soluble fraction 1/14/16	0.00	---	1.00	---	---	---	---	---	---	---	---	---	---	---	---
Soluble fraction 2/14/16	0.00	---	1.00	---	---	---	---	---	---	---	---				
Soluble fraction 1/16/15	0.00	---	1.00	---	---	---	---	---	---	---	---	---	---	---	---
Soluble fraction 2/16/15	0.00	---	1.00	---	---	---	---	---	---	---	---				
Ppt fraction 1/0/25	---	0.00	0.000	---	---	---	---	---	---	---	---	---	---	---	---
Ppt fraction 2/0/25	---	0.00	0.000	---	---	---	---	---	---	---	---				
Ppt fraction 1/2/23	---	0.00	0.000	---	---	---	---	---	---	---	---	---	---	---	---
Ppt	---	0.00	0.000	---	---	---	---	---	---	---	---				

fraction 2/2/23															
Ppt fraction 1/4/21	---	0.08	0.017	1.16	0.06	1.58	0.04	---	---	---	---	---	---	---	---
Ppt fraction 2/4/21	---	0.08	0.017	---	---	---	---	---	---	---	---				
Ppt fraction 1/6/20	---	0.88	0.190	0.72	0.04	1.01	0.02	---	---	---	---	0.64	0.09	1.00	0.09
Ppt fraction 2/6/20	---	0.88	0.190	0.66	0.05	1.09	0.03	0.60	0.08	1.00	0.13				
				0.54	0.05	0.91	0.03								
Ppt fraction 1/8/19	---	2.65	0.570	0.32	0.08	0.61	0.05	---	---	---	---	0.36	0.06	0.63	0.04
Ppt fraction 2/8/19	---	2.65	0.570	0.40	0.06	0.66	0.04	---	---	---	---				
Ppt fraction 1/10/18	---	4.60	0.986	-0.11	0.07	-0.09	0.04	-0.05	0.09	-0.08	0.02	0.00	0.09	0.01	0.10
				0.01	0.06	-0.06	0.03								
Ppt fraction 2/10/18	---	4.60	0.986	0.09	0.08	0.12	0.04	0.06	0.05	0.09	0.05				
				0.02	0.05	0.05	0.03								
Ppt fraction 1/12/17	---	4.66	1.00	---	---	---	---	---	---	---	---	---	---	---	---
Ppt fraction 2/12/17	---	4.66	1.00	---	---	---	---	---	---	---	---				
Ppt fraction 1/14/16	---	4.66	1.00	-0.11	0.06	-0.15	0.03	---	---	---	---	-0.08	0.04	-0.11	0.07
Ppt	---	4.66	1.00	-0.05	0.06	-0.06	0.04	---	---	---	---				

fraction 2/14/16															
Ppt fraction 1/16/15	---	4.66	1.00	---	---	---	---	---	---	---	---	---	---	---	---
Ppt fraction 2/16/15	---	4.66	1.00	-0.08	0.04	-0.03	0.03	---	---	---	---				
F4 Culture - 80 cm															
Soluble fraction 1/0/25	4.74	---	0.000	-0.20	0.05	-0.24	0.02	---	---	---	---	-0.18	0.03	-0.28	0.07
Soluble fraction 2/0/25	4.74	---	0.000	-0.16	0.08	-0.33	0.04	---	---	---	---				
Soluble fraction 1/2/24	5.16	---	0.000	---	---	---	---	---	---	---	---	---	---	---	---
Soluble fraction 2/2/24	5.16	---	0.000	-0.18	0.05	-0.28	0.03	---	---	---	---				
Soluble fraction 1/4/23	4.87	---	0.000	---	---	---	---	---	---	---	---	---	---	---	---
Soluble fraction 2/4/23	4.87	---	0.000	-0.22	0.05	-0.24	0.03	---	---	---	---				
Soluble fraction 1/6/22	5.25	---	0.000	---	---	---	---	---	---	---	---	---	---	---	---
Soluble fraction 2/6/22	5.25	---	0.000	-0.56	0.07	-0.87	0.03	-0.54	0.02	-0.83	0.06				
				-0.53	0.05	-0.80	0.03								
Soluble fraction 1/8/21	4.67	---	0.016	---	---	---	---	---	---	---	---	---	---	---	---

Soluble fraction 2/8/21	4.67	---	0.016	-0.44	0.07	-0.64	0.04	-0.46	0.04	-0.63	0.01				
				-0.51	0.05	-0.63	0.02								
				-0.43	0.03	-0.62	0.03								
Soluble fraction 1/10/20	4.42	---	0.067	-0.76	0.05	-1.04	0.03	---	---	---	---	-0.78	0.06	-1.15	0.10
Soluble fraction 2/10/20	4.42	---	0.067	-0.73	0.08	-1.19	0.04	-0.79	0.09	-1.20	0.02				
				-0.85	0.06	-1.22	0.03								
Soluble fraction 1/12/19	4.02	---	0.152	---	---	---	---	---	---	---	---	---	---	---	---
Soluble fraction 2/12/19	4.02	---	0.152	---	---	---	---	---	---	---	---				
Soluble fraction 1/14/18	3.80	---	0.198	---	---	---	---	---	---	---	---	---	---	---	---
Soluble fraction 2/14/18	3.80	---	0.198	-1.27	0.08	-1.85	0.04	-1.27	0.00	-1.85	0.00				
				-1.27	0.06	-1.85	0.04								
Soluble fraction 1/16/17	3.13	---	0.339	---	---	---	---	---	---	---	---	---	---	---	---
Soluble fraction 2/16/17	3.13	---	0.339	---	---	---	---	---	---	---	---				
Soluble fraction 1/18/16	2.68	---	0.434	-1.31	0.04	-1.90	0.03	---	---	---	---	-1.35	0.05	-1.94	0.06
Soluble fraction 2/18/16	2.68	---	0.434	-1.39	0.05	-1.98	0.02	---	---	---	---				
Soluble fraction 1/20/15	1.80	---	0.621	-2.48	0.04	-3.63	0.03	---	---	---	---	---	---	---	---

Soluble fraction 2/20/15	1.80	---	0.621	---	---	---	---	---	---	---	---				
Ppt fraction 1/0/25	---	0.00	0.000	---	---	---	---	---	---	---	---	---	---	---	---
Ppt fraction 2/0/25	---	0.00	0.000	---	---	---	---	---	---	---	---				
Ppt fraction 1/2/24	---	0.00	0.000	---	---	---	---	---	---	---	---	---	---	---	---
Ppt fraction 2/2/24	---	0.00	0.000	---	---	---	---	---	---	---	---				
Ppt fraction 1/4/23	---	0.00	0.000	---	---	---	---	---	---	---	---	---	---	---	---
Ppt fraction 2/4/23	---	0.00	0.000	---	---	---	---	---	---	---	---				
Ppt fraction 1/6/22	---	0.00	0.000	1.14	0.06	1.71	0.02	---	---	---	---	1.05	0.12	1.62	0.14
Ppt fraction 2/6/22	---	0.00	0.000	0.97	0.07	1.52	0.04	---	---	---	---				
Ppt fraction 1/8/21	---	0.08	0.016	---	---	---	---	---	---	---	---	---	---	---	---
Ppt fraction 2/8/21	---	0.08	0.016	0.93	0.06	1.38	0.04	0.90	0.03	1.36	0.02				
				0.88	0.04	1.34	0.02								
Ppt fraction 1/10/20	---	0.32	0.067	0.44	0.06	0.73	0.03	0.51	0.09	0.75	0.03	0.52	0.07	0.74	0.04
				0.57	0.04	0.77	0.03								

Ppt fraction 2/10/20	---	0.32	0.067	0.48	0.09	0.68	0.05	0.53	0.07	0.72	0.07				
				0.58	0.05	0.77	0.03								
Ppt fraction 1/12/19	---	0.72	0.152	---	---	---	---	---	---	---	---	---	---	---	---
Ppt fraction 2/12/19	---	0.72	0.152	---	---	---	---	---	---	---	---				
F4 Culture - 80 cm cont.															
Ppt fraction 1/14/18	---	0.94	0.198	0.32	0.05	0.46	0.03	---	---	---	---	0.31	0.02	0.40	0.05
Ppt fraction 2/14/18	---	0.94	0.198	0.33	0.06	0.38	0.04	0.31	0.03	0.37	0.02				
				0.29	0.07	0.35	0.03								
Ppt fraction 1/16/17	---	1.61	0.339	---	---	---	---	---	---	---	---	---	---	---	---
Ppt fraction 2/16/17	---	1.61	0.339	---	---	---	---	---	---	---	---				
Ppt fraction 1/18/16	---	2.06	0.434	0.44	0.04	0.63	0.02	---	---	---	---	0.36	0.12	0.60	0.05
Ppt fraction 2/18/16	---	2.06	0.434	0.28	0.05	0.56	0.03	---	---	---	---				
Ppt fraction 1/20/15	---	2.95	0.621	0.24	0.06	0.43	0.04	---	---	---	---	---	---	---	---
Ppt fraction 2/20/15	---	2.95	0.621	---	---	---	---	---	---	---	---				

F4 Culture - 120 cm															
Soluble fraction 1/0/25	4.90	---	0.000	-0.22	0.06	-0.28	0.04	---	---	---	---	---	---	---	---
Soluble fraction 2/0/25	4.90	---	0.000	---	---	---	---	---	---	---	---				
Soluble fraction 1/2/24	5.23	---	0.000	-0.19	0.03	-0.17	0.03	---	---	---	---	-0.15	0.05	-0.19	0.02
Soluble fraction 2/2/24	5.23	---	0.000	-0.12	0.05	-0.21	0.03	---	---	---	---				
Soluble fraction 1/4/23	4.97	---	0.000	-0.22	0.05	-0.30	0.03	---	---	---	---	-0.21	0.02	-0.31	0.00
Soluble fraction 2/4/23	4.97	---	0.000	-0.19	0.06	-0.31	0.03	---	---	---	---				
Soluble fraction 1/6/22	5.47	---	0.000	-0.41	0.04	-0.58	0.03	---	---	---	---	---	---	---	---
Soluble fraction 2/6/22	5.47	---	0.000	---	---	---	---	---	---	---	---				
Soluble fraction 1/8/21	5.29	---	0.000	-0.32	0.06	-0.45	0.03	---	---	---	---	-0.28	0.05	-0.44	0.01
Soluble fraction 2/8/21	5.29	---	0.000	-0.25	0.05	-0.43	0.04	---	---	---	---				
Soluble fraction 1/10/20	5.42	---	0.000	-0.48	0.07	-0.73	0.04	---	---	---	---	---	---	---	---
Soluble fraction	5.42	---	0.000	---	---	---	---	---	---	---	---				

2/10/20															
Soluble fraction 1/12/19	5.27	---	0.000	-0.43	0.07	-0.63	0.03	---	---	---	---	-0.43	0.01	-0.67	0.04
Soluble fraction 2/12/19	5.27	---	0.000	-0.44	0.03	-0.70	0.03	---	---	---	---				
Soluble fraction 1/14/18	5.38	---	0.000	-0.74	0.04	-1.10	0.03	---	---	---	---	---	---	---	---
Soluble fraction 2/14/18	5.38	---	0.000	---	---	---	---	---	---	---	---				
Soluble fraction 1/16/17	4.91	---	0.000	-0.70	0.08	-0.98	0.04	---	---	---	---	---	---	---	---
Soluble fraction 2/16/17	4.91	---	0.000	---	---	---	---	---	---	---	---				
Soluble fraction 1/18/16	4.80	---	0.020	-0.70	0.03	-1.01	0.03	---	---	---	---	---	---	---	---
Soluble fraction 2/18/16	4.80	---	0.020	---	---	---	---	---	---	---	---				
Soluble fraction 1/20/15	4.24	---	0.134	---	---	---	---	---	---	---	---	---	---	---	---
Soluble fraction 2/20/15	4.24	---	0.134	-0.66	0.05	-0.94	0.04	-0.68	0.03	-0.99	0.07				
				-0.70	0.04	-1.04	0.02								
Ppt fraction 1/0/25	---	0.00	0.000	---	---	---	---	---	---	---	---	---	---	---	---
Ppt fraction	---	0.00	0.000	---	---	---	---	---	---	---	---				

2/0/25															
Ppt fraction 1/2/24	---	0.00	0.000	---	---	---	---	---	---	---	---	---	---	---	---
Ppt fraction 2/2/24	---	0.00	0.000	---	---	---	---	---	---	---	---				
Ppt fraction 1/4/23	---	0.00	0.000	---	---	---	---	---	---	---	---	---	---	---	---
Ppt fraction 2/4/23	---	0.00	0.000	---	---	---	---	---	---	---	---				
Ppt fraction 1/6/22	---	0.00	0.000	0.98	0.06	1.45	0.03	---	---	---	---	---	---	---	---
Ppt fraction 2/6/22	---	0.00	0.000	---	---	---	---	---	---	---	---				
Ppt fraction 1/8/21	---	0.00	0.000	1.48	0.06	2.27	0.04	---	---	---	---	---	---	---	---
Ppt fraction 2/8/21	---	0.00	0.000	---	---	---	---	---	---	---	---				
Ppt fraction 1/10/20	---	0.00	0.000	---	---	---	---	---	---	---	---	---	---	---	---
Ppt fraction 2/10/20	---	0.00	0.000	---	---	---	---	---	---	---	---				
Ppt fraction 1/12/19	---	0.00	0.000	0.94	0.06	1.48	0.03	---	---	---	---	---	---	---	---
Ppt fraction	---	0.00	0.000	---	---	---	---	---	---	---	---				

2/12/19															
Ppt fraction 1/14/18	---	0.00	0.000	0.55	0.07	0.86	0.03	0.59	0.06	0.87	0.02	---	---	---	---
				0.63	0.05	0.88	0.02								
Ppt fraction 2/14/18	---	0.00	0.000	---	---	---	---	---	---	---	---				
Ppt fraction 1/16/17	---	0.00	0.000	0.76	0.09	1.12	0.04	---	---	---	---	---	---	---	---
Ppt fraction 2/16/17	---	0.00	0.000	---	---	---	---	---	---	---	---				
Ppt fraction 1/18/16	---	0.10	0.020	0.68	0.05	1.08	0.03	---	---	---	---	---	---	---	---
Ppt fraction 2/18/16	---	0.10	0.020	---	---	---	---	---	---	---	---				
Ppt fraction 1/20/15	---	0.65	0.134	0.35	0.05	0.52	0.02	---	---	---	---	0.27	0.08	0.44	0.11
Ppt fraction 2/20/15	---	0.65	0.134	0.30	0.06	0.42	0.03	0.24	0.06	0.42	0.11				
				0.25	0.05	0.53	0.02								
				0.17	0.06	0.30	0.03								
Uninoculated Control															
Soluble fraction 1/0/25	4.98	0.00	---	-0.18	0.06	-0.27	0.04	---	---	---	---	-0.16	0.03	-0.20	0.09
Soluble fraction 2/0/25	4.98	0.00	---	-0.14	0.07	-0.14	0.04	---	---	---	---				
Soluble fraction 1/2/24	5.45	0.00	---	-0.24	0.06	-0.30	0.03	-0.20	0.06	-0.23	0.09	-0.20	0.04	-0.24	0.07
				-0.16	0.09	-0.17	0.04								
Soluble	5.45	0.00	---	-0.21	0.05	-0.24	0.04	---	---	---	---				

fraction 2/2/24															
Soluble fraction 1/4/23	5.33	0.00	---	-0.19	0.05	-0.26	0.02	---	---	---	---	-0.15	0.06	-0.22	0.06
Soluble fraction 2/4/23	5.33	0.00	---	-0.11	0.06	-0.18	0.03	---	---	---	---				
Soluble fraction 1/6/22	5.79	0.00	---	-0.26	0.08	-0.34	0.04	---	---	---	---	-0.26	0.01	-0.32	0.02
Soluble fraction 2/6/22	5.79	0.00	---	-0.27	0.05	-0.31	0.03	---	---	---	---				
Soluble fraction 1/8/21	5.83	0.00	---	-0.16	0.04	-0.21	0.03	---	---	---	---	-0.13	0.04	-0.21	0.01
Soluble fraction 2/8/21	5.83	0.00	---	-0.09	0.04	-0.20	0.02	---	---	---	---				
Soluble fraction 1/10/20	6.20	0.00	---	-0.24	0.08	-0.35	0.04	---	---	---	---	-0.19	0.07	-0.29	0.08
Soluble fraction 2/10/20	6.20	0.00	---	-0.14	0.07	-0.24	0.04	---	---	---	---				
Soluble fraction 1/12/19	6.31	0.00	---	-0.11	0.07	-0.14	0.04	---	---	---	---	-0.14	0.04	-0.20	0.08
Soluble fraction 2/12/19	6.31	0.00	---	-0.17	0.07	-0.26	0.03	---	---	---	---				
Soluble	7.00	0.00	---	-0.26	0.07	-0.31	0.03	-0.18	0.09	-0.22	0.11	-0.21	0.09	-0.24	0.11
fraction				-0.08	0.06	-0.09	0.03								
1/14/18				-0.21	0.05	-0.25	0.03								
Soluble	7.00	0.00	---	-0.27	0.04	-0.32	0.03	---	---	---	---				

fraction 2/14/18															
Soluble fraction 1/16/17	6.92	0.00	---	-0.16	0.05	-0.14	0.03	---	---	---	---	-0.11	0.06	-0.16	0.03
Soluble fraction 2/16/17	6.92	0.00	---	-0.07	0.05	-0.18	0.03	---	---	---	---				
Soluble fraction 1/18/16	7.77	0.00	---	-0.18	0.05	-0.25	0.03	---	---	---	---	-0.14	0.06	-0.23	0.03
Soluble fraction 2/18/16	7.77	0.00	---	-0.10	0.05	-0.21	0.03	---	---	---	---				
Soluble fraction 1/20/15	7.88	0.00	---	-0.11	0.06	-0.21	0.04	---	---	---	---	-0.16	0.07	-0.22	0.01
Soluble fraction 2/20/15	7.88	0.00	---	-0.21	0.05	-0.22	0.03	---	---	---	---				
Dark Control															
Soluble fraction 1/0/25	5.01	0.00	---	---	---	---	---	---	---	---	---	---	---	---	---
Soluble fraction 2/0/25	5.01	0.00	---	---	---	---	---	---	---	---	---				
Soluble fraction 1/2/25	5.42	0.00	---	-0.21	0.09	-0.31	0.04	---	---	---	---	-0.18	0.04	-0.28	0.04
Dark control cont.															
Soluble fraction 2/2/25	5.42	0.00	---	-0.15	0.05	-0.25	0.03	---	---	---	---				

Soluble fraction 1/4/24	5.25	0.00	---	-0.17	0.06	-0.24	0.04	---	---	---	---	-0.20	0.05	-0.27	0.04
Soluble fraction 2/4/24	5.25	0.00	---	-0.24	0.04	-0.29	0.03	---	---	---	---				
Soluble fraction 1/6/23	5.75	0.00	---	-0.22	0.05	-0.29	0.03	---	---	---	---	-0.24	0.03	-0.32	0.04
Soluble fraction 2/6/23	5.75	0.00	---	-0.26	0.04	-0.35	0.03	---	---	---	---				
Soluble fraction 1/8/22	5.83	0.00	---	-0.15	0.08	-0.30	0.04	---	---	---	---	-.18	0.04	-0.28	0.04
Soluble fraction 2/8/22	5.83	0.00	---	-0.21	0.04	-0.25	0.02	---	---	---	---				
Soluble fraction 1/10/21	6.10	0.00	---	-0.18	0.05	-0.26	0.03	---	---	---	---	---	---	---	---
Soluble fraction 2/10/21	6.10	0.00	---	---	---	---	---	---	---	---	---				
Soluble fraction 1/12/20	6.40	0.00	---	-0.11	0.05	-0.17	0.04	---	---	---	---	-0.12	0.01	-0.17	0.00
Soluble fraction 2/12/20	6.40	0.00	---	-0.13	0.05	-0.17	0.03	---	---	---	---				
Soluble fraction 1/14/19	6.89	0.00	---	-0.19	0.05	-0.33	0.03	---	---	---	---	-0.20	0.02	-0.30	0.04
Soluble fraction 2/14/19	6.89	0.00	---	-0.22	0.05	-0.27	0.03	---	---	---	---				

Soluble fraction 1/16/18	7.10	0.00	---	-0.18	0.07	-0.17	0.04	---	---	---	---	-0.17	0.02	-0.16	0.01
Soluble fraction 2/16/18	7.10	0.00	---	-0.16	0.04	-0.15	0.03	---	---	---	---				
Soluble fraction 1/18/17	7.73	0.00	---	-0.27	0.07	-0.31	0.04	---	---	---	---	-0.20	0.09	-0.27	0.05
Soluble fraction 2/18/17	7.73	0.00	---	-0.14	0.06	-0.24	0.03	---	---	---	---				
Soluble fraction 1/20/16	8.28	0.00	---	-0.16	0.06	-0.28	0.03	---	---	---	---	-0.19	0.03	-0.26	0.12
Soluble fraction 2/20/16	8.28	0.00	---	-0.22	0.05	-0.37	0.03	-0.20	0.03	-0.26	0.17				
				-0.18	0.05	-0.14	0.04								

Molecular techniques

Denaturing gradient gel electrophoresis (DGGE)

To define and compare the phylogenetic diversity within the enrichment cultures to strain F4, genomic DNA was extracted from cultures of the two enrichments and strain F4 grown photoautotrophically on Fe(II) according to the protocol of Wilson (1995). In addition, approximately 5 mg of sodium hydrosulfite was added to the DNA extraction to reduce and solubilize Fe(III) precipitates in the culture. The extracted genomic DNA was used as a template for 16S rDNA amplification by standard PCR methods on a MasterCycler Gradient PCR machine (Eppendorf) using the primers GM5-GC (5' to 3': CGCCCGCCGCGCCCCGCGCCCGTCCCGCCGCCCCCGCCCGCCTACGGGAGGCAGCAG and 907M (5' to 3': CCGTCAATTCMTTTGAGTTT). The PCR program was as follows: 95°C for 1 min and then 24 cycles of 95°C for 1 min., 50°C for 1 min., and 72°C for 1.5 min, after which there was a 10 min extension time at 72°C. Amplification was confirmed by agarose gel electrophoresis (1% agarose). Following the protocols of Muyzer et al. (1998a), the amplified PCR products were separated on a 1.5 mm thick, polyacrylamide (6% (w/v)) gel containing a gradient of 20-60% urea and formamide as denaturants (where 100% denaturant contained 7 M urea and 40% v/v formamide). The gradient gel was made using a Bio-Rad model 385 gradient former and a Bio Rad EconoPump model EPI (10 ml/min) (Hercules, CA) and DGGE was conducted with a Bio-Rad D-gene system in TAE buffer at 200 Volts for 4 hours at 60°C.

Restriction fragment length polymorphism (RFLP)

For community analysis by RFLP, genomic DNA from the three cultures grown photoautotrophically on Fe(II) was extracted with the DNeasyTM Tissue Kit (Qiagen, Valencia, CA). Again, the extracted DNA was used as a template for 16S rDNA amplification as described above, in this case, using the primers 8F (5' to 3': AGAGTTTGATCCTGGCTCAG) and 1492R (5' to 3': GGTTACCTTGTTACGACTT). The PCR program here was: 94°C for 3 min and then 30 cycles of 94°C for 1 min., 55°C for 1 min., and 72°C for 1 min, after which there was a 10 min extension time at 72°C. After confirmation of amplification by agarose gel electrophoresis, the PCR products were cloned using the TOPO TA Cloning kit (Invitrogen, Carlsbad, CA) and transformed into E. coli. Plasmids were purified from approximately 95 clone-containing E. coli colonies for each of the three cultures by a high-throughput alkaline lysis procedure [127], and the purified plasmid product was used as a template to re-amplify the 16S rDNA insert using primers T3 (5' to 3': TAATACGACTCACTATA), and T7 (5' to 3': ATTAACCCTCACTAAAGGGA). The subsequent PCR products were digested with the enzymes HinP1 I and Msp I (New England Biolabs, final concentrations of 20 and 40 units of enzyme/ml respectively) overnight at 37°C and separated by electrophoresis on a 2.5% low melting point agarose gel. The clones were visually grouped into unique restriction pattern groups and representative clones from the largest groups were partially sequenced using the primer T3 and preliminarily identified using the Basic Local Alignment Search Tool (BLAST) [2]. For complete sequencing of the 16S rDNA gene clone of strain F4, the primers

T3, T7, and the bacterial primers 50F (5' to 3': AACACATGCAAGTCGAACG), 356F (5' to 3': ACTCCTACGGGAGGCAGCA), 515F (5' to 3': GTGCCAGCMGCCGCGGTAA), 805F (5' to 3': ATTAGATACCCTGGTAGTC), 926R (5' to 3': ACCGCTTGTGCGGGCCC) and 1200R (5' to 3': TCGTAAGGGCCATGATG) were used. Sequencing was performed at the DNA Sequencing Core Facility at the Beckman Institute at Caltech. The resultant sequences were edited and aligned using Sequencher (GeneCodes Corp.). Distance, parsimony and maximum likelihood phylogenetic trees were constructed using the ARB software package [165], and compared to determine the relative robustness of the resulting phylogenetic tree topologies.

Mineral analyses

Raman spectroscopy

For analysis of the biological precipitates by Raman spectroscopy, approximately one-week-old cultures of strain F4 and the two enrichments were transferred to an anaerobic chamber where 1 ml of culture containing rust-colored precipitates was taken with a syringe and transferred to a microcentrifuge tube. The precipitates were collected by centrifugation and incubated at room temperature for approximately 12 hours in 2.25% sodium hypochlorite (Chlorox) to remove residual organic materials. Controls where the precipitates were not subjected to sodium hypochlorite showed that this treatment only increased the signal to noise ratio and did not alter the Fe mineral phases (data not shown). The precipitates were washed three times with ultra-pure H2O that had been

equilibrated with an anoxic atmosphere and the precipitates were immediately analyzed on a Renishaw Micro Raman spectrometer operating with a 514.5 nm argon laser at a power of 0.5 mW using a 5x, 20x, and/or 100x objective. Multiple areas of the precipitates in all the cultures were analyzed to address the homogeneity of the material. Phases of the precipitates were identified by comparison to a standard database as well as to 2-line ferrihydrite and goethite (α-FeOOH) prepared according to Schwertmann and Cornell (1991).

Powder X-Ray diffraction

For analysis of the biological precipitates by powder x-ray diffraction (XRD), an approximately two and a half week-old culture of strain F4 was transferred to an anoxic chamber where 1 ml was removed with a syringe. The precipitates were collected by centrifugation and residual organic materials were oxidized with sodium hypochlorite as described above. The precipitates were washed three times with ultra-pure H2O that was equilibrated with an anoxic atmosphere, spread on a glass disk, and allowed to dry in an anaerobic chamber. XRD patters were obtained on a Scintag Pad V X-ray Powder Diffractometer using Cu-Kα radiation operating at a 35 kV and 30 mA and a θ-2θ goniometer equipped with a germanium solid-state detector. Each scan used a 0.04° step size starting at 10° and ending at 80° with a counting time of 2 seconds per step. Phases of the precipitates were identified by comparison to spectra in the PCPDFWIN program, © JCPDS-International Centre for Diffraction

Data, 1997, as well as to spectra obtained from synthetic 2-line ferrihydrite and α-FeOOH.

Standards and nomenclature

The two Fe isotope ratios measured in this study are reported as $^{56}Fe/^{54}Fe$ and $57Fe/^{54}Fe$ ratios in standard δ notation in units of per mil (‰), where:

(1) $\delta^{56}Fe\ ‰ = [(^{56}Fe/^{54}Fe)_{SAMPLE}/(^{56}Fe/^{54}Fe)_{WHOLE\text{-}EARTH})\text{-}1]\ 10^3$

and

(2) $\delta^{57}Fe‰ = [(^{57}Fe/^{54}Fe)_{SAMPLE}/(^{57}Fe/^{54}Fe)_{WHOLE\text{-}EARTH})\text{-}1]\ 10^3$

The $^{56}Fe/^{54}Fe$ whole-earth ratio is the average of 46 igneous rocks that have $\delta^{56}Fe = 0.00\pm0.05‰$. On this scale, the IRMM-14 Fe standard, available from the Institute for Reference Materials and Measurements in Belgium, has a $\delta^{56}Fe$ value of -0.09±0.05‰ and $\delta^{57}Fe$ value of -0.11±0.07‰ [11]. Co-variations in $\delta^{56}Fe$ and $\delta^{57}Fe$ values plot along a linear array, whose slope is consistent with mass-dependent fractionation, which provides an internal check for data integrity [11]. Differences in isotope composition between two components A and B are expressed in standard notation as:

3) $\Delta_{A\text{-}B} = \delta^{56}Fe_A - \delta^{56}Fe_B$

Experimental details

For the first set of Fe isotope fractionation experiments, single cultures of the two enrichments and an uninoculated medium blank were incubated at a distance of 40 cm from the incandescent light source. The isotopic compositions

of the starting reagents and culture inoculums for this experiment are listed in Table 4-1. All sampling was conducted under strictly anoxic conditions in an anaerobic chamber. At each sampling point throughout the growth period, the cultures were shaken vigorously to homogenize the contents. The total $Fe(II)_{aq}$ concentration was measured by the *Ferrozine* assay [159], to calculate "*F*", the fraction of $Fe(II)_{aq}$ oxidized, and 1 ml from each culture was removed for isotope analysis. This 1 ml sample was divided into two 0.5 ml fractions, each of which was transferred to a separate microcentrifuge tube, producing two duplicate samples for each time point; these duplicates provide an assessment of the accuracy of separation of solid and liquid phases. Because the medium preparation procedures described above appeared to eliminate the formation of Fe(II) precipitates during photosynthetic Fe(II)-oxidation, the Fe(III) precipitate was isolated from $Fe(II)_{aq}$ solely by centrifugation. The Fe(II)-containing supernatant was removed with a pipette and filtered through a 0.22 μm nylon filter; the Fe(III) precipitate was washed twice with ultra-pure H_2O. The small changes to the total culture volume that occurred from successive sampling were accounted for in the calculation of *F*. All samples were stored at -80°C until chemical processing for isotope analysis could be performed.

In the second set of experiments, Fe isotope fractionation produced by strain F4 was measured. The experimental setup in this case was similar to that for the enrichments but with two differences. First, the overall rate of Fe(II)-oxidation was varied by incubating duplicate cultures of strain F4 inoculated with approximately the same number of cells at 40, 80 and 120 cm distances from the

light source, and second, duplicate cultures were incubated in the dark as a control, in addition to duplicate uninoculated controls that were incubated in the light. Preparation followed the same methods as those used for the enrichment cultures.

Methods for isotopic analysis

Samples were quantitatively dissolved in 7 M HCl and chemically separated from other cations and organic material by a previously described column separation procedure [155, 164]. Briefly, the samples were subjected to two passages through an anion exchange resin (Bio-Rad AG 1X4 200-400 mesh) with 7.0 M double-distilled HCl as the eluent for matrix removal, and 0.5 M HCl as the eluent for Fe collection. Yields were quantitative to avoid possible mass fractionation during separation. After elution of the sample from the anion exchange column and HCl was removed by evaporation. Samples were then diluted to 400 ppb Fe using 0.1% Optima grade HNO_3 for isotope analysis. High-precision Fe isotope measurements were made using a Micromass IsoProbe multiple-collector inductively-coupled-plasma mass spectrometer (MC-ICP-MS) at the University of Wisconsin-Madison. Technical aspects of the MC-ICP-MS methods have been published in detail elsewhere [11, 155]. Instrumental mass bias corrections were made using a standard-sample-standard approach. The data were compared to theoretical models such as Rayleigh fractionation or closed-system equilibration (*e.g.*, equations 3.28 and 3.20b, respectively, in Criss, 1999), using α=1.0015.

RESULTS

Physiological and phylogenetic characterization of the cultures

Photoautotrophic oxidation of Fe(II)

All three cultures used in this study are able to grow photoautotrophically using $Fe(II)_{aq}$ as an electron donor. An increase in cell numbers (data not shown) accompanied by oxidation of $Fe(II)_{aq}$ to rust-colored Fe(III) precipitates occurs in all three cultures over a period of 7 to 10 days after inoculation into anoxic medium where Fe(II) is the sole source of electrons (Figure 4-1). The maximal rates of Fe(II)-oxidation in these cultures at a 40 cm distance from the light source are ~1.5 mM Fe(II)/day for strain F4 (between days 6 and 8), ~1.9 mM Fe(II)/day for enrichment 1 (between days 9 and 11) and ~1.5 mM Fe(II)/day for enrichment 2 (between days 11 and 13); the fraction of the total Fe(II)-oxidized in these cultures at the end of the experiment was 100%, 92%, and 93%, respectively. Neither an increase in cell numbers nor Fe(II)-oxidation is observed when these cultures are incubated in the dark. No cell growth occurs when Fe(II) (*i.e.*, the electron donor) is omitted and the cultures are incubated in the light. Moreover, no component of the medium is able to oxidize Fe(II) abiotically as shown by the lack of Fe(II)-oxidation in uninoculated controls (Figure 4-1). Together, these results indicate that the observed Fe(II)-oxidation is biologically-mediated by a light-dependent reaction that is correlated to an increase in biomass. Stoichiometric demonstrations of growth on Fe(II) have been reported previously [52, 69, 70, 163].

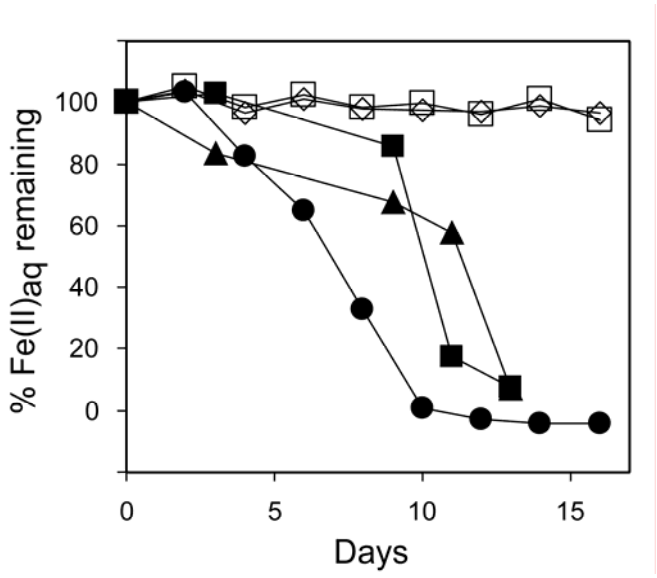

Figure 4-1: Fe(II)-oxidation by the two enrichment cultures and *Thiodictyon* strain F4. ● - F4, ■ - enrichment 1, ▲ - enrichment 2, □ - uninoculated control, ◇ - medium inoculated with F4, incubated in the dark. All cultures, except the dark control, were incubated at 40 cm from the 40 W light source. The dark control is representative of dark controls performed with the two enrichment cultures. Iron contents for the uninoculated and dark controls are consistent over time within analytical errors. Data for the enrichment cultures and *Thiodictyon* strain F4 were collected in separate experiments.

The effect of light intensity on the overall rate of biological Fe(II)-oxidation was investigated using duplicate cultures of strain F4 that were inoculated with approximately the same number of cells and incubated at various distances from the 40 W light source (40, 80, and 120 cm). As expected, the farther the cultures were from the light, the slower was their maximal rate of Fe(II)-oxidation (Figure 4-2). Maximal rates of ~1.5 mM Fe(II)/day, ~0.4 mM Fe(II)/day, and ~0.2 mM

Fe(II)/day were observed for the cultures at 40, 80, and 120 cm light distances, respectively. As a result, Fe(II) was oxidized to completion only in the strain F4 culture that was incubated at 40 cm from the light source within the timescale of the experiment (20 days).

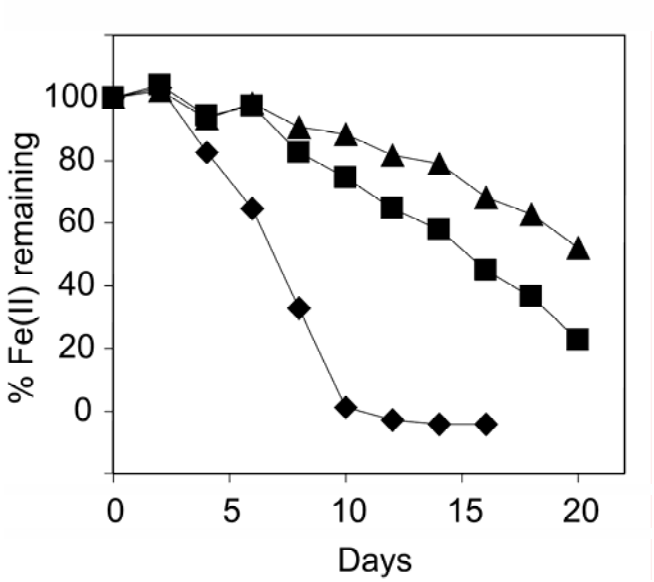

Figure 4-2: Fe(II)-oxidation by cultures of *Thiodictyon* strain F4 inoculated with approximately the same number of cells and incubated at 40, 80, and 120 cm from the light source. ◆ - F4 incubated at 40 cm from the light, ■ - 80 cm, ▲ - 120 cm. The data shown are representative of duplicate cultures.

Microscopy

Differential interference contrast (DIC) microscopy was used to visually characterize the three cultures. In the enrichment cultures, several morphotypes can be seen: all are rod-shaped, ranging in size from 0.5-1 μm wide and 1.5-2 μm long for the smallest cell type, to 1-1.5 μm wide and 4-5 μm long for the

largest, with some cells containing gas vacuoles (Figure 4-3A). Cells of strain F4 are approximately 1.5-2 µm wide and 5-7 µm long, contain gas vacuoles (Figure 4-3B), form long chains with side branches that give rise to net-like cell arrangements, and have a purple-violet pigmentation when grown photoheterotrophically on acetate. The variety of morphologies observed indicates that multiple types of bacteria are represented among the three cultures, although some cells in the enrichment cultures (*e.g.*, Type I, Figure 4-3A) appear similar to strain F4.

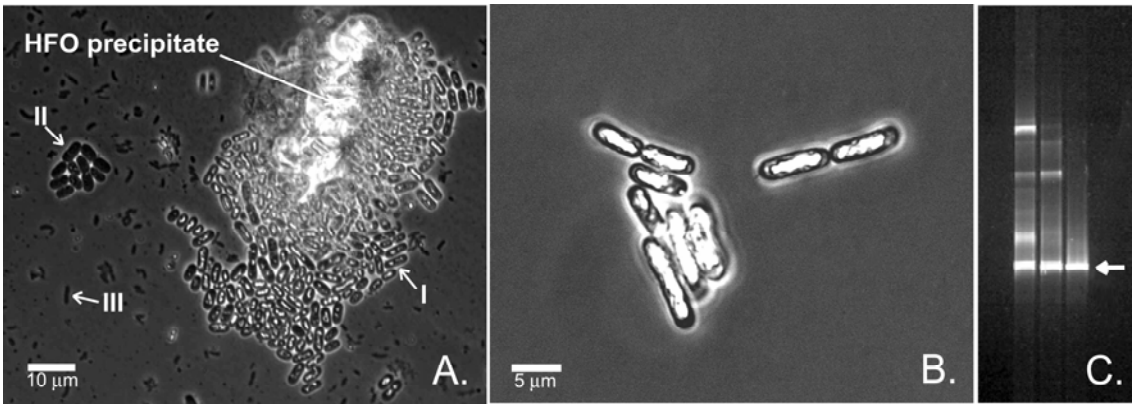

Figure 4-3: Differential interference contrast (DIC) micrographs of the enrichments and *Thiodictyon* strain F4. A. A representative micrograph of the two enrichments growing photosynthetically on 10 mM $Fe(II)_{aq}$ supplemented with 1 mM acetate. Three major cell morphologies are observed: approximately 1-1.5 µm by 4-5 µm, rod shaped cells with gas vacuoles (light areas within the cells) which tended to aggregate around the HFO precipitates (I), 1.5-2 µm by 3.5-4 µm rod shaped cells with no gas vesicles (II) and 0.5-1 µm by 1.5-2 µm rod shaped cells (III). B. DIC micrograph of *Thiodictyon* strain F4, growing photosynthetically on 10 mM $Fe(II)_{aq}$. Cells are approximately 1.5-2 µm by 5-7

μm and contain gas vacuoles. Note the similarity in size and shape between cells of *Thiodictyon* strain F4 and cells of type I in the enrichment culture. C. DGGE of the enrichments and *Thiodictyon* strain F4. From left to right lanes correspond to enrichment 1, enrichment 2 and *Thiodictyon* strain F4.

DGGE and RFLP analyses

To assess the diversity within our cultures, we used Denaturing Gradient Gel Electrophoresis (DGGE) and Restriction Fragment Length Polymorphism (RFLP) [30, 123]. DGGE and RFLP showed that multiple species are present in our enrichment cultures, corroborating the diversity of morphotypes observed by microscopy. An abundant organism in these cultures is very similar to strain F4 (DGGE results, Figure 4-3C; RFLP results not shown). Complete 16S rDNA sequence analysis of strain F4 showed that this isolate is a γ-Proteobacterium that groups with the *Thiorhodaceae* (Figure 4-4). The closest relative to this strain by 16S rDNA comparison (98% sequence identity, 1347 nucleotides considered) is the uncharacterized *Thiodictyon* strain Thd2 that is also able to oxidize Fe(II) phototrophically [52]. Other bacteria present in both of the enrichments were found to have sequences similar to the phototrophic Fe(II)-oxidizing strain *Chlorobium ferrooxidans* [69], and the Fe(III)-reducing heterotrophic genus *Geobacter* [110]. Preliminary RFLP data suggest that the abundance of Fe(III)-reducing organisms in the enrichments is low (data not shown), and thus it is unlikely that they appreciably affect the measured Fe isotope fractionations.

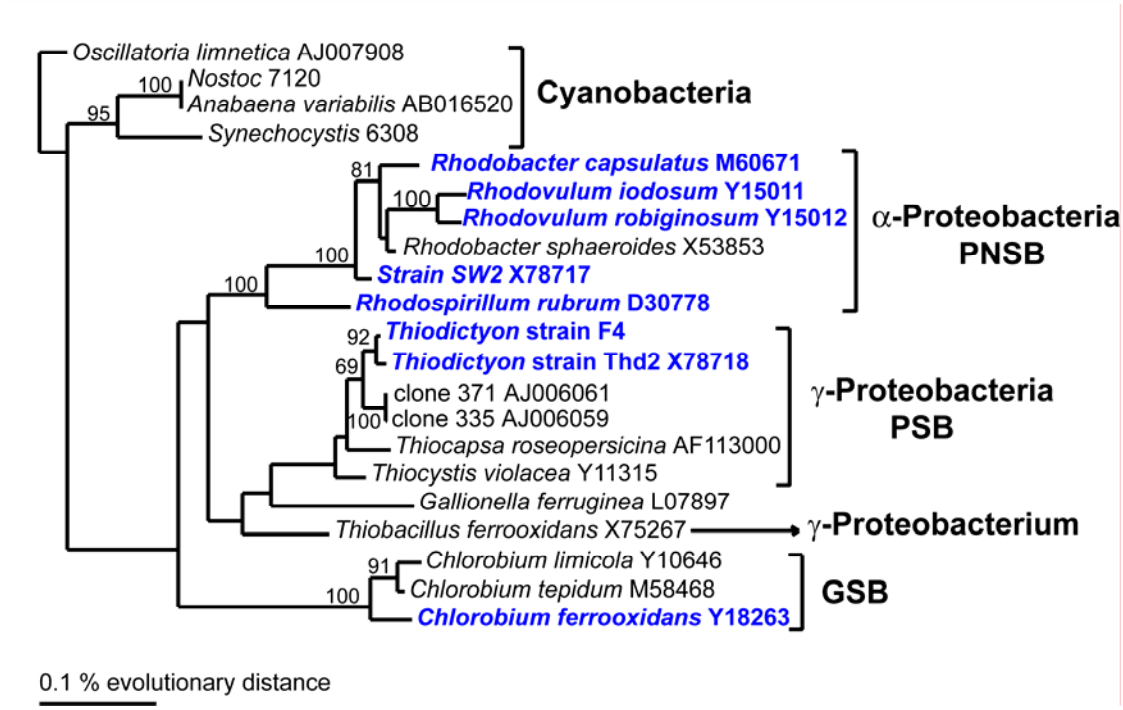

Figure 4-4: The phylogenetic relationship of *Thiodictyon* strain F4 inferred from 16S rDNA sequences. The tree was constructed by the maximum-likelihood method using the ARB software package with 1250 positions considered. Bootstrap values above 50% from 100 bootstrap analyses are given at branch nodes. Anaerobic phototrophs able to oxidize Fe(II) are in blue to illustrate the evolutionary diversity of organisms capable of this form of metabolism. Aerobic phototrophs (cyanobacteria) and other organisms capable of oxidizing Fe(II) non-photosynthetically are also shown for phylogenetic comparison. Accession numbers are listed after the bacterium. PNSB – purple non sulfur bacteria, PSB – purple sulfur bacteria, GSB – green sulfur bacteria.

Biological precipitates

The Raman spectra obtained using a 5x objective for the Fe(III) precipitates in all three cultures show either no distinctive peaks or generally resemble the spectrum obtained for synthetic 2-line ferrihydrite at the same laser power, with a broad peak ranging from approximately 950 to 1150 cm^{-1} (data not shown). The low signal to noise ratios in the spectra determined for the biological precipitates and the 2-line ferrihydrite synthetic reference, however, make it difficult to identify distinctive peaks. The peak at 950 to 1150 cm^{-1}, observed in our 2-line ferrihydrite standard, is not observed in the Raman spectrum of 2-line ferrihydrite published by Mazzetti and Thistlethwaite (2002). The spectrum of our 2-line ferrihydrite control analyzed under the 20x objective, however, more closely matches the published spectrum for this material with broad peaks at approximately 710, 1320, and 1550 cm^{-1}, and no broad peak at 950 to 1150 cm^{-1}. Subtle peaks at 290 and 400 cm^{-1} also exist in the spectrum we obtained for the 2-line ferrihydrite standard using the 20x objective. Under the 100x objective, these two peaks become more defined and intense and an additional intense peak at approximately 220 cm^{-1} is observed; these three peaks at approximately 200, 290 and 400 cm^{-1} are characteristic of hematite. A similar evolution of peaks was observed in the 2-line ferrihydrite spectrum of Mazzetti and Thistlethwaite (2002) after successive scans at increasing laser power. This suggests that thermal transformation of 2-line ferrihydrite to hematite occurred under the laser. As we increased the laser intensity on the biological precipitates, the spectra of the precipitates in all three cultures changed with

time, and eventually, spectra indicative of goethite were observed. This thermal transformation for both 2-line ferrihydrite and the biological precipitates occurs whether the same spot is analyzed at increasing laser intensity or new areas are chosen for analysis.

Because goethite is highly crystalline and our goethite standard produced a clear diagnostic spectrum at 5x objective power, if goethite had been present in significant amounts in our cultures, it would have been revealed using the 5x power objective. The fact that the ferric precipitates that formed in our cultures are easily transformed to goethite under the Raman laser suggests that they are unstable, and supports the interpretation that the primary precipitates are poorly crystalline hydrous ferric oxide (HFO); this is additionally supported by the 5x power Raman spectra on the solids, which gave little indication of diagnostic peaks. In no case were peaks in the Raman spectra found that correspond to vivianite or siderite.

Attempts to confirm the laser Raman spectroscopic results by XRD yielded inconclusive results due to the very fine-grained nature of the precipitates. Despite very slow scans (>18 hours), the two broad XRD peaks that are characteristic of 2-line ferrihydrite could not be discerned relative to background. Very small intensity peaks, only slightly higher than background, were observed for goethite and vivianite in the XRD spectra; no peaks matching those of siderite were observed (data not shown). As noted above, however, laser Raman spectra obtained at low power (where in situ conversion to goethite does not occur) did not reveal evidence for significant proportions of goethite,

vivianite, or siderite. We therefore conclude that poorly crystalline HFO constituted the only significant solid material in the biologically-induced precipitates.

Isotopic fractionation produced by the two enrichment cultures

Throughout the experiment with the enrichment cultures, the δ^{56}Fe values for $Fe(II)_{aq}$ are always lower than those of the HFO precipitate in both enrichment 1 and 2 (Figure 4-5A and 5B). The isotopic fractionation between $Fe(II)_{aq}$ and the HFO precipitate was relatively constant at early stages in reaction progress in each of the cultures (Table 4-2). No Fe(II)-oxidation was observed in the uninoculated control and no change in Fe isotope composition for $Fe(II)_{aq}$ over time relative to the δ^{56}Fe value of the initial Fe(II) reagent in the medium was observed (Figure 4-5C). This confirms that no significant precipitation of ferrous solids or abiotic Fe(II)-oxidation (followed by precipitation of ferric (hydr)oxides) occurred over the course of the experiment.

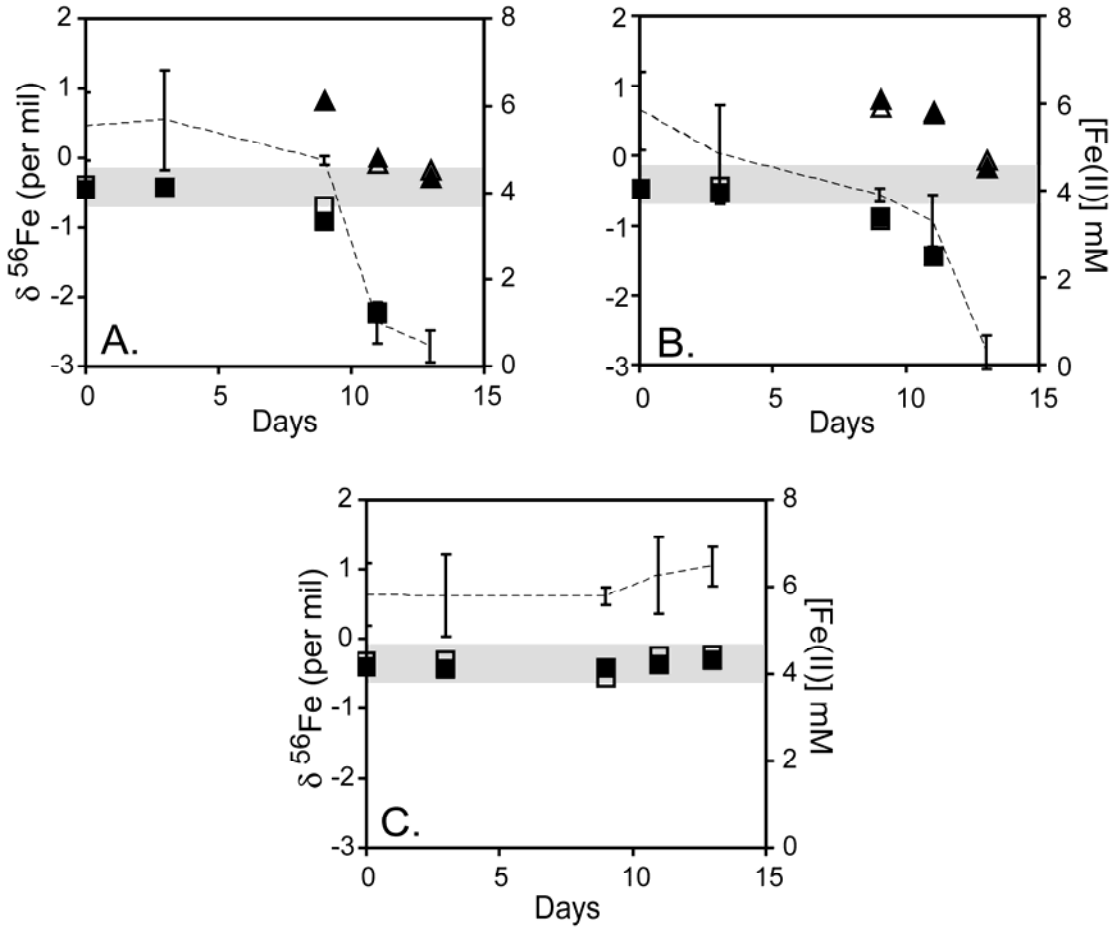

Figure 4-5: Isotopic data for the two enrichments incubated at 40 cm from the light source and the uninoculated control. The δ^{56}Fe values for duplicate samples of the $Fe(II)_{aq}$ and HFO fractions taken from single cultures are plotted as a function of time. A. Enrichment 1. ■ and □ - duplicate $Fe(II)_{aq}$ fractions. ▲ and △ - duplicate HFO fractions. B. Enrichment 2. ■ and □ - duplicate $Fe(II)_{aq}$ fractions. ▲ and △ - duplicate HFO fractions. C. The uninoculated control. ■ and □ - duplicate $Fe(II)_{aq}$ fractions. The dashed line plots on graphs A., B., and C. are $Fe(II)_{aq}$ concentrations (mM) as determined by *Ferrozine* assay and the error bars represent the error on triplicate assays for each time point. The shaded box on each of the graphs illustrates the error on the isotopic

measurements from the uninoculated control. In some cases the points are larger than the error.

Isotopic fractionation produced by Thiodictyon strain F4

Study of *Thiodictyon* strain F4 allowed us to circumvent the potential isotopic effects of multiple species in the enrichment cultures. In addition, using strain F4, we were able to assess potential kinetic or equilibrium isotope effects linked to the rate of overall Fe(II)-oxidation through variations in light intensity. As in the enrichment cultures, the data from the *Thiodictyon* strain F4 cultures show that $Fe(II)_{aq}$ had lower ^{56}Fe /^{54}Fe ratios as compared to the Fe(III) precipitate (Figure 4-6A, 6B and 6C). The isotopic fractionation between $Fe(II)_{aq}$ and the HFO precipitate remained relatively constant during the early stages of reaction progress (Table 4-3). The isotopic composition of the HFO precipitate at the end of the experiment was different for each incubation distance due to incomplete Fe(II)-oxidation in the 80 to 120 cm cultures vs. complete oxidation in the 40 cm cultures (Figure 4-6A, 6B, 6C and Table 4-3). The uninoculated and dark controls for *Thiodictyon* strain F4 showed no significant deviation in Fe isotope composition throughout the 20 days and the results from the two controls are identical within analytical error (Figure 4-6D, 6E and Table 4-3).

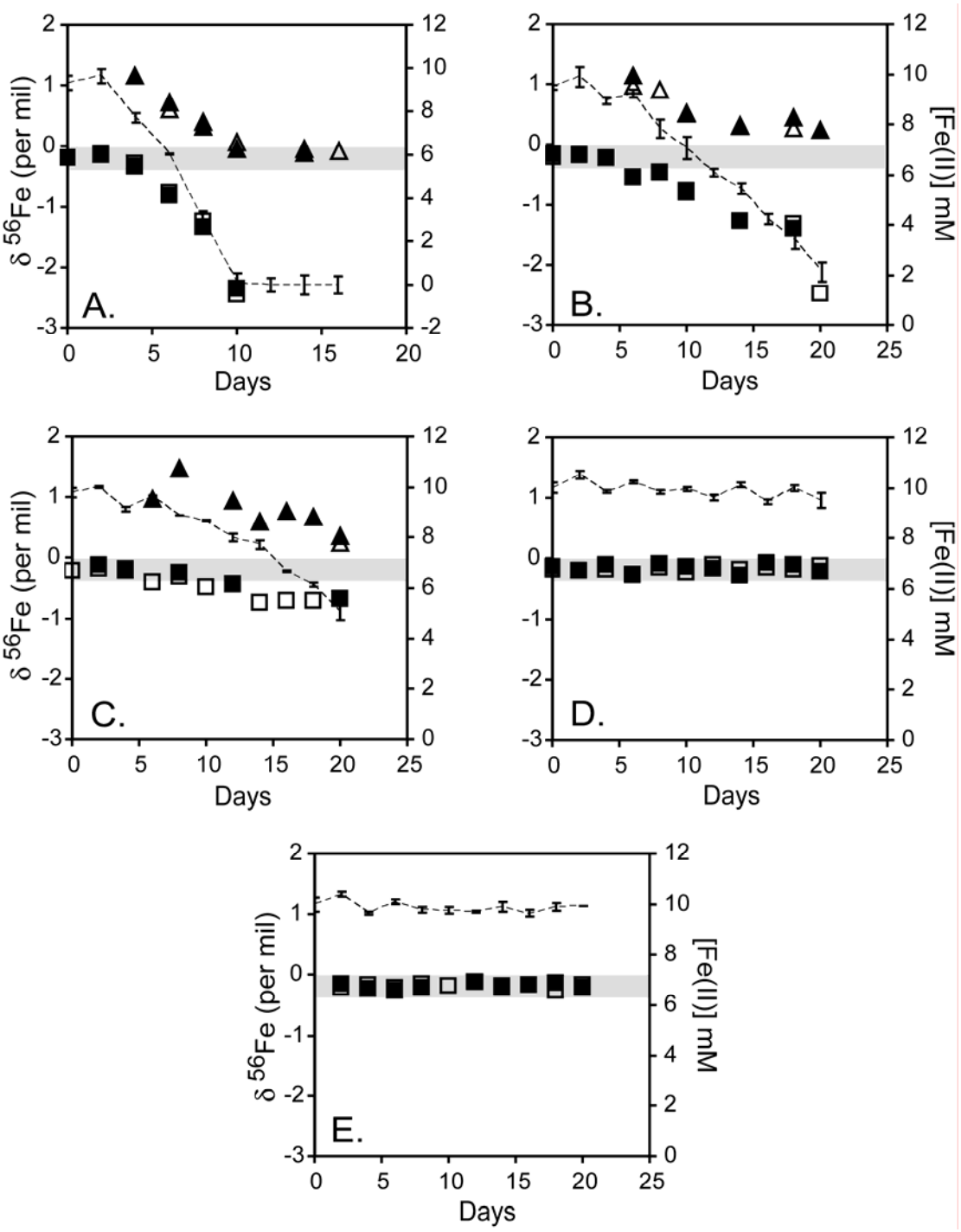

Figure 4-6: Isotopic data for *Thiodictyon* strain F4 incubated at 40, 80, and 120 cm from the light source and the uninoculated and dark controls. The $\delta^{56}Fe$ values for duplicate samples of the $Fe(II)_{aq}$ and HFO fractions taken from single cultures are plotted as a function of time. A. F4 incubated at 40 cm from the

light. ■ and □ - duplicate $Fe(II)_{aq}$ fractions. ▲ and △ - duplicate HFO fractions. B. F4 incubated at 80 cm from the light. ■ and □ - duplicate $Fe(II)_{aq}$ fractions. ▲ and △ - duplicate HFO fractions. C. F4 incubated at 120 cm from the light. ■ and □ - duplicate $Fe(II)_{aq}$ fractions. ▲ and △ - duplicate HFO fractions. D and E. The uninoculated and dark controls, respectively. ■ and □ - duplicate $Fe(II)_{aq}$ fractions. The dashed line plots on graphs A., B., and C. are $Fe(II)_{aq}$ concentrations (mM) as determined by *Ferrozine* assay and the error bars represent the error on triplicate assays for each time point. The shaded box on each of the graphs illustrates the error on the isotopic measurements from the uninoculated and dark controls. In some cases the plotted points are larger than the error.

DISCUSSION

Isotopic fractionation mechanisms: general observations

The isotopic fractionation between $Fe(II)_{aq}$ and the HFO precipitate is relatively constant (~ -1.5±0.2‰) for the enrichment and *Thiodictyon* strain F4 experiments during early stages in the reaction progress ("*F*") (Figure 4-7A, 7B, and Table 4-4) and appear to be independent of the Fe(II)-oxidation rate (Figure 4-7B). When the data are compared to the trends that would be expected for both a Rayleigh fractionation model (where the reaction product is isolated from further isotopic exchange with the system after formation) and a closed-system equilibrium model (where the reaction components remain open to isotopic exchange throughout the duration of the reaction), we find that our data fall in

between. Finally, isotopic mass-balance between $Fe(II)_{aq}$ and the solid precipitate is attained in all cases for solid-liquid pairs early in the experiments (where the true fractionations are best constrained) within the 2σ error of the isotopic measurements and calculated F values. The exception to this is the *Thiodictyon* strain F4 culture at 120 cm light distance. In this experiment, the $\delta^{56}Fe$ values of $Fe(II)_{aq}$ change between days 2 and 12, despite no significant change in $Fe(II)_{aq}$ contents, resulting in an F value of zero (Table 4-3). This observation suggests that small amounts of precipitate were forming early in the experiment that were below our detection limit.

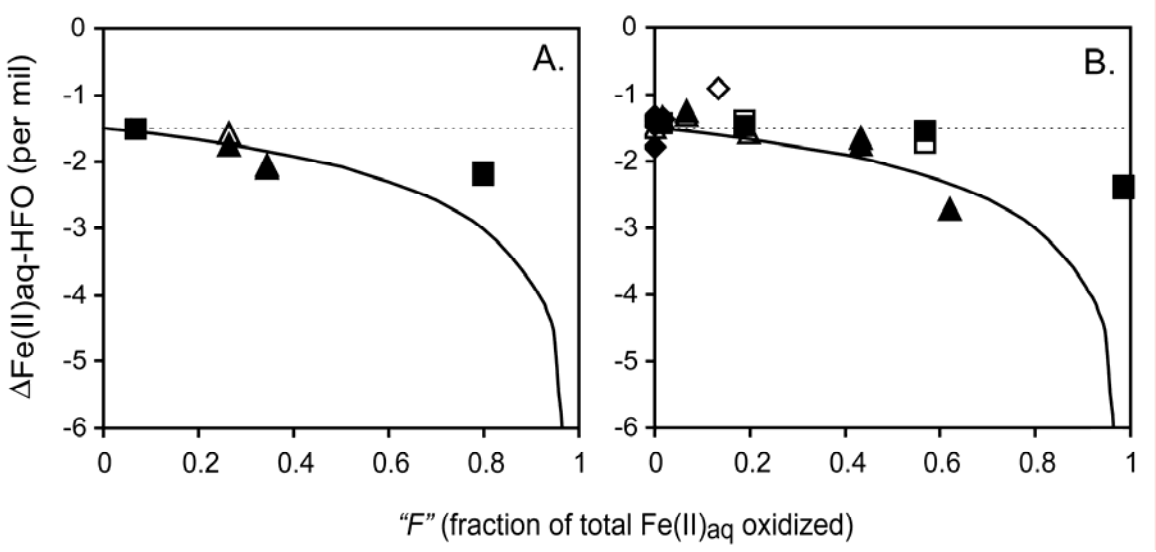

Figure 4-7: Fe isotope fractionations between $Fe(II)_{aq}$ and HFO in the enrichments and *Thiodictyon* strain F4 cultures. $\Delta_{Fe(II)aq\text{-}HFO}$ values are plotted as a function of "*F*", defined as the fraction toward complete oxidation of initial $Fe(II)_{aq}$. Note that the true isotopic fractionation factor (assuming it is constant over the reaction progress) is most closely constrained at low "*F*" values. Open

and closed symbols of the same type represent the difference between the $\delta^{56}Fe$ values of $Fe(II)_{aq}$ and HFO samplings, in duplicate, for a particular culture. A. The enrichments. ■ and □ - enrichment 1. ▲ and △ - enrichment 2. B. *Thiodictyon* strain F4. ■ and □ - the 40 cm culture. ▲ and △ - the 80 cm culture. ◆ and ◇- the 120 cm culture. Rayleigh (solid curved line) and closed-system (dashed straight line) equilibrium models are shown for comparison.

Table 4-4: Summary of fractionation factors using initial precipitates. Errors for individual experiments based on 1-standard deviation of the duplicate aliquots. Error for the Grand Average is based on the square root of the sum of the squares of the errors for the individual experiments.

Experiment	$\Delta_{Fe(II)-HFO}$
Enrichment 1 (Day 9)	-1.59 ± 0.15 ‰ (1σ)
Enrichment 2 (Day 9)	-1.68 ± 0.09 ‰ (1σ)
Thiodictyon strain F4, 40 cm, light (Day 4)	-1.46 ± 0.07 ‰ (1σ)
Thiodictyon strain F4, 80 cm, light (Day 6)	-1.60 ± 0.13 ‰ (1σ)
Thiodictyon strain F4, 120 cm, light (Day 6)	-1.39 ± 0.07 ‰ (1σ)
Grand Average	**-1.54 ± 0.24 ‰ (1σ)**

It is surprising that our data do not follow a Rayleigh fractionation model because the product of Fe(II)-oxidation is a ferric (hydr)oxide solid that is not expected to significantly exchange with the fluid after formation. Isotopic exchange experiments using enriched ^{57}Fe tracers have shown that although there is isotopic exchange between aqueous Fe and three nanometer (nm)

particles of ferrihydrite, this exchange is dominated by interaction with surface sites over timescales of days to weeks [133]. While it is difficult to measure the particle size of the culture precipitates because they aggregate, we may approximate their individual diameters as between 2-25 nm based on studies of natural and synthetic 2-line ferrihydrite [151]. Given the potentially high surface-to-volume ratio of these particles, isotopic exchange between aqueous Fe and ferrihydrite surface sites may have contributed to the difference between our measured values and the Rayleigh model. It is also possible that small nanoparticles of HFO passed through the filter during sample processing, and thus could have decreased the magnitude of the measured $\Delta_{Fe(II)\text{-}HFO}$ fractionation. This effect would be very small at the beginning of the reaction, when $Fe(II)_{aq}$ contents were high, but could become pronounced toward the end of the experiments where $Fe(II)_{aq}$ contents were low.

There are a number of steps in which Fe isotope fractionation could be occurring in our experimental system. First, isotopic fractionation could occur during binding of Fe(II) from the medium to a receptor ligand on or in the cell. Fractionation may also occur in a second step, during oxidation of the biologically bound Fe(II) to an aqueous Fe(III) species. Third, isotopic fractionation may occur between free or cell-associated Fe(II) and Fe(III) species. Fourth, precipitation of HFO might fractionate Fe, as might adsorption of Fe(II) onto HFO and/or cell surfaces. Finally, isotopic exchange between aqueous Fe and the HFO product might contribute. For each of these possibilities, isotopic fractionations may occur through kinetic or equilibrium processes.

Isotopic fractionation mechanisms: possible abiotic mechanisms

The approximately -1.5‰ fractionation between $Fe(II)_{aq}$ and HFO measured in our photosynthetic Fe(II)-oxidizing experiments is similar to that obtained in an abiotic system studied by Bullen et al. (2001). In these experiments, an $Fe(II)Cl_2$ solution was oxidized to ferrihydrite by raising the pH through the addition of $NaHCO_3$. Bullen et al. (2001) interpreted their measured Fe isotope fractionations to reflect isotopic exchange between $Fe(II)_{aq}$ and $Fe(II)(OH)X_{(aq)}$ species, noting that $Fe(II)(OH)X_{(aq)}$ is the most reactive species, and therefore an important precursor to ferrihydrite. While similar reactions might have occurred in our experiments, two major differences between the present study and that of Bullen et al. (2001) are 1.) that the later was performed under aerobic conditions, whereas our study was performed strictly anaerobically, and 2.) that the overall oxidation and precipitation rates of the Bullen et al. (2001) experiment were ~10^3 times faster than those used in our study. Although the final fractionation factor measured by Bullen et al. (2001) is indistinguishable from that measured early in our experiments (Table 4-4), the initial fractionation factor (-0.9±0.2‰) measured by Bullen et al. (2001) is significantly different. This makes it difficult to conclude that the fractionation factors observed in the two experiments result entirely from a common mechanism.

Despite these differences, a kinetic isotope effect during precipitation may have partially contributed to the fractionations measured in this study and that of Bullen et al. (2001). Drawing upon analogy with the study of Fe(III)-hematite fractionations by Skulan et al. (2002), who observed that kinetic $\Delta_{Fe(III)\text{-}Hematite}$

fractionations increased with increasing precipitation rates, we would expect rapid precipitation to produce significant Fe(III)-HFO fractionations (provided that the precipitation is not quantitative; [173]). Although we were able to control the rate of biological Fe(II)-oxidation in our experiments, which limited the overall precipitation rate by controlling the amount of Fe(III) available for precipitation, we were unable to control the rate at which aqueous Fe(III) converted to HFO. If, for example, a kinetic isotopic fractionation existed between Fe(III) and HFO in our experiments, and the $\Delta_{Fe(III)\text{-}HFO}$ kinetic fractionation is positive, then the measured $\Delta_{Fe(III)\text{-}HFO}$ fractionations would be smaller than those that truly existed between aqueous Fe(III) and Fe(II) pools in our experiments.

One final abiotic Fe isotope fractionation mechanism that may be common to our experiments and those of others, is that associated with Fe(II) sorption onto Fe (hydr)oxide minerals [75]. Assuming an HFO surface area of 600 m^2/g and a sorption capacity of 3×10^{-6} mol Fe(II)/m^2 [140], we calculate that only a small amount (<1%) of Fe(II) could have sorbed to HFO during early stages in the reaction progress. A surface area of 600 m^2/g is probably a maximum value, and if the HFO precipitates in our experiments consisted of larger crystals, or were highly clumped, the effective surface area would be much smaller. Nevertheless, even assuming a high surface area, we would not expect sorption to affect the isotopic composition of the system unless the fractionation during sorption was many 10's of per mil or greater, which seems unlikely.

Isotopic fractionation mechanisms: possible biological mechanisms

Identifying a biological mechanism for producing Fe isotope fractionation by Fe(II)-oxidizing phototrophs is challenging due to our lack of understanding of how these bacteria oxidize Fe(II) at the molecular level. For example, it is not yet clear whether oxidation of Fe(II) occurs inside or outside the cell. It has been proposed that oxidation of Fe(II) occurs at the cell surface and that electrons are shuttled to the phototrophic reaction center within the cytoplasmic membrane via a periplasmic transport system [52]. Alternatively, Fe(II) may be oxidized intracellularly by an enzyme located in the periplasm, as is the case for photoautotrophic sulfide oxidation by the sulfide-quinone reductase of Rhodobacter capsulatus [150]. If Fe(II) is oxidized intracellularly, we might expect that cell-produced Fe-chelators would help prevent intracellular precipitation of Fe(III) and/or mediate the export of Fe out of the cell. Alternatively, it is possible that Fe(III) is coordinated by inorganic ligands and that subtle changes in local pH control Fe(III) precipitation. The details of the metabolic steps involved in biological Fe(II)-oxidation may have significant implications for our interpretation of the Fe isotope fractionations produced by these bacteria, and a priority for future work is to elucidate the oxidation pathway.

Despite these uncertainties, our results suggest that equilibrium exchange between biological ligands is a possible explanation for the measured iron isotope fractionation. Although both theoretical and experimental work suggest that there are ligands that preferentially bind Fe(II) with strong covalent bonds [117, 132, 146], it seems more likely that the observed Fe isotope fractionations

are due to isotopic exchange between Fe(II) and Fe(III) species, given that some of the largest Fe isotope fractionations are predicted to occur between ferric and ferrous species [86, 132, 146, 181]. While we cannot be certain that our system was in isotopic equilibrium, it is striking (although perhaps coincidental) that different strains of the Fe(III)-reducing species *Shewanella alga*, grown using ferrihydrite or hematite as an electron acceptor, produce an approximately -1.3 ‰ fractionation in ^{56}Fe /^{54}Fe ratios between Fe(II) and ferric (hydr)oxide substrates [10, 11]. This isotopic fractionation is similar to the Fe isotope fractionations measured in this study, despite the fact that the phototrophic and *S. alga* cultures convert Fe via different redox reaction pathways, and at different rates.

If isotopic exchange between Fe(II) and Fe(III) is an important mechanism for the fractionation observed in the Fe(II)-oxidizing and Fe(III)-reducing biological experiments, this would seem to require ligands with similar binding strengths to be present in both systems. Whether these ligands are present as free species or cell-associated (*i.e.*, bound to a protein or a cell surface polymer) is unknown. However, given the abundance of Fe(II) in our experiments, it seems unlikely that Fe(II) would be chelated by a free biological ligand. Although we could not measure an aqueous pool of Fe(III) in our experiments, it is possible that the exchangeable Fe(III) pool is very small and below the detection limit of our assay. The characterization of Fe binding ligands (be they in solution or cell-associated) in both Fe(II)-oxidizing and Fe(III)-reducing biological systems is a necessary next step to better understand Fe isotope fractionation.

CONCLUSIONS

Iron isotope fractionation produced by diverse Fe(II)-oxidizing anaerobic phototropic bacteria results in poorly crystalline HFO products that have $^{56}Fe/^{54}Fe$ ratios that are ~1.5±0.2‰ higher than the $Fe(II)_{aq}$ electron donor. The measured isotope fractionations appear to be independent of the overall rate of Fe(II)-oxidation. Equilibrium isotope exchange between Fe(II) and Fe(III) bound to biological ligands may explain the observed fractionation. Alternatively, a kinetic isotope effect of rapid HFO precipitation overlying an equilibrium effect produced by ligand exchange is also consistent with the data. Despite a number of uncertainties in the mechanisms that underlie the observed isotopic fractionations, these results show that photosynthetic Fe(II)-oxidation, under anaerobic conditions, will produce ferric (hydr)oxide precipitates that have high $\delta^{56}Fe$ values relative to $Fe(II)_{aq}$ sources.

Can an Fe isotope "fingerprint" of anaerobic photosynthetic Fe(II)-oxidizing bacteria be recognized in the rock record? Johnson et al. (2003) noted that the moderately positive $\delta^{56}Fe$ values found in some oxide layers of the 2.5 Ga Kuruman and Griquatown Iron Formations might be explained by the +1.5‰ HFO-$Fe(II)_{aq}$ fractionations produced by Fe(II)-oxidizing phototrophs, assuming that ancient Fe(II) sources had moderately negative $\delta^{56}Fe$ values (~ -0.5‰), such as those of modern mid-ocean ridge hydrothermal fluids [12, 152]. If ambient oxygen contents were low at 2.5 Ga, as has been argued by many workers [58, 74, 91, 145], photoautotrophic Fe(II)-oxidizing bacteria may indeed be the best explanation for the occurrence of ferric oxides that have high $\delta^{56}Fe$ values in the

Archean rock record. It is as yet unknown what the Fe isotope effects would be of UV-photo-oxidation, which is an alternative means for producing ferric oxides in an anoxic environment [24]. If, however, ambient oxygen levels were sufficiently high in the Archean that oxidation of Fe(II) by oxygen could have occurred, similarly high δ^{56}Fe values for ferric oxides may have been produced. It therefore seems likely that interpretation of the Fe isotope record in terms of oxidative processes will require independent evidence regarding ambient oxygen contents in a particular environment.

5. Identification of genes involved in Fe(II) oxidation by *Rhodopseudomonas palustris* TIE-1 and *Rhodobacter* sp. SW2

ABSTRACT

Oxidation of Fe(II) by anoxygenic photoautotrophic bacteria is thought to be one of the most ancient forms of metabolism and it is hypothesized that these bacteria catalyzed the deposition of a class of Precambrian sedimentary rocks known as Banded Iron Formations. Testing this hypothesis requires knowledge of the molecular mechanism and components of this metabolism. To begin to identify these components and elucidate the mechanism of photoautotrophic Fe(II) oxidation, we have taken two approaches: 1) we have performed a transposon mutagenesis screen of the Fe(II)-oxidizing strain *Rhodopseudomonas palustris* TIE-1 and 2) we have expressed a genomic cosmid library of the genetically intractable, Fe(II)-oxidizing strain *Rhodobacter* sp. SW2 in *Rhodobacter capsulatus* SB1003 - a strain unable to grow photoautotrophically on Fe(II). In TIE-1, two genes, one predicted to encode an integral membrane protein that appears to be part of an ABC transport system and the other a homolog of CobS, an enzyme involved in cobalamin (vitamin B_{12}) biosynthesis, were identified. This suggests that components of the Fe(II) oxidation system of this bacterium may reside at least momentarily in the

periplasm and that a protein involved in Fe(II) oxidation may require cobalamin as cofactor. In the heterologous expression approach, four cosmids that confer Fe(II) oxidation activity to *Rhodobacter capsulatus* SB1003 were identified. Sequence analysis suggests that the gene(s) responsible for this phenotype encode a permease or a protein with binding domain for the redox cofactor pyrroloquinoline quinone (PQQ).

INTRODUCTION

Bacteria able to oxidize Fe(II) photoautotrophically are phylogenetically diverse and isolated strains include members of the purple sulfur (*Thiodictyon sp.* strain F4), purple non-sulfur (*Rhodobacter* strain SW2, *Rhodovulum sp.* strains N1 and N2, and *Rhodomicrobium vannielii BS-1*) and green sulfur bacteria (*Chlorobium ferrooxidans* KoFox) [41, 52, 69, 70, 163, 182]. These bacteria carry out a form of metabolism that likely represents one of the first to have evolved [20, 41, 185], and it has been proposed that direct photoautotrophic Fe(II) oxidation may have catalyzed the deposition of Banded Iron Formations (BIFs), a class of ancient sedimentary iron ore deposits [67, 101, 182]. In this respect, the effect these bacteria may have had on the Fe cycle of an ancient anaerobic Earth is of particular interest.

Indirect Fe(II) oxidation mediated by cyanobacteria, however, is also likely to have played a role in BIF deposition once the concentrations of O_2 produced by these organisms reached sufficient levels in the atmosphere and oceanic systems of the ancient Earth [37]. To distinguish these two biological processes

from each other in the rock record, as well as from other proposed abiotic mechanisms of Fe(II) oxidation [32], biological signatures that uniquely represent the activity of Fe(II)-oxidizing organisms and that are capable of being preserved in the rock record must be identified.

A first step towards identifying such biosignatures and quantifying the contribution of photoautotrophic Fe(II)-oxidizing bacteria to BIF deposition over time, is understanding the molecular mechanisms of Fe(II) oxidation by extant relatives of these ancient bacteria. Although first reported over a decade ago [182], very little is known about the molecular mechanism of Fe(II) oxidation in phototrophic bacteria. Thus, at present, there are no unique organic biomarkers associated with this physiology, nor are there clear inorganic biosignatures [41].

Here, in an effort to characterize the mechanism of photoautotrophic Fe(II) oxidation, we performed a transposon mutagenesis screen to identify genes involved in Fe(II) oxidation in the newly isolated, genetically tractable, *Rhodopseudomonas palustris* TIE-1 [83]. Two genes were identified; one predicted to encode an integral membrane protein that appears to be part of an ABC transport system and the other a homolog of CobS, an enzyme involved in cobalamin (vitamin B_{12}) biosynthesis. The role these gene products may play in Fe(II) oxidation by this phototroph is discussed.

In addition, to identify genes involved in Fe(II) oxidation in the genetically intractable Fe(II)-oxidizing photoautotroph, *Rhodobacter* strain SW2, a genomic cosmid library of this strain was expressed in *Rhodobacter capsulatus* SB1003 - a closely related strain unable to grow photoautotrophically on Fe(II). Four

cosmid clones that confer Fe(II) activity to *Rhodobacter capsulatus* SB1003 were identified and the specific gene(s) responsible for this phenotype was localized to an approximately 9.4 kilobase (kb) region on the insert of one of these cosmids. The identity of this gene(s) remains to be determined, but potential candidates identified through sequence analysis include genes predicted to encode a permease or a protein with binding domain for the redox cofactor pyrroloquinoline quinone (PQQ).

EXPERIMENTAL PROCEDURES

Bacterial strains, cosmids, and plasmids

Strains used are listed in Table 5-1. *Rhodobacter sp*. strain SW2 (SW2), *Rhodobacter capsulatus* strain SB1003 (1003), *Rhodobacter sphaeroides* CM06 (CM06) and *Rhodopseudomonas palustris* CGA009 (CGA009) were gifts from F. Widdel (MPI, Bremen, Germany), R. Haselkorn (U. Chicago), S. Kaplan (UT-Houston Medical School), and C. Harwood (UW-Seattle), respectively. *Rhodopseudomonas palustris* TIE-1 was isolated in our lab by Yongqin Jiao [83]. 1003, TIE-1and CGA009 were routinely grown in YP medium (3 g Bacto Yeast Extract and 3 g Bacto Peptone per Liter (BD, Franklin Lakes, New Jersey) and incubated at 30°C. CM06 and all *E. coli* strains were grown on Luria-Bertani (LB) medium and were incubated at 30°C and 37°C, respectively. When testing CM06 for complementation of the *trpB* mutation it carries, this strain was replica plated to Sistrom's minimal medium agar plates [154]. SW2 was maintained in a previously described anoxic minimal salts medium for freshwater cultures (basal

phototrophic medium) [52] and incubated at 16°C. This basal phototrophic medium was used for phototropic growth of all strains. Drug and other supplements were added as necessary. For *Rhodobacter* strains SW2, 1003 and CM06, concentrations of 1 µg/ml tetracycline, 5 µg/ml kanamycin, and 20 µg/ml gentamicin were used. For gentamicin in liquid, the concentration needed to be dropped to 5 µg/ml. Kanamycin and tetracycline were used at 200 and 75 µg/ml, respectively, for TIE-1. Drug and supplement concentrations for *E. coli* strains were: 15 µg/ml tetracycline, 50 µg/ml kanamycin, 50 µg/ml gentamicin, 0.2 mM diaminopimelic acid (DAP), 8.5 mg/ml isopropyl-ß-D-thiogalactopyranoside) (IPTG) and 30 mg/ml 5-bromo-4-chloro-3-indolyl-beta-D-galactopyranoside (X-gal). For phototrophic growth, strains were incubated approximately 30 cm from a 34 W tungsten, incandescent light source. All cultures containing tetracycline that were incubated in the light were incubated behind UV light filters to minimize the light mediated degradation of tetracycline [45]. Electron donors for photosynthetic growth were added to the basal phototrophic medium as follows: H_2 was provided as a headspace of 80% H_2: 20% CO_2, acetate was added from a 1 M, filter sterilized, anoxic solution at pH 7 to a final concentration of 10 mM and Fe(II) was added from a filter sterilized, anoxic 1 M Fe(II)$Cl_2 \cdot H_2O$ stock solution to a final concentration of 1 mM. The precipitate that forms after the addition of the Fe(II)$Cl_2 \cdot H_2O$ to the medium is likely a mixture of the ferrous minerals vivianite ($Fe_3(PO_4)_2 \cdot 8H_2O$) and siderite ($FeCO_3$) [41]. For cultivation of TIE-1 cultures, this precipitate was removed by filtration as previously described [41]. *E. coli* strains UQ950 and DH10β were

used for routine cloning and *E. coli* strains WM3064 or β2155 were used for transferring mobilizable plasmids and cosmids to *Rhodobacter* and *Rhodopseudomonas* strains.

Table 5-1: Bacterial strains and plasmids used in this study.

Strain or plasmid	Genotype, markers, characteristics and uses	Source and/or reference(s)
Bacterial Strains		
E. coli β2155	Donor strain for conjugation; *thrB1004 pro thi strA hsdS lacZΔM15* (F´ *lacZΔM15 lacIq trajD36proA+ proB+*) *ΔdapA::erm* (Erm^R) *pir*::RP4 *(::kan* (Km^R) from SM10)	[48]
E. coli WM3064	Donor strain for conjugation; *thrB1004 pro thi rpsL hsdS lacZΔM15 RP4–1360 Δ(araBAD)567 ΔdapA1341::[erm pir(wt)]*	W. Metcalf (UI-Urbana-Champaign)
E. coli UQ950	*E. coli* DH5α λ (pir) host for cloning; F-*Δ*(*argF-lac)169 Φ80dlacZ58(ΔM15*) *glnV44(AS) rfbD1 gyrA96*(Nal^R) *recA1 endA1 spoT1 thi-1 hsdR17 deoR λpir+*	D. Lies (Caltech)
E. coli DH10β	Host for *E. coli* cloning; F- *mcrA Δ*(*mrr-hsdRMS-mcrBC*) *Δ*80d*lacZΔ*M15 *ΔlacX74 deoR recA1 endA1 araD139 Δ*(*ara leu*)7697 *galU galK rpsL nupG* (Str^R)	D. Lies (Caltech)
Rhodobacter capsulatus SB1003	*rif-10*	R. Haselkorn (U. Chicago), [192]
Rhodobacter sphaeroides CM06	2.4.1*Δ*S CII *trpB*::Tn*5*TpMCS (Tp^R Trp^-)	S. Kaplan (UT-Houston Medical School), [112]
Rhodopseudomonas palustris CGA009	Wild type (ATCC BAA-98)	Caroline Harwood (UW-Seattle), [93]
Rhodopseudomonas palustris TIE-1	Wild type	Y. Jiao (Caltech), [83]

Rhodobacter sp. SW2	Wild type	F. Widdel (MPI, Bremen, Germany), [52]
Plasmids		
pRK415	10.5 kb incP-1 (pK2) Tc^R, *lacZα*	[92]
pT198	T198 PCR fragment, including the promoter region, cloned into the *XbaI* site of pRK415	This work
pT498	T498 PCR fragment, including the promoter region, cloned into the *XbaI* site of pRK415	This work
pLAFR5	21.5-kb broad-host-range cosmid cloning vector derivative of pLAFR3, *ori* RK2 (Tc^R, *lacZα*)	[92]
pBBR1MCS2	Derivative of pBBR1, (Km^R)	[102]
pBBR1MCS3	Derivative of pBBR1, (Tc^R)	[102]
pBBR1MCS5	Derivative of pBBR1, (Gm^R)	[102]
p2B3	Contains SW2 genomic DNA cloned into the *BamHI* site of pLAFR5 that confers Fe(II) oxidation activity and Tc^R to 1003	This work
p9E12	Contains SW2 genomic DNA cloned into the *BamHI* site of pLAFR5 that confers Fe(II) oxidation activity and Tc^R to 1003	This work
p11B3	Contains SW2 genomic DNA cloned into the *BamHI* site of pLAFR5 that confers Fe(II) oxidation activity and Tc^R to 1003	This work
p12D4	Contains SW2 genomic DNA cloned into the *BamHI* site of pLAFR5 that confers Fe(II) oxidation activity and Tc^R to 1003	This work
pP1	Sub-clone of an ~24 kb *PstI* fragment of p9E12 in pBBR1MCS3 (Tc^R)	This work
pP2	Sub-clone of an ~13 kb *PstI* fragment of p9E12 in pBBR1MCS3 (Tc^R)	This work
pP3	Sub-clone of an ~9.4 kb *PstI* fragment of p9E12 in pBBR1MCS3	This work

	(Tc^R)	
pP4	Sub-clone of an ~6.5 kb *PstI* fragment of p9E12 in pBBR1MCS3 (Tc^R)	This work
pP5	Sub-clone of an ~4 kb *PstI* fragment of p9E12 in pBBR1MCS3 (Tc^R)	This work
pP6	Sub-clone of an ~1.8 kb *PstI* fragment of p9E12 in pBBR1MCS3 (Tc^R)	This work
pP7	Sub-clone of an ~1.7 kb *PstI* fragment of p9E12 in pBBR1MCS3 (Tc^R)	This work
pH5	Sub-clone of an ~4 kb *HindIII* fragment of p9E12 pBBR1MCS2 (Km^R)	This work
pH6	Sub-clone of an ~1.5 kb *HindIII* fragment of p9E12 in pBBR1MCS2 (Km^R)	This work
pP3-gm1	Sub-clone of an ~9.4 kb *PstI* fragment of p9E12 pBBR1MCS5 (Gm^R)	This work
pP3-gm2	Sub-clone of an ~9.4 kb *PstI* fragment of p9E12 pBBR1MCS5 (Gm^R)	This work

Transposon mutagenesis of Rhodopseudomonas palustris TIE-1

Genetic screen for mutants defective in Fe(II) oxidation

To generate a library of transposon mutants to screen for Fe(II)-oxidation defects, the plasmid pSC189, carrying the kanamycin resistant hyperactive mariner transposon [35], was moved via conjugation from the donor strain, *E. coli* β2155, to TIE-1. A deletion of the *dapA* gene of *E. coli* β2155 renders it unable to grow without the exogenous addition of DAP to the growth medium [48]. Thus, TIE-1 exconjugants with transposon insertions can be selected on YP agar plates

containing kanamycin but no DAP. Transposon containing TIE-1 exconjugants were picked to 96 well microtiter plates containing YP plus kanamycin and incubated aerobically at 30°C overnight with shaking. Transposon containing isolates were tested for Fe(II) oxidation activity by a cell suspension assay. 20 µl of each clone grown in YP was transferred to conical bottom 96 well microtiter plates containing 200 µl phototrophic basal medium. These plates were incubated anaerobically in the light under an atmosphere of 80% N_2:15% CO_2:5% H_2 in an anaerobic chamber (Coy Laboratory Products, Grasslake, MI). After 3 days of incubation, the plates were centrifuged (3500 rpm for 7 min, JS 5.9 rotor Beckman rotor) and the supernatant was removed. In an anaerobic chamber, cell pellets were washed in 100 µl of anoxic buffer containing 50 mM Hepes, 20 mM NaCl, 20 mM NaHCO3 and 200-300 µM of Fe(II)$Cl_2 \cdot H_2O$ at pH 7. After 5-hour incubation in the light, the amount of remaining Fe(II) was determined by the *Ferrozine* assay [159]. 100 µl of *Ferrozine* solution (1g of *Ferrozine* and 500 g of ammonia acetate in 1 L of dH_2O) was added into each well and the OD_{570} was read after a 10 min incubation. Putative mutants were identified in instances where the total Fe(II) removed from the system was less than ~50% relative to the wild type. At least three independent checks were performed for each mutant.

Southern blot

To verify that the mariner transposon inserted in a random fashion, we performed southern blot on 10 randomly selected mutants from different mating

events. *SmaI* and *SphI* digested genomic DNA from the mutants was separated on a 1% agarose gel and transferred to nylon membrane using a positive pressure blotting apparatus (Stratagene, CA) according to the manufacturer's instructions. Probe DNA was prepared from a gel-purified *MluI* restriction fragment of pSC189 that contained an internal part of the mariner transposon including the kanamycin resistance gene. Approximately 25 ng of probe DNA was labeled with 50 µCuries of alpha-P32-dCTP using the Ready-To-Go labeling beads (Amersham Pharmacia Biotech). Prior to hybridization, unincorporated radioactive nucleotides were removed from the reaction by centrifugation through sephadex columns (ProbeQuant G-50 Microspin columns, Amersham Pharmacia Biotech) according to the manufacturer's instructions. Nylon membranes were hybridized overnight at 65˚C. Hybridized membranes were washed 3 times for 5 minutes each in 2x SSC buffer (20 x SSC: 175.3 g/L NaCl plus 88.2 g/L of trisodium citrate) plus 0.1% SDS (sodium dodecyl sulfate) at room temperature, then twice for 15 minutes each with 0.1x SSC plus 0.1% SDS at 65˚C. The membrane was exposed to X-ray film at -80°C for 48 hr prior to development.

Cloning of mariner-containing fragments

To identify the DNA sequence flanking the transposon in the mutants, genomic DNA was digested with restriction enzyme *SacII* followed by ligation at a DNA concentration (2-3 µg/ml) that favored intramolecular ligation [136]. Ligated DNA was washed and concentrated using a DNA purification kit (Qiagen) and transformed into *E. coli* UQ950 cells. Plasmid DNA was extracted from overnight

cultures of kanamycin resistant clones. The sites of transposon insertions of these mutants were determined by sequencing with primers Mar3 (5'-CTTCTTGACGAGTTCTTCTGAGC-3') and Mar4 (5'-TAGGGTTGAGTGTTGTTCCAGTT -3') that anneal near the ends of the mariner transposon in opposite directions.

Complementation of Fe(II) oxidation mutants

Plasmid pT198 and pT498 were constructed to complement the genetic defect in mutants 76H3 and A2, respectively. Primers were designed based on the corresponding gene sequences in *R. palustris* CGA009 that were analogous to the disrupted genes in the mutants. For mutant 76H3, a 1.4 kb gene fragment was amplified through PCR from wild type TIE-1 with primers T198L (5'-GGCTCTAGATCAACCAGAAACCAGCTTCC-3') and T198R (5'-GGCTCTAGATGTGAGCCACTCTGTCATCC-3'). For mutant A2, a 1.3 kb gene fragment was generated with primers T498L (5'-GGCTCTAGACAATTGCGACAGCTTACGAC-3') and T498R (5'-GGCTCTAGA AGAACCGCCTTCTTGGTCT-3'). The purified PCR products were digested and ligated to the *XbaI* cloning site of the broad host plasmid pRK415 vector to generate the vectors pT198 and pT498 for complementation. pT198 and pT498 were introduced into *E. coli* UQ950 by transformation. Transformants with the inserts were isolated through a blue/white screen on LB plates with tetracycline (15 µg/ml). The plasmids pT198 and pT498 were purified from *E. coli* UQ950, transformed by heat shock into the donor strain *E. coli* WM3064 and moved via

conjugation into the mutant TIE-1 strains. Similar to *E. coli* β2155, *E. coli* WM3064 not only contains the genes required for plasmid transfer on its chromosome, but also requires DAP for growth. TIE-1 exconjugants containing vector pT198 and pT498 were selected on YP agar plates supplemented with 75 µg/ml of tetracycline. Colonies were picked and grown up in YP liquid medium with tetracycline (75 µg/ml). YP cultures were washed and sub-cultured in the basal medium plus tetracycline (75 µg/ml) with H_2 as the electron donor. Cells were then collected by centrifugation and tested for complementation of Fe(II)-oxidation activity by the cell suspension assay as described above.

Heterologous expression of a genomic cosmid library of Rhodobacter sp. SW2 in Rhodobacter capsulatus SB1003

Preparation of a genomic cosmid library of Rhodobacter SW2 in E. coli WM3064

Genomic DNA from SW2 was isolated according to standard protocols [43]. 25 mls of SW2 grown phototrophically on acetate was harvested for 10 minutes at 5000 rpm on a JA 25.50 Beckman rotor. The pellet was resuspended in 25 mls of lysis buffer (0.25 mls 1 M Tris·HCL pH7.4, 0.5 mls 0.5 M EDTA pH 7.4, 2.5 mls 1 mg/ml proteinase K, 21.75 mls dH_2O), after which 1.25 mls of 10% SDS was added. After a 4 hour incubation at 37°C, 0.75 ml 5 M NaCl was added. Following sequential phenol and chloroform extractions, genomic DNA was precipitated with 100% EtOH, harvested by centrifugation, washed with 70% EtOH and resuspended in 1 ml of TE buffer (10 mM Tris·HCL pH 8, 1 mM EDTA

pH 8). pLAFR5 and all other cosmid DNA was purified using the Qiagen HiSpeed Plasmid Midi Kit (Qiagen, Valencia, CA).

After optimization of partial digestion conditions on a small scale, 13.2 µg of SW2 genomic DNA was digested at 37°C for 3-4 min with 0.2 Units of *Sau3AI*. After incubation at 65°C for 20 min, the genomic DNA fragments were dephosphorylated for 45 min with HK Thermolabile Phosphatase (Epicentre, Madison, WI) according to the manufacturer's instructions. 26.9 µg of the pLAFR5 cosmid vector [92] was digested sequentially with *ScaI* and *BamHI* at 37°C.

Ligations containing 7.5 µg total DNA were carried out at a 9:1 molar ratio of insert to vector. Appropriate volumes of vector and insert were combined, brought up to 500 µl with dH_2O and the mixture was concentrated to ~14.5 µl using a Pall Nanosep 30K Omega filter spin column (Pall, East Hills, New York). T4 DNA liagase (Roche, Basel, Switzerland), ligase buffer and ATP (5 mM final concentration to inhibit blunt ligations) were added, the reactions were brought up to 20 µl with dH_2O and incubated at 16°C overnight.

The Stratagene Gigapack III XL packaging extract (Stratagene, La Jolla, CA) was used to package the ligation reaction (0.375 µg total DNA) into recombinant λ phage. An undiluted portion of the packaging reaction was used to infect *E. coli* DH10β according to the manufacturer's instructions. *E. coli* containing cosmids with inserts were selected on LB + tetracycline, DAP, IPTG and X-gal. Cosmids were purified from 10 random white colonies for restriction digest with *EcoRI* to verify that the library was random and determine the

average insert size. After this diagnostic, the rest of the packaging reaction was used to infect *E. coli* WM3064. The library in this strain was stored at -80°C in LB containing tetracycline, DAP, and 10% glycerol.

Introduction of the SW2 cosmid library into Rhodobacter capsulatus SB1003

The SW2 cosmid library was introduced into 1003, a strain unable to grow phototrophically on Fe(II), via conjugation from the WM3064 hosts. Each cosmid containing WM3064 strain was mated to 1003 independently to ensure complete representation of the cosmid library. WM3064 clones were grown in 1 ml of LB + tetracycline and DAP in 96 deep well plates overnight at 37°C with shaking. The cells were harvested by centrifugation (3500 rpm for 15 min using a JS 5.9 rotor Beckman rotor) and washed once with LB to remove traces of tetracycline. To the each of the pellets, 1 ml 1003 was added and the plate was centrifuged again. Cell pellets were resuspended in 20 µl of YP and spotted individually to a 245 mm by 245 mm YP agar plate. The mating plate was incubated at 30°C for 18-22 hours after which the mating spots were resuspended in 200 µl YP + 1 µg/ml tetracycline. The entire mating was plated to a 60 mm by 15 mm agar pate of YP + 1 µg/ml. Exconjugants were inoculated into 96 well microtiter plates containing YP + 1 mg/ml tetracycline and incubated overnight at 30°C with shaking. After growth, sterile glycerol was added to a final concentration of 10% and the library was preserved at -80°C.

Identification of cosmid clones conferring Fe(II) oxidation activity by cell suspension assay

Cosmid containing 1003 exconjugants were tested for Fe(II) oxidation activity by a cell suspension assay similar to that described above. Here, 10 µl of each clone grown in YP was transferred to conical bottom 96 well microtiter plates containing 200 µl phototrophic basal medium. These plates were incubated anaerobically in the light in a GasPak 150 large anaerobic jar under a headspace of 80% H_2:20%CO_2. Residual O_2 was eliminated from the headspace using a BBL GasPak Brand Disposable H_2 and CO_2 Envelope (BD, Franklin Lakes, NJ). After growth, the plates were centrifuged and the supernatant was removed. In an anaerobic chamber (Coy Laboratory Products, Grasslake, MI), cell pellets were washed in 200 µl of assay buffer (an anoxic buffer containing 50 mM Hepes, 20 mM NaCl at pH 7) to remove traces of the medium and centrifuged. The pellets were then resuspended in 100 µl of assay buffer containing 0.1 mM of $FeCl_2$ and 20 mM $NaHCO_3$. After an approximately 20-hour incubation in the light, the amount of remaining Fe(II) was determined by the *Ferrozine* assay [159]. Here, 100 µl of *Ferrozine* solution was added into each well. The plates were then centrifuged, 100 µl of the supernatant was transferred to a flat bottom 96 well plate and the OD_{570} was read after a 10 min incubation. Putative Fe(II) oxidizing clones were identified as those clones that had less remaining Fe(II) that the negative control, 1003 + pLAFR5. SW2 served as a positive control. Putative clones were retested in triplicate. Clones that came

through as positive after the retesting were reconstructed and retested in triplicate.

For cell suspension assays where the total concentration of Fe as well as Fe(II) was followed, exponential phase cultures of cosmid containing 1003 cells grown phototrophically on H_2 + 1 µg/ml tetracycline were diluted to the same OD_{600}. 5 mls of these cultures were harvested by centrifugation (10,000 rpm on a Beckman JLA 10.5 rotor for 20 min) and then, under anaerobic conditions, the cell pellets were washed once with an equal volume of assay buffer and resuspended in 2.5 mls of assay buffer containing 0.1 mM $Fe(II)Cl_2 \cdot H_2O$ and 20 mM $NaHCO_3$. Cell suspensions were incubated at 30°C in 12 ml stoppered serum bottles 30 cm from a 34 W tungsten incandescent light bulb under a headspace of 80% N_2:20% CO_2. Fe(II) and Fe(III) concentrations were measured in triplicate by the *Ferrozine* assay where 50 µl of cell suspension was added to either 50 µl of 1N HCl (Fe(II) measurement) or 50 µl of a 10% hydroxylamine hydrochloride solution in 1N HCL (Fe total measurement). 100 µl of *Ferrozine* solution was then added and after 10 minutes the absorbance at OD_{570} was read. Fe concentrations were determined by comparison to Fe(II) standards.

Sub-cloning of cosmid clones

To identify a smaller fragment of cosmid 9E12 that conferred Fe(II)-oxidation activity, restriction fragments of this cosmid were cloned into broad-host-range vectors of the pBBR1 series [102]. p9E12 was digested with *PstI* and

HindIII, pBBR1MCS-2 was digested with *HindIII* and pBBR1MCS-3 and pBBR1MCS-5 were digested with *PstI*. All vectors were dephosphorylated with Antarctic Phosphatase (New England Biolabs, Beverly, MA) according to the manufacturer's instructions. The restriction fragments were gel purified using Qiagen kits (Qiagen, Valencia, CA). Fragments less than 10 kb were purified using the QIAquick Gel Extraction kit and fragments greater than 10 kb were purified using the QIAEX II Gel Extraction kit. Ligation reactions contained an approximately 6:1 volume ratio of insert to vector and were transformed into *E. coli*DH10β. Clones containing inserts were selected on the appropriate drug containing plates supplemented with DAP, IPTG, and X-gal. Plasmids were purified from putative clones using a QIAprep Spin Miniprep Kit and digested with the appropriate restriction enzyme to verify the insert size. Clones with the correct size insert were introduced into *E. coli* WM3064 by transformation and subsequently introduced into 1003 via conjugation. Exconjugants were tested for Fe(II) oxidation activity in the 96 well plate cell suspension assay format described above.

Sequencing and analysis

All sequencing was performed by Laragen (Los Angeles, CA). Putative ORFs were identified using ORF finder (http://www.ncbi.nlm.nih.gov/gorf/gorf.html). Proteins in the database similar to the translated ORFs were identified by BlastP (http://www.ncbi.nlm.nih.gov/blast/), and conserved domains were identified

using the NCBI Conserved Domain Database (CDD) (http://www.ncbi.nlm.nih.gov/Structure/cdd/wrpsb.cgi). Additional protein analyses (*e.g.,* sub-cellular localization and motif identification) were preformed using the tools on the ExPAsy proteomics server (http://us.expasy.org/). Predicted promoters were identified using BPROM (http://www.softberry.com/berry.phtml?topic=bprom&group=programs&subgroup=gfindb), a bacterial σ^{70} promoter recognition program with ~80% accuracy and specificity.

RESULTS

Genes involved in photoautotrophic Fe(II)-oxidation by Rhodopseudomonas palustris strain TIE-1

To identify genes involved in phototrophic Fe(II) oxidation in TIE-1 we performed transposon mutagenesis on this strain using a hyperactive mariner transposon. We chose this transposon because it exhibits a relatively high transposition frequency in diverse gram-negative bacteria and integrates into the host chromosome with little sequence specificity [35]. The frequency of transposon insertion obtained for TIE-1 was ~10^{-5} with this transposon. Southern blot analysis of 10 randomly selected isolates derived from independent transposition events indicated that the transposon integrates as a single event in random locations (data not shown).

We performed a limited screen of ~12,000 transposon insertion mutants for defects in phototrophic Fe(II) oxidation using a cell suspension assay. Based

on the assumption that strain TIE-1 has the same number of genes as strain CGA009 and that the transposition is purely random, this screen is ~88% saturated assuming a Poisson distribution [36]. Fourteen mutants were identified as being defective in Fe(II) oxidation: eight mutants had general photosynthetic growth defects; the other six were specifically defective in Fe(II) oxidation. BLAST analysis performed on DNA sequences flanking the mariner insertions revealed that the sequence flanking the transposon has significant similarity to sequences from the genome of *R. palustris* strain CGA009 [105] in all cases.

The eight mutants exhibiting general growth defects grew at least 50% less on acetate and H_2 compared to the wild type (data not shown). Two of these mutants were disrupted in genes that are homologs of *bchZ* and *bchX*, known to encode proteins involved in bacteriochlorophyll synthesis [29]. These mutants will not be discussed further here, however, it is not surprising that our screen picked up components of the general photosynthetic electron transport system given the large variance in cell density in the step prior to the cell suspension assay. Two mutants, however, were identified that are specifically defective in Fe(II) oxidation: 76H3 and A2. 76H3 is a representative of 5 mutants that have transposon insertions at different locations in the same gene, whereas A2 was only isolated once. Both mutants exhibit normal photosynthetic growth in minimal medium with H_2 as the electron donor, but their ability to oxidize Fe(II) is less than 10% of the wild type (Figure 5-1A and 1B). Complementation of the disrupted genes indicates that their expression is necessary and sufficient to

restore nearly wild-type levels of activity, suggesting that Fe(II) oxidation defects were not caused by the downstream genes (Figure 5-1C and 1D).

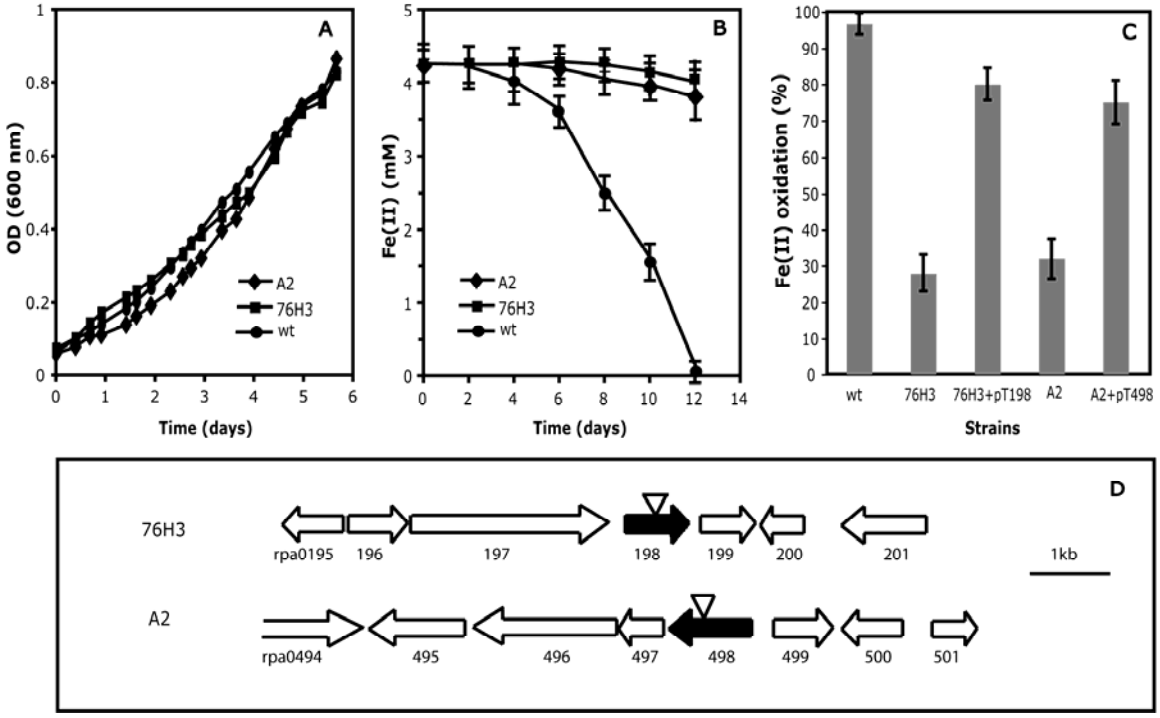

Figure 5-1: Mutants 76H3 and A2 are specifically defective in Fe(II) oxidation. A. Normal growth of mutant 76H3 and A2 with H_2 as the electron donor. Data are representative of two independent cultures. B. Defects in phototrophic growth on Fe(II) for mutants 76H3 and A2 compared to wild type. Growth was stimulated with H_2 present in the headspace initially. Data are representative of duplicate cultures. C. Mutant 76H3 and A2 carrying plasmids pT198 and pT498, respectively, show 80% of Fe(II) oxidation compared to the wild type in the cell suspension assay. D. Organization of the genomic regions surrounding the mutated genes in mutants 76H3 and A2. The black arrows indicate the disrupted genes and the transposon insertion sites are marked by the open triangles. The

numbers provided below the open reading frames (all arrows) are consistent with the numbers given for the identical regions from the CGA009 genome.

Because the sequence fragments from TIE-1 flanking the transposon insertions were highly similar to sequences from strain *R. palustris* CGA009, we designed primers based on the CGA009 genome to sequence the regions surrounding the transposon insertions in 76H3 and A2 (Figure 5-1D). Both regions contained homologs of genes found in the same order in CGA009. Mutant 76H3 has a transposon insertion in a gene that shares 99% identity over the entire gene sequence (791 base-pairs) to gene RPA0198 in CGA009 that encodes a putative integral membrane protein. BLAST search predicts that the protein encoded by this gene shares 100% identity to a possible transport protein in *R. palustris* CGA009, 85% identity to a probable ABC transport permease in *Bradyrhizobium japonicum*, and 60% identity to a hypothetical transmembrane protein from *Magnetospirillum* sp. MS-1. It is predicted to encode a cytoplasmic membrane protein with 6 internal helices based on sequence analysis with the Psort program (http://www.psort.org/) and no known motifs could be identified in this protein by the Motifscan program (http://myhits.isb-sib.ch/cgi-bin/motif_scan). Based on the annotation of the CGA009 genome, the upstream genes encode a putative ABC transporter permease (RPA0197) and a putative ABC transporter ATP-binding protein (RPA0196). The downstream gene (RPA0199) encodes a putative phosphinothricin acetyltransferase.

Mutant A2 has a transposon insertion in a gene (995 base-pairs) with 99% identity to gene RPA0498 in *R. palustris* CGA009 that is annotated as a *cobS* gene. The translated protein sequence is 100% identical to a putative CobS in strain CGA009, 93% identical to a putative CobS from *Bradyrhizobium japonicum*, 80% identical to a well studied CobS from *Pseudomonas denitrificans* and 76% and 71% identical to MoxR-like ATPases from *Rhodospirillum rubrum* and *Rhodobacter sphaeroides*, respectively. Studies of CobS function in *P. denitrificans* have shown that CobS is a cobaltochelatase: a cytoplasmic protein involved in cobalt insertion into porphyrin rings [47]. MoxR-like ATPases belong to a superfamily of proteins with associated ATPase activity (AAA) [78]. Not surprisingly, members of the MoxR family function as chaperons/chelatases in the assembly of specific metal-containing enzymatic complexes. Based on the annotation of the CGA009 genome, the genes downstream appear to encode a GCN5-related N-acetyltransferase (RPA0497), a CobT homolog (RPA0496), and a conserved hypothetical protein (RPA0495).

Preparation of a Genomic Cosmid Library of Rhodobacter SW2 in E. coli WM3064

The goal of this work was to identify genes involved in photoautotrophic Fe(II) oxidation in *Rhodobacter* sp. SW2. Because SW2 is not amenable to genetic analysis, our approach was to express a genomic cosmid library of this strain in *Rhodobacter capsulatus* SB1003, a strain that is unable to grow

phototrophically on Fe(II), and screen for clones that confer Fe(II) oxidation activity.

The SW2 genomic library was constructed in the broad host range cosmid vector pLAFR5 [92]. This cosmid vector has tandem *cos* cassettes (the recognition sequence for λ phage) separated by a unique *ScaI* site. Digestion of pLAFR5 with *ScaI* and *BamHI* generates two vector arms, each containing a *cos* cassette. During ligation, these arms are joined via a *Sau3AI* digested insert at the *BamHI* site of pLAFR5. Dephosphorylation of the insert DNA prior to ligation decreases the potential for insert-insert ligation. All DNA between the *cos* cassettes is subsequently packaged into λ phage heads and used to transduce the genomic library into the *E. coli* host of choice. The nature of the packaging reaction used here is such that 47-51 kb cosmids are preferentially packaged, thus, inserts of approximately 25.5 - 29.5 kb are expected. Additionally, because the multiple cloning site of pLAFR5 lies within the *lacZ*α gene, clones containing inserts can easily be identified as white colonies on plates containing IPTG and X-gal.

To verify that the cosmid library was representative of the SW2 genome and determine the average insert size, DH10β was infected with a portion of the library-containing phage lysate. 94% of the clones obtained were white on LB plates containing X-Gal and IPTG, indicating that they contained cosmids with inserts. Restriction digest analysis of ten randomly selected cosmids revealed that these cosmids contained different inserts with an average size of approximately 23.5 kb (Figure 5-2). Although the size of the SW2 genome is

unknown, by comparison to other *Rhodobacter* strains*, (Rhodobacter sphaeroides* 2.4.1: 4500 kb and *Rhodobacter capsulatus*: 3600 kb), an average insert size of 23.5 kb suggests that a library of approximately 700 - 880 clones would be sufficient to guarantee 99% representation of the SW2 genome [36].

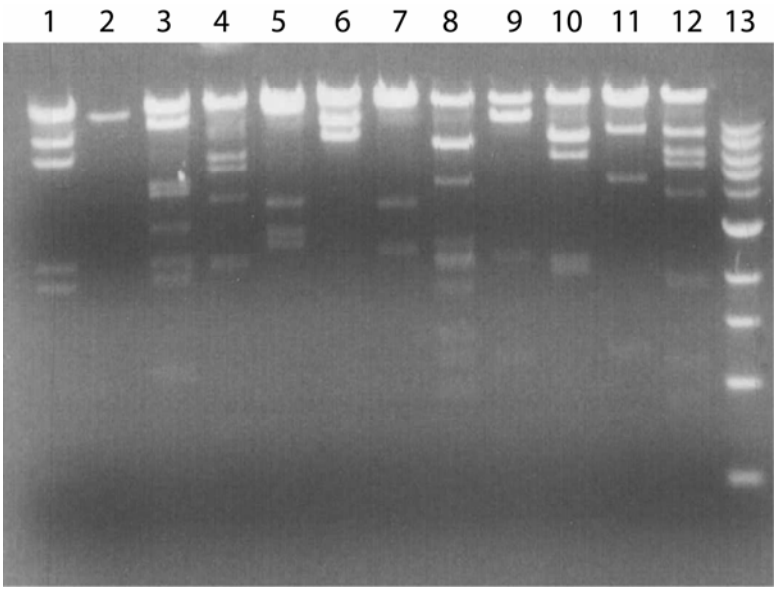

Figure 5-2: Restriction digests of ten randomly selected cosmids with *EcoRI* reveal that the cosmid genomic library of SW2 is representative of the SW2 genome and that the average insert size is approximately 23.5 kb. Lane 1 – λ *HindIII* molecular weight marker; lanes 2-12 – ten randomly selected cosmids digested with *EcoRI*; Lane 13 – 1 kb molecular weight marker (Bio-Rad).

Heterologous expression of the SW2 genomic library in Rhodobacter capsulatus SB1003 and identification of four cosmids that confer Fe(II) oxidation activity

After moving the SW2 genomic library into 1003 via conjugation from WM3064, we verified that DNA from SW2 could be expressed in other *Rhodobacter* species by successfully using the library to complement a *trpB* mutant of *Rhodobacter sphaeroides* 2.4.1 (CM06, data not shown). After this demonstration, 1536 cosmid containing WM3064 strains were mated independently to 1003. All exconjugants were pre-screened for Fe(II)-oxidation activity using a cell suspension assay in 96 well format. Four cosmids, designated p2B3, p9E12, p11B3, and p12D4, showed a decrease in Fe(II) that was at least 99% greater than the negative control, 1003 + pLAFR5 (Figure 5-3).

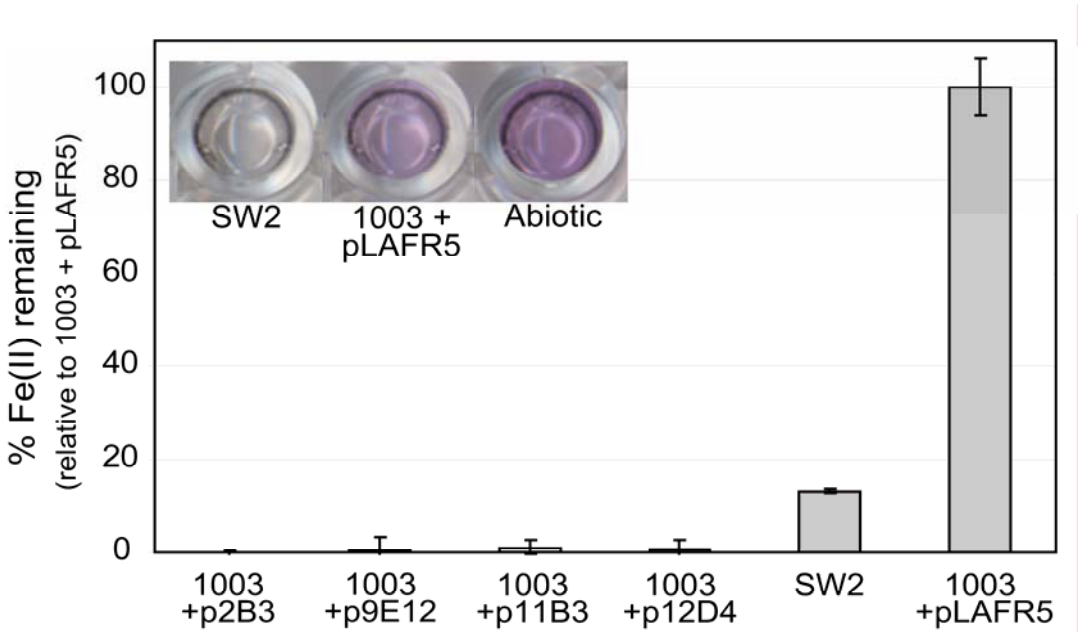

Figure 5-3: Strains of *Rhodobacter capsulatus* SB1003 containing cosmid clones p2B3, p9E12, p11D3 and p12D4 show a decrease in Fe(II) that is 99% greater than the negative control, 1003 + pLAFR5. Error bars represent the error for cell suspension assays of 24, 14, 24, 10, and 9 independent colonies of 1003 containing p2B3, p9E12, p11D3, p12D4 and pLAFR5 respectively, and 4 independent cultures of SW2. The inset shows the color difference between the positive control, SW2 and the abiotic control after the addition of *Ferrozine* during a 96 well plate format cell suspension assay.

Interestingly, we found that 1003 seemed to have Fe(II) oxidation activity in our assay, albeit less than that conferred to the p2B3, p9E12, p11B3, and p12D4 containing 1003 strains. Here a decrease in Fe(II), equivalent to approximately 73% of the total Fe(II) added, was observed (Figure 5-4).

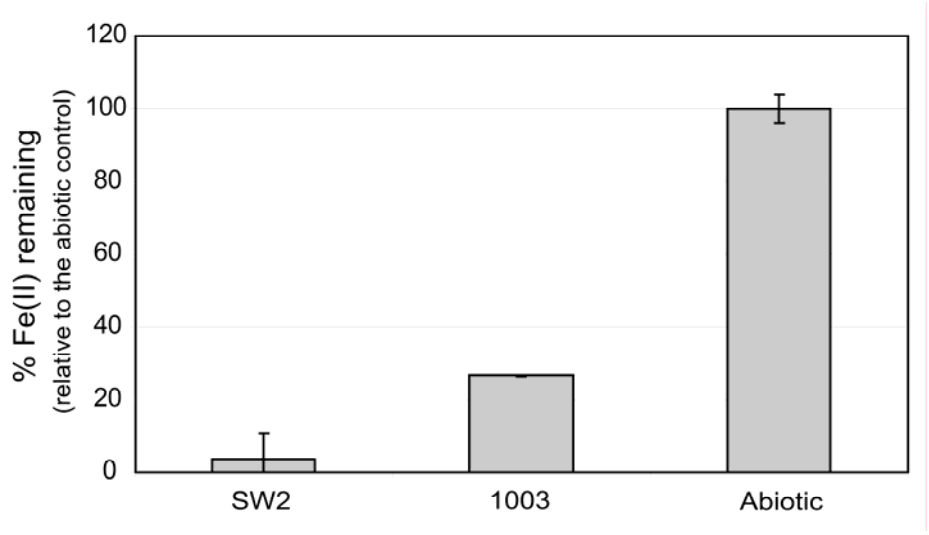

Figure 5-4: In our 96 well format cell suspension assay, *Rhodobacter capsulatus* SB1003 shows a decrease in Fe(II), equivalent to approximately 73%

of the total Fe(II) added. This decrease, however is less than that observed for the p2B3, p9E12, p11B3, and p12D4 containing 1003 strains.

Because only Fe(II) was followed in the plate assay, we could not conclude that the decrease in Fe(II) was due to oxidation as opposed to Fe(II) uptake by the cells or strong Fe(II) chelation by cell surface components or other cell produced molecules. Therefore, to verify that these cosmids were in fact conferring Fe(II) oxidation activity, reconstructed strains containing these four cosmids were retested in a cell suspension assay where the concentration of both Fe(II) and total Fe were followed over time. During these assays, the total amount of Fe stayed constant while Fe(II) decreased. This indicated that the decrease in Fe(II) observed in the cosmids containing strains was attributable to oxidation of Fe(II) (Figure 5-5). Although these cosmids did confer Fe(II)-oxidation activity to 1003, they were not sufficient to confer photoautotrophic growth on Fe(II) (Figure 5-6).

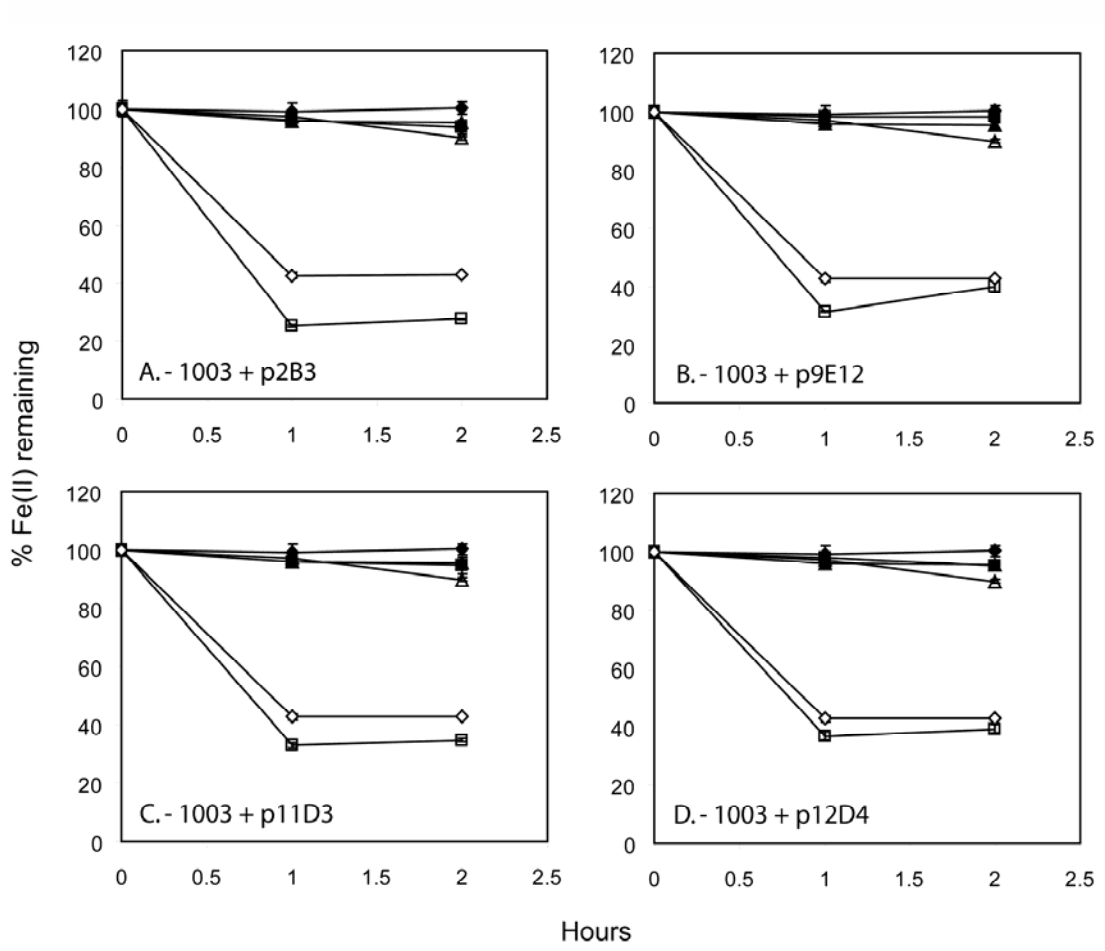

Figure 5-5: Fe(II) oxidation by 1003 + p2B3 (A), p9E12 (B), p11D3 (C), and p12D4 (D) in comparison to SW2 and 1003. On all graphs, ■ – Fe total for 1003 + cosmid; ▲ – Fe total for SW2; ♦ – Fe total for 1003; □ – Fe(II) for 1003 + cosmid strain; ◇ – Fe(II) for SW2; ∆ – Fe(II) for 1003. When both the concentration of Fe(II) and total Fe were followed in cell suspension assays over time, a decrease in the amount of Fe(II) was observed while the total amount of Fe stayed constant. This shows that Fe(II) is being oxidized by these cosmid containing strains rather than being sequestered within the cells or chelated by cell surface components or other cell produced molecules. Assays were normalized for cell number and the error bars represent the error on triplicate

Ferrozine measurements. In these assays, it seem as though Fe(II) is not oxidized to completion by SW2 or the cosmid strains. This, however, is due to OD_{570} absorbance by the high number of cells in the sample taken for the [Fe] measurement.

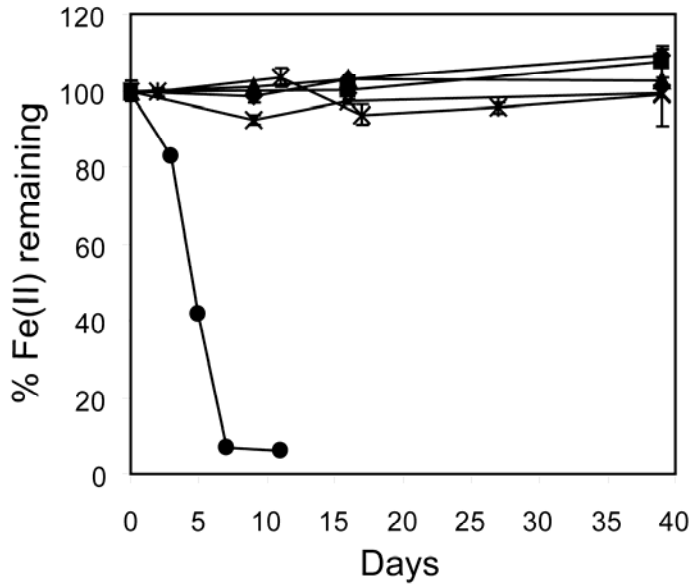

Figure 5-6: Fe(II) oxidation conferring cosmids p2B3, p9E12, p11D3 and p12D4 do not confer the ability to grow photoautotrophically on Fe(II) to 1003. ♦ – p2B3; ■ – p9E12; ▲ - p11D3; X – p12D4; ⨯ – 1003; ● – SW2.

Identification of genes on p9E12 that confer Fe(II) oxidation activity

In an initial approach to identify the specific genes on these cosmids responsible for the observed Fe(II) oxidation phenotype, p9E12 was mutagenized *in vitro* using the Epicentre EZ-Tn5™ <T7/KAN-2> Promoter Insertion Kit. After mutagenesis, the transposon derivative cosmid library was

transformed into WM3064, introduced into 1003 via conjugation and exconjugants were screened for loss of Fe(II) oxidation activity. This approach, however, was unsuccessful . Here we found that all of the transposon containing cosmids that no longer conferred the ability to oxidize Fe(II) contained the transposon in different sites in the pLAFR5 backbone, rather than the SW2 DNA insert. Genes in the sequence flanking the transposon insertions of these cosmids included *trfA*, *tetA*, *kfrA*, *trbD/E*, and *korF/G*, indicating that the disruptions may affect plasmid stability, replication and/or maintenance [71, 79].

Moving on to a sub-cloning strategy, the four cosmids were digested with *PstI*, *HindIII* and *EcoRI* (Figure 5-7) so that the inserts of these cosmids could be mapped and common regions among them identified and cloned.

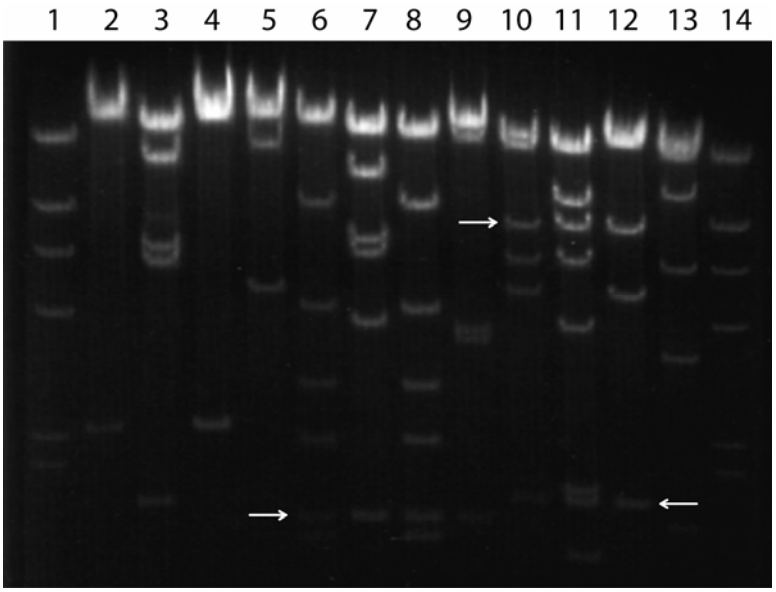

Figure 5-7: Digestion of p2B3, p9E12, p11D3 and p12D4 with *EcoRI*, *HindIII* and *PstI* reveals common restriction fragments among three or more of these cosmids. The common fragments are highlighted by the white arrows. Lanes 1

and 14 – λ *HindIII* molecular weight marker; lanes 2-5 – p2B3, p9E12, p11D3 and p12D4 digested with *EcoRI*, respectively; lanes 6-9 – p2B3, p9E12, p11D3 and p12D4 digested with *HindIII*, respectively; lanes 10-13 – p2B3, p9E12, p11D3 and p12D4 digested with *PstI*, respectively. Some small pieces are missing from this gel. These include *HindIII* fragments of p2B3 (~0.5 kb) and p11D3 (~0.5 kb) and *PstI* fragments of p2B3 (~0.6 and 0.2 kb), p9E12 (~0.2 kb), p11D3 (~0.2 kb) and p12D4 (~0.6 and 0.7 kb).

A restriction map of the four cosmids digested with *PstI* is shown in Figure 5-8. Map for the *EcoRI* and *HindIII* digests were not constructed. Here, discrepancies in the data seemed to suggest that the inserts among these cosmids may be from different regions of the SW2 genome. For example, the only *PstI* restriction fragment that p12D4 shares with any of the other cosmids is an approximately 0.75 kb fragment, present only in p2B3 (fragments 7 of p2B3 and p12D4). However, although the insert of p9E12 spans this region and should also contain this piece, it does not. Interestingly, the *PstI* restriction fragments 6, 4, 5, and 2 of p12D4 are very similar in size to restriction fragments 8, 5, 6, and 2 of the 9E12 *PstI* digest (Figure 5-7 and 5-8).

It is possible that genes in disparate regions of the SW2 genome can confer an Fe(II) oxidation phenotype, and that these different regions are represented among the inserts of the four cosmids. It is also possible that during the ligation of pLAFR5 to SW2 genomic DNA, fragments of DNA from different regions of the SW2 genome were ligated together to form the insert of p12E4,

despite measures taken to prevent such insert-insert ligations. If, however, genes in different regions of the SW2 genome can confer Fe(II) oxidation activity and are represented among the inserts of these four cosmids, it seems that these regions may share similarities in sequence structure.

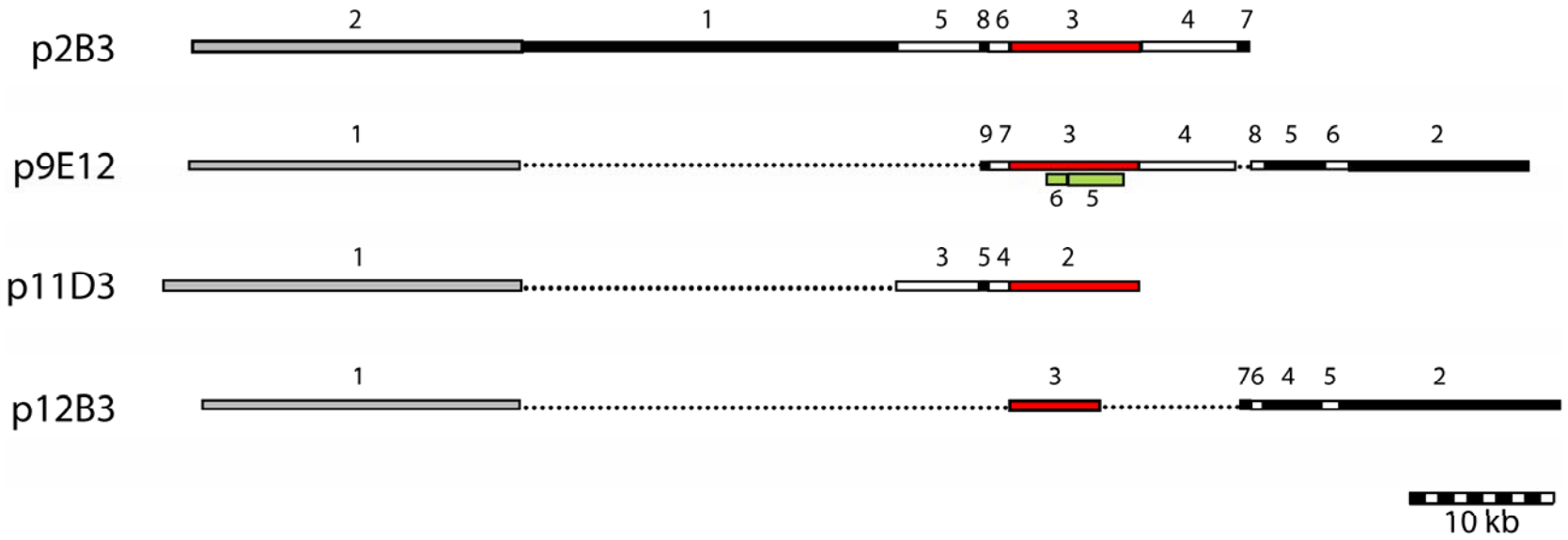
p2B3
2
1
5
8
6
3
4
7
p9E12
1
9
7
3
4
8
5
6
2
6
5
p11D3
1
3
5
4
2
p12B3
1
3
7
6
4
5
2
10 kb

Figure 5-8.

Figure 5-8: Restriction map of p2B3, p9E12, p11B3 and p12D4 digested with *PstI*. The red bars represent fragments in the *PstI* digest common among p2B3, p9E12 and p11D3. The position of fragment 3 in the p12D4 *PstI* digest is inferred from the sizes of the other fragments in this digest relative to those in the digests of p2B3 and p9E12. This fragment likely represents a smaller piece of the common fragment in red due to partial digest conditions. The green bars represent the positions of the pH5 and pH6 inserts on fragment 3 of the p9E12 *PstI* digest inferred from sequence data. Fragment 6 in the *HindIII* digest of p9E12 was common among all the cosmids. From sequence data, fragments 7 and 3 in the p9E12 *PstI* digest are contiguous as are fragments 5, 6, and 2, and 1, although, the position of *PstI* fragment 7 with respect to fragment 3 is arbitrary (*i.e.,* fragment 7 could be on the other side of fragment 3). The positioning, however, is likely accurate given the nature of the sequence at the end of the P3 T7 and the sequence on fragment 4 (P4, 100% identical at the DNA and protein level to E. coli) in comparison to the sequence at the beginning of P3 T7 (97% identical at the protein level to *Rhodobacter sphaeroides* 2.4.1. The positions of p9E12 *PstI* fragments 4, 8 and 9 are inferred from comparison to the digests of the other cosmids

Nonetheless, digestion of the four cosmids with *PstI* and *HindIII* did reveal four fragments that were shared among three or more of the cosmids. In the *PstI* digest, fragments of ~9.4, 1.7 and 0.2 kb were shared among p2B3, p9E12 and p11B3 (Figure 5-7 and 5-8) and in the *HindIII* digest an approximately 1.5 kb

piece was shared among all four cosmids (Figure 5-7). That a *PstI* fragment is not shared among the four cosmids likely results from the fact that the initial digestion of the SW2 genome was a partial digest with *Sau3AI*. Thus, some fragment in the *PstI* digest of p12D4 may represent smaller piece of one of the shared fragments among p2B3, 9E12 and 11B3 (likely the~6.5 kb fragment, Figure 5-8). To test if one of these common fragments contained the genes sufficient to confer an Fe(II) oxidation phenotype, the 9.4 and 1.7 kb fragments of the *PstI* digest were cloned into the broad-host-range vector, pBBR1MCS3 (Tc^R) and the 1.5 kb piece of the *HindIII* digest was cloned into a kanamycin resistant derivative of the same plasmid, pBBR1MCS2 (Km^R) to construct pP3, pP7 and pH6, respectively. None of these clones, conferred Fe(II) oxidation activity upon 1003 (data not shown), however, we later discovered the tetracycline resistance gene located on the vector of pBBR1MCS3 (Tc^R) is not well expressed in *Rhodobacter* strains [168]. Thus, the fact that we did not observe Fe(II) oxidation activity with any of these sub-clones may result from the fact that the construct was not well maintained.

Our next approach was to sequence the insert of p9E12 in hopes that the genes conferring Fe(II) oxidation activity could be identified through sequence data analysis. Here our guiding expectations were that these genes may not be found in the sequenced phototrophs that are unable to oxidize Fe(II), that they may contain cofactor binding motifs that would be indicative of redox activity (*e.g.*, heme binding or multi-Cu oxidase motifis or Fe-S clusters), that they may have no homologs in the database, as no Fe(II)-oxidizing proteins involved in

photoautotrophic growth have been reported thus far, or that they would bear similarity to the genes involved in Fe(II) oxidation identified in TIE-1. In addition, given the observed Fe(II) oxidation activity of 1003 in our cell suspension assays, we also kept in mind the possibilities that the genes responsible for this phenotype may include transcriptional regulators or that gene dosage effects may play a role and introduction of additional copies of these genes could increase Fe(II) oxidation activity.

To reduce the ~ 35 kb insert of p9E12 to a more manageable size for sequencing, the *PstI* restriction fragments 1, 2, 4, 5, and 6 were cloned into pBBR1MCS3 (Tc^R) and an additional *HindIII* fragment, 5, was cloned into pBBR1MCS2 (Km^R). These clones were designated pP1, pP2, pP4, pP5, pP6, and pH5, respectively. The inserts of pP2, pP3, and pP4, were shotgun cloned and sequenced and the inserts of pP5, pP6, pP7, pH5, and pH6 were sequenced by primer walking. Initial sequencing of pP1 using the T7 and T3 primers (primer sites are located on the pBBR1MCS backbone) showed that the insert consisted primarily of pLAFR5 (Table 5-2), thus the insert of this construct was not sequenced further. The *PstI* fragments 8 and 9 were not cloned and sequenced because their restriction fragment size suggested that they would not contain more than one gene. In the end, approximately 78% of the p9E12 insert was sequenced. Only the inserts of pP4, pP5, pP6, and pP7 were sequenced enough to be assembled into contigs. The sequences obtained are presented in Appendix 1 and the results of the sequence analysis using ORF finder, BlastP and the CDD are summarized in Table 5-2.

ORFs on the inserts of pP1, pP2, pP5 and pP6 formed a contiguous stretch of DNA that was largely homologous in gene identity and organization to a region of the *Rhodobacter sphaeroides* 2.4.1 genome (locus tags Rsph03003804 to Rsph03003821). Of 17 predicted ORFs, only one in this sequence did not have a homolog in 2.4.1 (Table 5-2). The translated sequence of this ORF encodes a protein with 53% identity to a putative lipoprotein in *Silicibacter pomeroyi* DSS-3 and 40% identity to the putative RND (resistance-nodulation-cell division) multi-drug efflux membrane fusion protein, MexC, in *Rhodopseudomonas palustris* CGA009. In place of this ORF on the genome of *R. sphaeroides* 2.4.1, there is a 903 kb stretch of DNA with no predicted genes. On the pP2 insert portion of this sequence there is a predicted MoxR-like ATPase (COG0714). Although this predicted protein is in the same COG (Cluster of Orthologous Group) as the TIE-1 mutant A2 (putative CobS with similarity to a MoxR-like ATPase from *Rhodobacter sphaeroides* 2.4.1), this predicted protein is not a homolog of the putative CobS protein, nor is the predicted histone acetyltransferase HPA2 downstream of it a homolog of the predicted acetyltransferase downstream of CobS in TIE-1. In fact, direct homologs of the genes involved in Fe(II) oxidation in TIE-1 are not present in the sequence of the p9E12 insert that we have obtained thus far.

ORFs on the pP4 insert were identical in nucleotide and amino acid sequence to genes involved in fimbrial biosynthesis in *E. coli* (Table 5-2). This perfect identity was surprising given the large difference in GC content between *E. coli* and *Rhodobacter* species (50% vs. 68% and 69% for *Rhodobacter*

capsulatus and *sphaeroides*, respectively). Consistent with this, these ORFs have a GC content of 49% versus 63% on average for the rest of the sequenced insert. The possibility exists that these ORFs may not actually be present in SW2, and may represent contamination of *E. coli* DNA during the cosmid library construction. If true, this may also help to explain some of the ambiguities in the *PstI* restriction map surrounding this fragment (Figure 5-8). Further, genes involved in fimbrial biosynthesis in *E. coli* have no obvious function related to Fe(II)-oxidation; therefore, these predicted ORFs were not considered further.

The inserts of pP3 and pP7 could be linked together based on sequence analysis and contained 10 predicted ORFs. Four of these ORFs had no homolog in *Rhodobacter*. These include: 1) a hypothetical protein with 100% amino acid (aa) identity to a hypothetical protein in *E. coli*, 2) AraJ, a transcriptional regulator (100% aa identity to AraJ of *E. coli*), 3) an ATP binding protein of an ABC transporter (56% aa identity to an ATP binding protein of an ABC transporter in *Erwinia carotovora*), and 4) a predicted permease (80% aa identity to a predicted permease in *Silicibacter* TM1040) (Table 5-2). Given the proximity of the first two ORFs to pP4, for the reasons described above regarding the uncertain origin of the pP4 insert, we are skeptical that these ORFs are endogenous to SW2, and thus, involved in photoautotrophic Fe(II) oxidation. Further, sequence analysis of the pH5 insert reveals that the ORF predicted to encode the ATP binding protein of an ABC transporter lies within the predicted permease ORF, and the expectation value for the permease is lower than that for the ATP binding protein. Finally, all these ORFs, but the permease lie entirely in the region of P3 that is

not predicted to be shared among the cosmids. It seems, therefore, that among these four candidates, the only one with potential to be involved in Fe(II) oxidation in SW2 is the predicted permease. This conclusion is consistent with our results with TIE-1, where we found a putative, cytoplasmic membrane permease that appears to be part of an ABC transport system to be involved in Fe(II) oxidation

Another ORF of interest on the pP3 insert sequence shares 45% aa identity to a putative serine/threonine protein kinase related protein of *Methanothermobacter thermautotrophicus* Delta H and 39% aa identity to a WD40-like repeat containing protein in *Rhodobacter sphaeroides* 2.4.1 (Table 5-2). This translated ORF contains a domain conserved in bacterial dehydrogenases [5] and serine/threonine kinases [131] containing the redox cofactor pyrroloquinoline quinone (PQQ), suggesting potential redox capabilities of this putative protein. In the PQQ containing methanol dehydrogenase from *Methylobacterium extorquens* and other related dehydrogenases, the PQQ cofactor is located in a large subunit of this protein that forms an eight bladed β-propeller structure [5]. Each of the eight blades in this structure is made up of four anti-parallel β-sheets and the interactions between these propeller blades are stabilized by series of 11 residue consensus sequences present in the sequence of all but one of the propeller motifs. Similarly, in proteins with WD-40 repeat domains, these repeats form a β-propeller structure [156]. Members of the WD-40 protein family include proteins with regulatory function and the WD repeats are assumed to be involved in protein-protein interactions [124].

Originally thought to be unique to eukaryotes, proteins with WD-40 repeats have recently been found in a number of prokaryotes including serine/threonine kinases found in *Streptomycin coelicolor* and *Thermomonospora curvata* [88, 131]. No proteins with WD-40 domains, however, have been found to contain PQQ. Thus, while it seems likely that the predicted protein from SW2 contains a β-propeller structure, whether it also contains a PQQ cofactor and possesses redox capability, remains to be determined. Encouragingly, however, recent evidence supports a role for a quinoprotein in Mn(II)-oxidation: the Mn(II) oxidizing activity of cell free extracts of *Erythrobacter* sp. SD21 is enhanced by the addition of PQQ and mutants of *Pseudomonas putida* MnB1 with disruptions in *trpE* that are defective in Mn(II) oxidation can be rescued *in vitro* when supplemented with PQQ [87].

The remaining ORFs encode predicted proteins with homologs in *Rhodobacter sphaeroides* 2.4.1 involved in amino acid biosynthesis (IlvC), carbohydrate transport and metabolism (ManB), folic acid biosynthesis (FolP and B), poly-isoprenoid biosynthesis (IspA), a protein-export membrane protein (SecF) and a permease of the drug/metabolite transporter superfamily (Table 5-2). These predicted proteins have no obvious function related to Fe(II) oxidation, although a role for a permease and a protein–export membrane protein can be envisioned given our results with TIE-1, where we found a putative, cytoplasmic membrane permease that appears to be part of an ABC transport system to be involved in Fe(II) oxidation. The putative protein–export membrane protein,

however, is located on a *PstI* restriction fragment that is not thought to be common among the four cosmids.

Table 5-2: Summary of ORF finder, BlastP and Conserved Domain Database search results from the p9E12 insert sequence. The top BlastP matches to predicted ORFs in the pP1, pP2, pP3, pP4, pP5, pP6, pP7 pH5 and pH6 insert sequences are listed, as are conserved domains within the predicted ORF when they are present. When the top match is not a *Rhodobacter* species, the highest *Rhodobacter* or related purple non-sulfur bacterium match, when it exists, is also listed. [1]The number of amino acid residues that encode the predicted ORF. [2,3]Amino acid identity and similarity between the predicted ORF translation and the proteins in the database that showed the best BlastP matches. [4]The expectation value; the lower the E value, the more significant the score. [5]Translated fragments of the same ORF detected in different reading frames, likely due to mistakes in the sequence that result in a frame shift mutation. [6]The ORF of this predicted ABC transporter ATP-binding protein lies within that of this predicted permease (COG0730). bp = base-pairs.

Table 5-2:

Conserved domains (function)	Protein name (**C**luster of **O**rthologous **G**roups)	Matching species	Amino acids[1]	Identities[2]	Positives[3]	E value[4]
pP1 – 397 bp contig from T3 end						
	non-functional *lacZ* alpha peptide	unidentified cloning vector	151	25/29 (86%)	26/29 (89%)	5e-05
pfam04956, Conjugal transfer protein TrbC	TelB	Cloning vector pLAFR	125	103/108 (95%)	104/108 (96%)	6e-51
pP1 – 709 bp contig from T7 end						
pfam06271, RDD family (function unknown).	Predicted membrane protein/domain (COG1714)	*Rhodobacter sphaeroides* 2.4.1	151	102/145 (70%)	119/145 (82%)	3e-51
pP2 – 7264 bp contig from the T3 end						
	ATP-dependent transcriptional regulator (COG2909)[5]	*Rhodobacter sphaeroides* 2.4.1	344	195/330 (59%)	236/330 (71%)	e-105
	ATP-dependent transcriptional regulator (COG2909)[5]	*Rhodobacter sphaeroides* 2.4.1	54	31/51 (60%)	39/51 (76%)	3e-10
COG3825, Uncharacterized protein conserved in bacteria (function unknown) COG3552, CoxE, Protein containing von Willebrand factor type A (vWA) domain (general function prediction only)	Uncharacterized protein conserved in bacteria (COG3825)	*Rhodobacter sphaeroides* 2.4.1	394	313/394 (79%)	345/394 (87%)	0.0
COG0586, DedA, Uncharacterized membrane-associated protein (function unknown)	Rhodanese-related sulfurtransferase (OG0607) Uncharacterized membrane-associated protein (COG0586)	*Rubrivivax gelatinosus* PM1 *Rhodobacter sphaeroides* 2.4.1	198	64/200 (32%) 44/139 (31%)	99/200 (49%) 66/139 (47%)	2e-15 1e-08
pfam01435, Peptidase_M48, Peptidase family M48 COG4783, Putative Zn-dependent protease,	Putative Zn-dependent protease, contains TPR repeats (COG4783)	*Rhodobacter sphaeroides* 2.4.1	145	102/134 (76%)	110/134 (82%)	2e-51

contains TPR repeats (general function prediction only)						
	hypothetical protein Rsph03003811	*Rhodobacter sphaeroides* 2.4.1	112	75/109 (68%)	87/109 (79%)	7e-37
COG1092, Predicted SAM-dependent methyltransferase (general function prediction only)	Predicted SAM-dependent methyltransferase (COG1092)	*Rhodobacter sphaeroides* 2.4.1	341	158/206 (76%)	178/206 (86%)	2e-87
	Putative lipoprotein	*Silicibacter pomeroyi* DSS-3	249	91/246 (36%)	131/246 (53%)	9e-35
	putative RND multi-drug efflux membrane fusion protein MexC	*Rhodopseudomonas palustris* CGA009		36/124 (29%)	50/124 (40%)	7.1
	Dihydroxyacid dehydratase/ phosphogluconate dehydratase	*Silicibacter* sp. TM1040	83	41/71 (57%)	49/71 (69%)	3e-14
pP2 – 1822 bp contig from the T7 end						
	DnaK suppressor protein (COG1734)	*Silicibacter* sp. TM1040	96	39/56 (69%)	47/56 (83%)	8e-17
	DnaK suppressor protein (COG1734)	*Rhodobacter sphaeroides* 2.4.1		26/30 (86%)	28/30 (93%)	2e-07
d00009, AAA, AAA-superfamily of ATPases (membrane fusion, proteolysis, and DNA replication) COG0714, MoxR-like ATPases (general function prediction only)	MoxR-like ATPases	*Rhodobacter sphaeroides* 2.4.1	279	243/279 (87%)	263/279 (94%)	e-138
pfam00583, Acetyltransf_1, Acetyltransferase (GNAT) family (N-acetyltransferase functions)	Histone acetyltransferase HPA2 and related acetyltransferases (COG0454)	*Rhodobacter sphaeroides* 2.4.1	205	77/134 (57%)	91/134 (67%)	1e-37
pP2 – 970 bp contig of an internal fragment						
	phosphogluconate	*Silicibacter pomeroyi* DSS-3	126	81/110	92/110	3e-41

	dehydratase			(73%)	(83%)	
pP3 – 1095 bp contig from T3 end						
	hypothetical protein b0395	*Escherichia coli* K-12	72	71/72 (98%)	72/72 (100%)	6e-36
COG1940, NagC, Transcriptional regulator/sugar kinase (transcription/ carbohydrate transport and metabolism)	AraJ Transcriptional regulator/sugar kinase (COG1940)	*Escherichia coli* K-12 *Rhodospirillum rubrum* ATCC 11170	51	45/45 (100%) 22/41 (53%)	45/45 (100%) 28/41 (68%)	2e-20 2e-05
COG4987, CydC, ABC-type transport system (energy production and conversion/ posttranslational modification, protein turnover, chaperones) COG1132, MdlB, ABC-type multi-drug transport system (defense mechanisms)	ABC transporter ATP-binding protein[6]	*Erwinia carotovora* subsp. *atroseptica* SCRI1043	130	32/93 (34%)	53/93 (56%)	6e-06
pP3 – 7231 bp contig from T7 end						
pfam01450, IlvC, Acetohydroxy acid isomeroreductase, catalytic domain (catalyses the conversion of acetohydroxy acids into dihydroxy valerates)	Ketol-acid reductoisomerase (COG0059)	*Rhodobacter sphaeroides* 2.4.1	214	208/214 (97%)	210/214 (98%)	e-118
cd00216, PQQ_DH, Dehydrogenases with pyrroloquinoline quinone (PQQ) as a cofactor COG1520, WD40-like repeat (function unknown)	serine/threonine protein kinase related protein WD40-like repeat (COG1520)	*Methanothermobacter thermautotrophicus* Delta H *Rhodobacter sphaeroides* 2.4.1	362	72/248 (29%) 69/287 (24%)	113/248 (45%) 112/287 (39%)	2e-14 2e-05
pfam00892, DUF6, Integral membrane protein DUF6 (function unknown)	Permeases of the drug/metabolite transporter (DMT) superfamily (COG0697)	*Silicibacter* sp. TM1040 *Rhodobacter sphaeroides*	301	131/282 (46%) 106/278	172/282 (60%) 157/278	5e-59 1e-41

	Permeases of the drug/metabolite transporter (DMT) superfamily (COG0697)	2.4.1		(38%)	(56%)	
COG1109, ManB, Phosphomannomutase (carbohydrate transport and metabolism)	Phosphomannomutase (COG1109)	*Rhodobacter sphaeroides* 2.4.1	447	377/446 (84%)	400/446 (89%)	0.0
COG0294, FolP, Dihydropteroate synthase and related enzymes (coenzyme metabolism) cd00423, Pterin_binding, Pterin binding enzymes. This family includes dihydropteroate synthase (DHPS) and cobalamin-dependent methyltransferases	Dihydropteroate synthase and related enzymes (COG0294)	*Rhodobacter sphaeroides* 2.4.1	337	226/331 (68%)	259/331 (78%)	e-121
	Dihydroneopterin aldolase (COG1539)	*Rhodobacter sphaeroides* 2.4.1	88	29/34 (85%)	32/34 (94%)	4e-09
pfam00583, Acetyltransferase (GNAT) family (N-acetyltransferase functions)	Acetyltransferase, GNAT family Sortase and related acyltransferases Acetyltransferases (COG0456)	*Silicibacter pomeroyi* DSS-3 *Rhodobacter sphaeroides* 2.4.1 *Rhodobacter sphaeroides* 2.4.1	274	85/158 (53%) 42/151 (27%) 27/75 (36%)	103/158 (65%) 63/151 (41%) 35/75 (46%)	2e-37 0.006 0.040
	Predicted permeases (COG0730)[6]	*Silicibacter* sp. TM1040	47	27/41 (65%)	33/41 (80%)	5e-08
pP4 – 6281 bp consensus sequence						
pfam00419, Fimbrial protein	FimA	*Escherichia coli* K-12	80	72/72 (100%)	72/72 (100%)	3e-33
pfam00419, Fimbrial protein	FimI	*Escherichia coli* K-12	212	212/212 (100%)	212/212 (100%)	e-120
pfam00345,	FimC	*Escherichia coli* K-12	218	218/218	218/218	e-120

Pili_assembly_N, Gram-negative pili assembly chaperone, N-terminal domain. C2 domain-like beta-sandwich fold pfam02753, Pili_assembly_C, Gram-negative pili assembly chaperone, C-terminal domain. Ig-like beta-sandwich fold COG3121, FimC, P pilus assembly protein, chaperone PapD (cell motility and secretion / intracellular trafficking and secretion)				(100%)	(100%)	
pfam00577, Fimbrial Usher protein (biogenesis of gram negative bacterial pili) COG3188, FimD, P pilus assembly protein, porin PapC (cell motility and secretion/intracellular trafficking and secretion)	FimD[5]	*Escherichia coli* K-12	444	403/439 (91%)	408/439 (92%)	0.0
pfam00577, Fimbrial Usher protein (biogenesis of gram negative bacterial pili) COG3188, FimD, P pilus assembly protein, porin PapC (cell motility and secretion/intracellular trafficking and secretion)	FimD[5]	*Escherichia coli* K-12	468	454/454 (100%)	454/454 (100%)	0.0
pfam00419, Fimbrial protein COG3539, FimA, P pilus assembly protein, pilin FimA	FimF	*Escherichia coli* K-12	176	176/176 (100%)	176/176 (100%)	4e-96

(cell motility and secretion/intracellular trafficking and secretion)						
pfam00419, Fimbrial protein COG3539, FimA, P pilus assembly protein, pilin FimA (cell motility and secretion/intracellular trafficking and secretion)	FimG	*Escherichia coli* K-12	169	167/167 (100%)	167/167 (100%)	3e-89
pfam00419, Fimbrial protein	FimH	*Escherichia coli* K-12	307	287/287 (100%)	287/287 (100%)	e-164
pP5 – 3955 bp consensus sequence						
	hypothetical protein Rsph03003817	*Rhodobacter sphaeroides* 2.4.1	43	34/38 (89%)	36/38 (94%)	3e-12
COG1391, GlnE, Glutamine synthetase adenylyltransferase (posttranslational modification, protein turnover, chaperones/signal transduction mechanisms)	Glutamine synthetase adenylyltransferase (COG1391)[5]	*Rhodobacter sphaeroides* 2.4.1	340	174/245 (71%)	196/245 (80%)	2e-92
COG1391, GlnE, Glutamine synthetase adenylyltransferase (posttranslational modification, protein turnover, chaperones/signal transduction mechanisms)	Glutamine synthetase adenylyltransferase (COG1391)[5]	*Rhodobacter sphaeroides* 2.4.1	373	276/351 (78%)	298/351 (84%)	e-153
COG1391, GlnE, Glutamine synthetase adenylyltransferase (posttranslational modification, protein turnover, chaperones/signal transduction mechanisms)	Glutamine synthetase adenylyltransferase (COG1391)[5]	*Rhodobacter sphaeroides* 2.4.1	172	110/165 (66%)	124/165 (75%)	4e-53
cd00002, YbaK, protein family (function unknown) COG2606, EbsC,	Uncharacterized conserved protein (COG2606)	*Rhodobacter sphaeroides* 2.4.1	156	110/155 (70%)	122/155 (78%)	9e-56

Uncharacterized conserved protein (function unknown)						
	hypothetical protein STM1w01000948 hypothetical protein Rsph03003820	*Silicibacter* sp. TM1040 *Rhodobacter sphaeroides* 2.4.1	117	57/91 (62%) 56/95 (58%)	66/91 (72%) 66/95 (69%)	2e-25 4e-24
pP6 – 1770 bp consensus sequence						
COG0800, Eda, 2-keto-3-deoxy-6-phosphogluconate aldolase (carbohydrate transport and metabolism)	2-keto-3-deoxy-6-phosphogluconate aldolase (COG0800)	*Rhodobacter sphaeroides* 2.4.1	258	72/96 (75%)	78/96 (81%)	4e-32
pfam00920, ILVD_EDD, Dehydratase family.	Dihydroxyacid dehydratase/ phosphogluconate dehydratase (COG0129)	*Rhodobacter sphaeroides* 2.4.1	90	62/90 (68%)	69/90 (76%)	2e-25
fam06983, 3-dmu-9_3-mt, 3-demethylubiquinone-9 3-methyltransferase COG3865, Uncharacterized protein conserved in bacteria (function unknown)	Uncharacterized protein conserved in bacteria (COG3865)	*Rhodobacter sphaeroides* 2.4.1	153	87/157 (55%)	101/157 (64%)	1e-37
pP7 – 1299 bp consensus sequence						
COG0059, IlvC, Ketol-acid reductoisomerase (amino acid transport and metabolism/ coenzyme metabolism)	Ketol-acid reductoisomerase (COG0059)	*Rhodobacter sphaeroides* 2.4.1	185	60/65 (92%)	62/65 (95%)	5e-27
COG0142, IspA, Geranylgeranyl pyrophosphate synthase (coenzyme metabolism)	Geranylgeranyl pyrophosphate synthase (COG0142)	*Rhodobacter sphaeroides* 2.4.1	102	33/40 (82%)	35/40 (87%)	4e-10
pfam02355, SecD_SecF (protein export membrane proteins) COG0341, SecF, Preprotein translocase subunit SecF (intracellular trafficking and	SecF - Protein-export membrane protein Preprotein translocase subunit SecF (COG0341)	*Rhodobacter capsulatus* SB1003 *Rhodobacter sphaeroides* 2.4.1	70	43/60 (71%) 41/60 (68%)	52/60 (86%) 52/60 (86%)	2e-17 3e-17

secretion)						
pH5 – 949 bp from T3 end						
	Phosphomannomutase (COG1109)	*Rhodobacter sphaeroides* 2.4.1		201/241 (83%)	209/241 (86%)	e-109
pH5 – 912 bp from T7 end						
	Predicted permeases (COG0730)[6]	*Silicibacter* sp. TM1040	219	42/57 (73%)	44/57 (77%)	1e-15
COG4987, CydC, ABC-type transport system (energy production and conversion/ posttranslational modification, protein turnover, chaperones) COG1132, MdlB, ABC-type multi-drug transport system (defense mechanisms)	ABC transporter ATP-binding protein[6]	*Erwinia carotovora* subsp. *atroseptica* SCRI1043		32/93 (34%)	53/93 (56%)	6e-06
pH6 – 269 bp from T3 end						
	No significant hits to the three predicted ORFs		41, 76, & 85			
pH6 – 322 bp from T7 end						
COG1109, ManB, Phosphomannomutase (carbohydrate transport and metabolism)	Phosphomannomutase (COG1109)	*Rhodobacter sphaeroides* 2.4.1	74	51/73 (69%)	57/73 (78%)	4e-20

Because the sequence of the pP3 insert is only approximately 89% complete, more ORFs may exist in the unsequenced region. The inserts of pH5 and pH6 lie within the pP3 sequence (Figure 5-8), but do not provide additional sequence information beyond that which was obtained from the pP3 insert sequence.

The number of predicted ORFs not present in other *Rhodobacter* species on the sequence of the pP3 insert, the lack of conserved organization to a region of the 2.4.1 genome (as was observed with the inserts of pP1, pP2, pP5 and pP6), the fact that this P3 fragment is common to three of the four identified cosmids (with a region of this fragment likely being common to the to the fourth cosmid as well) and that a *HindIII* fragment within it is common to all four cosmids (Figure 5-7 and 5-8) seemed to suggest that pP3 may contain the genes required for the observed Fe(II) oxidation activity. Revisiting our sub-cloning results where we found that the pP3 clone did not confer Fe(II) oxidation activity to 1003, we realized that the particular tetracycline resistance gene located on the vector of this construct (from pBR322) is not well expressed in *Rhodobacter* strains [168]. Thus, as stated earlier, we could not tell if this sub-clone did not confer Fe(II) oxidation activity to 1003 because it did not contain the required genes or because the construct was not well maintained. Therefore, this restriction fragment was re-cloned in both orientations into pBBR1MCS5 (Gm^R) to generate pP3-gm1 and pP3-gm2. When tested, both of these constructs conferred Fe(II) oxidation activity upon 1003 (Figure 5-9).

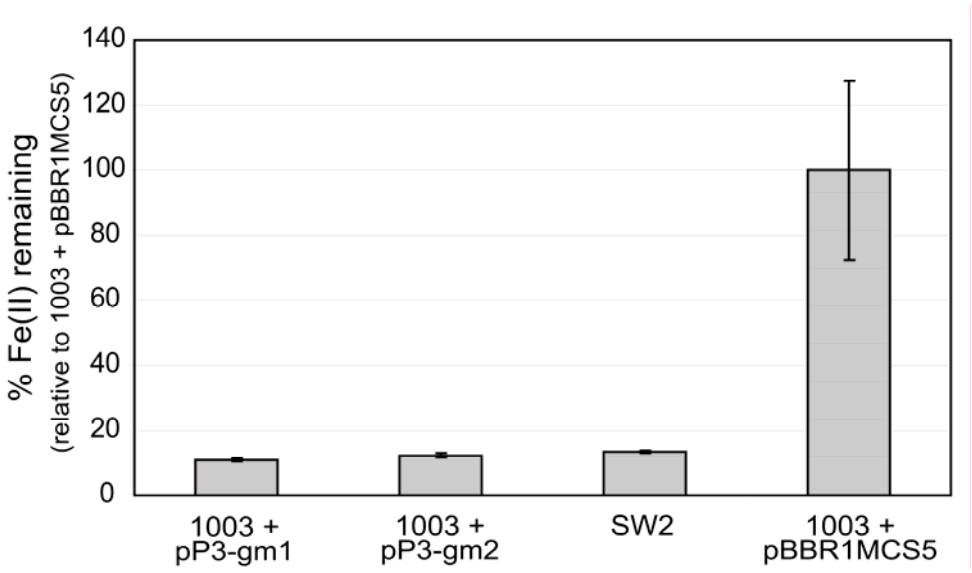

Figure 5-9: The 9.4 kb *PstI* fragment of p9E12 confers Fe(II) oxidation activity to *Rhodobacter capsulatus* SB1003 when cloned into pBBR1MCS5(Gm^R). This activity is independent of the orientation in which the fragment is cloned suggesting that the gene(s) responsible for the observed phenotype is cloned with its endogenous promoter.

That this activity is independent of the orientation in which the fragment is cloned suggests that the gene(s) responsible for the observed phenotype are cloned with their endogenous promoter. Promoter prediction analysis indicates that σ^{70} promoter consensus sequences lie 182 bp upstream of the putative PQQ containing protein, 655 bp upstream from the predicted permease with no homolog in *Rhodobacter*, and 198 bp upstream of the predicted permease of the drug/metabolite transporter superfamily.

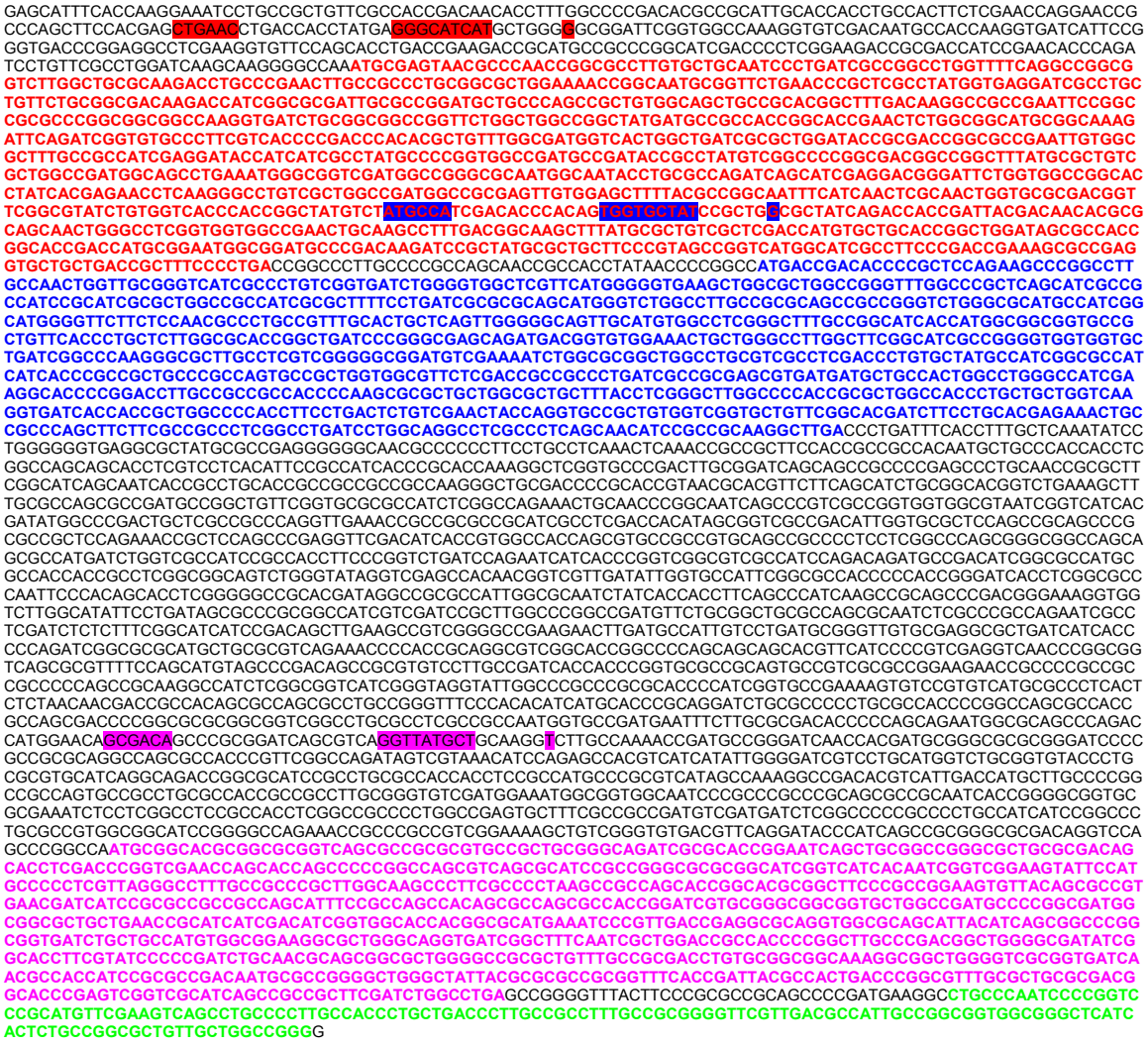

Figure 5-10: Sequence region of the pP3 insert that contains genes predicted to encode a putative PQQ containing protein (bold red), a permease of the drug/metabolite transporter superfamily (bold blue) an acetyltransferase of the GNAT family (bold pink), and a permease with no homolog in *Rhodobacter* (bold green). Candidate promoters for these genes are highlighted in the color representative of the gene sequence.

DISCUSSION AND FUTURE WORK

Fe(II) oxidation activity of Rhodobacter capsulatus SB1003 and Rhodopseudomonas palustris CGA009.

It is intriguing that *Rhodobacter capsulatus* SB1003 pre-grown on H_2 has Fe(II) oxidation activity in our cell suspension assays (albeit less than that of the cosmid containing strains) (Figure 5-4). In addition, it has been observed that photoheterotrophically-grown cells of *Rhodopseudomonas palustris* CGA009 also have Fe(II) oxidation activity [83]. In the case of CGA009, the observed activity is equivalent to that of *Rhodopseudomonas palustris* TIE-1 under these conditions. This indicates that Fe(II) oxidation can be decoupled from growth, as neither 1003 or CGA009 can grow photoautotrophically on Fe(II).

The cell suspension assay, however, did not decouple Fe(II) oxidation from the photosynthetic apparatus, as no Fe(II) oxidation occurred in the dark (data not shown). This suggests that either we have not yet identified the specific conditions which allow 1003 and CGA009 to grow photoautotrophically on Fe(II) or TIE-1 and SW2 contain components not present in CGA009 or 1003 that allow them to conserve energy for growth from Fe(II) oxidation. Given that both of the genes identified in our transposon mutagenesis screen are also present in *R. palustris* strain CGA009, if the latter is the case, it is possible that essential genes for this process are missing from 1003 and CGA009, mutated, or not expressed. To resolve this, a screen to identify TIE-1 mutants that are incapable of phototrophic growth on Fe(II), rather than oxidation activity, could be

performed. Alternatively, CGA009 or 1003 could be complemented for growth on Fe(II) through provision of genes from TIE-1 or SW2.

Identification of genes involved in photoautotrophic Fe(II)-oxidation by Rhodopseudomonas palustris strain TIE-1

Of 12,000 mutants screened for loss of Fe(II) oxidation activity, six were identified as being specifically defective in Fe(II) oxidation, with only two different genes being represented among these mutants. Theoretically, our screen is only ~88% saturated. Thus, that five of six mutants identified contained disruptions in the same gene suggests that our screening strategy is not ideal to identify mutants defective in Fe(II) oxidation.

Nonetheless, the two mutants identified in this study provide new insight into the mechanism of Fe(II) oxidation in *Rhodopseudomonas palustris* TIE-1. Mutant strain A2 contains a disruption in a homolog of a cobalt chelatase (CobS). Because the structures of cobaltochelatases and ferrochelatases (which insert Fe(II) into porphyrin rings) are alike, it has been suggested that they have similar enzymatic activities [42, 144]. While it is possible that the phenotype of A2 might be due to the disruption of an enzyme that inserts Fe(II) into a protein or a cofactor that is involved in Fe(II)-oxidation, this seems unlikely because cobaltochelatases and ferrochelatases are typically different at the amino acid level [42]. Instead, a protein involved in Fe(II) oxidation may require cobalamin as cofactor; if true, this would represent a novel use for cobalamin [144]. Mutant strain 76H3 is disrupted in a gene that appears to encode a component of an

ABC transport system that is located in the cytoplasmic membrane. While a variety of molecules could be transported by this system, whatever is being transported (*e.g.,* the Fe(II) oxidase or a protein required for its assembly) likely resides at least momentarily in the periplasm. This raises the question of where Fe(II) is oxidized in the cell? Because Fe(II) is known to enter the periplasmic space of gram negative bacteria through porins in the outer membrane [179], it is conceivable that Fe(II) could be oxidized in this compartment. Alternatively, the Fe(II) oxidase could reside in the outer-membrane and face the external environment, as has been inferred for Fe(II) oxidizing acidophilic bacteria [7, 190]. Determining what catalyzes Fe(II) oxidation and where it is localized is an important next step in our investigation of the molecular basis of phototrophic Fe(II) oxidation.

Identification of candidate genes involved in photoautotrophic Fe(II)-oxidation by Rhodobacter sp. SW2

Identification of the gene(s) on the insert of p9E12 that confer the observed Fe(II) oxidation phenotype proved challenging. Our attempt to identify these genes through *in vitro* mutagenesis was unsuccessful, as all cosmids that lost the ability to confer Fe(II) oxidation contained transposons in different sites in the pLAFR5 backbone rather than the SW2 DNA insert. Given the nature of the genes that these insertions disrupt (*trfA*, *tetA*, *kfrA*, *trbD/E*, and *korF/G)*, it is likely that the loss of the Fe(II) oxidation phenotype results from defects in cosmid stability, replication, and/or maintenance. Why the transposon preferentially

inserts into the pLAFR5 backbone was not investigated, however, it is known that the *tetA* gene on pBR322 contains numerous “hot-spots” for Tn*5* insertion [15]. Although the *tetA* gene located on pBR322 is different from that on pLAFR5 [168], these genes share 75% sequence identity (determined using Blast 2 sequences; http://www.ncbi.nlm.nih.gov/blast/bl2seq/wblast2.cgi). Thus, such hot-spots likely exist within the *tetA* gene of pLAFR5 and perhaps other genes on the backbone of this cosmid.

At this point, it is still unclear which gene(s) from *Rhodobacter* SW2 on the insert of pE12 (or pB3, p11D3, and p12D4) confer the observed Fe(II) oxidation activity to *Rhodobacter capsulatus* SB1003; however, sub-cloning of the *PstI* restriction fragment 3 in pBBR1MCS5 (Gm^R) has allowed us to confine our search to the genes present on this fragment. Sequence analysis of this 9.4 kb fragment suggests that a potential gene responsible for the Fe(II) oxidation phenotype may encode a predicted permease based on the fact it is the only ORFs in sequence common to the four cosmids for which a homolog in other *Rhodobacter* species was not found. In addition, one of the genes found to be involved in Fe(II) oxidation in TIE-1 encodes a predicted permease. Directly upstream of this permease in SW2 is a putative acetyltransferase. In TIE-1, an predicted acetyltransferase is found downstream of the permease involved in Fe(II) oxidation. The similarities here are encouraging and warrant further investigation.

In accordance with our findings that genes required for Fe(II) oxidation in TIE-1 are also present in CGA009, a strain unable to grow photoautotrophically

on Fe(II), a protein containing a β-propeller structure and possibly the redox cofactor pyrroloquinoline quinone (PQQ) with similarity to a WD-like protein in *Rhodobacter sphaeroides* 2.4.1 also represents a potential Fe(II) oxidation gene candidate. A quinoprotein has recently been implicated in the Mn(II)-oxidizing activity of *Erythrobacter* sp. SD21 and *Pseudomonas putida* MnB1 [87], providing precedent for the involvement of PQQ containing enzymes in metal oxidation reactions. In addition, a permease of the drug/metabolite transporter superfamily with a homolog in *Rhodobacter sphaeroides* 2.4.1 represents a candidate based on similarity to TIE-1 mutant 76H3 and the fact that it lies in a region common to the four cosmids.

We find that this 9.4 kb fragment confers Fe(II) oxidation activity upon 1003 independent of the orientation in which it is cloned. This suggests that the gene(s) responsible for this phenotype is cloned with its endogenous promoter. Analysis of the sequence upstream of these predicted candidate ORFs reveals putative σ^{70} promoter consensus sequences 182 bp upstream of the predicted start of translation (T_L start) for the putative PQQ containing protein, 1427 bp upstream from the T_L start for the predicted permease with no homolog in *Rhodobacter*, and 198 bp upstream of the T_L start for the predicted permease of the drug/metabolite transporter superfamily. For comparison, in genes of *E.coli* K12, the distance between the transcription start site associated with the promoter and the translation start site is between 0–920 bp with 95% of 771 promoters analyzed being at a distance <325 bp upstream of the T_L start site [28].

The promoter 1427 bp upstream from the T_L start for the predicted permease with no homolog in *Rhodobacter* is well out of this range, however, it is possible that this permease is co-transcribed with the upstream acetyltransferase. This predicted promoter lies 655 bp upstream of the acetyltransferase and while this distance is above average by comparison to *E. coli*, it is within range.

To identify the specific genes responsible for the observed Fe(II) oxidation phenotype, we may take two approaches which include: 1) cloning these candidates to test them specifically for their ability to confer Fe(II) oxidation activity to 1003; 2) making directed knock-outs of these candidates using the method of Datsenko and Wanner [44]. In this method, particular genes on a chromosome or a construct can be replaced with an antibiotic resistance gene (generated by PCR and designed to have a 36 nucleotide extension with homology to the gene(s) of interest) using the phage λ Red recombinase to promote recombination. In anticipation of the possibility that the genes involved are not present in our current sequence, we are also closing the sequence gaps of the pP3 insert. Lastly, given that the pP3-gm1 and pP3-gm2 clones contain a smaller fragment of the p9E12 insert and are cloned in the BBR1MCS5 vector (which confers gentamicin resistance) rather than pLAFR5, if our direct approaches do not work, we will again attempt to use an *in vitro* mutagenesis approach to identify these genes.

Once these genes are identified we will be able to address whether the Fe(II) oxidation system is these phototrophs is similar to that in other Fe(II)-oxidizing bacteria such as *A. ferrooxidans.* Uncovering the degree to which

electron transfer from Fe(II) is conserved amongst phylogenetically divergent species may in turn provide information on the origins of this ancient metabolism.

6. *C*-type cytochrome, soluble and membrane protein analysis of *Rhodobacter* sp SW2 and *Rhodopseudomonas palustris* TIE-1

ABSTRACT

The ability to grown on Fe(II) is thought to be a primitive metabolism and of the bacteria able to use Fe(II) as a source of energy for growth, it is believed that the anoxygenic phototrophs are the most ancient. Substantiation of this hypothesis requires phylogenetic investigations of the enzymes involved in this metabolism, particularly the enzyme that catalyzes the oxidation of Fe(II); however, the identity of this enzyme remains unknown. The high reduction potentials of Class I *c*-type cytochromes and existing precedent for the involvement of *c*-type cytochromes in Fe(II) oxidation by *Acidithiobacillus ferrooxidans* make a protein of this type a strong candidate for the role of Fe(II) oxidase in Fe(II)-oxidizing phototrophs. To identify components involved in photoautotrophic Fe(II) oxidation, and potentially the Fe(II) oxidase, we characterized the soluble, membrane and *c*-type cytochrome protein profiles of the Fe(II)-oxidizing phototrophs, *Rhodobacter* sp SW2 and *Rhodopseudomonas palustris* TIE-1, grown on different electron donors, and in particular on Fe(II). *C*-type cytochromes and other proteins unique or more highly expressed under Fe(II) growth conditions in *Rhodobacter* sp SW2 and *Rhodopseudomonas palustris*

TIE-1 were observed. Whether these proteins are involved in phototrophic Fe(II)-oxidation by these strains is under current investigation.

INTRODUCTION

The photosynthetic electron transport chain of purple non-sulfur bacteria of the *Rhodospirillaceae* family contains two multi-subunit transmembrane proteins: the reaction center and the cytochrome bc_1 complex. While exceptions exist, in these types of bacteria, the cyclic electron flow between these two complexes that results in ATP formation is mediated by the membrane soluble quinone pool in the cytoplasmic membrane and cytochrome c_2 (Cyt c_2), located in the periplasmic space [119]. Electrons from inorganic substrates such as H_2 or S^{2-}, enter the cyclic electron transport chain via these soluble carriers in a reaction that is catalyzed by enzymes specific to growth on the respective substrate [64, 178].

In a bicarbonate containing system the relevant Fe couple, $Fe(OH)_3$ + $HCO_3^-/FeCO_3$, has a high redox potential of +0.2 V [52]. Thus, in purple non-sulfur, anoxygenic phototrophs able to use Fe(II) as an electron donor for photosynthesis, a carrier(s) that mediates electron transfer between Fe(II) and the photosynthetic electron transport chain must have a redox potential higher than +0.2 V. Because the reduction potential of the ubiquinone pool (+0.113 V) is higher than that of the Fe(II) couple, it is unlikely that electrons from Fe(II) enter the chain at this point. It has been proposed that electrons from Fe(II) enter the electron transport chain of these organisms via Cyt c_2 directly [52].

However, it is also possible that entry of these electrons into the cyclic electron flow is mediated by an enzyme unique to growth on Fe(II) (*i.e.*, an Fe(II) oxidase), similar to the case of H_2 and S^{2-}.

Class I *c*-type cytochromes, of which bacterial Cyt c_2 is a representative [16], have reduction potentials that vary from +0.2 - +0.35 V [9], making them able to accept electrons from Fe(II). Given this, and the fact that *Rhodobacter capsulatus* has at least 12 *c*-type cytochromes and *Rhodopseudomonas palustris* and *Rhodobacter sphaeroides* each have at least 21 (some of which have no known function) [118], a *c*-type cytochrome is a likely candidate for the role of Fe(II) oxidase. In addition, a number of *c*-type cytochromes have been implicated in Fe(II) respiratory chain of *Acidithiobacillus ferrooxidans* [189], an obligately autotrophic and acidophilic bacterium capable of aerobic respiration on Fe(II) and reduced forms of sulfur (H_2S, S^o, $S_2O_3^{2-}$) [53, 139]. Further, it has been proposed that one of them, the product of the *cyc2* gene, Cyc2, is the primary acceptor for electrons from Fe(II) [7].

Another protein implicated in the Fe(II) respiratory chain of *Acidithiobacillus ferrooxidans* that is also postulated to be the primary electron acceptor in some strains is the high potential iron-sulfur protein (HiPIP), encoded by the *iro* gene [63, 104]. HiPIPs, have redox potentials in the range of +0.05 to +0.45 V and are also commonly found in purple photosynthetic bacteria [120]. These soluble ferredoxins are found primarily in purple sulfur bacteria of the *Chomatiaceae and Ectothiorhodospiraceae* families, but are also found in some *Rhodospirillaceae* [118]. In these bacteria, it is thought that these HiPIPs can

serve the same purpose as Cyt c_2, that is, to mediate electron flow between the reaction center and the cytochrome bc_1 complex [118]. Thus, another potential candidate for the role of Fe(II) oxidase may be a HiPIP.

Because *c*-type cytochromes can be easily detected through specific staining on polyacrylamide gels [61], we characterized the *c*-type cytochrome contents of the Fe(II) oxidizing phototrophs, *Rhodobacter* sp SW2 and *Rhodopseudomonas palustris* TIE-1, grown on different electron donors and in particular, on Fe(II). We have also begun investigations of the membrane and soluble proteins of these two bacteria to identify proteins expressed exclusively under Fe(II) growth conditions. Protocols with which to identify proteins with Fe(II) oxidation activity in polyacrylamide gels exist [46] and it is our goal to identify a protein(s) with such activity.

EXPERIMENTAL PROCEDURES

Organisms and cultivation

Cultures of *Rhodopseudomonas palustris* TIE-1 (TIE-1) and *Rhodobacter* sp. SW2 (SW2) were maintained in a previously described anoxic minimal salts medium for freshwater cultures [52] and were incubated 20 to 30 cm from a 34 W tungsten, incandescent light source at 30°C for TIE-1 and 16°C for SW2. *Rhodobacter capsulatus* SB1003 (1003) grown photoheterotrophically on RCV [180] and incubated at 30°C. Electron donors for photosynthetic growth were added to the basal medium as follows: thiosulfate was added from an anoxic filter sterilized stock to a final concentration of 10 mM; acetate was added from a 1 M,

filter sterilized, anoxic solution at pH 7 to a final concentration of 10 mM, and H_2 was provided as a headspace of 80% H_2: 20% CO_2. For growth on Fe(II), 4 mls of a filter sterilized, anoxic 1 M Fe(II)$Cl_2 \cdot H_2O$ stock solution was added per 1 liter (L) of anaerobic, basal medium (final concentration ~4 mM). To avoid the precipitation of ferrous Fe minerals that results upon addition of Fe(II)$Cl_2 \cdot H_2O$ to the bicarbonate buffered basal medium and the precipitation of ferric Fe minerals that form during the growth of these bacteria on Fe, the metal chelator, nitrilotriacetic acid (NTA, disodium salt from Sigma), was supplied from a 1 M filter sterilized stock solution to a final concentration of 10 mM. This NTA addition greatly facilitated the harvesting of cells, free of Fe minerals, from Fe(II) grown cultures.

Soluble and membrane protein extraction

To extract soluble and membrane protein fractions from SW2, 1 L cultures of this strain grown phototrophically on H_2, acetate and Fe(II) were harvested in exponential phase by centrifugation (10,000 rpm in a Beckman JLA 10.5 rotor for 20 min). The pellets were resuspended in 3 mls of 10 mM HEPES buffer at pH 7 and sonicated on ice for a total of 5 minutes using a 10 second on/10 second off program. 18 µl of a 0.2 M PMSF stock (0.0348 g in 1 ml 100% EtOH) and 1 µl of a 50 mg/ml DNAse stock were added and the lysate was incubated 30 min on ice. After incubation, cell debris was removed by centrifugation (6000 rpm on a Beckman JLA 10.5 rotor for 30 min at 4ºC). The supernatant from this centrifugation was subjected to ultracentrifugation at 200,000 x g for 90 min at

4ºC. The resultant supernatant represented the soluble protein fraction. The resultant pellet was resuspended in 50 µl buffer to give the membrane protein fraction. Soluble and membrane protein fractions from *Rhodobacter capsulatus* SB1003 grown phototrophically on RCV, a condition under which *c*-type cytochromes are known to be expressed in a similar manner to that described above.

To extract soluble and membrane protein fractions from TIE-1, ~10 L of cells grown phototrophically on H_2, thiosulfate and ~ 50 L of cells grown phototrophically on Fe(II) were harvested in exponential phase by centrifugation (10,000 rpm on a Beckman JLA 10.5 rotor for 20 min). The pellets were washed and resuspended in 20 mls of buffer (50 mM HEPES, 20 mM NaCl, pH 7), DNAase and protease inhibitors were added and the suspension was subjected to 3 passages through a French pressure cell at 18,000 psi. Cell debris was removed by low speed centrifugation (10,000 x g for 20 minutes) and soluble and membrane protein fractions were isolated as described above.

Protein concentrations were measured using the Bio-Rad protein assay (Hercules, CA). For SW2 sample storage, glycerol was added to a final concentration of 10% before freezing the sample at -20ºC. TIE-1 samples were frozen with liquid N_2 and stored at -80 C.

Sodium dodecyl sulfate-polyacrylamide gel electrophoresis (SDS-PAGE) and gel staining

SDS-PAGE was performed by standard procedures according to the Laemmli method [1], using dithiothreitol (DTT) as the reducing agent in the Laemmli sample buffer. For SW2, 15 µg protein samples of the soluble and membrane protein fractions from the different cultures were incubated with sample buffer for 5 min at 25°C. These samples were then separated on a 12% polyacrylamide gel at a current of 20 mA. For TIE-1, 100 µg samples of crude cell extract and soluble fraction and 60 µg of the membrane fraction from the different cultures were prepared as described above. Here, the samples proteins were separated on a 4-20% Tris·HCl mini-gradient pre-cast gel from Biorad at a current of 25 mA.

Gels were stained for protein with the Bio-Safe Coomassie Stain from Bio-Rad. Gels were stained for heme-containing proteins according to the in-gel peroxidase activity assay of Francis and Becker [61]. Here, the gel was first incubated in 12.5% trichloroacetic acid for 30 minutes and then washed with dH_2O for 30 minutes. After these incubations, the gel was transferred to a solution containing 20 mls of 0.5 M Na-citrate buffer (pH 4.4), 0.4 mls of 30% H_2O_2 and180 mls of a freshly prepared solution of *o*-dianisidine (200 mg *o*-dianisidine (Sigma), 180 mls dH_2O). The staining reaction was allowed to proceed from 2 hours to overnight.

RESULTS

C-type cytochromes and other proteins unique to Fe(II) growth in SW2

Heme and protein stains of soluble and membrane proteins of SW2 grown on Fe(II), H_2, and acetate, separated by SDS-PAGE, are shown in Figure 6-1A and 6-1B, respectively. Here, a *c*-type cytochrome of approximately 15 kDa (kiloDaltons) that appears unique to the membrane fraction of Fe(II)-grown cells was observed (Figure 6-1A). This cytochrome was not present in 1003, a strain that is unable to grow photoautotrophically on Fe(II). High molecular weight non-*c*-type cytochrome proteins that appear to be unique to the membrane fraction of Fe(II)-grown SW2 cells were also observed (Figure 6-1B). It is important to note, however, that the concentration of protein loaded here was low (15 µg). For example, the *c*-type cytochromes (likely cyc_1 or cyc_y [81]), present in 1003 of approximately 30 kDa, are very faint. Thus, it is possible that the cytochrome present under Fe(II) growth conditions also exists in the cells grown on H_2 and acetate, but its concentration in our sample is below the detection limit of the peroxidase activity assay. This caveat stands for the unique proteins identified in the gel stained for protein as well.

A.

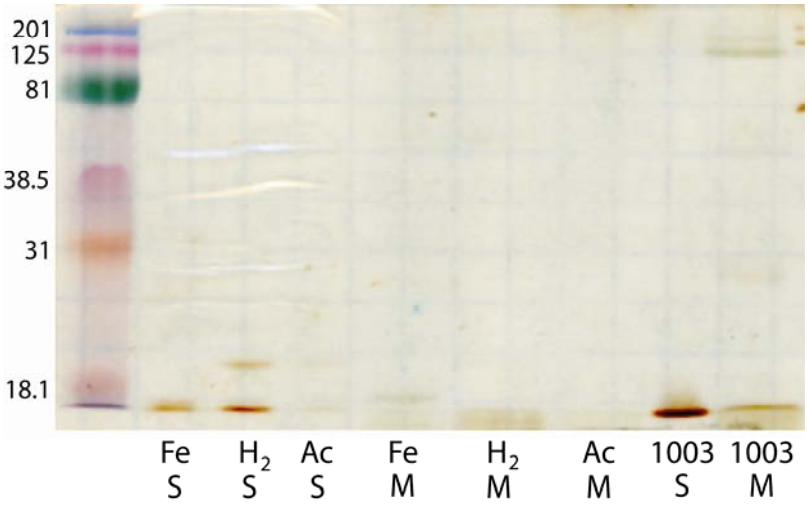
201
125
81
38.5
31
18.1
Fe S
H2 S
Ac S
Fe M
H2 M
Ac M
1003 S
1003 M

B.

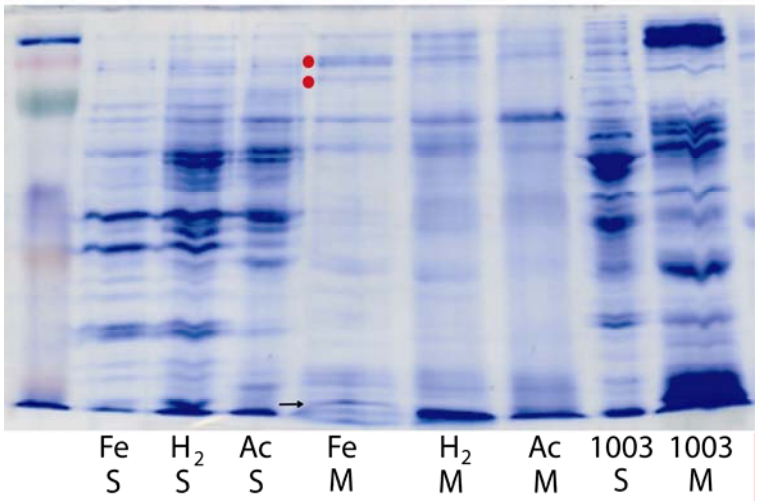
Fe S
H2 S
Ac S
Fe M
H2 M
Ac M
1003 S
1003 M

Figure 6-1: A. Heme stain of soluble (S) and membrane (M) proteins of SW2 cells grown phototrophically on Fe(II), H_2, and acetate, and *Rhodobacter capsulatus* SB1003 grown photoheterotrophically on RCV. The arrow highlights a *c*-type cytochrome of approximately 15 kDa that appears unique to the membrane fraction of Fe(II)-grown SW2 cells. B. Total soluble and membrane protein profiles of SW2 grown on Fe(II), H_2, and acetate. The red dots highlight proteins that appear unique to the membrane fraction of Fe(II)-grown cells and the arrow identifies the protein that corresponds to the heme in part A.

C-type cytochromes upregulated under Fe(II) growth conditions and other proteins unique to Fe(II) growth conditions in TIE-1

Heme and protein stains of soluble and membrane proteins of TIE-1 cells grown on Fe(II), H_2, and thiosulfate, separated by SDS-PAGE, are shown in Figure 6-2A and 6-2B, respectively. In the heme stain, we observed *c*-type cytochromes of approximately 35 kDa that were much more highly expressed in the crude and soluble fractions of Fe(II)-grown TIE-1 cells (Figure 6-2A). In addition, it seems an approximately 90 kDa *c*-type cytochrome associated with the membrane fraction that is more highly expressed under Fe(II) growth conditions (Figure 6-2A). On a gel stained for protein, an approximately 23 kDa, non-*c*-type cytochrome protein that appears unique to Fe(II) grown cells is present in soluble protein fraction (Figure 6-2B).

A.

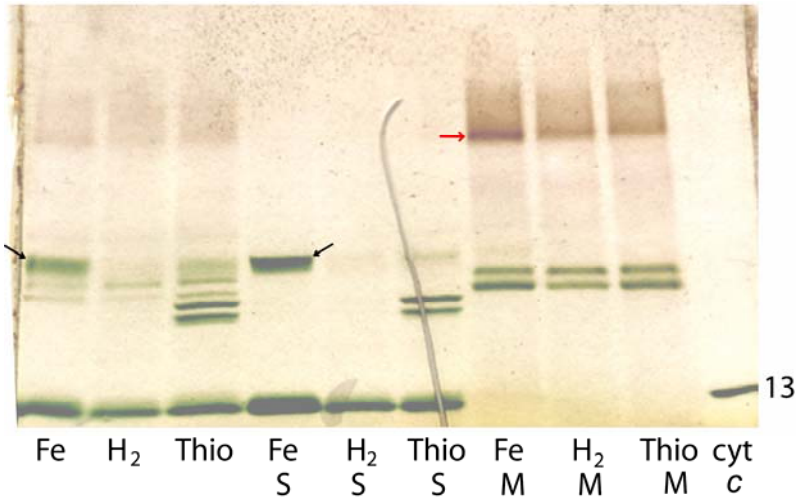
13
Fe
H2
Thio
Fe S
H2 S
Thio S
Fe M
H2 M
Thio M
cyt c

B.

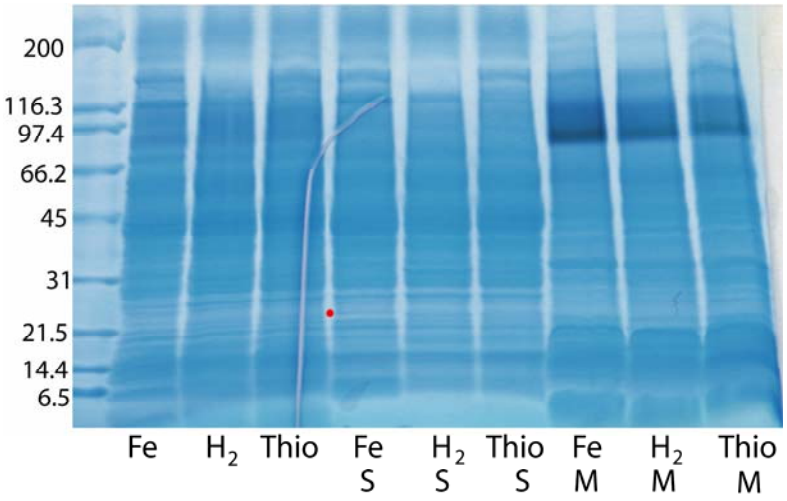
200
116.3
97.4
66.2
45
31
21.5
14.4
6.5
Fe
H2
Thio
Fe S
H2 S
Thio S
Fe M
H2 M
Thio M

Figure 6-2: A. Heme stain of soluble (S) and membrane (M) proteins of TIE-1 cells grown on Fe(II), H_2, and thiosulfate, separated by SDS-PAGE. The black arrows highlight *c*-type cytochromes of approximately 35 kDa that are much more highly expressed in the crude and soluble fractions of Fe(II)-grown cells. In addition, there is a *c*-type cytochrome of approximately 90 kDa that is more highly expressed in the membrane fraction (indicted by the red arrow). B. Total soluble and membrane protein profiles of TIE-1 grown on Fe(II), H_2, and acetate. The red dots highlight proteins that appear unique to the soluble fraction of Fe(II)-grown cells.

DISCUSSION AND FUTURE WORK

Preliminary work presented here provides evidence that *c*-type cytochromes and other proteins unique or more highly expressed under Fe(II) growth conditions are present in *Rhodobacter* sp. SW2 and *Rhodopseudomonas palustris* TIE-1. Whether these proteins are involved in phototrophic Fe(II)-oxidation by these strains remains to be investigated, however precedent for *c*-type cytochromes being involved in Fe(II) respiratory processes exists [6, 38, 174, 177, 189]. Further, the redox potentials of *c*-type cytochromes are consistent with the hypothesis that the enzyme that shuttles electrons from Fe(II) to the photosynthetic electron transport chain is a *c*-type cytochrome.

Interestingly, the product of the *cyc2* gene of *Acidithiobacillus ferrooxidans* is a high molecular weight *c*-type cytochrome (46 kDa) that is localized to the outer membrane and this protein is proposed to catalyze the first step in the

transfer of electrons from Fe(II) to O_2 by this organism [6]. While the 35 kDa *c*-type cytochrome we observed in TIE-1 appears to be soluble, the similarity here is encouraging. In addition, a gene that is predicted to encode a putative deca-heme *c*-type cytochrome with similarity at the C-terminal to MtrA (a cytochrome involved in Fe(III) respiration in *Shewanella oneidensis* MR-1), is found in the genome of *Rhodopseudomonas palustris* CGA009 (CGA009), a strain unable to growth photosynthetically on Fe(II), and can be amplified by PCR from TIE-1 (Figure 6-3, [82]). The predicted product of this gene has a multi-copper oxidase copper binding motif at the N-terminal. Proteins with such motifs have been implicated in divalent metal oxidation coupled to growth in *Acidithiobacillus ferrooxidans*, *Leptothrix discophora*, *Pseudomonas putida, Bacillus SG-1* and some eukaryotic organisms [26].

A gene with similarity to the *iro* gene of *Acidithiobacillus ferrooxidans* (predicted to encode an Fe oxidase in some strains of this organism) is also found in the genome of CGA009, and is detected in TIE-1 (Figure 6-3). A gene that is predicted to encode a cytochrome of 90 kDa, however, is not found in the genome of CGA009. Thus, it is possible that this cytochrome is unique to *Rhodopseudomonas palustris* strains able to growth on Fe(II). Finally, a gene predicted to encode an outer membrane protein, homologous to MtrA, an outer membrane protein involved in Fe(III) respiration in *Shewanella oneidensis*, is found in the same cluster as the two genes described above (Figure 6-3).

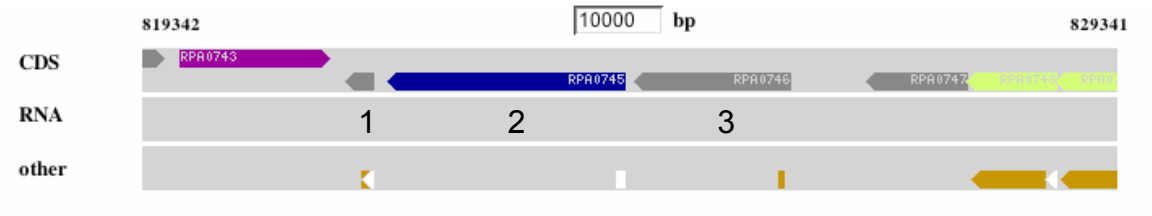

Figure 6-3: Gene cluster in *Rhodopseudomonas palustris* GCA009 with homologs in TIE-1 containing genes encoding proteins with possible function in photoautotrophic Fe(II) oxidation. 1: A gene predicted to encode a high redox potential Fe-S protein that is homologous to the *iro* (possible iron oxidase) in *Acidithiobacillus ferrooxidans*. 2: A gene predicted to encode an outer membrane protein, homologous to MtrA, (an outer membrane protein involved in Fe(III) respiration in *Shewanella oneidensis*. 3: The predicted product of this gene has a multi-copper oxidase copper binding motif at the N-terminal and a C-terminal sequence is homologous to a deca-heme cytochrome *c* in *Shewanella*.

Current efforts are underway to construct mutants of these genes in TIE-1 and test their Fe(II) oxidation capabilities. Finally, we are also working to obtain N-terminal sequence for the observed *c*-type cytochromes of TIE-1 and SW2 and to develop an in-gel assay to test if these cytochromes or the other proteins unique to Fe(II) growth conditions in these strains have Fe(II)-oxidation activity.

Once components of photoautotrophic growth on Fe(II) are identified, we can begin to uncover the degree to which electron transfer from Fe(II) is conserved among phototrophs and other bacteria able to oxidize Fe(II). In addition, knowledge of the components involved in this form of metabolism will direct our efforts to identify traces of Fe(II) oxidation in the rock record [41].

7. Conclusions and Implications

One of the major contributions of this thesis is our finding that phylogenetically distinct Fe(II)-oxidizing phototrophs fractionate Fe isotopes via apparently equilibrium processes. While our work could not distinguish between an equilibrium fractionation mediated by biological or abiotic processes, it demonstrated that equilibrium processes prevail in biological systems rather than kinetic process as previously hypothesized [10]. Further the likely possibilities we provided for the mechanism of Fe isotope fractionation by these organisms guided subsequent investigations where our hypothesis that the fractionation represented equilibrium exchange between aqueous Fe(II) and Fe(III) species overlain by kinetic effects produced by precipitation of ferric minerals was proven true [8]. Finally, while we found that these organisms fractionate Fe isotopes in a way that is consistent with Fe isotopic values found in Precambrian BIFs, we concluded that it is unlikely that this fractionation can be used as a biosignature for this metabolism given its similarity to fractionations produced by abiotic Fe(II) oxidation reactions, thus, making further study in this area largely unnecessary.

Organisms that oxidize Fe(II) are difficult to study from a genetic perspective. This is largely due to the challenges inherent in growing these organisms. For example, aerobic neutrophilic Fe(II)-oxidizers must outcompete the rate of abiotic oxidation of Fe(II) by molecular oxygen (O_2) to harvest energy for growth. The requirement of specific O_2 and Fe(II) concentrations for these

bacteria is met by growing them in tubes of solid medium with opposing gradients of Fe(II) and O_2 [54]. Such culturing requirements are not easily amenable to large scale genetic screens. Thus, a second contribution of this work is the development of an assay for the identification of genes involved in Fe(II) photoautotrophy in genetically intractable strains. With this assay, we are afforded a means to identify the molecular components of Fe(II) oxidation and using this assay we have identified the first genes known to be involved in this metabolism. Future work to identify additional components of this metabolism are now enabled and should include the identification of the enzyme that catalyzes Fe(II) oxidation, its localization in the cell, and investigations of the degree to which this enzyme is conserved among phylogenetically distinct organisms able to oxidize Fe(II). We anticipate that such phylogenetic investigations will provide insight, not only into the mechanism of this metabolism, but also its origins.

Overall, this thesis provides an example of what one might call “metabolic paleontology,” that is: the investigation of the mechanisms of modern metabolisms as a means to uncover how ancient related metabolisms may have affected the geochemical evolution of the Earth. It is important to note, however, that a fundamental assumption in this work is that the metabolisms of modern microbes are representative of those of ancient organisms. The uncertainty in this assumption is irresolvable, as we can never know to what extent ancient metabolisms may differ from modern metabolisms. However, a thorough understanding of the molecular components of a particular metabolism of interest

and how their expression is regulated in a diversity of modern organisms can help to reduce this uncertainty by giving us a feel for the range of variability in the rates and particular components of these metabolisms. Moreover, with molecular investigations, we can uncover the degree to which aspects of this these metabolisms have been conserved throughout their evolution, as it is in these aspects were our most robust conclusions can be drawn. With such comprehensive comparative studies we can make progress towards the identification and unambiguous interpretation of biosignatures in the rock record.

Given the extensive time-period over which BIFs were deposited, it is probable that a combination of biotic (both an- and oxygenic) and abiotic mechanisms contributed to the deposition of these rocks and that the relative contributions of biotic and abiotic Fe oxidation varied over geologic time. Therefore, it is important to note that a model for the contribution of Fe(II) oxidizing phototrophs in the deposition of BIFs does not preclude a role for abiotic mechanisms of Fe(II) oxidation and recognize that an understanding of the chemistry of the Earth at the time of BIF deposition is critical in determining which Fe(II) oxidizing metabolisms were involved in the formation of BIFs over time. Furthermore, such temporal variations in the role of direct biological and inorganic processes may produce identifiable morphological or chemical variances in BIFs of different ages and may present a potential target for biosignature development.

In conclusion, studying extant microbes to identify chemical signatures unique to these organisms may provide us with tools to investigate how the

metabolism of ancient related organisms shaped the chemistry of the Earth. Although I was not able to identify a biosignature unique to the metabolism of these organisms, my research makes significant contributions toward this lofty goal and it is my hope that these investigations will lay the groundwork for future studies with this directive.

Appendix 1. Partial sequence of p9E12, a cosmid that confers Fe(II) oxidation activity to *Rhodobacter capsulatus* SB1003

To identify the genes responsible for the observed Fe(II) oxidation activity conferred onto *Rhodobacter capsulatus* SB1003 by p9E12, the insert of this cosmid was sub-cloned and partially sequenced. The sequence data obtained are presented here and represent ~78% of the p9E12 insert. pP1, pP2, pP3, pP4, pP5, pP6, pP7 are clones with *PstI* restriction fragments of pE12 in pBBR1MCS3 (Tc^R) and pH5 and pH6 are clones with *HindIII* restriction fragments of pE12 in pBBR1MCS2 (Km^R). For further details see Chapter 5.

pP1 – 397 bp from T3 end
66% GC

CTTAATCGCCTTGCAGCACATCCCCCTTTCGCCAGCTGGCGTAATAGCGAAGAGGCCCGCACCGATCGCCCCGAAC
ACGAGCACGGCACCCGCGACCACTATGCCAAGAATGCCCAAGGTAAAAATTGCCGGCCCCGCCATGAAGTCCGTGA
ATGCCCCGACGGCCGAAGTGAAGGGCAGGCCGCCACCCAGGCCGCCGCCCTCACTGCCCGGCACCTGGTCGCTG
AATGTCGATGCCAGCACCTGCGGCACGTCAATGCTTCCGGGCGTCGCGCTCGGGCTGATCGCCCATCCCGTTACTG
CCCCGATCCCGGCAATGGNAAGGACTGCCAGCGCTGCCATTTTTGGGGTGAGGCCGTTCGCGGCCGAGGGGCGCA
GCCCCTGGGGGGATGGGAGG

pP1 – 709 bp from T7 end
66% GC

TTGCCGAAACCAGCGGTTCGGGCGCAAACTGATGCTGAAGGGAGGGCCCCTTGCCGGGGCCTTCCCCCTTTCCACA
AGGAATGGCTGCGATGACCTACGACACCATGCTTCCCGACCCCGACCGCCATGCCGAGTTCTATGCCGGCGTGCCG
ACCAAGCGCGCGCTGGCCTGGGTGGCGGATATGGTGCTGATCGCCGTGGTCACCGCGATCATCGTGCCGTTCACC
GCCTTTACCGCGCTGTTTTTCCTGCCCTTCCTGTATCTGGTGGTGGGCTTTGTCTATCGCACCCTGACCCTTGCGGG
CGGCTCTGCCACCTGGGGGATGCGGCTGATGGCGATCGAGTTGCGCGACTATCGCGGCCAGCGGTTTGATCTGGC
CACCGCGATCCTGCACACGCTGGGCTACAGCATTTCCATCGGCATGGTGGCGCCGCAGGTGCTTTCGGCCGGGCT
GATGCTGGTCACGCCGCGGGCGCAGGGGCTGACCGACCTTTTGATGGGCAGCGTGGCGATCAACCGCGCCGCCC
GCTACTGACCCTTGGGGGCGCGGCAAAGACAGTCCTTGGCGGCAGCCGCGCGGCTTGCTAACGTGGCGGCGGATC
CCCTTTGAATGTCGATCATGCGCCACACTCTGCCGATCCACGAGACCCTGAAACGCGGCCATACCAAGCCCGCGCC
CTGGACGGTGATCCGCTCCTTGCCGCCCCA

pP2 – 7264 bp from the T3 end
68% GC

ATTCGTTGTGCCTTGCCAGTGTCCTTGCCCTGTCGGGCTGTGTCCCCGCCGCCCCGCCGCTGGTGACGATGACCCG
CGCCACCGCCGTGCTGGCGCTGGACGGGTTGCCCCGCGATGAAAACCTTCGGGCCGCAGCGCGCCCCCGCCCCCA
CCCGCAGCAATGCCGAGATCGCGCAGGACTTTCTGGCGCTGGAGTTTCGCATGGAAAGCGGGCGGGCGCTGCCGG
TGCTCAGCCGCTTTGACGGCCCGATCACCGTGGCGCTGACCGGCGCCGTGCCTGCCACCGCCGCCCGCGATCTGG
CCGCCGTGGTCGCCCGCTTCCGGGCCGAGGCCGGGATCGACATCCGCCAGACCGACAGCGCCGCCCGCATCACC
GTTGAATTCATCCCGCGGGCGCAAATCCAGGGCGTCTATGCCAATGTCGCCTGTTTCGTGGTGCCAAGGGTGTCGT
CCTGGGCCGACTACCGCGCTGCCCGTGGCGCGGCCAGGCTGGATTGGGCCACAGTGACCGCCCGCGAGCAGGCC
GCGATCTTCGTGCCCGCCGACACCAGCCCGCAAGAGGTGCGCGACTGTCTGCACGAGGAACTGGCGCAGGCGATG
GGGCCGCTCAACGATCTGTATTCGCTGTCGGATTCGGTGTTCAACGACGACAATTTCCACACCACGCTGACCGGCTT
CGACATGCTGGTGCTGCGCGCGCATTACGCGCCGGAACTGCGATCCGGCATGACCGAGGCCGAGGTGGCGGCGCT
GTTGCCCGACCTGCTGGCGCGACTGAACCCAGGCGGCCGCCATGCGGGAAACCCGGTCAGCAGCGCCACGCCGC
GGGCCTGGATCGACGCGATGGAAAAGGCGCTTGGCGGGCAGGCACCGGTCGCCGCCCGCCGGGCCGCCGCCCG
CCGCACGCTGGAAATTGCCACGGCGCAAGGCTGGCACGACAGCCGCCTTGCCTTCAGCCAGTTCGCGGTGGGGCG
GCTGAACATCGGCCACGACCCCGCAACCGCCCTTGTGGCCTTTACCGCCGCCGCAGCACTTTACCGCAGCCTGCCC
GGCGGCCAGATCCAwGsaGCsmATgTCsAkcAtgCAgCTkGCsGCCgTTacTaGCCCTGCGGCAGGGCGATGCCAAGGG
CGCGCTGGTGCTGGCCGATCGGGCCATTCCGGTGGTCACCTCGGCGCAGAACGCAGCCCTCTTGGCCACGCTGCT
GATGGTCAAGGCCGAGGCGCTGGAGGCGCTTGGCCGCACGGCGCAGGCGCAGGCCGTCCGGCTCGACAGCCTTG
GCTGGGCGCGCTATGGTTTCGGCTCGGCGCAAGCGGTGCAGACCCGGATGGCCGAGATTGCCGCCCTGACCCCGC
CACGGGAAAAGGGCTGATCCGCCGGGGGCCACATGTTCGTGCCGTTCTTCCAGACCCTGCGGCAGTTCGGCGTGC
CGGTCAGCTTGCGCGAATACCTGTCGTTTCTGGAAGGCATGGCCGCGGGGCTTGCCACCTATGACCCGGACGGCTT
CTACCACCTCGCCCGCCTGACCATGGTCAAGGACGAACGCCACCTCGACCGCTTCGACCGCGCCTTTGCCAGCAGT
TTTCACGGGCTGGACAGCATCACCGCCGAACAGGTGCTGGAGGCGGTCGATCTGCCGCGCGACTGGCTGGAAAAG
CTGGCCGAATCCACCCTGACGCCGGAAGAACGCGCCGAACTCAAGGCCCTGGGCAGCTTTGATGCGCTGATGGAG
GCGCTGCGGGCGCGGCTGGCCGAACAGCAGGGGCGGCATCAGGGCGGCGCGAAATGGATCGGCACGGCGGGCA
CCTCGCCCTTCGGCGCCTACGGCGCCAACCCCGAAGGCGTGCGGATCGGTCAGGACGGCTCGCGCCACCGCACC
GCGGTCAAGGTCTGGGACCAGCGCCTCTTTCGCAATCTGGACGACCGGGTGGAACTGGGCACCCGCAACATCAAG
GTCGCCCTGCGCCGCCTGCGCCACTGGGCCCGCGACGGTGCGGAACAGGAGCTTGACTTGGCCGGCACCATCCGC
GCCACCGCCGAGCATGGCTGGCTGGACGTGCAAACCCGCCCCGAGCGGCGCAATGCGGTCAAGGTGCTGCTGTTC
CTCGATATCGGCGGCAGCATGGACCCGCATGTGCAGGTGATGGAGGAGTTGTTCTCCGCCGCCCGCGCCGAGTTCA
AGCACCTGATCCCGTTCTACTTTCACAACTGCCTTTATGAAGGCGTGTGGCGCGACAACGCCCGCCGCTGGGATGC
CCAGACCCCCACCGCCGAGGTGCTGCACAGCTATGGCGCGGATTACAAATGCATTTTCGTAGGCGACGCCAGCATG
AGCCCCTACGAGATCCTGCACCCCGGCGGCGCCAACGAACACTGGAACCCGGAGACCGGCCAGACCTGGCTGACC
CGCGCCGCACAGGCCTGGCCCGCGCATCTGTGGATCAACCCGGTGCCCGAGGCGCATTGGTCTTACACGCCGTCC
ATCCGGCTGATCCAGCAGATATTCGACGGCCGCATGGTGCCGATGACGCTGGAGGGCATCGCCCGCGGGATCAAG
GCGCTGGGACGATGAAACATCTGTGGCAGACCCACCGCTGGCTGGTGCTGGCTTTCCTTGTCGCCGCCAGCCTGTC
GATGTTCTTCGGCATCCGCGCCGCCCTGTTCGTGCCGCGCTGGCATCTGCACCTCGACTATGCAGCCCAGCCGGTG
CAGCCCTGGATGACGCCGAAGCTGATCGTCAAGACCTACGGCGTCCCGCCGGAAGTTCTGGAACAAGTGCTTGGCC
TGCCTGAAAAATTCCACCCGCGGCAAACCCTGGCCGAGATTGCCGCAGATCAGGGCATCGACTCTGCGGCGCTGGC
AGCAAGGGTCGAGGCGGCAGTGCGCGCCGCCAGAGGCCACTTGCAGCAATGACCGAAACCCTGTTGGAACTGGTG
CCGACCTGGGGCGCCTTGCTGGTGCTGGTGGCCACCTTGCTGTCATGCCTCGCACTTCCCGTGCCATCGTCGCTGA
TCATGCTGGCGGCGGGGGCCTTTGTCAGTGCCGGCGATCTGAACTTGCTGGCGGTCGCCGCGGCGGCGCTGGGC
GGGGCGCTGCTGGGCGATCAGTTGGGCTACTTCGCCGGCCGCTTCGGTGGCACGCCGATCTGGGCACACTTCACC
CGCCGCCCCGCCACCGCCGCCCTCGCTGCCCGCGCCGAAGCCAACCTGAAGCGGCATGACCTGCTGGCGGTGTAT
TTCAGCCGCTGGCTGTTCAGCCCGCTGGGGCCGTATGTCAACCTCTTGGGCGGCGCCACCGCGATGAACTGGGCC
CGCTTCACCGCCGCTGACCTTGTGGGCGAGGCCACCTGGGTGGCGCTTTACGTCGGCCTTGGCATGGCGTTCTCCA
GCCAGATCGAGGCGGTCAGCGCAGCACTTGGCAACATCGCAGGTGCCCTTGCCGCAGGCCTTGTCACCCTCTTGCT
GGCCCGCGCCCTGTGGCACGCCGCCCGCGAACCCCGCGCCTGACCCATTCACACTCGCCTAAATATCCCCGCCGG
AGGCTCCTGCCCTTCCGCCATCCTGCCGTTGCTTTCCGGCCCCGAACCCCCATATTCCCCCCATGCTGAAATTCACC
CCGCTGATCCTCGCCCTGCTTTACGCCTTCGCGATGTATCGCTTTTCGGTCTGGCGCACGCTGAAGGCGCTGGATG
CGCAGTCGCATCCGCTGGCCGAACCCGAGATCACCGCGCTGACCGACCGGATGGCGCAGGCGCTGGGGCTGCCG
CGTATCGCGGTGCAGGTCTATGAGGTCGATCCGGTCAACGGCCTGGCCGCCCCCGATGGCCGCATCTTCCTGACCC
GCGGTTTCTTGCAGAAATACCGCGCGGGCGAAGTGACGGCGGCGGAACTGGCTTCGGTGATCGCCCACGAGTTGG
GCCATGTGGCGCTGGGCCATGCGCGGCGAAGGATGATCGACTTCAmcGGsCaGAAcgcggTgTtCaTGCwGmTrTCCAt
CaCaCTGgCtGraCCGCtttTtgCccGaGCATcGgCrTgCTaGATCGCCCGCACCGTCGCCAACACGCTTGCCGCCAGCCTG
TCGCGGCGCGACGAGCACGAGGCCGACGCCTATGCCTCGGCCTTGCTGGTGAAATCCGGCATCGGCACCGCGCCG
CAGAAGTCGCTGTTTCGCAAACTGGAGGCGCTGACCGGCGCGCCCGGCGCCAACGCCCCGGCCTGGTTGCTGAGC
CACCCGAAAACCCAGGACCGCATCGCCGCGATCGAAGACCGCGAGGCCCGCTGGGATCAGGCCTGAGCCACCGCC
TTGGCCAGACGCGGCAGTTTCGCGCGTTTGAGCAGGGATTTCAGCGTCACCGGCGCGCCGGAAAGGCGTTCCGCC
TCGGCGCGCACCGCCTCCAGCACGAGGCCCATCGCCTGCGGCTGCGACGACCACAACTCCCACAGAAACCCGTCC
GGCTCGCGCCGCTGCACCCCTTCGGCGGCCAGCACATGCCGGGGGAAATCGGCGTTGTTCAGGGTCAGGATGGCA
TCGGCGCTGCCCGCCACCGCCACCGCCAGAACATGCGTGTCATTCTCGTCCGGCAGATGCAGCCGCGCCTCCAGC
CCCGGGGCGGCGGCCAGCATCGCCTTGGGAAAGCCAGCCTTGGTCAGCGCCACGCTGATGCGGGCCTGCGCCTC
GGCCGCTGGTCCCAGCTTGCGGGTGGCGCGGGCCCATTCTTCCAGAATCCGTTCCGACCAAAGCGGTTCAAAAAGC
CCGGCCTTGGCCGCCCCCAGCAGGATGTCCCGCAGGATCGGCGGATAAAGCACGCAGGCGTCGAGAACCAGCTTC
ACCCGTCAAGCCGGAAGAACAGGGCCTTCAGGTAACCCGATTCCGCCAGTTGCGGCAAAAGCGGATGGTCCGGCC

CGGCAAAGCCGGTGTGCAGCAGTTGCGCCCGCCGCCCGCCGCGGCCGATGCCACGCCCGCAGGCGTTGCGGAAC
GCGACAAGATCGGCGGCATGGCTGCACGAGCACAGCACCAGATAGCCGCCCGGCGCCACCAGCGGCGCCGCCAG
CCGCGCCACCCGTTCATAGGCGCGCAAACCAGCTTCCAACGCGGGCTTGTTCGGAGCAAAGGCCGGCGGGTCGCA
AATCAGCAGATCGAACTGCGAAGCTTGGGTGCCCAGATCCTCCAGCACCGCGAAGGCATCGCCCTGCCGCGTGGTG
AACTGGCCCGAAAAGCCCGAAACCGCCGCCCCCTGTTCGGCCAGTGCCAGCGCCGGGGCCGAGCCATCCACCGCC
AACACCGACGCCGCCCCGCCAGCCAGCGCCGCCAGCCCGAAACCGCCGACATGGGCGAACACGTCCAGCACCCG
CGCACCCTGCGCGtAacGGCtCGCggCArwGtGCgTGGaaTTCGsgCgCTtGGTCGAAGAACAGCCCGGTTTTCTGGCCG
CCGATCACATCGGCCAGATAGGTGGCGCCGTTCATCGGCACCTTGATCGGCGCATCGACAGCGCCACGGATCAGCA
GGGTTTCTTCCGAAAGCCCCTCCAGCCCGCGCGCGCCCGGTGCCGTTCTTGACCACATTCGCCACCCCGGTTAC
CGCCACAAGCGCGGCCACCAGCGCCTCCAGATGCGCCTCGGCCCAGGCGGCGTTGGGCTGCACCACCGCCGTATC
GCCAAAGCGGTCGATCACCACACCGGGCAGCGCGTCGGCCTCGGCATGCACCAGCCGGTAATAGGGCTGCGGATA
AAGCCGCGCCCGCAAGGCCAGCGCCCGCCCGATCCGCGCTTCGAACCACGCCTGATCAATCTGCGCCAAAGGATC
ACGGTCCAGCACCCGGGCGATGATCTTCGAGGCCGTGTTCACCGTCACCAGCGCCAGCGGCCGCCGATCGGCATC
CTCCAGCACCGCCAGCGCGCCGGGGACAAGGTTTTGGGTGCGCCGGTCGGTCACCAACTCATCGGCATAGACCCA
CGGGAACCCATGGCGGATGGCGCGGGCCTCGGCTTTCGGTTTCAGGCGGACAACCGGGCGTCCCGCGTAACCCGA
AGGTTCGGCGGCGGTATCGGCATCGGGGCGGGGCACATGCGGCAGGGAGGGCGTCATGCCCTCCCTCCTACTGTG
TTCTGCGGGCTTGGGAAAGAGCCGCGGTCAGTCGCGCAGCGCCACCGGCGTCAGGATCAGATCGCTTTCCAGCCG
CGAGGTCGGCACGGCACCGGCATCCGGCAGCGGCTGCGGTTGCGACAGTTCCTGCCGGATCACCTGTGCCAGACG
TTCCAGCACCACCACGCGCTGGGTGCGCCCGGCCAATTCCTCGGCCAGCGCCCGGTTGCCGCCGGATGCCTTGAC
ATCAGCCACCACAAGTCGCGGCCCGTCGATGATCTGGCCAGTCGCGGCGTCGCGCAGCGTCAGGGTGAATTTCATC
GAATGGGTGCCGCCAACGGTATAGCGGGTCTTTTCGGTCAGGCAGTGAAACCGCGTGACTTCGGCCTCGACGATCA
CCTTGCGGCCCTGGTGCATGGCCTGGGTGCCAGTGGCAAAGGCTTCCTCGAAGATCGCCTTGACCTGGGCATGGC
GGTCGCCCAGCGGTTCGCCGCGCCAGACGATATCGGCGATCGGATAGAACATGTTGGCTTCCGACACCCGCAGGTT
TTGCGGCACGCTGATGCGCACTTCGGCCACGTCATATTGCGCAGCGGGGGCCACCATGTTCGGCCCGCTTTTCGAG
GTGATCGACAGCGCCGTGGCGTCGGGCAGGCTGGCCCGCGACACCGGCTGCATCCCGCCGCACGCGCTCAGCGA
TACGGCCAATCCCAAAGCGGCGATCAAACGAAGCGTTTTCAwctsGGcGaaTTCcTccGsrGgAtATtCCatCaCaCTGktCGa
ctGCCsCtCGwGcATGCrtCtaGaGggCAATTGCGACTGAATTGCGAAAACCTTGCAGCAAAGTTGAGGTTTCGTTAACCTT
GTTCCAGCGCCCCGACAGGATAACGCCGCGGCGGAAGGCAGCAGTTGTTAGCGGTAACAGCATCTGCTAGACCCG
GCGCAACCAGAGCTCGCGAGGACGCAAATGACGCTTGACCGCACCATCGCCCGGGTCACCGACCGCATCCGCGCC
CGCTCGGAAACCAGCCGCGGGGCGTATCTGGAGCGGTTGGGCAAGGCCGCCGCCGCGGGGCCGGCGCGGGCGC
ATCTGTCTTGCGGCAACCAGGCGCATGCCTATGCGGCGATGGGGGTGGACAAGGCGGCACTGGCGGCCGCACGG
GCACCCAATCTGGGCATCG

pP2 – 1822 bp from the T7 end
64% GC

CACACAGGAAACAGCTATGACCATGATTACGCCAAGCTTGGTACCGAGCTCGGATCCACTAGTAACGGCCGCCAGT
GTGCTGGAATTCGCCCTTGGCCCTCGATGGTTTCCGCGCTTTGCGACATCAATTCCTGTTTCCAGACCACCAGCTTG
CGGCGGAAATACTCCAGTTGCCGCTCGTTCATGAACGGCTCGGTTTCGGCCGGACGGTAGTCTTCGGGAATAAAGA
CCTCTGCCTTCATCACTGCACTCTCCATCTCCCCGGACCGCACCGACAGGCGGCGTTTGAGGTCGGGCGCTCCTGC
TGGCGGTGCCATATCGCAAGCCAAAGCCGTTGTCACTAGCGTTCAGCCGGGGTTGCGGGTGGGTTGGGCCGTGCTA
GTCTGTGTCTTCCCAAGCTGCGAAGGCCAAAGATGAAATTCCGCTCAACCGCCAGTTACATCGCCACCACCGACCTC
GCCCATGCGGTCAATGCGGCGGTGACGTTGCAACGCCCCTTGCTGGTGAAGGGCGAGCCGGGCACCGGCAAGACC
GAACTGGCGCGGCAGGTGGCGCTGGCGCTGCAACTGCCGATCATCGAATGGCATGTGAAATCCACCACCAAGGCG
CAGCAGGGGCTTTACGAATACGACGCGGTCAGCCGGTTGCGCGACAGCCAGTTGGGCGACGCGCGGGTGAACGAT
GTCGCCAACTACATCCGCAAGGGCAAGCTGTGGCAGGCCTTCGAGGCACCGGGCCGGGTGGTCTTGCTGATCGAC
GAGGTGGACAAGGCCGATATCGAGTTTCCCAACGACCTGTTGCAGGAACTCGACCGCATGGAGTTTCACGTCTACG
AGACCGGCGAAACCGTGCGGGCGCAGCATCGGCCGGTGGTGATCATCACCTCGAACAACGAAAAGGAACTGCCCG
ACGCCTTCCTGCGCCGCTGTTTCTTCCACTACATCCGCTTCCCGGACATCGACACCCTGCGCGCCATCGTCGAGGTG
CATTTTCCCGGCATCAAGGAAGCCTTGCTGACCACGGCGCTGACCCAGTTCTATGAGCTGCGCGAGATGCCGGGGC
TGAAGAAAAAGCCCTCCACCTCCGAGGTGCTGGACTGGCTGAAGCTGTTGCTGGCCGAAGACCTCGGCCCCGAGGA
TCTGAAGCGCGAGGGCAAGGCGGTGTTGCCAAAGCTGCACGGCGCGCTGCTGAAAACCGAGCAGGATCTGCATCT
GTTCGAGCGGCTGGCCTTCATGGCGCGGCGCCAGGGCTAGGCGGCGCGGCGCCGCTTACCCGGCGCCCGCGGCC
TTGACCTACCCCCCGCGCGTGCCGCAAGGTCCAGAAGTTGCCGCACCCCGGTCGCCTTGCTGCCGCAGCCCCGGG
GTTAGCTGCGGCAAGCCCTTTCAGAACCAGACAGATTGCGCCATGACCCAAAGCCTGCCCGTCGCCATCCGCCCCA
TCACCGAAGCCGACCGCCCGGTCTGGCAGGCGCTGTGGCACGACTATCTGTTGTTCTACAAGACCGCCCTGCCGCA
GGCGGTTTATGACAGCACCTTCGCGCGGCTGATCGCGGGCAACGCAGGCATCCATGGCTTGCTGGCCGAACGCGG
CGGCGTGGCGCTGGGGTTGACGCATTTCATCTTTCACCCCTCCTGCTGGAAGATCGAGCCTGCCTGCTATCTGCAAG
ACCTGTTCACCACCCCTGCCGCCCGTGGCTCGGGCGTGGGCCGGGCGCTGATCGAGGCGGTCTATGCCCGCGCCG
ATGCCGCCGGAGCGCCCGGGGTCTATTGGCTGACCGCCGAGAACAACTATCCGGGGCGGATGCTTTATGATCAGGT
TGCAA

pP2 – 970 bp of an internal fragment
63% GC

CACTAGTAACGGCCGCCAGTGTGCTGGAATTCGCCCTTCGCTGTTCTCGCGCGACGTGATCGCGCTGGCCGCGGCG
GTGGCGCTGTCGCACAACACCTTTGACGCCGCGCTGTTTCTGGGGGTCTGCGACAAGATCGTGCCCGGTCTGGTGA
TCGCGGCGGCCAGTTTCGGCCATATCCCGGCGGTGTTCGTGCCGGCCGGGCCGATGGCCTCGGGCCTGCCGAATG
ACGAAAAATCCAAGGTCCGCAATGCCTTCGCCGCCGGCGAAGTGGGCCGCGAGGTGCTGATGGCGGCGGAAATGG
CCAGCTATCACGGCCCCGGAACCTGCACCTTCTACGGCACCGCCAACACCAACCAGATGCTGATGGAGTTCATGGG
GCTGCACCTGCCGGGCGCCTCTTTCGTGCATCCCGGCTCGCCCCTGCGCGCGGCGCTGACCGAGGCGGCGGTGG
AACGCGCGGCGAGGATCACCGCGCTTGGCAACGATTTCCGCCCGGTGGGAGAGTTGCTGGACGAGCGGGCCTTCG
TCAAAGGGCGAATTCTGCAGATATCCATCACACTGGCGGCCGCTCGAGCATGCATCTAGAGGGCCCAATTCGCCCTA
TAGTGAGTCGTATTACAATTCACTGGCCGTCGTTTTACAACGTCGTGACTGGGAAAACCCTGGCGTTACCCAACTTAA
TCGCCTTGCAGCACATCCCCCTTTCGCCAGCTGGCGTAATAGCGAAGAGGCCCGCACCGATCGCCCTTCCCAACAG
TTGCGCAGCCTGAATGGCGAATGGACGCGCCCTGTAGCGGCGCATTAAGCGCGGCGGGTGTGGTGGTTACGCGCA
GCGTGACCGCTACACTTGCCAGCGCCCTAGCGCCCGCTCCTTTCGCTTTCTTCCCTTCCTTTCTCGCCACGTTCGCC
GGCTTTCCCCGTCAAGCTCTAAATCGGGGGCTCCCTTTAGGGTTCCGATTTAGTGCTTTA

pP3 – 1095 bp from T3 end
63% GC

CTTATCCGCCCTACGCGGTTCTGGCACATTTTGCAGGCCTGATAAGACGCGGCAAGCGTCGCATCAGGCATCGGAG
CACTTATTGCCGGATGCGGCGTGAACGCCTTATCCGGCCTACGGTTCTGGCACCTTTTGTAGGCCTGATAAGACGCG
GCAAGCGTCGCATCAGGCATGATGCGCCAATTGCCTACGTTTTTTACTCTTGTGGCCATAACCACGCAGCGCCGCGT
ACGCCGCTGGAATCACCGTGCTTCGCCTTACGCACCGGCGTTTCACATTCGCCGCCGAAGACAAATTGTTTAATCAA
CTGCCCAACCGTTTGATATAAACGGTCTGGTCGACGGATCACCATTATCGCGCGTGATAAGCGGCGTCAGCCCGCTA
GGAACGCCGCCATATACCTGCCGAGAAGCAGGAGAACCGGCGCCGCCAGAACCAGTAACATCACCCGCGCCATCC
GAACCCCCAAGAGCCTGCCGAAGCGTCGGCATGGAATTTTGGCCAGCATAAATGCCGCCCACCTTGGGCCGCAAGG
TCAGCGACATGACCTTTTGCCGCAGCACAGTGTTTTCCTGTGCAAGGGCATTGGTTTTCGAGAGTTTGGCCTCGTCC
TGGCGTTTCGCCAGATTATCCGCAAGGATCAGCCTGGGCGGCTGGGCGGTTGCGGACTGGCCAGAGGCCGACCTG
CGGGCGGGCCTGACCCTGCTGCCGCAACGCAGCACGCTGATGGCCGGAACCGTGGCCGAGGCGCTGCGGCTGGC
CGGCCCCGCCGAGGACGCGCACCTGTGGCAGGTGCTGGCGGCCGTGCAGATGGACGGGATCATCCGCGAACGCG
ACGGCCTGGCCGCCCGGATCTGCGCCACGCCCATGGCCAGCCCGATGCCCCACCACGGCGCGCCATAGGCGGCA
AACACCGCCAGCGCGCCGAGGTTGGAGGCGAAGTTCAGCAGCTTGGTATGCGCCGTGGCCTTCAGCACGCCATGC
CCCGCCAGCACCACAAAAGCCGATCATGTAGAACGCCCCCGCCCCCGGCCCGATCAGCCCGTCATAGCCGCCGAT
CAGTGGCACCACGAAGGCGGTGAAAGCAGTGGGCGA

pP3 – 7231 bp from T7 end
66% GC

CAGCTTGATTCGTTGGCCGACACCTACCGCAAATACGTGCATGACAACCTGCGCGAAGGCGCTGCCATTGCCTTTGC
CCATGGACTGAACGTGCATTTCGGCCTGATCGAGCCGAAACCCGGCGTCGATGTCATCATGATGGCACCCAAAGGC
CCCGGCCACACCGTGCGCGGCGAATACACCAAGGGCGGCGGCGTGCCCTGCCTGGTGGCGGTGCATAACGACGC
CACCGGCAAGGCGATGGAAATCGGCCTGTCCTACTGTTCCGCCATCGGCGGCGGCCGCTCGGGCATCATCGAGAC
CAACTTCCGCCAGGAATGTGAAACCGACCTGTTCGGCGAACAGGCGGTGCTGTGTGGCGGTCTGGTCGAACTGATC
CGCATGGGCTTCGAGACCCTGGTCGAAGCCGGCTACGAGCCGGAAATGGCCTATTTCGAATGTCTGCACGAGGTGA
AGCTGATCGTCGATCTGATCTATGAAGGCGGCATCGCCAACATGAACTACTCGATCTCCAACACCGCCGAATATGGC
GAATACGTCAGCGGCCCGCGCATCCTGCCTTACGCCGAAACCAAGGCCCGGATGAAGGAAGTGCTGACCGACATCC
AGACCGGCAAGTTCGTGCGCGACTTCATGCAGGAAAATGCCGTCGGCCAGCCGTTCTTCAAGGCCACCCGCCGCAT
CAACGACGAACACCAGATCGAGAAGGTCGGCGAGAAACTGCGGGCGATGATGCCGTGGATCTCGAAGGGCAAGAT
GGTGGACCGCTCGCGCAACTAAGCCGGAAAAACCTGCATTTTCAATGCACTGATTCGGAAAGGGGCGCTTTATTGCG
CCCTTTTTCATCAGTTTTCGCCAATTTGCGCAACCACCGGTAGAAGTCCGGCCGAAATTCGCGTTTGATTTGACAGGC
CCCTCACGTTCTCGTTACCGTCAGACCATGGTCGGTATATTTTCGACCAAGTCTGTATTGAGAAGCCCCCTCGTCAGA
ATTTTCTGGCAAGAATCTCATGAGCCCTGCCCCCGCTTGCACCGCGTGAAACCTGGTCGATTTTACGCCCGAAAAAA
TGACCCTTTGGGAGGATGAAATGCTGGACAGAATGAAAGGTGGCTTTGCCGCCACGGCCTTGCTTTGCCTGGGCCTT
GCCAACCCGCTTGCCGCCGATACCAGGACGCTTTCACAGCAGTATCTTGACGATGTGCGCAGCGGTGCCATCGTGA
TCGAGGGTGACAGCGCGGCGGTGTCGGAACTGATCCTGAAACGCGATATTCCGATCCCCTACAGCTATATCGCGCA
GCTGTTTGCCACACCGAACGCCTTCGGCTCGGGTCCGGCCTGCATCATCTGCCACGGCTCGAACAACCCGACCCAT
GCCTACCGCGGCCTCAATCTTTCCACCTGCGACGGCCTGCGCAACGGCTCGACCGAGCAACCGGCCCGCGCCATC
TTTACCCCCGGCGAAGACCCCAAGAACGCCATCATCGGCCGCCGCCTGCGCGCGAACCGCATGCCGCTGGGCATC
GCCTTCAACAACCCCACCGATTCCGCACCGATCCTGGCGATCAAGGAATGGATCCTGGCGGGGGCGCCGAACGAC
GAGCATTTCACCAAGGAAATCCTGCCGCTGTTCGCCACCGACAACACCTTTGGCCCCGACACGCCGCATTGCACCA
CCTGCCACTTCTCGAACCAGGAACCGCCCAGCTTCCACGAGCTGAACCTGACCACCTATGAGGGCATCATGCTGGG
GGCGGATTCGGTGGCCAAAGGTGTCGACAATGCCACCAAGGTGATCATTCCGGGTGACCCGGAGGCCTCGAAGGT
GTTCCAGCACCTGACCGAAGACCGCATGCCGCCCGGCATCGACCCCTCGGAAGACCGCGACCATCCGAACACCCA

GATCCTGTTCGCCTGGATCAAGCAAGGGGCCAAATGCGAGTAACGCCCAACCGGCGCCTTGTGCTGCAATCCCTGA
TCGCCGGCCTGGTTTTCAGGCCGGCGGTCTTGGCTGCGCAAGACCTGCCCGAACTTGCCGCCCTGCGGCGCTGGA
AAACCGGCAATGCGGTTCTGAACCCGCTCGCCTATGGTGAGGATCGCCTGCTGTTCTGCGGCGACAAGACCATCGG
CGCGATTGCGCCGGATGCTGCCCAGCCGCTGTGGCAGCTGCCGCACGGCTTTGACAAGGCCGCCGAATTCCGGCC
GCGCCCGGCGGCGGCCAAGGTGATCTGCGGCGGCCGGTTCTGGCTGGCCGGCTATGATGCCGCCACCGGCACCG
AACTCTGGCGGCATGCGGCAAAGATTCAGATCGGTGTGCCCTTCGTCACCCCGACCCACACGCTGTTTGGCGATGG
TCACTGGCTGATCGCGCTGGATACCGCGACCGGCGCCGAATTGTGGCGCTTTGCCGCCATCGAGGATACCATCATC
GCCTATGCCCCGGTGGCCGATGCCGATACCGCCTATGTCGGCCCCGGCGACGGCCGGCTTTATGCGCTGTCGCTG
GCCGATGGCAGCCTGAAATGGGCGGTCGATGGCCGGGCGCAATGGCAATACCTGCGCCAGATCAGCATCGAGGAC
GGGATTCTGGTGGCCGGCACCTATCACGAGAACCTCAAGGGCCTGTCGCTGGCCGATGGCCGCGAGTTGTGGAGC
TTTTACGCCGGCAATTTCATCAACTCGCAACTGGTGCGCGACGGTTCGGCGTATCTGTGGTCACCCACCGGCTATGT
CTATGCCATCGACACCCACAGTGGTGCTATCCGCTGGCGCTATCAGACCACCGATTACGACAACACGCGCAGCAACT
GGGCCTCGGTGGTGGCCGAACTGCAAGCCTTTGACGGCAAGCTTTATGCGCTGTCGCTCGACCATGTGCTGCACCG
GCTGGATAGCGCCACCGGCACCGACCATGCGGAATGGCGGATGCCCGACAAGATCCGCTATGCGCTGCTTCCCGT
AGCCGGTCATGGCATCGCCTTCCCGACCGAAAGCGCCGAGGTGCTGCTGACCGCTTTCCCCTGACCGGCCCTTGCC
CCGCCAGCAACCGCCACCTATAACCCCGGCCATGACCGACACCCCGCTCCAGAAGCCCGGCCTTGCCAACTGGTTG
CGGGTCATCGCCCTGTCGGTGATCTGGGGTGGCTCGTTCATGGGGGTGAAGCTGGCGCTGGCCGGGTTTGGCCCG
CTCAGCATCGCCGCCATCCGCATCGCGCTGGCCGCCATCGCGCTTTTCCTGATCGCGCGCAGCATGGGTCTGGCCT
TGCCGCGCAGCCGCCGGGTCTGGGCGCATGCCATCGGCATGGGGTTCTTCTCCAACGCCCTGCCGTTTGCACTGCT
CAGTTGGGGGCAGTTGCATGTGGCCTCGGGCTTTGCCGGCATCACCATGGCGGCGGTGCCGCTGTTCACCCTGCTC
TTGGCGCACCGGCTGATCCCGGGCGAGCAGATGACGGTGTGGAAACTGCTGGGCCTTGGCTTCGGCATCGCCGGG
GTGGTGGTGCTGATCGGCCCAAGGGCGCTTGCCTCGTCGGGGGCGGATGTCGAAAATCTGGCGCGGCTGGCCTGC
GTCGCCTCGACCCTGTGCTATGCCATCGGCGCCATCATCACCCGCCGCTGCCCGCCAGTGCCGCTGGTGGCGTTCT
CGACCGCCGCCCTGATCGCCGCGAGCGTGATGATGCTGCCACTGGCCTGGGCCATCGAAGGCACCCCGGACCTTG
CCGCCGCCACCCCAAGCGCGCTGCTGGCGCTGCTTTACCTCGGGCTTGGCCCCACCGCGCTGGCCACCCTGCTGC
TGGTCAAGGTGATCACCACCGCTGGCCCCACCTTCCTGACTCTGTCGAACTACCAGGTGCCGCTGTGGTCGGTGCT
GTTCGGCACGATCTTCCTGCACGAGAAACTGCCGCCCAGCTTCTTCGCCGCCCTCGGCCTGATCCTGGCAGGCCTC
GCCCTCAGCAACATCCGCCGCAAGGCTTGACCCTGATTTCACCTTTGCTCAAATATCCTGGGGGGTGAGGCGCTATG
CGCCGAGGGGGGCAACGCCCCCCTTCCTGCCTCAAACTCAAACCGCCGCTTCCACCGCCGCCACAATGCTGCCCA
CCACCTCGGCCAGCAGCACCTCGTCCTCACATTCCGCCATCACCCGCACCAAAGGCTCGGTGCCCGACTTGCGGAT
CAGCAGCCGCCCCGAGCCCTGCAACCGCGCTTCGGCATCAGCAATCACCGCCTGCACCGCCGCCGCCGCCAAGGG
CTGCGACCCCGCACCGTAACGCACGTTCTTCAGCATCTGCGGCACGGTCTGAAAGCTTTGCGCCAGCGCCGATGCC
GGCTGTTCGGTGCGCGCCATCTCGGCCAGAAACTGCAACCCGGCAATCAGCCCGTCGCCGGTGGTGGCGTAATCG
GTCATCACGATATGGCCCGACTGCTCGCCGCCCAGGTTGAAACCGCCGCGCCGCATCGCCTCGACCACATAGCGGT
CGCCGACATTGGTGCGCTCCAGCCGCAGCCCGCGCCGCTCCAGAAACCGCTCCAGCCCGAGGTTCGACATCACCG
TGGCCACCAGCGTGCCGCCGTGCAGCCGCCCCTCCTCGGCCCAGCGGGCGGCCAGCAGCGCCATGATCTGGTCG
CCATCCGCCACCTTCCCGGTCTGATCCAGAATCATCACCCGGTCGGCGTCGCCATCCAGACAGATGCCGACATCGG
CGCCATGCGCCACCACCGCCTCGGCGGCAGTCTGGGTATAGGTCGAGCCACAACGGTCGTTGATATTGGTGCCATT
CGGCGCCACCCCCACCGGGATCACCTCGGCGCCCAATTCCCACAGCACCTCGGGGGCCGCACGATAGGCCGCGC
CATTGGCGCAATCTATCACCACCTTCAGCCCATCAAGCCGCAGCCCGACGGGAAAGGTGGTCTTGGCATATTCCTGA
TAGCGCCCGCGGCCATCGTCGATCCGCTTGGCCCGGCCGATGTTCTGCGGCTGCGCCAGCGCAATCTCGCCCGCC
AGAATCGCCTCGATCTCTCTTTCGGCATCATCCGACAGCTTGAAGCCGTCGGGGCCGAAGAACTTGATGCCATTGTC
CTGATGCGGGTTGTGCGAGGCGCTGATCATCACCCCCAGATCGGCGCGCATGCTGCGCGTCAGAAACCCCACCGC
AGGCGTCGGCACCGGCCCCAGCAGCAGCACGTTCATCCCCGTCGAGGTCAACCCGGCGGTCAGCGCGTTTTCCAG
CATGTAGCCCGACAGCCGCGTGTCCTTGCCGATCACCACCCGGTGCGCCGCAGTGCCGTCGCGCCGGAAGAACCG
CCCCGCCGCCGCCCCCAGCCGCAAGGCCATCTCGGCGGTCATCGGGTAGGTATTGGCCCGCCCGCGCACCCCATC
GGTGCCGAAAAGTGTCCGTGTCATGCGCCCTCACTCTCTAACAACGACCGCCACAGCGCCAGCGCCTGCCGGGTTT
CCCACACATCATGCACCCGCAGGATCTGCGCCCCCTGCGCCACCCCGGCCAGCGCCACCGCCAGCGACCCCGGCG
CGCGGCGGTCGGCCTGCGCCTCGCCGCCAATGGTGCCGATGAATTTCTTGCGCGACACCCCCAGCAGAATGGCGC
AGCCCAGACCATGGAACAGCGACAGCCCGCGGATCAGCGTCAGGTTATGCTGCAAGGTCTTGCCAAAACCGATGCC
GGGATCAACCACGATGCGGGCGCGCGGGATCCCCGCCGCGCAGGCCAGCGCCACCCGTTCGGCCAGATAGTCGT
AAACATCCAGAGCCACGTCATCATATTGGGGATCGTCCTGCATGGTCTGCGGTGTACCCTGCGCGTGCATCAGGCA
GACCGGCGCATCCGCCTGCGCCACCACCTCCGCCATGCCCGCGTCATAGCCAAAGGCCGACACGTCATTGACCATG
CTTGCCCCGGCCGCCAGTGCCGCCTGCGCCACCGCCGCCTTGCGGGTGTCGATGGAAATGGCGGTGGCAATCCCG
CCCGCCCGCAGCGCCGCAATCACCGGGGCGGTGCGCGAAATCTCCTCGGCCTCCGCCACCTCGGCCGCCCCTGG
CCGAGTGCTTTCGCCGCCGATGTCGATGATCTCGGCCCCCGCCCCTGCCATCATCCGGCCCTGCGCCGTGGCGGC
ATCCGGGGCCAGAAACCGCCCGCCGTCGGAAAAGCTGTCGGGTGTGACGTTCAGGATACCCATCAGCCGCGGGCG
CGACAGGTCCAGCCCGGCCAATGCGGCACGCGGCGCGGTCAGCGCCGCGTGCCGCTGCGGGCAGATCGCGCA
CCGGAATCAGCTGCGGCCGGGCGCTGCGCGACAGCACCTCGACCCGGTCGAACCAGCACCAGCCCCCGGCCAGC
GTCAGCGCATCCGCCGGGCGCGCGGCATCGGTCATCACAATCGGTCGGAAGTATTCCATGCCCCCTCGTTAGGGCC
TTTGCCGCCCGCTTGGCAAGCCCTTCGCCCCTAAGCCGCCAGCACCGGCACGCGGCTTCCCGCCGGAAGTGTTACA
GCGCCGTGAACGATCATCCGCGCCGCCGCCAGCATTTCCGCCAGCCACAGCGCCAGCGCCACCGGATCGTGCGGG
CGGCGGTGCTGGCCGATGCCCCGGCGATGGCGGCGCTGCTGAACCGCATCATCGACATCGGTGGCACCACGGCG
CATGAAATCCCGTTGACCGAGGCGCAGGTGGCGCAGCATTACATCAGCGGCCCGGCGGTGATCTGCTGCCATGTG
GCGGAAGGCGCTGGGCAGGTGATCGGCTTTCAATCGCTGGACCGCCACCCCGGCTTGCCCGACGGCTGGGGCGAT
ATCGGCACCTTCGTATCCCCCGATCTGCAACGCAGCGGCGCTGGGGCCGCGCTGTTTGCCGCGACCTGTGCGGCG
GCAAAGGCGGCTGGGGTCGCGGTGATCAACGCCACCATCCGCGCCGACAATGCGCCGGGGCTGGGCTATTACGCG
CGCCGCGGTTTCACCGATTACGCCACTGACCCGGCGTTTGCGCTGCGCGACGGCACCCGAGTCGGTCGCATCAGC
CGCCGCTTCGATCTGGCCTGAGCCGGGGTTTACTTCCCGCGCCGCAGCCCCGATGAAGGCCTGCCCAATCCCCGG

TCCCGCATGTTCGAAGTCAGCCTGCCCCTTGCCACCCTGCTGACCCTTGCCGCCTTTGCCGCGGGGTTCGTTGACG
CCATTGCCGGCGGTGGCGGGCTCATCACTCTGCCGGCGCTGTTGCTGGCCGGGG

pP4 – 6281 bp consensus sequence
49% GC

CTCTAGAACTAGTGGATCCCCCGGGCTGCAGAGTTCAGCTGCGGGTAGCGCAACAAACGTTGGTGTGCAGATCCTG
GACAGAACGGGTGCTGCGCTGACGCTGGATGGTGCGACATTTAGTTCAGAAACAACCCTGAATAACGGAACCAATAC
CATTCCGTTCCAGGCGCGTTATTTTGCAACCGGGGCCGCAACCCCGGGTGCTGCTAATGCGGATGCGACCTTCAAG
GTTCAGTATCAATAACCTACCCAGGTTCAGGGACGTCATTACGGGCAGGGATGCCCACCCTTGTGCGATAAAAATAA
CGATGAAAAGGAAGAGATTATTTCTATTAGCGTCGTTGCTGCCAATGTTTGCTCTGGCCGGAAATAAATGGAATACCA
CGTTGCCCGGCGGAAATATGCAATTTCAGGGCGTCATTATTGCGGAAACTTGCCGGATTGAAGCCGGTGATAAACAA
ATGACGGTCAATATGGGGCAAATCAGCAGTAACCGGTTTCATGCGGTTGGGGAAGATAGCGCACCGGTGCCTTTTGT
TATTCATTTACGGGAATGTAGCACGGTGGTGAGTGAACGTGTAGGTGTGGCGTTTCACGGTGTCGCGGATGGTAAAA
ATCCGGATGTGCTTTCCGTGGGAGAGGGGCCAGGGATAGCCACCAATATTGGCGTAGCGTTGTTTGATGATGAAGG
AAACCTCGTACCGATTAATCGTCCTCCAGCAAACTGGAAACGGCTTTATTCAGGCTCTACTTCGCTACATTTCATCGC
CAAATATCGTGCTACCGGGCGTCGGGTTACTGGCGGCATCGCCAATGCCCAGGCCTGGTTCTCTTTAACCTATCAGT
AATTGTTCAGCAGATAATGTGATAACAGGAACAGGACAGTGAGTAATAAAAACGTCAATGTAAGGAAATCGCAGGAAA
TAACATTCTGCTTGCTGGCAGGTATCCTGATGTTCATGGCAATGATGGTTGCCGGACGCGCTGAAGCGGGAGTGGC
CTTAGGTGCGACTCGCGTAATTTATCCGGCAGGGCAAAAACAAGAGCAACTTGCCGTGACAAATAATGATGAAAATA
GTACCTATTTAATTCAATCATGGGTGGAAAATGCCGATGGTGTAAAGGATGGTCGTTTTATCGTGACGCCTCCTCTGT
TTGCGATGAAGGGAAAAAAAGAGAATACCTTACGTATTCTTGATGCAACAAATAACCAATTGCCACAGGACCGGGAAA
GTTTATTCTGGATGAACGTTAAAGCGATTCCGTCAATGGATAAATCAAAATTGACTGAGAATACGCTACAGCTCGCAA
TTATCAGCCGCATTAAACTGTACTATCGCCCGGCTAAATTAGCGTTGCCACCCGATCAGGCCGCAGAAAAATTAAGAT
TTCGTCGTAGCGCGAATTCTCTGACGCTGATTAACCCGACACCCTATTACCTGACGGTAACAGAGTTGAATGCCGGA
ACCCGGGTTCTTGAAAATGCATTGGTGCCTCCAATGGGCGAAAGCACGGTTAAATTGCCTTCTGATGCAGGAAGCAA
TATTACTTACCGAACAATAAATGATTATGGCGCACTTACCCCCAAAATGACGGGCGTAATGGAATAACGCAGGGGGA
ATTTTTCGCCTGAATAAAAAGAATTGACTGCCGGGTGATTTTAAGCCGGAGGAATAATGTCATATCTGAATTTAAGACT
TTACCAGCGAAACACACAATGCTTGCATATTCGTAAGCATCGTTTGGCTGGTTTTTTTGTCCGACTCGTTGTCGCCTG
TGCTTTTGCCGCACAGGCACCTTTGTCATCTGCCGACCTCTATTTTAATCCGCGCTTTTTAGCGGATGATCCCCAGGC
TGTGGCCGATTTATCGCGTTTTGAAAATGGGCAAGAATTACCGCCAGGGACGTATCGCGTCGATATCTATTTGAATAA
TGGTTATATGGCAACGCGTGATGTCACATTTAATACGGGCGACAGTGAACAAGGGATTGTTCCCTGCCTGACACGCG
CGCAACTCGCCAGTATGGGGCTGAATACGGCTTCTGTCGCCGGTATGAATCTGCTGGCGGATGATGCCTGTGTGCC
ATTAACCACAATGGTCCAGGACGCTACTGCGCATCTGGATGTTGGTCAGCAGCGACTGAACCTGACGATCCCTCAGG
CATTTATGAGTAATCGCGCGCGTGGTTATATTCCTCCTGAGTTATGGGATCCCGGTATTAATGCCGGATTGCTCAATT
ATAATTTCAGCGGAAATAGTGTACAGAATCGGATTGGGGGTAACAGCCATTATGCATATTTAAACCTACAGAGTGGGT
TAAATATTGGTGCGTGGCGTTTACGCGACAATACCACCTGGAGTTATAACAGTAGCGACAGATCATCAGGTAGCAAAA
ATAAATGGCAGCATATCAATACCTGGCTTGAGCGAGACATAATACCGTTACGTTCCCGGCTGACGCTGGGTGATGGT
TATACTCAGGGCGATATTTTCGATGGTATTAACTTTCGCGGCGCACAATTGGCCTCAGATGACAATATGTTACCCGAT
AGTCAAAGAGGATTTGCCCCGGTGATCCACGGTATTGCTCGTGGTACTGCACAGGTCACTATTAAACAAAATGGGTA
TGACATTTATAATAGTACGGTGCCACCGGGGCCTTTTACCATCAACGATATCTATGCCGCAGGTAATAGTGGTGACTT
GCAGGTAACGATCAAAGAGGCTGACGGCAGCACGCAGATTTTTACCGTACCTTATTCGTCAGTCCCGTTTTGCAACG
TGAAGGGCATACTCGTTATTCCATTACGGCAGGAGAATACCGTAGTGGAAATGCGCAGCAGGAAAAACCCCGCTTTT
TCCAAGAGTACATTACTCCACGGCCTTCCGGCTGGCTGGACAATATATGGTGGAACGCAACTGGCGGATCGTTATCG
TGCTTTTAATTTTCGGTATCGGGAAAAACATGGGGGCACTGGGCGCTCTGTCTGTGGATATGACGCAGGCTAATTCC
ACACTTCCCGATGACAGTCAGCATGACGGACAATCGGTGCGTTTTCTCTATAACAAATCGCTCAATGAATCAGGCACG
AATATTCAGTTAGTGGGTTACCGTTATTCGACCAGCGGATATTTTAATTTCGCTGATACAACATACAGTCGAATGAATG
GCTACAACATCGAAACACAGGACGGAGTTATTCAGGTTAAGCCGAAATTCACCGACTATTACAACCTCGCTTATAACA
AACGCGGGAAATTACAACTCACCGTTACTCAGCAACTCGGGCGCACATCAACACTGTATTTGAGTGGTAGCCATCAA
ACTTATTGGGGAACGAGTAATGTCGATGAGCAATTCCAGGCTGGATTAAATACTGCGTTCGAAGATATCAACTGGACG
CTCAGCTATAGCCTGACGAAAAACGCCTGGCAAAAAGGACGGGATCAGATGTTAGCGCTTAACGTCAATATTCCTTTC
AGCCACTGGCTGCGTTCTGACAGTAAATCTCAGTGGCGACATGCCAGTGCCAGCTACAGCATGTCACACGATCTCAA
CGGTCGGATGACCAATCTGGCTGGTGTATACGGTACGTTGCTGGAAGACAACAACCTCAGCTATAGCGTGCAAACCG
GCTATGCCGGGGGAGGCGATGGAAATAGCGGAAGTACAGGCTACGCCACGCTGAATTATCGCGGTGGTTACGGCAA
TGCCAATATCGGTTACAGCCATAGCGATGATATTAAGCAGCTCTATTACGGAGTCAGCGGTGGGGTACTGGCTCATG
CCAATGGCGTAACGCTGGGGCAGCCGTTAAACGATACGGTGGTGCTTGTTAAAGCGCCTGGCGCAAAAGATGCAAA
AGTCGAAAACCAGACGGGGGTGCGTACCGACTGGCGTGGTTATGCCGTGCTGCCTTATGCCACTGAATATCGGGAA
AATAGAGTGGCGCTGGATACCAATACCCTGGCTGATAACGTCGATTTAGATAACGCGGTTGCTAACGTTGTTCCCACT
CGTGGGGCGATCGTGCGAGCAGAGTTTAAAGCGCGCGTTGGGATAAAACTGCTCATGACGCTGACCCACAATAATA
AGCCGCTGCCGTTTGGGGCGATGGTGACATCAGAGAGTAGCCAGAGTAGCGGCATTGTTGCGGATAATGGTCAGGT
TTACCTCAGCGGAATGCCTTTAGCGGGAAAAGTTCAGGTGAAATGGGGAGAAGAGGAAAATGCTCACTGTGTCGCCA
ATTATCAACTGCCACCAGAGAGTCAGCAGCAGTTATTAACCCAGCTATCAGCTGAATGTCGTTAAGGGGGCGTGATG
AGAAACAAACCTTTTTATCTTCTGTGCGCTTTTTTGTGGCTGGCGGTGAGTCACGCTTTGGCTGCGGATAGCACGATT
ACTATCCGCGGCTATGTCAGGGATAACGGCTGTAGTGTGGCCGCTGAATCAACCAATTTTACTGTTGATCTGATGGA
AAACGCGGCGAAGCAATTTAACAACATTGGCGCGACGACTCCTGTTGTTCCATTTCGTATTTTGCTGTCACCCTGTGG
TAATGCCGTTTCTGCCGTAAAGGTTGGGTTTACTGGCGTTGCAGATAGCCACAATGCCAACCTGCTTGCACTTGAAAA
TACGGTGTCAGCGGCTTCGGGACTGGGAATACAGCTTCTGAATGAGCAGCAAAATCAAATACCCCTTAATGCTCCAT
CGTCCGCGCTTTCGTGGACGACCCTGACGCCGGGTAAACCAAATACGCTGAATTTTTACGCCCGGCTAATGGCGAC

ACAGGTGCCTGTCACTGCGGGGCATATCAATGCCACGGCTACCTTCACTCTTGAATATCAGTAACTGGAGATGCTCA
TGAAATGGTGCAAACGTGGGTATGTATTGGCGGCAATATTGGCGCTCGCAAGTGCGACGATACAGGCAGCCGATGT
CACCATCACGGTGAACGGTAAGGTCGTCGCCAAACCGTGTACGGTTTCCACCACCAATGCCACGGTTGATCTCGGC
GATCTTTATTCTTTCAGTCTTATGTCTGCCGGGGCGGCATCGGCCTGGCATGATGTTGCGCTTGAGTTGACTAATTGT
CCGGTGGGAACGTCGAGGGTCACTGCCAGCTTCAGCGGGGCAGCCGACAGTACCGGATATTATAAAAACCAGGGG
ACCGCGCAAAACATCCAGTTAGAGCTACAGGATGACAGTGGCAACACATTGAATACTGGCGCAACCAAAACAGTTCA
GGTGGATGATTCCTCACAATCAGCGCACTTCCCGTTACAGGTCAGAGCATTGACAGTAAATGGCGGAGCCACTCAGG
GAACCATTCAGGCAGTGATTAGCATCACCTATACCTACAGCTGAACCCGAAGAGATGATTGTAATGAAACGAGTTATT
ACCCTGTTTGCTGTACTGCTGATGGGCTGGTCGGTAAATGCCTGGTCATTCGCCTGTAAAACCGCCAATGGTACCGC
TATCCCTATTGGCGGTGGCAGCGCCAATGTTTATGTAAACCTTGCGCCCGTCGTGAATGTGGGGCAAAACCTGGTCG
TGGATCTTTCGACGCAAATCTTTTGCCATAACGATTATCCGGAAACCATTACAGACTATGTCACACTGCAACGAGGCT
CGGCTTATGGCGGCGTGTTATCTAATTTTTCCGGGACCGTAAAATATAGTGGCAGTAGCTATCCATTTCCTACCACCA
GCGAAACGCCGCGCGTTGTTTATAATTCGAGAACGGATAAGCCGTGGCCGGTGGCGCTTTATTTGACGCCTGTGAG
CAGTGCGGGCGGGGTGGCGATTAAAGCTGGCTCATTAATTGCCGTGCTTATTTTGCGACAGACCAACAACTATAACA
GCGATGATTTCCAGTTTGTGTGGAATATTTACGCCAATAATGATGTGGTGGTGCCTACTGGCGGCTGCGATGTTTCTG
CTCGTGATGTCACCGTTACTCTGCCGGACTACCCTGGTTCAGTGCCAATTCCTCTTACCGTTTATTGTGCGAAAAGCC
AAAACCTGGGGTATTACCTCTCCGGCACAACCGCAGATGCGGGCAACTCGATTTTCACCAATACCGCGTCGTTTTCA
CCTGCACAGGGCGTCGGCGTACAGTTGACGCGCAACGGTACGATTATTCCAGCGAATAACACGGTATCGTTAGGAG
CAGTAGGGACTTCGGCGGTGAGTCTGGGATTAACGGCAAATTATGCACGTACCGGAGGGCAGGTGACTGCAGGAAT
TCGATATCAAGCTTATCGATACCGTCGAC

pP5 – 3955 bp consensus sequence
69% GC

GGGGGTGGATAGCGTCAGCGGCAGGCTCAGCGCCCAATCGACGAAGATCGAGCGGCATTCGGCGGCGGTGATGC
CGTCGATGGCATAGCTTTCGCGCACCAGCCCCTTGGGGTCCGCCTCAGTCAGTTGCATCGCCTGCCCCGTCCTTTTC
GCCCAGCCGTTCCGAAATCACCGCCGCCGCTGCCGCCACCAAGGCCTCCAGCCGTGCCGACAGGGCATCGGCGTC
GGCCTCGCCGGTTTCGCGCACCAGAAACGCCCGGCCACCGCTGCCCAGCCGGTCCAGCTCCAACTTGCGGTCGGT
CAGAAGCCGGGTGCCCGCCTGCAACCGCCAGCACAGCCTGTAGGCCGCCAGCAGCGCCGTCTCGCCCGCTTGCGA
CAGGAAACCGCCCTTTACGCCGGCCCGCAACTGCGCTTCCACCCGCCGCGCAGGGTCGGCCAGCCGCAGCGCGCA
GGTCTGCGCCAGCAGTTCGATGTCCATCAGGCGCCCCGCGCCGTTCTTCGCCTCCCAGGCGCCTTCGGGGGGTTT
GGCGGCTTGCAGGCGGCTGCGCATCTCGGCCACGTCGGCCAGCACCTTCGGCCCCTGCCCGGTGGCGGCGAACA
CCTCGCGGCGGAAGGCCTCGACCTCGGCGGCCAGATCGGGGTTGCCCGCCAGCGGCCGGGCGCGGGTCAGGGC
CAGGTGTTCCCAGGTCCAGGCCTCGGTCATCTGGTAGGCGCGGAAGGATTCGATCGAGGTCGCCACCGGCCCTTG
CCGACCGGAGGGGCGCAGCCGCATGTCCACCTCGTAAAGCCGACCTTCGGCCATCGGGGCGGTCAGGGCTGTCAC
CATGGCTTGCGTCAGGCGGGCGTAGTACAGGCGCGGTGGCAGCGGGCGGGGCCGTCCGAGGCCTCGGCATCGGC
GCTGTCGTAGATAACGATCAGGTCGAGGTCGGACCCGGCGTTCAGCCGCGCCGCACCCAGGCTGCCCATGCCCAG
CAGCACCGCCCCCCGCCCCGGCGCTGCCCCATGCTTGCGGGCATATTCCGCGCCCACCACCGGCCAGAGGGCGG
CCACCACCGCCTCGGCCAGATCGGCATAGTGCTTGCCCGCCTCGAAAGCGTCGATCAGCCCGCGCAGGTGGTGGA
CGCCGACGCGGAAGTGCCATTCGCGGGTCCAGCGGCGGGCGGCGTCAAGCTTGCCTTCGTAGTCAGTGACCCCCG
AAAGATGCTCGGCCAACAGCCCGGTCAGGGCGGCACAGCCCGGCCAGGGCGCGAAGAAACTGGCCGCCGATCAC
CGCATCCAGCACTGCGGCGTTGCGCGACAGATACCGCGCCAGCACCGGGGCGGTGGCGGCGATATCTACAATCAA
TTCAACGAGTTGCGGGTTGGCTTCGAACAGCGAGAAGATCTGCACGCCCGAGGGCAGGCCGATCAGAAAGCCGTCA
AACGCCACCAGCGCCTCGTCGGGGTTGGCGGCGGCCATCAGGCTGCGCAGCAGGCTGGGGCGCAGGCGCTGAAA
GATCGCCACGGCACGATCCGAGCGCAGGGCGGGATAGTTGGCCCAGGCATCGACGATGGCGCGGGCGCTGTCGG
AAAGCTCGGGGCCGTCTTCGACCTGGCCGGGGGCAAAGAAGCCTTCGGTCAGGAAATCGGTCTGCTCCAGCCGGG
CGGTCAGGGCGGCACGAAAGCCTGCCACATCCTCGGTGCCGCTGAAAAAGGCAATGCGGGCAACGCCTTGGGCGG
TGGCGGGCATGTCGTGGGTCTGGGCGTCACCGACCATTTGCAAGCGGTGCTCGACCTCGCGGTGGGCGCGGTAAA
GCGCGGTCAGATCCTCGGCCACCTCGGGCGGCACCCAGCCTTTTTCGGCCAGCGCCGCAAGGCTGCCAACGGTGG
TGCGACCGCGCAAGGCGGTGTCACGGCCCCCGGCGATCAACTGGCGGGTCTGGGTGAAGAACTCGATCTCGCGGA
TGCCGCCGACGCCGAGTTTCATGTTGTGACCCTCGATCACGATGGGGCCGTGAAGCCCGCGATGGTCGCGGATGC
GCAGGCGCATGTCGTGGGCGTCCTGGATGGCGGCGAAATCCAGATGCTTGCGCCAGACGAAGGGGGTCAGGCTGT
GCAGGAACCGCTGCCCGGCGGCAAGGTCGCCGCCGCAGGGCCGGGCCTTGATATAGGCGGCGCGTTCCCAGGTG
CGGCCGACGCTTTCGTAATAGCTTTCCGCCGCCGCCATCGACAGGCACACCGGCGTCACCGCCGCATCGGGGCGC
AGCCGCAGGTCGGTGCGGAACACGTAGCCCTCGCCGGTCAGGTCCGACAGCAGGGCGGTCATCCGCCGCGTGAC
GCGGATGAAGGCCGCCCGCGCCTCGGGGGCATCGCCGCCATAGCGGGTCTCGTCGAACAGACAGATCAGGTCGAT
GTCGGAGGAATAGTTCAGTCGTGCGCGCCCATCTTGCCCATGGCCAGCGCCACCATGCCCGCGCCGGTTTCGGCAT
CATCCGGCCCCTGCCCCGGCAGCTTGCCGCGCCTGATTTCCTCGGCCACCAGCCGCGTCAGGCACAGGTGCACCG
CCCGGTCGGCGAGTTGCGTCAGGGCGCCCGTCACCGCCTCCAGCCGCCAGACGCCGCCCAGATCGGCGAGGCCG
ATCAGCAGCGCCACCCGCCGCTTGGCGATGCGCAGACCGGCGCCGAGGGTATCGACGGACAGGGTGTCGAGCGG
CTCCAGCACTTCGGCCAAGGCGGCTTCGGGCGAGATCGTCAAGGCCGCACGCAGCCAGTCGGCCTCGCGCAGCAT
CAGGCCTTTCAGGTAGGGGCTGCACCCGGCGGTGCCGTGGATCAGCGGCAGAAGGTCCGGGCCTAGGTCGGCAA
GGCTGCGGGCGGCATCGGCGGCGGCATCGGCGGCGAAGGCGATGGGATGGCGGGTCAGCCGGGCGGCAAAGGG
CGCATGGGTCATGGCGCCAGCATGGCCGGGGCCGGGTGCCGGGTCAACCGGGGGGATTGCAAGCGTCACCCGGC
TTGCGGATAAAGCCGGGGAAGGAGACGCCGATGAGCAAAAGCCTCGCCCGGGTGAAAGCCGCCCTTGCCGCGCAT
GGGATTGACGCCCCGGTGCTGGAAATGCCGCAGGAAACCCGCACCGCCCCGCAAGCTGCCGAGGCTGCGGGCTGT
GCGCTGGACCAGATCGTGAAGTCGATCCTGTTTCGCGGCGAAGGCTCGGGGCAGTTGCGGCTGTTCCTGACGGCG
GGTGGCAATCAGGTCTGCGCCGACAAGGCCTCGGCGCTGGCGGGCGAGGCTTTGGGGCGGGCCGATGCCGATCA

GGTGCGCAAGACCACCGGCTTTGCCATCGGCGGCGTGGCCCCCATCGGCCACCTGACCCCGCTGCCCTGCTGGTT
CGACGCGCGGCTGCTGGAGTTTCCGCAGGTCTGGGCCGCCGCCGGCACCCCGCGCCACATCTTCGCCGCCCCGC
CGCATCTGCTGTTGCGGATCACTGCGGCGCATCTGGCCGATTTCACCGCCTGAGGCCCATGTAAAAATGTTTTACAT
CGGGTCTTGAACCTGCCCCCGGCAATACCGATCTCCGTTCATGTGAAACACCTTCACATCGACCTGCAACCCTGAAC
GGGAGACCGCCATATGTATACCGCTTCTTCCCCTGCCGCATCTGGCAGCGTCACCACGTGGTTCAACCGCGCGGTC
GCCTGGCTGGATGACCGTGGCAAAGGCGCCTGGATCGCCGCCATGGTGCTGTCCTTCATCTTCGTCTGGCCGCTTG
GCCTGTTCATCCTTGGCTACATGATCTGGAGCAAACGCATGTTCAAACGCAATGGCTGCGGCCACCATCACGCTTTC
CACGGCGCTTACCGCAGCAGCGGCAACACCGCCTTCGACGCCTACAAGGCCGAAACCATGCGCCGCCTGGAAGAC
GAACAGGACGCGTTCAATTTCCTTCCTGCAGGAATTCGATATCAAGCTTATCGATACCGTCG

pP6 – 1770 bp consensus sequence
66% GC

GCGGGGCGGCCGCTCNGAACTAGTGGATCCCCCGGGCTGCAGGCAGGCCTTGCCGCGCCCCTNTANAGGGNGCC
GCAAGGGTGGCCGCTCCACCCGCGNTCGNCTTTTGAGNGGCGCAAGCTGCGCCCGCTGGCCTGAGGTCAACCGCG
GGCAGCGGCCTCCAGTGCGGCAATGTCAATCTTCACCATGCCCATCATCGCCTGCATCACCCGCCCCGAGGTGTCG
GTCTGCAAAAGCCGCGGCAGCACCCGCGGCGTGATCTGCCAGGACAGCCCGAAGCGGTCGGTCAGCCAGCCGCA
GCGGCTTTCGACACCGCCTTCCAGCAAGGCGTCCCACAGCCGGTCCACCTCGGCCTGAGTATCGACATGCACCCCC
AGCGACACCGCGGGCGTCAGCGCGTAATGCGACCCGCCGTTCAGCGCCAGATAGCGCTGGCCCAGCAGATCGAAA
TACACCGCCAGCGCCTGGCCTGGGTCGTCGGGCTTTTGTAGGATTTCAGTGATGCGGGCGCCCTCGAACAGGCTGC
AATAGAACCGCGCGGCGGCTTCGGCCTGGGTGTCGAACCACAGGCAGGTGGACAGCGAAGGCTCGGTCATCGGCA
TTTCCCCCTTTTGCAAGGCATTGAAAACTTAGCGCAGATCGCAGGCCTCGCGCGCCAGCCGGGTGATCCCGGCCCA
GTCGCCCTTGACCATCATCGCCTTGGGTGCCACCCAACTGCCGCCGACGCACAGCACGTTGGACAGCGCCAGATAG
TCCCGCGCATTGCCCAGCCCGATGCCGCCGGTGGGGCAGAAACTGACCTGCGGCAACGGCGCACCAATCGCCTTC
AGCGCCGCCGCCCCGCCCGAGGCTTCGGCGGGAAAGAACTTCTGCACCGTATAGCCGCGSTcCAGCAGCGCCATC
ACTTCGGTYGCCGTYGCCGCCCCCGCMAGCAGCGGcAAGCCnTCGGCCTCGCAGgNGGSCAGCAAACGGTCGGTG
NCCCCCCGGAGACACCCCGAAGGTNGCCCCCGCCGCCTTGGCCGCCCGCACATCCTCNGGCGTCAGCAATGTGCC
CGCGCCGACCACGCCGCCCGGCACCCCGGCCATGGCACGGATCACCTCCAGCGCCGCCGGCGTGCGCAGCGTCA
CCTCCAGCACCGGCAAGCCGCCCGCCACCAGANCCTCGGCCAAAGGTNGGGCATGGCGCACATCCTCGATAACCA
GCACCGGAATGACCGGCGCCAGACGGCAGATTTNGGCAGCGCGGGCGGATTGTTNGGCGGGGGTCATCATCGGCT
CCTTGTGGTCCGCCACGGCTCGGGCGGAAACTGCGGGTGCCTCCGGCGGGGATATTTAGAAACAGATGAAATCACG
AGGCATTCATCTGTTCTCAAATATCCTCGCCGAAGGCCAGAAGTTCTCTATTTTTCNGTCACACCACCACGCCGGCAC
CCTCGGTGGCCGGGCCGACATTGCGGCGGAAGGCGTCGAACAGATCGCGGCCCATGCCGTGACCGTTTTNGGACA
GATCGGCGACCACCGGGCTGCGGGTTGCGAAGTCCTCGGCCCCCAGCACGGACAGCGTGCCCGCCGGCGCGTCC
AGTCGCACAATGTCGCCATCGCGCAGCCGGGCCAGCGGGCCACCGCAGGCAGCTTCGGGCGAGACGTGGATGGC
GGCGGGCACCTTTNNAAAAGCCCCCGACATCCGGCCATCGGTCACCAATGCCCNATNAAANGGCCGCGGTCCTGCA
GGAATTCGATATCAAGCTTATCGATACCTCGACTCAGGGG

pP7 – 1299 bp consensus sequence
62% GC

ANGGGCCCCCTCGANGTCGAGGTATCGATAAGCTTGATATCGAATTCCTGCAGCTCGTCGGCNNTTTAATGAANATG
ATCAGGTCGCACCAGGCGGCGGCTTCGCCCNTTTNAAATCACCTTCAGGCCCTCGCCCTCGGCCTTCTTGGCACTG
GGCGAACCGGGGCGCAGCGCCACGACCAGGTTTTTCGCGCCGCTGTCGCGCAGGTTCAGCGCGTGGGCATGGCC
CTGGCTGCCGTAGCCGAGgATKGCAACcTTCTTgTYCTTGATCAGGTTGATgTCGCAGTCACgGTCATAATACACGCGC
ATGGGGCGTTCcTTTGCTGGTTGATTGCCGCGCAGCATAGGCGGTTTGCGGCGATGGTTCGTGCAAAGTTTGACATA
TCTAGGGGGATnGGGGGAAAAGTCATGCGCGAATGTGGCGATTGGTGGATGAAACATGCAGATCGACGATACCGAC
CGGCGGGTGCTGCGGCAGTTGATGGCGGAACCTGGGCTGGCGATGGCCGATCTGGCGGAACGCGCCGGCGTCAC
GCAGGCGACCTGCTGGCGGCGGATCGAGATGGCAGGGCGCGAAGTGCATTTCCGCTCGAAATCCGATGCGGTGGC
GCAGGGCATCGGCATCGTGTTTCAGGAGCTGAACCTGTTTCCCAACCTCAGCGTTGCCGAAAACATCTTCATCGCCC
GCGAGCCGGTGCGGGCGGGCATCGACATCGACGCGGGTGCGCAGCGGGTGGCGGCGCGGGCCTTGATGCGGCG
GCTGGAGCAGGACATCGACCCCGATGCCGACCTTGGCACCCTGCGCATCGGCCAGCAGCAGATTGTCGAGATCGC
CGCCGCCGCCGAAACCGCATTTTCCGCGGCAATGCCGTGCAGCCGGGCCGATTCGAGCACCAGAAACCCGCGCAA
CCGTTTGCCGCCCTGGGTGGCATAGCGCATCGCCTGCACCACCGGCTGATCAGCATCGCCTCAGGCTTTGGCCTGC
GACGGCATCGAGCCATCGTCTTTCGGCTTTTCGCTGCGGTCCAGCCCCAGGAACAGCACGATGTTCTTGGCCACGA
ACACCGAGGAATAGGTGCCCAGAATCACCCCGAAGAAGATGGCAAAGGTGAAGCCGCGGATCACGTCGCCGCCGA
AGATCAGCATGGCGATCAGCGCGAGCAGCGTGGTGAACGAGGTCATCANCGTAAAGGNTCAGCGTCTGGTTGACCG
AGATGTTCATCACCANCTATAAAGGGGCGTGGTCTTGTATTTCTGCAGCCCGGGGGATCCACTAGTCAGAGCGGCC
GCCCCGCGGTTG

pH5 – 949 bp from T3 end
61% GC

CCCTGAGTGAGGTATCGATAAGCTTTGCGCCAGCGCCGATGCCGGCTGTCCTTNTANAGGNNTCTCGGNCANAAAC
TGCAACCCGGCAATCACCTTCTTTANGGGGGGGTGGCGTAATCGGTCATCACGATATGGCCCGACTGCTCGCCGCC
CAGGTTGAAACCGCCGCGCCGCATCGCCTCGACCACATAGCGGTCGCCGACATTGGTGCGCTCCAGCCGCAGCCC
GCGCCGNTCCAGAAACCGCTCCAGCCCGAGGTTCGACATCACCGTGGCCACCAGCGTGCCGCCGTGCAGCCGCCC
CTCCTCGGCCCAGNGGGCGGCCAGCAGCGCCATGATCTGGTCGCCATCCGCCACCTTCCCGGTCTGATCCANAATC
ATCACCCGGTCGGCGTCGCCATCCANACAGATGCCGACATCGGCGCCATGCGCCACCACCGCCTCGGCGGCAGTC
TGGGTATAGGTCGAGCCACAACGGTCGTTGATATTGGTGCCATTCGGCGCCACCCCCACCGGGATCACCTCGGCGC
CCAATTCCCACAGCACCTNGGGGGCCGCACGATAGGCCGCGCCATTGGCGCAATCTATCACCACCTTCAGCCCATC
AAGCCGCAGCCCGACGGGAAAGGTGGTCTTGGCATATTCCTGATAGCGCCCGCGGCCATNNTCGATCCGCTTGGCC
CNGCNGATGTTCTGCGGCTGCGCCAGCGCAATCTCGCCCNCCAGAATCGCCTCGATCTCTCTTTCGGCATCATCCG
ACAGCTTGAAGCCGTCGGGGCCNAANAACTTGATGCCATTGTCCTGATGCGGGTTGTGCGAGGCGCTNATCATCAC
CCCCAGATCGGNGCGNATGCTGCGNATNAAAAACCCAACGGANGNGTCGGNACNGGGCCCANCAACAGCANTTCAT
CCCGTCAAGTNACCNGGNGGTCAGCGCNTTTCAAAATGTA

pH5 – 912 bp from T7 end
64% GC

ACCGCGGGCGGCCGCTCTGACTAGTGGATCCCCCGGGCTGCAGGAATTCGATATCAAGCCNNTTNANNTAGGGTCG
ACGGATCACCATTATCGCGCGTGATAAGCCTTTTTAAGNCCGCTAGGAACGCCGCCATATACCTGCCGAGAAGCAGG
AGAACCGGCGCCGCCAGAACCAGTAACATCACCCGCGCCATCCGAACCCCCAAGAGCCTGCCGAAGCGTCGGCAT
GGAATTTTGGCCAGCATAAATGCCGCCCACCTTGGGCCGCAAGGTCAGCGACATGACCTTTTGCCGCAGCACAGTG
TTTTCCTGTGCAAGGGCATTGGTTTTCGAGAGTTTGGCCTCGTCCTGGCGTTTCGCCAGATTATCCGCAAGGATCAG
CCTGGGCGGCTGGGCGGTTGCGGACTGGCCAGAGGCCGACCTGCGGGCGGGCCTGACCCTGCTGCCGCAACGCA
GCACGCTGATGGCCGGAACCGTGGCCGAGGCGCTGCGGCTGGCCGGCCCCGCCGAGGACGCGCACCTGTGGCAG
GTGCTGGCGGCCGTGCAGATGGACGGGATCATCCGCGAACGCGACGGCCTGGCCGCCCGGATCTGCGCCACGCC
CATGGCCAGCCCGATGCCCCACCACGGCGCGCCATAGGCGGCAAACACCGCCAGCGCGCCGAGGTTGGAGGCGA
AGTTCAGCAGCTTGGTATGCGCCGTGGCCTTCAGCACGCCATGCCCCGCCAGCACCACAAAGCCGATCATGTAGAA
CGCCCCCGCCCCCGGCCCGATCAGCCCGTCATAGCCGCCGATCAGTGGCACCACNAAGGCGGTGAAAAGCAGTGG
GGCGAAATGCGGCGGGNGCGGTCNTCNTCGNACAGCCCCTTCTTGAAGNAAAAAANCCNGNGATGCCAATCAGGAT
CACCGGAG

pH6 – 269 bp from T3 end
51% GC

TCGNAANANGGGCCCCCTGNGNCGANGTATCGATAAGCTTNATGCGNTGTCGCTCGACCATGTGCCCCTNACCGNA
GGGNTAGNGNNATTGGAACAGANNATGNGGAACCTTNNTAAGGGGACAAGATCNGTTATGNGCTGCTTCCCGTAGC
CGGNCATGGCATCNCCNGCCCAACCGAAAGCGCCNAGGAGANGCTGACCGCTTTCCCCTGACCGGNCCTTGCCCC
GNCAGNAACCGNNANNTATAANCCNGGNCATGANCNANACCC

pH6 – 322 bp from T7 end
64% GC

AACCGCGGGGCGGCCGCTCTAGAACTAGTGGATCCCCCGGGCTGCAGGAATTCGATATCAAGCCCNNTTATANGGG
CCGCAGATGCTGAAGAACGTGCGTTACGGNCCNTNGACGCAGCCCTTGGCGGCGGCGGCGGTGCAGGCGGTGATT
GCTGATGCCGAAGCGCGGTTGCAGGGCTCGGGGCGGCTGCTGATCCGCAAGTCGGGCACCGAGCCTTTGGTGCGG
GTGATGGCGGAATGTGAGGACGAGGTGCTGCTGGCCGAGGTGGTGGGCAGCATTGTGGCGGCGGTGGAAGCGGC
GGTTTGAGTTTGAGGCAGGAAG

References

1. 2003 *Denaturing (SDS) discontinuous PAGE: Laemmli method*, in *Short Protocols in Protein Science*, J.E. Coligan, B.M. Dunn, D.W. Speicher, and P.T. Wingfield, Editors. John Wiley & Sons, Inc.: New York. p. 10-4 -10-7.
2. Altschul, S.F., W. Gish, W. Miller, E.W. Myers, and D.J. Lipman. (1990) Basic local alignment search tool*. J. Mol. Biol.*, **215**(3): p. 403-410.
3. Anbar, A.D. and A.H. Knoll. (2002) Proterozoic ocean chemistry and evolution: a bioinorganic bridge? *Science*, **297**: p. 1137-1142.
4. Anbar, A.D., J.E. Roe, J. Barling, and K.H. Nealson. (2000) Nonbiological fractionation of iron isotopes*. Science*, **288**: p. 126-128.
5. Anthony, C. (2004) The quinoprotein dehydrogenases for methanol and glucose*. Arch. Biochem. Biophys.*, **428**: p. 2-9.
6. Appia-Ayme, C., A. Bengrine, C. Cavazza, M. Bruschi, M. Chippaux, and V. Bonnefoy. (1998) The *cyc1* and *cyc2* genes encoding the cytochrome *c*4 (*c*552) and a high molecular weight cytochrome *c* from *Thiobacillus ferrooxidans* are co-transcribed*. FEMS Microbiol. Lett.*, **167**: p. 171-177.
7. Appia-Ayme, C., N. Guiliani, J. Ratouchniak, and V. Bonnefoy. (1999) Characterization of an operon encoding two *c*-type cytochromes, an *aa*(3)-type cytochrome oxidase, and rusticyanin in *Thiobacillus ferrooxidans* ATCC 33020*. Appl. Environ. Microbiol.*, **65**(11): p. 4781-7.
8. Balci, N., T.D. Bullen, K.W. Lien, W.C. Shanks, M. Motelica, and K.W. Mandernack. (2005) Iron isotope fractionation during microbially stimulated Fe(II) oxidation and Fe(III) precipitation*. Geochim. Cosmochim. Acta*, submitted.
9. Battistuzzi, G., M. Borsari, J.A. Cowan, A. Ranieri, and M. Sola. (2002) Control of cytochrome *c* redox potential: axial ligation and protein environment effects*. J. Am. Chem. Soc.*, **124**(19): p. 5315-5324.
10. Beard, B.L., C.M. Johnson, L. Cox, H. Sun, K.H. Nealson, and C. Aguilar. (1999) Iron isotope biosignatures*. Science*, **285**(5435): p. 1889-92.
11. Beard, B.L., C.M. Johnson, J.L. Skulan, K.H. Nealson, J.D. Coates, and H. Sun. (2003) Application of Fe isotopes to tracing the geochemical and biological cycling of Fe*. Chem. Geol.*, **195**: p. 87-117.
12. Beard, B.L., C.M. Johnson, K.L. Von Damm, and R.L. Poulson. (2003) Iron isotope constraints on Fe cycling and mass balance in oxygenated Earth oceans*. Geology*, **31**(7): p. 629–632.
13. Bengrine, A., N. Guiliani, C. Appia-Ayme, E. Jedlicki, D.S. Holmes, M. Chippaux, and V. Bonnefoy. (1998) Sequence and expression of the rusticyanin structural gene from *Thiobacillus ferrooxidans* ATCC33020 strain*. Biochim. Biophys. Acta*, **1443**(1-2): p. 99-112.
14. Benz, M., A. Brune, and B. Schink. (1998) Anaerobic and aerobic oxidation of ferrous iron at neutral pH by chemoheterotrophic nitrate-reducing bacteria*. Arch. Microbiol.*, **169**(2): p. 159-65.

15. Berg, D.E., M.A. Schmandt, and J.B. Lowe. (1983) Specificity of transposon Tn*5* insertion. *Genetics*, **1053**: p. 813-828.
16. Bersch, B., M.J. Blackledge, T.E. Meyer, and D. Marion. (1996) *Ectothiorhodospira halophila* ferrocytochrome c_{551}: solution structure and comparison with bacterial cytochromes *c. J. Mol. Biol.*, **264**(567-584).
17. Blake, R.C., 2nd and E.A. Shute. (1994) Respiratory enzymes of *Thiobacillus ferrooxidans*. Kinetic properties of an acid stable iron:rusticyanin oxidoreductase. *Biochemistry*, **33**: p. 9220-9228.
18. Blake, R.C., 2nd, E.A. Shute, M.M. Greenwood, G.H. Spencer, and W.J. Ingledew. (1993) Enzymes of aerobic respiration on iron. *FEMS Microbiol. Rev.*, **11**(1-3): p. 9-18.
19. Blake, R.C., 2nd, E.A. Shute, J. Waskovsky, and A.P.J. Harrison. (1992) Respiratory components in acidophilic bacteria that respire iron. *Geomicrobiol. J.*, **10**: p. 173-192.
20. Blankenship, R.E. and H. Hartman. (1998) The origin and evolution of oxygenic photosynthesis. *Trends Biochem. Sci.*, **23**(3): p. 94-7.
21. Boschker, H.T., S.C. Nold, P. Wellsbury, D. Bos, W. de Graaf, R. Pel, R.J. Parkes, and T.E. Cappenberg. (1998) Direct linking of microbial populations to specific biogeochemical processes by ^{13}C-labeling of biomarkers. *Nature*, **392**: p. 801-805.
22. Brantley, S.L., L. Liermann, and T.D. Bullen. (2001) Fractionation of Fe isotopes by soil microbes and organic acids. *Geology*, **29**(6): p. 535–538.
23. Brasier, M.D., O.R. Green, A.P. Jephcoat, A.K. Kleppe, M.J. Van Kranendonk, J.F. Lindsay, A. Steele, and N.V. Grassineau. (2002) Questioning the evidence for Earth's oldest fossils. *Nature*, **416**(6876): p. 76-81.
24. Braterman, P.S., A.G. Carins-Smith, and R.W. Sloper. (1983) Photo-oxidation of hydrated Fe^{2+} - significance for banded iron formations. *Nature*, **303**: p. 163-164.
25. Brocks, J.J., G.A. Logan, R. Buick, and R.E. Summons. (1999) Archean molecular fossils and the early rise of eukaryotes. *Science*, **285**(5430): p. 1033-6.
26. Brouwers, G.J., E. Vijgenboom, P.L. Corstjens, J.P. De Vrind, and E.W. De Vrind-De Jong. (2000) Bacterial Mn^{2+} oxidizing systems and multicopper oxidases: an overview of mechanisms and functions. *Geomicrobiol. J.*, **17**(1-24).
27. Bullen, T.D., A.F. White, C.W. Childs, D.V. Vivit, and M.S. Schultz. (2001) Demonstration of significant iron isotope fractionation in nature. *Geology*, **29**(8): p. 699-702.
28. Burden, S., Y.X. Lin, and R. Zhang. (2005) Improving promoter prediction for the NNPP2.2 algorithm: a case study using *Escherichia coli* DNA sequences. *Bioinformatics*, **21**(5): p. 601-607.
29. Burke, D.H., M. Alberti, and J.E. Hearst. (1993) The *Rhodobacter-capsulatus* chlorin reductase-encoding locus, *bchA*, consists of 3 genes, *bchX*, *bchY*, and *bchZ. J. Bacteriol.*, **175**(8): p. 2407-2413.

30. Burlage, R.S. 1998 *Molecular techniques*, in *Techniques in Microbial Ecology*, R.S. Burlage, R. Atlas, D. Stahl, G. Geesey, and G. Sayler, Editors. Oxford University Press, Inc.: New York. p. 328.
31. Canfield, D.E., K.S. Habicht, and B. Thamdrup. (2000) The Archean sulfur cycle and the early history of atmospheric oxygen. *Science*, **288**(5466): p. 658-61.
32. Carins-Smith, A.G. (1978) Precambrian solution photochemistry, inverse segregation, and banded iron formations. *Nature*, **276**(5690): p. 807-8.
33. Catling, D.C., K.J. Zahnle, and C. McKay. (2001) Biogenic methane, hydrogen escape, and the irreversible oxidation of early Earth. *Science*, **293**(5531): p. 839-43.
34. Chaudhuri, S.K., J.G. Lack, and J.D. Coates. (2001) Biogenic magnetite formation through anaerobic biooxidation of Fe(II). *Appl. Environ. Microbiol.*, **67**(6): p. 2844-8.
35. Chiang, S.L. and E.J. Rubin. (2002) Construction of a mariner-based transposon for epitope-tagging and genomic targeting. *Gene*, **296**(1-2): p. 179-85.
36. Clarke, L. and J. Carbon. (1976) A colony bank containing synthetic ColE1 hybrid plasmids representative of the entire *E. coli* genome. *Cell*, **9**(1): p. 91-99.
37. Cloud, P. (1973) Paleoecological significance of banded iron-formation. *Econ. Geol.*, **68**(7): p. 1135-1143.
38. Cobley, J.G. and B.A. Haddock. (1975) The respiratory chain of *Thiobacillus ferrooxidans*: the reduction of cytochromes by Fe^{2+} and the preliminary characterization of rusticyanin a novel 'blue' copper protein. *FEBS Lett.*, **60**(1): p. 29-33.
39. Colmer, A.R., K.L. Temple, and M.E. Hinkle. (1949) An iron-oxidizing bacterium from the drainage of some bituminous coal mines. *J. Bacteriol.*, **59**: p. 317-328.
40. Cox, J.C. and D.H. Boxer. (1978) The purification and some properties of rusticyanin, a blue copper protein involved in Fe(II) oxidation from *Thiobacillus ferrooxidans. Biochem. J.*, **174**: p. 497-502.
41. Croal, L.R., C.J. Johnson, B.L. Bread, and D.K. Newman. (2004) Iron isotope fractionation by Fe(II)-oxidizing photoautotrophic bacteria. *Geochim. Cosmochim. Acta*, **68**(6): p. 1227-1242.
42. Dailey, H.A., T.A. Dailey, C.K. Wu, A.E. Medlock, K.F. Wang, J.P. Rose, and B.C. Wang. (2000) Ferrochelatase at the millennium: structures, mechanisms and 2Fe-2S clusters. *Cell. Mol. Life Sci.,* **57**(13-14): p. 1909-1926.
43. Darbre, P.D. (1999) *Basic Molecular Biology : Essential Techniques*. Chichester, New York: John Wiley & Sons, Inc.
44. Datsenko, K.A. and B.L. Wanner. (2000) One-step inactivation of chromosomal genes in *Escherichia coli* K-12 using PCR products. *Proc. Natl. Acad. Sci. U S A*, **97**(12): p. 6640-6645.

45. Davis, J., T.J. Donohue, and S. Kaplan. (1988) Construction, characterization and complementation of a Puf$^-$ mutant of *Rhodobacter sphaeroides. J. Bacteriol.*, **170**(1): p. 320-329.
46. de Vrind-de Jong, E.W., P.L. Corstjens, E.S. Kempers, P. Westbroek, and J.P. de Vrind. (1990) Oxidation of manganese and iron by *Leptothrix discophora*: use of *N,N,N′,N′*-tetramethyl-*p*-phenylenediamine as an indicator of metal oxidation*. Appl. Environ. Microbiol.*, **56**(11): p. 3458-3462.
47. Debussche, L., M. Couder, D. Thibaut, B. Cameron, J. Crouzet, and F. Blanche. (1992) Assay, purification, and characterization of cobaltochelatase, a unique complex enzyme catalyzing cobalt insertion in hydrogenobyrinic acid *a*,*c*-diamide during coenzyme B_{12} biosynthesis in *Pseudomonas denitrificans. J. Bacteriol.*, **174**(22): p. 7445-7451.
48. Dehio, C. and M. Meyer. (1997) Maintenance of broad-host-range incompatibility group P and group Q plasmids and transposition of Tn5 in *Bartonella henselae* following conjugal plasmid transfer from *Escherichia coli. J. Bacteriol.*, **179**(2): p. 538-540.
49. Dutton, P.L., K.M. Petty, H.S. Bonner, and S.D. Morse. (1975) Cytochrome *c2* and reaction center of *Rhodospeudomonas sphaeroides* Ga. membranes: extinction coefficients, content, half-reduction potentials, kinetics and electric field alterations. *Biochim. Biophys. Acta*, **387**(3): p. 536-556.
50. Edwards, K.J., P.L. Bond, T.M. Gihring, and J.F. Banfield. (2000) An archaeal iron-oxidizing extreme acidophile important in acid mine drainage*. Science*, **287**(5459): p. 1796-9.
51. Edwards, K.J., D.R. Rogers, C.O. Wirsen, and T.M. McCollom. (2003) Isolation and characterization of novel psychrophilic, neutrophilic, Fe-oxidizing, chemolithoautotrophic alpha- and gamma-Proteobacteria from the deep sea*. Appl. Environ. Microbiol.*, **69**(5): p. 2906-13.
52. Ehrenreich, A. and F. Widdel. (1994) Anaerobic oxidation of ferrous iron by purple bacteria, a new type of phototrophic metabolism*. Appl. Environ. Microbiol.*, **60**(12): p. 4517-26.
53. Ehrlich, H.L. 2002 *Geomicrobiology of Iron*, in *Geomicrobiology*. Dekker: New York. p. 345-429.
54. Emerson, D. and C. Moyer. (1997) Isolation and characterization of novel iron-oxidizing bacteria that grow at circumneutral pH*. Appl. Environ. Microbiol.*, **63**(12): p. 4784-92.
55. Emerson, D. and C.L. Moyer. (2002) Neutrophilic Fe-oxidizing bacteria are abundant at the Loihi Seamount hydrothermal vents and play a major role in Fe oxide deposition*. Appl. Environ. Microbiol.*, **68**(6): p. 3085-93.
56. Emerson, D., J.V. Weiss, and J.P. Megonigal. (1999) Iron-oxidizing bacteria are associated with ferric hydroxide precipitates (Fe-plaque) on the roots of wetland plants*. Appl. Environ. Microbiol.*, **65**(6): p. 2758-61.
57. Ewers, W.E. 1983 *Chemical factors in the deposition and diagenesis of banded iron-formation*, in *Iron Formations: Facts and Problems*, A.F. Trendall and R.C. Morris, Editors. Elsevier: Amsterdam.

58. Farquhar, J. and B.A. Wing. (2003) Multiple sulfur isotopes and the evolution of the atmosphere. *Earth Planet. Sci. Lett.*, **213**: p. 1-13.
59. Fedo, C.M. and M.J. Whitehouse. (2002) Metasomatic origin of quartz-pyroxene rock, Akilia, Greenland, and implications for Earth's earliest life. *Science*, **296**(5572): p. 1448-1452.
60. Fernandez-Prini, R., J.L. Alvarez, and A.H. Harvey. (2003) Henry's constants and vapor-liquid distribution constants for gaseous solutes in H_2O and D_2O at high temperatures. *J. Phys. Chem. Ref. Data*, **32**(2): p. 903-916.
61. Francis, R.T. and R.R. Becker. (1984) Specific indication of hemoproteins in polyacrylamide gels using a double-staining process. *Anal. Biochem.*, **136**(2): p. 509-514.
62. Francois, L.M. (1986) Extensive deposition of banded iron formation was possible without photosynthesis. *Nature*, **320**: p. 352-354.
63. Fukumori, Y., T. Yano, A. Sato, and T. Yamanaka. (1988) Fe(II)-oxidizing enzyme purified from *Thiobacillus ferrooxidans. FEMS Microbiol. Lett.*, **50**: p. 169-172.
64. Griesbeck, C., G. Hauska, and M. Schutz. 2000 *Biological sulfide oxidation: sulfide quinone reductase (Sqr), the primary reaction*, in *Recent Research Developments in Microbiology*, S.G. Pandalai, Editor. Research Signpost: Trivadrum, India. p. 179-203.
65. Grotzinger, J.P. and J.F. Kasting. (1993) New constraints on Precambrian ocean composition. *J. Geol.*, **101**(2): p. 235-243.
66. Hall, J.F., S.S. Hasnain, and W.J. Ingledew. (1996) The structural gene for rusticyanin from *Thiobacillus ferrooxidans*: cloning and sequencing of the rusticyanin gene. *FEMS Microbiol. Lett.*, **137**(1): p. 85-9.
67. Hartman, H. 1984 *The evolution of photosynthesis and microbial mats: a speculation on banded iron formations*, in *Microbial Mats: Stromatolites*, Y. Cohen, R.W. Castenholz, and H.O. Halvorson, Editors. Alan. R. Liss: New York. p. 451-453.
68. Hauck, S., M. Benz, A. Brune, and B. Schink. (2001) Ferrous iron oxidation by denitrifying bacteria in profundal sediments of a deep lake (Lake Constance). *FEMS Microbiol. Ecol.*, **37**: p. 127-134.
69. Heising, S., L. Richter, W. Ludwig, and B. Schink. (1999) *Chlorobium ferrooxidans* sp. nov., a phototrophic green sulfur bacterium that oxidizes ferrous iron in coculture with a "*Geospirillum*" sp. strain. *Arch. Microbiol.*, **172**(2): p. 116-24.
70. Heising, S. and B. Schink. (1998) Phototrophic oxidation of ferrous iron by a *Rhodomicrobium vannielii* strain. *Microbiology*, **144**(Pt 8): p. 2263-9.
71. Hinrichs, W., C. Kisker, M. Düvel, A. Müller, K. Tovar, W. Hillen, and W. Saenger. (1994) Structure of the tet repressor-tetracycline complex and regulation of antibiotic resistance. *Science*, **264**: p. 418-420.
72. Holland, H.D. (1973) The oceans: A possible source of iron in iron-formations. *Econ. Geol.*, **68**: p. 1169-1172.
73. Holland, H.D. (1984) *The Chemical Evolution of the Atmosphere and Oceans*. Princeton, NJ: Princeton University Press. 109-122.

74. Holland, H.D. and J.F. Kasting. 1992 *The Environment of the Archean Earth*, in *The Proterozoic Biosphere: An Interdisciplinary Study*, J.W. Schopf and C. Klein, Editors. Cambridge University Press: Cambridge. p. 21-24.
75. Icopini, G.A., S.L. Brantley, S. Ruebush, M. Tien, and T.D. Bullen. (2002) Iron fractionation during microbial reduction of iron. *Eos Trans. AGU Fall Meeting Suppl.*, **83(47)** (Abstract B11A-0706).
76. Ingledew, W.J. and J.G. Cobley. (1980) A potentiometric and kinetic study on the respiratory chain of ferrous-iron-grown *Thiobacillus ferrooxidans. Biochim. Biophys. Acta*, **590**(2): p. 141-58.
77. Ingledew, W.J. and A. Houston. (1986) The organization of the respiratory chain of *Thiobacillus ferrooxidans. Biotech. Appl. Biochem.*, **8**: p. 242-248.
78. Iyer, L.M., D.D. Leipe, E.V. Koonin, and L. Aravind. (2004) Evolutionary history and higher order classification of AAA plus ATPases. *J. Struct. Biol.*, **146**(1-2): p. 11-31.
79. Jagura-Burdzy, G., J.P. Ibbotson, and C.M. Thomas. (1991) The *korF* region of broad-host-range plasmid RK2 encodes two polypeptides with transcriptional repressor activity. *J. Bacteriol.*, **173**(2): p. 826-833.
80. James, H.L. (1954) Sedimentary facies of iron-formation. *Econ. Geol.*, **49**: p. 235-293.
81. Jenney, F.E., Jr., R.C. Prince, and F. Daldal. (1996) The membrane-bound cytochrome c_y of *Rhodobacter capsulatus* can serve as an electron donor to the photosynthetic reaction of *Rhodobacter sphaeroides. Biochim. Biophys. Acta*, **1273**(2): p. 159-64.
82. Jiao, Y. unpublished results.
83. Jiao, Y., A. Kappler, L.R. Croal, and D.K. Newman. (2005) Isolation and characterization of a genetically tractable photoautotrophic Fe(II)-oxidizing bacterium *Rhodopseudomonas palustris* strain TIE-1. *Appl. Environ. Microbiol., in press*.
84. Johnson, C.M., B.L. Beard, N.J. Beukes, C. Klein, and J.M. O'Leary. (2003) Ancient geochemical cycling in the Earth as inferred from Fe isotope studies of banded iron formations from the Transvaal Craton. *Contrib. Mineral. and Petrol.*, **144**(523-547).
85. Johnson, C.M., B.L. Beard, S.A. Welch, and E.E. Roden. (2002) Iron isotope fractionation in the system Fe(III)-Fe(II)-hematite-magnetite-Fe carbonate, and implications for the origin of banded iron formations. *Geol. Soc. Ann. Meeting, Denver, CO*, (Abstract # 169-9).
86. Johnson, C.M., J.L. Skulan, B.L. Beard, H. Sun, K.H. Nealson, and P.S. Braterman. (2002) Isotopic fractionation between Fe(III) and Fe(II) in aqueous solutions. *Earth Planet. Sci. Lett.*, **195**: p. 141-153.
87. Johnson, H.A. (2005) Personal communication.
88. Joshi, B., L. Janda, Z. Stoytcheva, and P. Tichy. (2000) PkwA, a WD-repeat protein, is expressed in spore-derived mycelium of *Thermomonospora curvata* and phosphorylation of its WD domain could act as a molecular switch. *Microbiology*, **146**: p. 3259-3267.

89. Kappler, A. and D.K. Newman. (2004) Formation of Fe(III)-minerals by Fe(II)-oxidizing photoautotrophic bacteria. *Geochim. Cosmochim. Acta*, **68**(6): p. 1217-1226.
90. Kasting, J.F. (1993) Earth's early atmosphere. *Science*, **259**(5097): p. 920-6.
91. Kasting, J.F., H.D. Holland, and L.R. Kump. 1992 *Atmospheric evolution: the rise of oxygen.*, in *The Proterozoic Biosphere: An Interdisciplinary Study*, J.W. Schopf and C. Klein, Editors. Cambridge University Press: Cambridge. p. 159-163.
92. Keen, N.T., S. Tamaki, D. Kobayashi, and D. Trollinger. (1988) Improved broad-host-range plasmids for DNA cloning in gram-negative bacteria. *Gene*, **70**(1): p. 191-7.
93. Kim, M.K. and C.S. Harwood. (1991) Regulation of benzoate-CoA ligase in *Rhodopseudomonas-palustris. FEMS Microbiol. Lett.*, **83**(2): p. 199-203.
94. Klein, C. and N.J. Beukes. 1983 *Proterozoic Iron-Formations*, in *Iron Formations: Facts and Problems*, A.F. Trendall and R.C. Morris, Editors. Elsevier: Amsterdam. p. 383-469.
95. Klein, C. and N.J. Beukes. (1989) Geochemistry and sedimentology of a facies transition from limestone to iron-formation deposition in the early Proterozoic Transvaal Supergroup, South Africa. *Econ. Geol.*, **84**: p. 1773-1774.
96. Klein, C. and N.J. Beukes. 1992 *Time Distribution, Stratigraphy, and Sedimentologic Setting and Geochemistry of Precambrian Iron-Formations*, in *The Proterozoic Biosphere: An Interdisciplinary Study*, J.W. Schopf and C. Klein, Editors. Cambridge University Press: Cambridge. p. 139-146.
97. Knauth, L.P. and D.R. Lowe. (2003) High Archean climatic temperature inferred from oxygen isotope geochemistry of cherts in the 3.5 Ga Swaziland Supergroup, South Africa. *Geol. Soc. Am. Bull.*, **115**(5): p. 566-580.
98. Knoll, A.H. (2003) The geological consequences of evolution. *Geobiology*, **1**: p. 3-14.
99. Knoll, A.H. and D.E. Canfield. (1998) Isotopic inferences on early ecosystems. *Paleontol. Soc. Papers*, **4**: p. 212-243.
100. Knoll, A.H. and S.A. Carroll. (1999) Early animal evolution: emerging views from comparative biology and geology. *Science*, **284**(5423): p. 2129-2137.
101. Konhauser, K.O., T. Hamade, R. Raiswell, R.C. Morris, F.G. Ferris, G. Southam, and D.E. Canfield. (2002) Could bacteria have formed the Precambrian banded iron formations? *Geology*, **30**(12): p. 1079-1082.
102. Kovach, M.E., P.H. Elzer, D.S. Hill, G.T. Robertson, M.A. Farris, R.M. Roop, and K.M. Peterson. (1995) Four new derivatives of the broad-host-range cloning vector pBBR1MCS, carrying different antibiotic-resistance cassettes. *Gene*, **166**: p. 175-176.

103. Kusano, T., K. Sugawara, C. Inoue, T. Takeshima, M. Numata, and T. Shiratori. (1992) Electrotransformation of *Thiobacillus ferrooxidans* with plasmids containing a *mer* determinant. *J. Bacteriol.*, **174**(20): p. 6617-23.
104. Kusano, T., T. Takeshima, K. Sugawara, C. Inoue, T. Shiratori, T. Yano, Y. Fukumori, and T. Yamanaka. (1992) Molecular cloning of the gene encoding *Thiobacillus ferrooxidans* Fe(II) oxidase. High homology of the gene product with HiPIP. *J. Biol. Chem.*, **267**(16): p. 11242-7.
105. Larimer, F.W., P. Chain, L. Hauser, J. Lamerdin, S. Malfatti, L. Do, M.L. Land, D.A. Pelletier, J.T. Beatty, A.S. Lang, F.R. Tabita, J.L. Gibson, T.E. Hanson, C. Bobst, J. Torres, C. Peres, F.H. Harrison, J. Gibson, and C.S. Harwood. (2004) Complete genome sequence of the metabolically versatile photosynthetic bacterium *Rhodopseudomonas palustris. Nat. Biotechnol.*, **22**(1): p. 55-61.
106. Lasaga, A.C. and H. Ohmoto. (2002) The oxygen geochemical cycle: dynamics and stability. *Geochim. Cosmochim. Acta*, **66**(3): p. 361-381.
107. Lepland, A., M.A. van Zuilen, G. Arrhenius, M.J. Whitehouse, and C.M. Fedo. (2005) Questioning the evidence for Earth's earliest life - Akilia revisited. *Geology*, **33**(1): p. 77-79.
108. Levasseur, S., R.J. Warthmann, and A.N. Halliday. (2002) Fractionation of Fe isotopes by anaerobic phototrophic bacteria. *Geochim. Cosmochim. Acta*, **66**(S1): p. A450.
109. Liu, Z., N. Guiliani, C. Appia-Ayme, F. Borne, J. Ratouchniak, and V. Bonnefoy. (2000) Construction and characterization of a recA mutant of T*hiobacillus ferrooxidans* by marker exchange mutagenesis. *J. Bacteriol.*, **182**(8): p. 2269-76.
110. Lonergan, D.J., H.L. Jenter, J.D. Coates, E.J. Phillips, T.M. Schmidt, and D.R. Lovley. (1996) Phylogenetic analysis of dissimilatory Fe(III)-reducing bacteria. *J. Bacteriol.*, **178**(8): p. 2402-8.
111. Lowe, D.R. (2005) Personal communication.
112. Mackenzie, C., A.E. Simmons, and S. Kaplan. (1999) Multiple chromosomes in bacteria: the yin and yang of *trp* gene localization in *Rhodobacter sphaeroides* 2.4.1. *Genetics*, **153**: p. 525-538.
113. Madigan, M.T., J.M. Martinko, and J. Parker. (2003) *Brock Biology of Microorganisms*. 10th ed. Upper Saddle River, NJ: Prentice Hall.
114. Madsen, E.L. (2005) Identifying microorganisms responsible for ecologically significant biogeochemical processes. *Nat. Rev. Microbiol.*, **3**(5): p. 439-46.
115. Malasarn, D., C.W. Saltikov, K.M. Campbell, J.M. Santini, J.G. Hering, and D.K. Newman. (2004) *arrA* is a reliable marker for As(V) respiration. *Science*, **306**(5695): p. 455.
116. Mandernack, K.W., D.A. Bazylinski, W.C. Shanks, 3rd, and T.D. Bullen. (1999) Oxygen and iron isotope studies of magnetite produced by magnetotactic bacteria. *Science*, **285**(5435): p. 1892-6.
117. Matthews, A., X. Zhu, and K. O'Nions. (2001) Kinetic iron stable isotope fractionation between iron (-II) and (-III) complexes in solution. *Earth Planet. Sci. Lett.*, **192**: p. 81-92.

118. Meyer, T.E. and M.A. Cusanovich. (2003) Discovery and characterization of electron transfer proteins in the photosynthetic bacteria. *Photosyn. Res.*, **76**: p. 111-126.
119. Meyer, T.E. and T.J. Donohue. 1995 *Cytochromes, iron-sulfur, and copper proteins mediating electron transfer from the cyt bc_1 complex to photosynthetic reaction center complexes*, in *Anoxygenic Photosynthetic Bacteria*, R.E. Blankenship, M.T. Madigan, and C.E. Bauer, Editors. Kluwer Academic Publishers: Netherlands. p. 725-745.
120. Meyer, T.E., C.T. Przysiecki, J.A. Watkins, A. Bhattacharyya, R.P. Simondsen, M.A. Cusanovich, and G. Tollin. (1983) Correlation between rate constant for reduction and redox potential as a basis for systematic investigation of reaction mechanisms of electron transfer proteins. *Proc. Natl. Acad. Sci. U S A*, **80**(22): p. 6740-4.
121. Mojzsis, S.J., G. Arrhenius, K.D. McKeegan, T.M. Harrison, A.P. Nutman, and C.R.L. Friend. (1996) Evidence for life on Earth before 3,800 million years ago. *Nature*, **384**(6604): p. 55-59.
122. Morel, F.M.M. and J.G. Hering. (1993) *Principles and Applications of Aquatic Chemistry*. New York: John Wiley & Sons, Inc.
123. Muyzer, G. and K. Smalla. (1998) Application of denaturing gradient gel electrophoresis (DGGE) and temperature gradient gel electrophoresis (TGGE) in microbial ecology. *Antonie Van Leeuwenhoek*, **73**(1): p. 127-41.
124. Neer, E.J., C.J. Schmidt, R. Nambudripad, and T.F. Smith. (1994) The ancient regulatory-protein family of WD-repeat proteins. *Nature*, **371**(6495): p. 297-300.
125. Neubauer, S.C., D. Emerson, and J.P. Megonigal. (2002) Life at the energetic edge: kinetics of circumneutral iron oxidation by lithotrophic iron-oxidizing bacteria isolated from the wetland-plant rhizosphere. *Appl. Environ. Microbiol.*, **68**(8): p. 3988-95.
126. Newman, D.K. and J.F. Banfield. (2002) Geomicrobiology: how molecular-scale interactions underpin biogeochemical systems. *Science*, **296**(5570): p. 1071-7.
127. Ng, W.L., M. Schummer, F.D. Cirisano, R.L. Baldwin, B.Y. Karlan, and L. Hood. (1996) High-throughput plasmid mini preparations facilitated by micro-mixing. *Nucleic Acids Res.*, **24**(24): p. 5045-7.
128. Ohmoto, H. (1997) When did the Earth's atmosphere become oxic? *Geochem. News*, **93**: p. 12-13 & 26-27.
129. Orphan, V.J., C.H. House, K.U. Hinrichs, K.D. McKeegan, and E.F. DeLong. (2001) Methane-consuming archaea revealed by directly coupled isotopic and phylogenetic analysis. *Science*, **293**(5529): p. 484-7.
130. Peng, J.B., W.M. Yan, and X.Z. Bao. (1994) Plasmid and transposon transfer to *Thiobacillus ferrooxidans. J. Bacteriol.*, **176**(10): p. 2892-7.
131. Petrickova, K. and M. Petricek. (2003) Eukaryotic-type protein kinases in *Streptomyces coelicolor*: variations on a common theme. *Microbiology*, **149**: p. 1609-1621.

132. Polyakov, V.B. and S.D. Mineev. (2000) The use of Mossbauer spectroscopy in stable isotope geochemistry. *Geochim. Cosmochim. Acta*, **64**: p. 849-865.
133. Poulson, R.L., B.L. Beard, C.M. Johnson, and S.A. Welch. (2003) Investigating isotope exchange between dissolved aqueous and precipitated amorphous iron species. *NAI General Meeting, Tempe, AZ*, (Abstract # 12626).
134. Poulton, S.W., P.W. Fralick, and D.E. Canfield. (2004) The transition to a sulphidic ocean ~1.84 billion years ago. *Nature*, **431**: p. 173-177.
135. Radajewski, S., P. Ineson, N.R. Parekh, and J.C. Murrell. (2000) Stable-isotope probing as a tool in microbial ecology. *Nature*, **403**(6770): p. 646-9.
136. Raponi, M., I.W. Dawes, and G.M. Arndt. (2000) Characterization of flanking sequences using long inverse PCR. *Biotechniques*, **28**(5): p. 838-842.
137. Rawlings, D.E. (1994) Molecular genetics of *Thiobacillus ferrooxidans. Microbiol. Rev.*, **58**(1): p. 39-55.
138. Rawlings, D.E. (2001) The molecular genetics of *Thiobacillus ferrooxidans* and other mesophilic, acidophilic, chemolithotrophic, iron- or sulfur-oxidizing bacteria. *Hydrometallurgy*, **59**: p. 187-201.
139. Robertson, L.A. and J. Gijs Kuenun. 2002 *The Genus Thiobacillus*, in *The Prokaryotes [computer file] : an evolving electronic resource for the microbiological community. Release 3.9.*, M. Dworkin, Editor. Springer-Verlag. Access at: http://141.150.157.117:8080/prokPUB/index.htm: New York.
140. Roden, E.E. and J.M. Zachara. (1996) Microbial reduction of crystalline Fe(III)-oxides: influence of oxide surface area and potential for cell growth. *Environ. Sci. Technol*, **30**: p. 1618-1628.
141. Roe, J.E., A.D. Anbar, and J. Barling. (2003) Nonbiological fractionation of Fe isotopes: evidence of an equilibrium isotope effect. *Chem. Geol.*, **195**: p. 69-85.
142. Rosing, M.T. (1999) ^{13}C-depleted carbon microparticles in >3700-Ma sea-floor sedimentary rocks from West Greenland. *Science*, **283**(5402): p. 674-6.
143. Rosing, M.T. (2004) U-rich Archean sea-floor sediments from West Greenland - indications of >3700-Ma oxygenic photosynthesis. *Earth Planet. Sci. Lett.*, **217**: p. 237-244.
144. Roth, J.R., J.G. Lawrence, and T.A. Bobik. (1996) Cobalamin (coenzyme B_{12}): Synthesis and biological significance. *Ann. Rev. Microbiol*, **50**: p. 137-181.
145. Rye, R. and H.D. Holland. (1998) Paleosols and the evolution of atmospheric oxygen: a critical review. *Am. J. Sci.*, **88**: p. 621-672.
146. Schauble, E.A., G.R. Rossman, and H.P. Taylor. (2001) Theoretical estimates of equilibrium Fe-isotope fractionations from vibrational spectroscopy. *Geochim. Cosmochim. Acta*, **65**: p. 2487-2497.

147. Schidlowski, M. (1988) A 3,800-million-year isotopic record of life from carbon in sedimentary rocks. *Nature*, **333**: p. 313-318.
148. Schopf, J.W., A.B. Kudryavtsev, D.G. Agresti, T.J. Wdowiak, and A.D. Czaja. (2002) Laser--Raman imagery of Earth's earliest fossils. *Nature*, **416**(6876): p. 73-6.
149. Schrader, J.A. and D.S. Holmes. (1988) Phenotypic switching of *Thiobacillus ferrooxidans. J. Bacteriol.*, **170**(9): p. 3915-23.
150. Schutz, M., I. Maldener, C. Griesbeck, and G. Hauska. (1999) Sulfide-quinone reductase from *Rhodobacter capsulatus*: requirement for growth, periplasmic localization, and extension of gene sequence analysis. *J. Bacteriol.*, **181**(20): p. 6516-23.
151. Schwertmann, U. and R.M. Cornell. (1991) *Iron Oxides in the Laboratory: Preparation and Characterization*. Weinheim, Germany: VCH Publishers.
152. Sharma, M., M. Polizzotto, and A.D. Anbar. (2001) Iron isotopes in hot springs along the Juan de Fuca Ridge. *Earth Planet. Sci. Lett.*, **194**: p. 39-51.
153. Shen, Y., R. Buick, and D.E. Canfield. (2001) Isotopic evidence for microbial sulphate reduction in the early Archaean era. *Nature*, **410**(6824): p. 77-81.
154. Sistrom, W.R. (1960) A requirement for sodium in the growth medium of *Rhodopseudomonas sphaeroides. J. Gen. Microbiol.*, **22**: p. 77-85.
155. Skulan, J.L., B.L. Beard, and C.M. Johnson. (2002) Kinetic and equilibrium Fe isotope fractionation between aqueous Fe(III) and hematite. *Geochim. Cosmochim. Acta*, **66**(17): p. 2995-3015.
156. Smith, T.F., C. Gaitatzes, K. Saxena, and E.J. Neer. (1999) The WD repeat: a common architecture for diverse functions. *Trends Biochem. Sci.*, **24**(5): p. 181-185.
157. Sobolev, D. and E.E. Roden. (2001) Suboxic deposition of ferric iron by bacteria in opposing gradients of Fe(II) and oxygen at circumneutral pH. *Appl. Environ. Microbiol.*, **67**(3): p. 1328-34.
158. Sobolev, D. and E.E. Roden. (2004) Characterization of a neutrophilic, chemolithoautotrophic Fe(II)-oxidizing α-Proteobacterium from freshwater wetland sediments. *Geomicrobiol. J.*, **21**: p. 1-10.
159. Stookey, L.L. (1970) *Ferrozine* - a new spectrophotometric reagent for iron. *Anal. Chem.*, **42**(7): p. 779-781.
160. Straub, K.L., M. Benz, and B. Schink. (2001) Iron metabolism in anoxic environments at near neutral pH. *FEMS Microbiol. Ecol.*, **34**(3): p. 181-186.
161. Straub, K.L., M. Benz, B. Schink, and F. Widdel. (1996) Anaerobic, nitrate-dependent microbial oxidation of ferrous iron. *Appl. Environ. Microbiol.*, **62**(4): p. 1458-1460.
162. Straub, K.L. and B.E. Buchholz-Cleven. (1998) Enumeration and detection of anaerobic ferrous iron-oxidizing, nitrate- reducing bacteria from diverse European sediments. *Appl. Environ. Microbiol.*, **64**(12): p. 4846-56.
163. Straub, K.L., F.A. Rainey, and F. Widdel. (1999) *Rhodovulum iodosum* sp. nov. and *Rhodovulum robiginosum* sp. nov., two new marine phototrophic

ferrous-iron-oxidizing purple bacteria. *Int. J. Syst. Bacteriol.*, **49**(2): p. 729-35.
164. Strelow, F.W.E. (1980) Improved separation of iron from copper and other elements by anion-exchange chromatography on a 4% cross-linkage resin with high concentrations of hydrochloric acid. *Tatlanta*, **27**: p. 727-732.
165. Strunk, O., O. Gross, B. Reichel, M. May, S. Hermann, N. Stuchmann, B. Nonhoff, M. Lenke, A. Ginhart, A. Vilbig, W. Ludwig, A. Bode, K.H. Schleifer, and W. Ludwig. (1998) *Arb: A software environment for sequence data*. Munich, Germany: Department of Microbiology, Technische Universitat Munchen.
166. Summons, R.E., L.L. Jahnke, J.M. Hope, and G.A. Logan. (1999) 2-Methylhopanoids as biomarkers for cyanobacterial oxygenic photosynthesis. *Nature*, **400**(6744): p. 554-7.
167. Takamiya, K.I. and P.L. Dutton. (1979) Ubiquinone in *Rhodopseudomonas sphaeroides*: Some thermodynamic properties. *Biochim. Biophys. Acta*, **546**(1): p. 1-16.
168. Taylor, D.P., S.N. Cohen, W.G. Clark, and B.L. Marrs. (1983) Alignment of genetic and restriction maps of the photosynthesis region of the *Rhodopseudomonas capsulata* chromosome by a conjugation-mediated marker rescue technique. *J. Bacteriol.*, **154**(2): p. 580-590.
169. Temple, K.L. and A.R. Colmer. (1951) The autotrophic oxidation of iron by a new bacterium, *Thiobacillus ferrooxidans. J. Bacteriol.*, **62**(5): p. 605-11.
170. Tian, F., O.B. Toon, A.A. Pavlov, and H. De Sterck. (2005) A hydrogen-rich early Earth atmosphere. *Science*, **308**(5724): p. 1014-1017.
171. Tice, M.M. and D.R. Lowe. (2004) Photosynthetic microbial mats in the 3,416-Myr-old ocean. *Nature*, **431**(7008): p. 549-52.
172. Trendall, A.H. and R.C. Morris. (1983) *Iron Formation: Facts & Problems*. Amsterdam: Elsevier.
173. Turner, J.V. (1982) Kinetic fractionation of carbon-13 during calcium carbonate precipitation. *Geochim. Cosmochim. Acta*, **46**: p. 1183-1191.
174. Valkova-Valchanova, M.B. and S.H. Chan. (1994) Purification and characterization of two new *c*-type cytochromes involved in Fe^{2+} oxidation from *Thiobacillus ferrooxidans. FEMS Microbiol. Lett.*, **121**(1): p. 61-9.
175. van Zuilen, M.A., A. Lepland, and G. Arrhenius. (2002) Reassessing the evidence for the earliest traces of life. *Nature*, **418**: p. 627-630.
176. Venturoli, G., J.G. Fernandez-Velasco, A.R. Crofts, and B.A. Melandri. (1986) Demonstration of a collisional interaction of ubiquinol with the ubiquinol-cytochrome *c2* oxidoreductase complex in chromatophores from *Rhodobacter sphaeroides. Biochim. Biophys. Acta*, **851**(3): p. 340-352.
177. Vernon, L.P., J.H. Mangum, J.V. Beck, and F.M. Shafia. (1960) Studies on a ferrous-ion-oxidizing bacterium. II. Cytochrome composition. *Arch. Biochem. Biophys.*, **88**: p. 227-31.
178. Vignais, P.M. and A. Colbeau. (2004) Molecular biology of microbial hydrogenases. *Curr. Iss. Mol. Biol.*, **6**: p. 159-188.
179. Wandersman, C. and P. Delepelaire. (2004) Bacterial iron sources: from siderophores to hemophores. *Ann. Rev. Microbiol*, **58**: p. 611-647.

180. Weaver, P.F., J.D. Wall, and H. Gest. (1975) Characterization of *Rhodopseudomonas capsulata. Arch. Microbiol.*, **105**(3): p. 207-216.
181. Welch, S.A., B.L. Beard, C.M. Johnson, and P.S. Braterman. (2003) Kinetic and equilibrium Fe isotope fractionation between aqueous Fe(II) and Fe(III). *Geochim. Cosmochim. Acta*, **67**(22): p. 4231-4250.
182. Widdel, F., S. Schnell, S. Heising, A. Ehrenreich, B. Assmus, and B. Schink. (1993) Ferrous iron oxidation by anoxygenic phototrophic bacteria. *Nature*, **362**(6423): p. 834-6.
183. Woods, D.R., D.E. Rawlings, M.E. Barros, I. Pretorius, and R. Ramesar. (1986) Molecular genetic studies of *Thiobacillus ferrooxidans*: the development of genetic systems and the expression of cloned genes. *Biotechnol. App. Biochem.*, **8**: p. 231-241.
184. Wu, J., E. Boyle, W. Sunda, and L.S. Wen. (2001) Soluble and colloidal iron in the oligotrophic North Atlantic and North Pacific. *Science*, **293**(5531): p. 847-9.
185. Xiong, J., W.M. Fischer, K. Inoue, M. Nakahara, and C.E. Bauer. (2000) Molecular evidence for the early evolution of photosynthesis. *Science*, **289**(5485): p. 1724-30.
186. Yamanaka, T. and Y. Fukumori. (1995) Molecular aspects of the electron transfer system which participates in the oxidation of ferrous ion by *Thiobacillus ferrooxidans. FEMS Microbiol. Rev.*, **17**(4): p. 401-13.
187. Yamanaka, T., T. Yano, M. Kai, H. Tamegai, A. Sato, and Y. Fukumori. 1991 *The electron transfer system in an acidophilic iron-oxidizing bacterium*, in *New era of bioenergetics*, Y. Mukohata, Editor. Academic Press: Tokyo. p. 223-246.
188. Yarzabal, A., C. Appia-Ayme, J. Ratouchniak, and V. Bonnefoy. (2004) Regulation of the expression of the *Acidithiobacillus ferrooxidans rus* operon encoding two cytochromes c, a cytochrome oxidase and rusticyanin. *Microbiology*, **150**(Pt 7): p. 2113-23.
189. Yarzabal, A., G. Brasseur, and V. Bonnefoy. (2002) Cytochromes *c* of *Acidithiobacillus ferrooxidans. FEMS Microbiol. Lett.*, **209**(2): p. 189-95.
190. Yarzabal, A., G. Brasseur, J. Ratouchniak, K. Lund, D. Lemesle-Meunier, J.A. DeMoss, and V. Bonnefoy. (2002) The high-molecular-weight cytochrome *c* Cyc2 of *Acidithiobacillus ferrooxidans* is an outer membrane protein. *J. Bacteriol.*, **184**(1): p. 313-7.
191. Yarzabal, A., K. Duquesne, and V. Bonnefoy. (2003) Rusticyanin gene expression of *Acidithiobacillus ferrooxidans* ATCC 33020 in sulfur- and ferrous iron media. *Hydrometallurgy*, **71**: p. 107-114.
192. Yen, H.C. and B. Marrs. (1976) Map of genes for carotenoid and bacteriochlorophyll biosynthesis in *Rhodopsedudomonas capsulata. J. Bacteriol.*, **126**: p. 619-629.